Charles University in Prague
Faculty of Mathematics and Physics

DOCTORAL THESIS

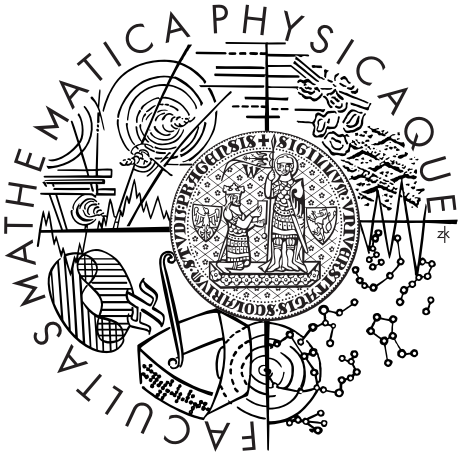

Miroslav Šulc

Excitation of molecules by cold electrons

Institute of Theoretical Physics

Supervisor of the doctoral thesis: prof. RNDr. Jiří Horáček, DrSc.
Study programme: Physics
Specialization: 4F1 Theoretical physics, astronomy and astrophysics

Prague 2011

Acknowledgements
First and foremost, I would like to heartily thank my advisor Prof. Jiří Horáček for his support and encouragement within my doctoral study. Further, I owe my deepest gratitude to Dr. Roman Čurík from J. Heyrovský Institute of Physical Chemistry of the Academy of Sciences of the Czech Republic. This thesis would have remained a dream without his guidance, physical insights, countless explanations of various scientific topics and friendly attitude.

My gratefulness goes likewise to Prof. David Field from the Department of Physics and Astronomy, University of Århus whose enthusiasm and generous help has been of tremendous value for me.

I am also very indebted to Prof. Jiří Vaníček for his kind hospitality and support during my stay and motivating work in the Laboratory of Theoretical Physical Chemistry of the École polytechnique fédérale de Lausanne. Special thanks belong to all members of the LCPT group. Their moral boost and great company made my time spent at the EPFL a wonderful experience.

Last but not least, I wish to thank to my family for creating and maintaining a pleasant background essential during my work on projects covered by the presented thesis.

I declare that I carried out this doctoral thesis independently, and only with the cited sources, literature and other professional sources.

I understand that my work relates to the rights and obligations under the Act No. 121/2000 Coll., the Copyright Act, as amended, in particular the fact that the Charles University in Prague has the right to conclude a license agreement on the use of this work as a school work pursuant to Section 60 paragraph 1 of the Copyright Act.

In Prague date August 15, 2011 .....

signature

Název práce: Excitace molekul studenými elektrony

Autor: Miroslav Šulc

Katedra / Ústav: Ústav teoretické fyziky, Univerzita Karlova v Praze

Vedoucí disertační práce: prof. RNDr. Jiří Horáček, DrSc.,
Ústav teoretické fyziky, Univerzita Karlova v Praze

Abstrakt: Pozornost je věnována vybraným metodám pro popis nízkoenergetických elektron-molekulových srážek. První část práce se zabývá aplikací metody R-matice v kombinaci s SL variačním principem pro potenciálový rozptyl v případě dalekodosahových interakcí. Další sekce se zaobírají aspekty konstrukce CP potenciálu v DMR metodě s využitím prostředků LDA DFT. Získané poznatky jsou následně aplikovány pro BF SEP výpočty v rámci analýzy experimentálních dat pro e^-–N_2 srážky představující součást širšího projektu věnovaného studiu rotačních excitací malých molekul v plynné fázi iniciovaných srážkami s elektrony. V případě N_2 bylo pozorováno potlačení dozadního průřezu pro energie pod 95 meV zdůvodnitelné z teoretického hlediska destruktivní interferencí parciálních vln s $l \leq 1$. Pro polární molekuly je naproti tomu výhodné zavést zobecněné fázové posuvy vzhledem k dipólové asymptotice, které jsou následně určené fitováním experimentálních dat integrálního a dozadního účinného průřezu. Příslušná metoda je demonstrována na datech pro CH_3Cl a SO_2.

Klíčová slova: R-matice, metoda DMR, nízkoenergetické elektron-molekulové srážky, dipólová interakce, Volterra propagátor

Title: Excitation of molecules by cold electrons

Author: Miroslav Šulc

Department / Institute: Institute of Theoretical Physics, Charles University in Prague

Supervisor of the doctoral thesis: prof. RNDr. Jiří Horáček, DrSc.,
Institute of Theoretical Physics, Charles University

Abstract: Several methods for low energy collisional processes are investigated. In the first part, attention is especially devoted to examination of applicability of the R-matrix method combined with SL variational principle for potential scattering with long-range forces. Next sections deal with the development of the interaction CP potential in the framework of the DMR method on LDA-DFT grounds. Obtained results are then utilized in BF SEP calculations within an analysis of experimental data for e^-–N_2 scattering comprising a part of a larger project addressing theoretical examination of rotational excitations of small molecules in the gas phase induced by electron impact. For N_2, a new phenomenon consisting in suppression of backward cross-section below 95 meV is observed and consequently attributed to destructive interference in the angular $l \leq 1$ space. Treatment for polar molecules introduces generalized dipole phase shifts determined by fitting to the experimental data. Their knowledge enables then to determine the differential as well as individual stat-to-state cross-sections. This approach is demonstrated on the experimental data for CH_3Cl and SO_2.

Keywords: R-matrix, Discrete Momentum Representation, low energy electron-molecule collisions, dipole interaction, Volterra integral propagator

CONTENTS

INTRODUCTION

The presented thesis intends to summarize and explain in more detail the work I have been involved in during my doctoral study at the Faculty of Mathematics and Physics of Charles University in Prague in the period from 2007 to 2011. From the conceptual point of view, the covered topics of interest could be divided into four essentially independent logical blocks.

Firstly, I have picked up on my master thesis (Šulc, 2007) and investigated several computational methods applicable for potential scattering problems. The attention was especially devoted to examination of the properties and numerical behavior of a newly proposed method capable of dealing with nonlocal potential terms. This approach profits from combination of the R-matrix method, the basic properties of which are summarized in Section 1.6, and Lanczos variational iterative procedure. For thorough clarification of the latter gambit we refer to the literature cited in Section 1.6. Consequently, we have also adapted this procedure to computational tasks, in which a long range interaction plays a dominant role. Corresponding details are briefly covered by Section 1.6 and discussed more thoroughly in Šulc et al. (2010). This publication is also included as a part of this thesis in Attachment A.

Within the next subproject we have focused on development of the interaction correlation-polarization potential in the framework of the Discrete Momentum Representation (DMR) method canvassed in Section 1.1. The electron-molecule scattering process is in the proposed approach described at the level of the Static Exchange approximation to which we devote the Chapter 2, especially the Section 2.1. In contrast to the "classical" approaches, where one typically employs more or less succesful tweaks in order to improve the adiabatic polarization potential (Section 2.3), we employ the Local Density Approximation (LDA) within the Density Functional Theory (DFT) to render the short range part of the correlation potential which is in turn matched with known asymptotic polarization form. Consequently, we apply this tack for description of electron scattering on small hydrocarbon molecules (Čurík and Šulc, 2010). Theoretical concepts are introduced mainly in Section 2.3 whereas corresponding results can be found in Attachment B.

The third topic comprising the main contribution to the presented thesis consisted in theoretical analysis of the experimental data regarding collisions of cold electrons (incident energy below $\sim 250\,\mathrm{meV}$) with small molecules in the gas phase. The work has been done in collaboration with the group of Prof. David Field from the Department of Physics and Astronomy of Århus University in Denmark. From the pure theoretical point of view, there is a marked difference between polar and non-polar molecular species.

In the former case, the electron-molecule interaction is governed by the dominant long-range dipole part of the potential (Appendix C) the presence of which can be actually conveniently utilized as explained in Subsection 4.1.1, where we demonstrate

the applicability potential of this approach on the experimental data regarding CH_3Cl. Roughly speaking, the scattering formalism is reformulated with respect to the solutions of the pure dipole interaction. In analogy with standard approach one is led to the generalized phase shifts which are attributed to (unknown) short-range perturbation to the dipole potential. These phase-shifts then play the role of free energy dependent parameters in the entire model and are fitted in order to reproduce the experimental integral and backward cross-sections data. Since we have two independent data sets at our disposal, we take into account just two most dominant generalized phase-shifts hoping in this sense for an one to one correspondence between the model and the measurement (Chapter 3). Utilizing the knowledge of the energy dependence of these phase shifts, we can consequently easily compute any scattering quantity, notably the differential cross-sections for individual rotational state-to-state transitions.

For non-polar molecules, the situation is more involved since the interaction misses a clearly dominant contribution. The identification of relevant fitting parameters as in the polar case is thus accordingly hampered. In order to resolve this issue, we have developed a computer program for laboratory frame close-coupling calculations in the SE approximation including a correlation-polarization potential constructed in a very similar DFT-fashion as for the hydrocarbons in the previous project. The numerical implementation was based on the Volterra propagator method tailored for scattering problems as elaborated succinctly in Section 1.5 and Appendix A. The resulting treatment has been tested on a model mimicking electron scattering off carbon monoxide (Section 1.4) representing a slightly polar molecule. For this particular system we have achieved good accordance with published results. However, for the non-polar N_2 molecule, it turned out to be very difficult to obtain reliable converged laboratory frame results. We have been thus forced to digress to the body frame (Section 1.2) and exploit the Rotational Frame Transformation (RFT) abstracted in Subsection 1.2.2. Decreasing the characteristic size of the problem by reducing the number of relevant channels led indeed to a significant improved numerical behavior. By comparing these *ab initio* results with available sources in the literature we have identified the body frame $\mathcal{K}$-matrix elements dominant for the prediction of the measured quantities. The procedure then runs along the lines of the polar case treatment. As a byproduct of this analysis, we have identified an interesting phenomena consisting in marked suppression of the backward cross-section below 95 meV. After some consideration, we have attributed this effect to a destructive interference in the $l \leq 1$ angular space. Corresponding publication is currently in the submission process and its actual version is included as Attachment B.

Finally, in the last part of my doctoral study during my stay in the group of Prof. Jiří Vaníček at the Laboratory of Theoretical Physical Chemistry (LCPT) of the École Polytechnique Fédérale de Lausanne (EPFL), I have devoted my interest to the study of properties and numerical behavior of selected semiclassical methods (Kay, 2005) in the framework of quantum dynamics with applicability in the field of time-resolved ultrafast spectroscopy. Specifically, we have implemented and consequently analyzed the Frozen Gaussian approach of Heller (1981) and the Heller-Herman-Kluk-Kay propagator proposed in Herman and Kluk (1984). These methods were tested on a set of low dimensional training systems, *i.a.* a two dimensional collinear model (Li et al., 1993) for the NCO molecule. Even for this rather simple setting, we were led to the apparently inevitable conclusion that the direct implementation of the original algorithms suffers from several conceptual (Walton and Manolopoulos, 1995) and also numerical drawbacks (Kay, 1994) reflecting itself in the fact that for sufficiently large time these methods are typically brought to their computational demise. In this sense, several improvements turned out to be of prominent importance (Elran and Kay, 1999; Kay,

1994; Walton and Manolopoulos, 1996; Wang et al., 2001). Another closely related aspect surprisingly overlooked in the literature is the possibility to employ simplectic integrators for solving the classical equations of motion. This ingredient represents actually a common denominator to a vast majority of semiclassical approximations to the quantum dynamics. More importantly, within this approach, the equations of motion for the stability matrix are naturally formulated by means of a straightforward iterative updating process amenable to simple implementation. Apart from standard propagation routines such as symplectic Euler's and Verlet's schemes, we have also implemented and tested a fourth order method (Chin, 1997) minimizing the number of terms in the split operator formula for the evolution operator at additional costs consisting in introducing an effective force containing terms depending on the Hessian matrix. This gambit turned out to yield better numerical accuracy, nevertheless the update process for the stability matrix then necessitates the knowledge of third derivatives of the potential the requirement of which could in principle complicate combination with *ab initio* calculation of the potential surfaces in an "on the fly" fashion. This work doesn't constitute a part of the presented thesis, nevertheless relevant references, more detailed discussion, and a concise summary of achieved results can be found in Wehrle, Šulc and Vaníček (2011).

CHAPTER
ONE

COMPUTATIONAL TOOLS

1.1 Discrete momentum representation

This method could be considered as an example of "direct" methods, in the spirit of which one tries to tackle the *Lippmann-Schwinger* (LS) equation for the transition operator[1] **T**.

The basic idea of the *Discrete Momentum Representation* (DMR) approach (Polášek et al., 2000) is that one tries to solve the LS equation directly in three dimensional momentum basis abandoning techniques such as partial wave decomposition. In one-channel formalism considering only elastic scattering, the LS equation takes (Gell-Mann and Goldberger, 1953) following form

$$\langle \vec{k}_f | \mathbf{T} | \vec{k}_i \rangle = \langle \vec{k}_f | \mathbf{U} | \vec{k}_i \rangle + \int \mathrm{d}\vec{k} \, \frac{\langle \vec{k}_f | \mathbf{U} | \vec{k} \rangle \langle \vec{k} | \mathbf{T} | \vec{k}_i \rangle}{k_0^2 - k^2 + \mathrm{i}\epsilon}, \tag{1.1}$$

with $k_0^2/2$ representing the energy of the incident electron, U denoting the potential multiplied by two[2] and finally presence of the term $\mathrm{i}\epsilon$ suggests the usual limiting process $\epsilon \to 0^+$ performed after the integration.

The problem is now twofold. First of all, in oder to ensure successfulness of the model, we certainly need to devise the interaction potential U as accurate as possible. In the following, we shall confine ourselves only on issues connected with numerical evaluation of the integral over $\vec{k}$ in Eq. (1.1). More detailed discussion regarding approximative treatments of the U-term can be found in Chapter 2.

The original paper (Polášek et al., 2000) doesn't give detailed explanation regarding simplifying procedure of the integral entering Eq. (1.1) and therefore in the following we would like to make a few comments concerning this issue.

To simplify the integral in Eq. (1.1) as much as possible, it is convenient to split up the integration into angular (over $\hat{k}$) and radial part (over k). This readily yields

$$\langle \vec{k}_f | \mathbf{T} | \vec{k}_i \rangle = \langle \vec{k}_f | \mathbf{U} | \vec{k}_i \rangle + \int_0^\infty \mathrm{d}k \, k^2 \frac{f(\vec{k}_f, \vec{k}_i, k)}{k_0^2 - k^2 + \mathrm{i}\epsilon}, \tag{1.2}$$

where the function f is defined in terms of **U** and **T** as

$$f(\vec{k}_f, \vec{k}_i, k) = \int \mathrm{d}\hat{n} \, \langle \vec{k}_f | \mathbf{U} | k\hat{n} \rangle \langle k\hat{n} | \mathbf{T} | \vec{k}_i \rangle. \tag{1.3}$$

[1] for economy of notation, we confine ourselves only to the one-channel Lippmann-Schwinger equation in this chapter

[2] atomic units are used throughout this chapter – in more precise notation $U = 2\mu V$,where μ is the reduced mass of the target-scatterer system

The radial integral in Eq. (1.2) is singular in the sense that the upper limit of integration is infinity and also due to the term in the denominator. In order to handle the iϵ-term, we can employ slight modification of the well-known *Plemelj-Sokhotsky* formula[3]

$$\frac{1}{x_0 - x + \mathrm{i}\epsilon} = \mathcal{P}\frac{1}{x_0 - x} - \mathrm{i}\pi\delta(x - x_0), \tag{1.4}$$

where both sides have to be understood in the sense of the theory of distributions. Using (1.4) for fixed $x_0 \neq 0$, the following identity is easily verified[4]

$$\begin{aligned}\frac{1}{x_0^2 - x^2 + \mathrm{i}\epsilon} &= \frac{1}{2x_0}\left(\frac{1}{x_0 - x + \mathrm{i}\epsilon} + \frac{1}{x_0 + x + \mathrm{i}\epsilon}\right) = \\ &= \mathcal{P}\frac{1}{x_0^2 - x^2} - \mathrm{i}\frac{\pi}{2x_0}\big(\delta(x - x_0) + \delta(x + x_0)\big).\end{aligned} \tag{1.5}$$

The distributions introduced in (1.4) and (1.5) act on functions defined on the entire real axis. However, the integration range in our integral of interest (1.1) is only the positive real axis. Nevertheless, this nuisance is easily circumvented for all terms except f appearing in the integrand of (1.1) are even in k. We can therefore replace the function f by its even extension $\tilde{f}$ and consequently expand the integration range to $(-\infty, \infty)$, utilize formula (1.5) and take only half of the resulting integral. Explicitly, one has

$$\begin{aligned}\int_0^\infty \mathrm{d}k\, k^2 \frac{f(\vec{k}_f, \vec{k}_i, k)}{k_0^2 - k^2 + \mathrm{i}\epsilon} &= \frac{1}{2}\int_{-\infty}^\infty \mathrm{d}k\, k^2 \frac{\tilde{f}(\vec{k}_f, \vec{k}_i, k)}{k_0^2 - k^2 + \mathrm{i}\epsilon} \\ &= \frac{1}{2}\mathcal{P}\int_{-\infty}^\infty \mathrm{d}k\, k^2 \frac{\tilde{f}(\vec{k}_f, \vec{k}_i, k)}{k_0^2 - k^2} - \mathrm{i}\frac{\pi}{2} k_0 \tilde{f}(\vec{k}_f, \vec{k}_i, k_0) \\ &= \mathcal{P}\int_0^\infty \mathrm{d}k\, k^2 \frac{f(\vec{k}_f, \vec{k}_i, k)}{k_0^2 - k^2} - \mathrm{i}\frac{\pi}{2} k_0 f(\vec{k}_f, \vec{k}_i, k_0).\end{aligned} \tag{1.6}$$

From practical point of view, we are thus now faced with an integral of the type

$$\mathcal{P}\int_0^\infty \mathrm{d}k\, k^2 \frac{f(\vec{k}_f, \vec{k}_i, k)}{k_0^2 - k^2}. \tag{1.7}$$

Original DMR approach (Ingr et al., 2000; Polášek et al., 2000) tries to improve the numerical behavior of (1.7) by a substitution chosen as

$$k = k_0 \frac{a + bx}{a - bx}, \text{ for } a, b > 0, \tag{1.8}$$

which maps the singularity $k = k_0$ to $x = 0$ and the points $k = 0$ and $k = \infty$ to $x = -a/b$ and $x = a/b$, respectively.[5] Alternative approaches based on principal value identities satisfied by Chebyshev polynomials of the first and second kind have been also reported (Pichl and Horáček, 1996).

By applying the transformation (1.8) to (1.7), we obtain

$$\mathcal{P}\int_0^\infty \mathrm{d}k\, k^2 \frac{f(\vec{k}_f, \vec{k}_i, k)}{k_0^2 - k^2} = -\frac{k_0}{2}\mathcal{P}\int_{-b/a}^{b/a} \mathrm{d}x\, \frac{\hat{f}(\vec{k}_f, \vec{k}_i, x)}{x}\frac{(a + bx)^2}{(a - bx)^2}, \tag{1.9}$$

with $\hat{f}(\vec{k}_f, \vec{k}_i, x) = f(\vec{k}_f, \vec{k}_i, k(x))$. Three minor observations regarding Eq. (1.9) deserve further comment.

[3] symbol $\mathcal{P}$ denotes *Cauchy principal value*

[4] limit $\epsilon \to 0^+$ is automatically assumed

[5] actually only the ratio b/a is important in (1.8) and therefore one can set $b = 1$ with impunity

- The integration in x is symmetric around 0. Because $\mathcal{P}\int_{-A}^{A} 1/x = 0$, one immediately sees that following identity (Polášek et al., 2000) holds

$$\mathcal{P}\int \frac{f(x)}{x} = \mathcal{P}\int \frac{f(x) - f(0)}{x}. \tag{1.10}$$

  It is therefore perfectly possible to evaluate the rest of the integrand in (1.9) at $x = 0$ and consequently subtract it from the original expression without changing the value of the integral (1.9).

- It might seem that the upper integration limit $x = b/a$ causes problems due to the $(a - bx)^2$ term. However, vicinity of $x = b/a$ corresponds to high momenta k and in this case it is not completely unreasonable to expect that the function $f(\vec{k}_f, \vec{k}_i, k(x))$ will decay fast enough to ensure convergence.

- If one uses Gauss-Legendre quadrature in x with even number of mesh points (which are then distributed symmetrically around the origin), it is justifiable simply to "forget" the principal value as had been already observed in the early days of computational science (Sloan, 1968).

As concerns the angular integration in (1.3), Polášek et al. (2000) suggested to use an efficient numerical scheme known in the literature as *Lebedev quadrature*. This method, originally introduced by Lebedev (1976, 1977), is intended for numerical integration of functions defined on a sphere. The grid points are chosen so that they are invariant under operations belonging to G_8^* – the octahedral point group augmented by inversion. It can be shown (Lebedev, 1976) that any point on a sphere has exactly 5,7,11,23 or 47 "conjugated" partners.[6] The final grid is then chosen as an union of several such "conjugated" groups and points belonging to the same group are equipped with the same integration weight. These weights are in turn determined from the natural requirement of exact integration of polynomials (or equivalently, spherical harmonics) up to a given order. This yields a set of nonlinear equations, which are consequently solved for the weights[7] in a numerical fashion.

Finally, introducing radial and angular numerical quadrature, the original LS equation (1.1) is thus converted into a matrix equation amenable to standard treatment by any of the plethora of methods available (Golub and Loan, 1996).

A detailed study regarding optimal choice of the radial as well as angular quadrature parameters can be found in Čársky (2010*a*). For these purposes, the author employs transformation (1.8) with $b = 1$ and presupposes that the error introduced by the numerical quadrature in Eq. (1.1) won't be significantly changed if one replaces the exact transition operator by the matrix U digressing thus actually to the Born approximation of second order. For $b = 1$, a value of a greater than 1 corresponds effectively to a cut-off in the momentum space (with x confined to the interval $[-1, 1]$). Čársky (2010*a*) therefore investigates the minimal value of a ensuring a prescribed relative error in the numerical integration of the second term in Eq. (1.1) (in the second Born approximation) as compared to the case $a = 1$ using several model potentials (H_2O, CH_4, cyclopropane, *etc.*). For this particular value of a, the author consequently supposes that the Lebedev's grid with 5 180 points (precise up to the order of 131) yields converged results. The angular grid density is then decreased until one reaches some preselected relative error. This methodology has been later tested (Čársky, 2010*b*) in

[6] *i.e.*, points belonging to one particular "conjugate" set are transformed among themselves with respect to the group G_8^*

[7] *e.g.*, Lebedev and Laikov (1999) give these weights in tabulated form up to order 131 (corresponding grid has then 5 810 points)

case of elastic electron scattering on small molecules, where the author also discusses numerical issues connected with the evaluation of matrix elements of the exchange contribution to the potential **U**-term.

The above described method has found many useful applications in the field of electron-molecule scattering. Ingr et al. (2000) have extended this approach also for polar molecules, where special care has to be taken concerning the singular behavior of the dipole potential. The underlying ideas are actually quite similar to the Born closure techniques described in Subsection 1.4.3. Formalism for two-channel vibrationally inelastic scattering has been established and applied for H_2 and H_2O molecules by Čurík and Čársky (2003). Study of elastic electron scattering on cyclopropane, where the short-range correlation potential is modeled at the local density approximation in the DFT framework has been recently given by Čurík and Šulc (2010). This paper is also included into this thesis as Attachment C.

1.2 Electron-molecule scattering formalism

In description of electron-molecule collisions one usually employs (Lane, 1980) Born-Oppenheimer approximation to simplify the theoretical treatment of the states of the target molecule which is assumed to be comprised of M nuclei located at $\{\vec{R}_i\}_{i=1}^{M}$ and N electrons with coordinates $\{\vec{r}_i\}_{i=1}^{N}$. Following Chang and Fano (1972), we will adhere to the convention[8] that unprimed coordinates refer to the frame of reference fixed in space (LF – *laboratory frame*) whereas primed coordinates are connected with a frame of reference attached to the molecule (BF – *body frame*).[9]

With this convention, the total Hamiltonian for the composite system comprised by an impinging electron with position vector $\vec{r}$ and the target molecule can be expressed as

$$\mathbf{H} = \mathbf{H}_{\mathrm{m}}^{(e)}(\vec{r}_i, \vec{R}_j) + \mathbf{H}_{\mathrm{m}}^{(n)}(\vec{R}_j) + \mathbf{T}_e(\vec{r}) + \mathbf{V}_{\text{e-m}}(\vec{r}, \vec{r}_i, \vec{R}_j), \tag{1.11}$$

where the meaning of the individual terms is as follows

- $\mathbf{T}_e(\vec{r})$ is simply the kinetic energy operator of the incident electron
- $\mathbf{H}_{\mathrm{m}}^{(e)}(\vec{r}_i, \vec{R}_j)$ stands for standard "electronic" Born-Oppenheimer Hamiltonian being merely given as a sum of kinetic energies of individual molecular electrons and Coulombic repulsion terms to wit

$$\mathbf{H}_{\mathrm{m}}^{(e)}(\vec{r}_i, \vec{R}_j) = -\frac{1}{2}\sum_{i=1}^{N}\Delta_i - \sum_{i=1}^{N}\sum_{j=1}^{M}\frac{Z_j}{|\vec{r}_i - \vec{R}_j|} + \sum_{\substack{i,j \\ i\neq j}}^{N}\frac{1}{|\vec{r}_i - \vec{r}_j|}$$

- $\mathbf{H}_{\mathrm{m}}^{(n)}(\vec{R}_j)$ contains in a very similar fashion the kinetic and potential terms regarding the nuclei, namely

$$\mathbf{H}_{\mathrm{m}}^{(n)}(\vec{R}_k) = -\frac{1}{2}\sum_{i=1}^{M}\frac{1}{M_i}\Delta_i + \sum_{i\neq j}^{M}\frac{1}{|\vec{R}_i - \vec{R}_j|}$$

- $\mathbf{V}_{\text{e-m}}(\vec{r}, \vec{r}_i, \vec{R}_j)$ represents the (Coulombic) interaction of the incident electron with the target molecule, *i.e.*,

$$\mathbf{V}_{\text{e-m}}(\vec{r}, \vec{r}_i, \vec{R}_j) = -\sum_{j=1}^{M}\frac{Z_j}{|\vec{r} - \vec{R}_j|} + \sum_{i=1}^{N}\frac{1}{|\vec{r} - \vec{r}_i|}$$

[8] Lane (1980); Morrison (1988) employ opposite notation

[9] coinciding in the rigid rotor approximation (Appendix E) with the principal axes of inertia

In order to simplify notation as much as possible, we shall confine ourselves in the following to diatomic targets having just one nuclear degree of freedom, the internuclear distance, R. To proceed further, one typically introduces (Morrison, 1988) a set of target Born-Oppenheimer electronic states $|\alpha\rangle$ to each of which there corresponds a potential energy curve $E_\alpha(R)$. By definition, these kets satisfy

$$\mathbf{H}_{\mathrm{m}}^{(e)} |\alpha\rangle = E_\alpha(R) |\alpha\rangle .$$

The nuclear degrees of freedom are collectively taken into account by introducing a common label ν. The target states $|\alpha\nu\rangle$ are consequently in the Born-Oppenheimer framework rendered as

$$\left[\mathbf{H}_{\mathrm{m}}^{(n)} + E_\alpha(R)\right] |\alpha\nu\rangle = E_{\alpha\nu} |\alpha\nu\rangle .$$

Central to the scattering process under investigation are the asymptotic free states (Taylor, 2006), which can be in the present setting labeled naturally by the scattered electron's momentum vector $\vec{k}_{\alpha\nu}$ and the target quantum numbers α, ν introduced above. Subscript on k denotes explicitly the dependence of the momentum on the channel indices α, ν. In accordance with Morrison (1988); Taylor (2006), we denote the stationary scattering states as $\left|\vec{k}_{\alpha\nu}, \alpha, \nu\right\rangle$. Since we are interested in low-energy collisions only, it is not completely unreasonable to expect that only the lowest electronic state will play a dominant role. This is manifested formally in the procedure (Burke, 1979; Morrison, 1988) in which one expands the sought total wave function $\left|\vec{k}_{\alpha\nu}, \alpha, \nu\right\rangle$ into individual electronic states, retains only the ground electronic state α_0 and finally applies the *bound-free* antisymmetrizer to enforce the indistinguishability of the incident (free) and the molecular (bound) electrons, *i.e.*,

$$\left|\vec{k}_{\alpha_0\nu}, \nu\right\rangle \equiv \mathcal{A} \sum_{\alpha'} \delta_{\alpha_0,\alpha'} \left|\alpha'\right\rangle \left\langle\alpha'\right| \left|\vec{k}_{\alpha\nu}, \alpha, \nu\right\rangle. \tag{1.12}$$

Projection of the Schrödinger equation corresponding to (1.11) for energy E onto the ground electronic state α_0 yields a Schrödinger-like equation in $\vec{r}, \vec{R}_j$ for $\left|\vec{k}_{\alpha_0\nu}, \nu\right\rangle$ since the electronic variables $\vec{r}_i$ have been integrated out. By denoting $\left|\vec{k}_{\alpha_0\nu}, \nu\right\rangle$ in coordinate representation as $\Psi_{\vec{k}_0,\nu_0}(\vec{r}, \vec{R}_j)$, the resulting equation takes the form

$$\left[-\frac{1}{2}\Delta_{\vec{r}} + \mathbf{H}_{\mathrm{m}}^{(n)} + E_{\alpha_0}(R) + \mathbf{V}_{\mathrm{int}} - E\right] \Psi_{\vec{k}_0,\nu_0}(\vec{r}, \vec{R}_j) = 0. \tag{1.13}$$

All information about the scattering process can be then extracted from the wave function $\Psi_{\vec{k}_0,\nu_0}$, *e.g.*, the scattering amplitude is closely linked with its asymptotic behavior

$$\Psi_{\vec{k}_0,\nu_0}(\vec{r}, \vec{R}_j) \overset{r\to\infty}{\sim} \mathrm{e}^{\mathrm{i}\vec{k}_0\cdot\vec{r}} \phi_{\nu_0}(\vec{R}_j) + \sum_\nu \frac{\mathrm{e}^{\mathrm{i}\vec{k}_\nu\vec{r}}}{r} f\big(\vec{k}_0, \nu_0 \to \vec{k}_\nu, \nu\big) \phi_\nu(\vec{R}_j). \tag{1.14}$$

Having obtained the scattering amplitude f, one consequently easily expresses the corresponding differential scattering cross-section

$$\left.\frac{\mathrm{d}\sigma}{\mathrm{d}\Omega}\right|_{\nu_0\to\nu} = \frac{k_\nu}{k_0} \left| f\big(\vec{k}_0, \nu_0 \to \vec{k}_\nu, \nu\big) \right|^2, \tag{1.15}$$

from which the integral cross-section $\sigma_{\nu_0\to\nu}$ is rendered by means of angular integration.

The interaction potential denoted by V_{int} in (1.13) consists of two important parts, the so-called *static* V_{st} and *exchange* V_{ex} potential. The former is merely the interaction potential $V_{\text{e-m}}$ averaged over the ground electronic state $|\alpha_0\rangle$ whereas the latter is

in general a nonlocal operator ensuing from the antisymmetrization in (1.12). Resulting approximation is widely known in the literature as *Static Exchange Approximation* (Huo and Gianturco, 1995, ch. 4) and is in more detail discussed in Section 2.1. The omission of excited electronic states in (1.12) is formally equivalent to neglecting of polarization effects, *i.e.*, distortion of the target charge density by the impinging electron, and it has to be accounted for by further modifications of the interaction potential V_{int} as briefly mentioned in Chapter 2.

1.2.1 Laboratory vs. Body frame approach

The plane wave representation inherently present in the central equation (1.13) of the static exchange approximation is not especially convenient for practical computational purposes especially at very low energies. Therefore one is forced to seek more convenient representations, two of which are the subject of the following discussion.

Laboratory frame approach (coupled angular momentum)

The laboratory frame approach in coupled angular momentum[10] representation is tantamount to considering one particular complete set of mutually commuting operators[11], namely

$$\mathbf{H}_{\mathrm{m}}^{(v)}, \mathbf{l}^2, \mathbf{j}^2, \mathbf{J}^2, \mathbf{J}_z, \tag{1.16}$$

i.e., one takes into account the vibrational Hamiltonian $\mathbf{H}_{\mathrm{m}}^{(v)}$, squared orbital angular momentum of the incident electron $\mathbf{l}^2$, squared rotational angular momentum $\mathbf{j}^2$ of the target diatomic molecule and also the total angular momentum $\mathbf{J}^2$ together with its projection $\mathbf{J}_z$ onto the space fixed z-axis. In coordinate representation, the relevant basis functions are expressed as

$$\Phi_{\upsilon jl}^{JM}\big(\hat{r},\vec{R}\,\big) = \chi_{\upsilon}(R) \sum_{m_j,m_l} (jl\, m_j m_l|\; J\, M)\, \mathrm{Y}_{j,\,m_j}\big(\hat{R}\big)\mathrm{Y}_{l,\,m}\big(\hat{r}\big), \tag{1.17}$$

with χ_{υ} representing the vibrational state υ. Transformation from the plane wave representation is effected (Morrison, 1988) in a straightforward way. In the basis (1.17), the wave function $\Psi_{\vec{k}_0,\nu_0}$ takes a similar form

$$\Psi_{\upsilon_0 j_0 l_0}^{JM}\big(\vec{r},\vec{R}\,\big) = \frac{1}{r}\sum_{\upsilon jl} \psi_{\upsilon jl,\upsilon_0 j_0 l_0}^{J}(r)\cdot\Phi_{\upsilon jl}^{JM}\big(\hat{r},\vec{R}\,\big), \tag{1.18}$$

where one is interested in solving the Schrödinger equation for the r-dependent "expansion coefficients", the "radial" equations (Chang and Fano, 1972, Eq. (21)) for which

$$\left[-\frac{1}{2}\frac{\mathrm{d}^2}{\mathrm{d}r^2} + \frac{l(l+1)}{2r^2} - \frac{1}{2}k_{\upsilon j}^2\right]\psi_{\upsilon jl,\upsilon_0 j_0 l_0}^{J}(r) = -\sum_{\upsilon' j' l'}\big\langle \upsilon jl\big|\mathbf{V}_{\mathrm{int}}\big|\upsilon' j' l'\big\rangle\psi_{\upsilon' j' l',\upsilon_0 j_0 l_0}^{J}(r) \tag{1.19}$$

are easily obtained by projecting the Schrödinger equation for the total wave function onto individual elements of the basis (1.17). Numerical methods designed for solving systems of equations of the type (1.19) are the subject of Section 1.5.

The channel momentum $k_{\upsilon j}$ entering (1.19) results from conservation of the total energy[12]

$$\vec{k}_{\upsilon j}^{\,2} = 2E - \omega(2\upsilon+1) - 2Bj(j+1). \tag{1.20}$$

[10] denoted as (LAB-CAM) by Huo and Gianturco (1995); Morrison (1988)

[11] since we are considering only diatomic molecules, the rotational part $\mathbf{H}_{\mathrm{m}}^{(r)}$ of the nuclear Hamiltonian $\mathbf{H}_{\mathrm{m}}^{(v)}$ is directly linked with the operator $\mathbf{j}^2$

[12] assumption of the diatomic case manifests itself in the expression for the rotational energy depending only on the quantum number j and the rotational constant B, ω stands for the vibrational frequency in the harmonic approximation

The interaction potential matrix element in (1.19) coupling individual channels depends on r and in general is a nonlocal operator due to the presence of the exchange potential. Approximate ways how to cope with its presence are discussed in Chapter 2. On the other hand, in the rigid rotor approximation, Eq. (1.19) can be further simplified as discussed in Section 1.4, where the LAB-CAM treatment is applied to investigation of rotational excitations caused by electron impact.

Body frame approach

Although the above described approach is formally "exact", it is easily seen that if the incident electron penetrates closer to the molecule (*i.e.*, for $r \to 0$), the LAB-CAM formalism is quite inconvenient. The reason for this (Lane, 1980) has to be accounted to the strong attractive behavior of the interaction in the vicinity of the molecule. Thus the movement (and therefore also the orbital angular momentum) of the electron is strongly coupled with the molecular axis $\hat{R}$. Consequently, the projection of the electron's angular momentum on $\hat{R}$ is approximately well-defined. However, this property is not directly reflected in (1.17) and therefore large number of basis functions will be in general necessary to reproduce this effect bringing any numerical method intended for solving (1.19) into considerable troubles.

Adequate description has to use therefore different set of commuting operators than (1.16) to take these considerations into account. Two choices are widely used depending whether one takes the vibrational Hamiltonian $\mathbf{H}_{\mathrm{m}}^{(v)}$ directly into account or not.

• **excluding $\mathbf{H}_{\mathrm{m}}^{(v)}$**

The first choice[13] ignores the vibrational Hamiltonian $\mathbf{H}_{\mathrm{m}}^{(v)}$ and as such hinges on the use of the following operators

$$\mathbf{l}^2, \mathbf{l}_{z'}, \mathbf{J}^2, \mathbf{J}_{z'}, \mathbf{J}_z, \tag{1.21}$$

namely the angular momenta of the incident electron, the total angular momentum and their projections onto the body-fixed z'-axis coinciding with the internuclear axis, the orientation of which is in the laboratory frame specified by a unit vector $\hat{R}$. In order to ensure completeness of the set of operators (1.21), it is necessary to take into account also the space-fixed projection $\mathbf{J}_z$ of the total angular momentum. Instead of (1.17) as in the LAB-CAM case one is thus led to slightly different basis[14]

$$|l\Lambda;\, JM\rangle \sim {}^{\mathrm{I}}X_{l\Lambda}^{JM} \equiv \sqrt{\frac{2J+1}{4\pi}}\, \mathcal{D}_{M,\Lambda}^{J}\big(\hat{R}\big) \mathrm{Y}_{l,\,\Lambda}\big(\hat{r}'\big) \tag{1.22}$$

with $\mathcal{D}_{M,\Lambda}^{J}$ being related to the symmetric top[15] rotational wave function as discussed in length in Appendix E. Along very similar lines as in the LAB-CAM approach, one can expand the total wave function with respect to the basis (1.22)

$$\Psi_{l_0\Lambda_0}^{JM}\big(\vec{r},\vec{R}\,\big) = \frac{1}{r}\sum_{l\Lambda} \phi_{l\Lambda,l_0\Lambda_0}^{J\upsilon_0}(r,R) \cdot {}^{\mathrm{I}}X_{l\Lambda}^{JM}\big(\hat{r},\hat{R}\,\big), \tag{1.23}$$

obtaining thus an analogue of the expansion (1.18). Since the basis (1.22) is not complete in the variable R, the resulting radial functions $\phi_{l\Lambda,l_0\Lambda_0}^{J\upsilon_0}(r,R)$ will be R-dependent

[13] denoted as BODY basis II by Morrison (1988) and also used in Lane (1980). Corresponding radial functions are introduced in Chang and Fano (1972, Eq. (24)) as $H_{l\Lambda}^{J\eta}(r,R)$

[14] for rigorous justification of the term containing the Wigner D-function $\mathcal{D}_{k,m}^{j}$ we refer to Appendix A in Chang and Fano (1972)

[15] the factor 4π instead of 8π is just a consequence of the fact that we are considering diatomic targets and therefore the Euler angle γ can be set to zero with impunity reducing thus the "volume of the angular space" to 4π

and it is also necessary to explicitly denote the initial vibrational state υ_0. Radial equations obtainable again by projecting the Schrödinger equation onto the individual basis elements (1.22) take the form (Lane, 1980; Morrison, 1988)

$$\left[-\frac{1}{2}\frac{\mathrm{d}^2}{\mathrm{d}r^2}+\frac{l(l+1)}{2r^2}+\mathbf{H}_{\mathrm{m}}^{(\upsilon)}-E\right]\phi_{l\Lambda,l_0\Lambda_0}^{J\upsilon_0}(r,R)+\sum_{l'\Lambda'}\Big[\big\langle l\Lambda;\,JM\big|\mathbf{V}_{\mathrm{int}}\big|l'\Lambda';\,JM\big\rangle\cdot\delta_{\Lambda,\Lambda'}+$$
$$\big\langle l\Lambda;\,JM\big|\mathbf{H}_{\mathrm{m}}^{(r)}\big|l'\Lambda';\,JM\big\rangle\cdot\delta_{l,l'}\Big]\phi_{l'\Lambda',l_0\Lambda_0}^{J\upsilon_0}(r,R)=0. \tag{1.24}$$

Since the target molecule is assumed to be diatomic, the interaction potential expressed in the molecular body frame is cylindrically symmetric and therefore its matrix elements are diagonal in Λ. Moreover, due to the overall rotational symmetry, they are also diagonal and actually independent on J, M. Similar considerations lead to the conclusion that $\mathbf{H}_{\mathrm{m}}^{(r)}$ is diagonal in J, M, l and independent on M.

Before proceeding to a slightly modified approach, we would like to make a few comments concerning Eq. (1.24)

- the action of the vibrational Hamiltonian $\mathbf{H}_{\mathrm{m}}^{(\upsilon)}$ on the radial functions (1.23) might seem too abstract nevertheless using the spectral decomposition of $\mathbf{H}_{\mathrm{m}}^{(\upsilon)}$ in the harmonic approximation

  $$\mathbf{H}_{\mathrm{m}}^{(\upsilon)}=\sum_{\upsilon}\omega(\upsilon+1/2)\,|\upsilon\rangle\langle\upsilon| \tag{1.25}$$

  easily furnishes in the coordinate R-representation ($\chi_\upsilon(R)$ denote individual vibrational wave functions)

  $$\mathbf{H}_{\mathrm{m}}^{(\upsilon)}\phi_{l\Lambda,l_0\Lambda_0}^{J\upsilon_0}(r,R)=\sum_{\upsilon}\omega(\upsilon+1/2)\int\mathrm{d}R'\,\chi_\upsilon^*(R)\chi_\upsilon(R')\phi_{l\Lambda,l_0\Lambda_0}^{J\upsilon_0}(r,R'). \tag{1.26}$$

  in accordance with third term of Eq. (26) in Chang and Fano (1972).

- complexity of the equations (1.24) can be significantly reduced in the so-called *rigid rotor* approximation, where one supposes that the internuclear distance R is held fixed at its equilibrium value R_e. In that case, we can afford to drop the R-dependence of $\phi_{l\Lambda,l_0\Lambda_0}^{J\upsilon_0}$ and also the initial vibrational label υ_0.

- finally, neglecting the rotational Hamiltonian decouples the equations in Λ, this approximation being known as *body frame fixed nuclei* (BF-FN) theory[16]

- presence of the rotational Λ-coupling $\big\langle l\Lambda;\,JM\big|\mathbf{H}_{\mathrm{m}}^{(r)}\big|l'\Lambda';\,JM\big\rangle$ term has also sort of unpleasant consequences for the asymptotic behavior of the radial functions. Since this term does not depend on r, it is effectively incompatible with the usual asymptotic form defining the scattering matrix. We have thus either to enforce some approximations disregarding this term or to employ some techniques in the frame transformation spirit as discussed below.

• taking $\mathbf{H}_{\mathrm{m}}^{(\upsilon)}$ into account

Farther from the molecule, the interaction potential becomes weaker and therefore the vibrational levels can not be considered as degenerate without impunity. The *vibrational frame transformation* (VFT) discussed in more detail in subsequent section is

[16] on the other hand, the FNO – *fixed nuclear orientation* – approximation amounts to neglecting the rotational Hamiltonian but allowing the molecule to vibrate

essentially a procedure for transition form the previously introduced body frame basis into a new one where one takes the vibrational Hamiltonian $\mathbf{H}_{\mathrm{m}}^{(\upsilon)}$ directly into consideration. Formally, this corresponds to augmenting the set (1.21) by the vibrational Hamiltonian $\mathbf{H}_{\mathrm{m}}^{(\upsilon)}$ yielding thus basis functions of the form

$$|\upsilon l\Lambda;\, JM\rangle \sim {}^{\mathrm{II}}X_{\upsilon l\Lambda}^{JM} \equiv \chi_{\upsilon}(R)\sqrt{\frac{2J+1}{4\pi}}\,\mathcal{D}_{M,\Lambda}^{J}\big(\hat{R}\big)\mathrm{Y}_{l,\,\Lambda}\big(\hat{r}'\big) \tag{1.27}$$

Employing the very same procedure as it has been done in the LAB-CAM and previous body frame approach furnishes coupled differential equations for the radial functions (the channels are in this case labeled by υ, l, Λ in accordance with (1.27))

$$\left[-\frac{1}{2}\frac{\mathrm{d}^2}{\mathrm{d}r^2}+\frac{l(l+1)}{2r^2}-\frac{1}{2}k_{\upsilon}^2\right]\phi_{\upsilon l\Lambda,\upsilon_0 l_0\Lambda_0}^{J}(r,R)+\sum_{\upsilon' l'\Lambda'}\Big[\big\langle \upsilon l\Lambda;\, JM\big|\mathbf{V}_{\mathrm{int}}\big|\upsilon' l'\Lambda';\, JM\big\rangle\cdot\delta_{\Lambda,\Lambda'}+$$
$$\big\langle \upsilon l\Lambda;\, JM\big|\mathbf{H}_{\mathrm{m}}^{(r)}\big|\upsilon' l'\Lambda';\, JM\big\rangle\cdot\delta_{l,l'}\delta_{\upsilon,\upsilon'}\Big]\phi_{\upsilon' l'\Lambda',\upsilon_0 l_0\Lambda_0}^{J}(r,R)=0. \tag{1.28}$$

Similarly as in (1.24), the matrix elements of the rotational Hamiltonian $\mathbf{H}_{\mathrm{m}}^{(r)}$ are diagonal in J, M, υ, l and independent on M, whereas the interaction potential $\mathbf{V}_{\mathrm{int}}$ couples channels differing only in υ, l and its matrix elements are independent on J, M. Channel momentum k_{υ} is again fixed by energy conservation[17]

$$\frac{1}{2}k_{\upsilon}^2 = E-\omega\big(\upsilon+1/2\big). \tag{1.29}$$

1.2.2 Frame transformation

In light of the preceding discussion, it is clear that the laboratory as well as the body frame approach are both convenient in different (mutually exclusive) portions of the $\vec{r}$-space, the former being tailored for description of the "asymptotic" motion of the electron (large r), where the individual angular momenta $\mathbf{j}^2$, $\mathbf{l}^2$ are approximately conserved provided the electron-molecule interaction decays fast enough. On the other hand, as it was already mentioned, the body frame approach is preferable for small r, where, roughly speaking, the interaction term dominates rotational and vibrational effects and one is thus tempted to employ the FN approximation due to the approximate degeneracy of the target (rovibrational) energy levels.

Therefore it might seem natural to profit from the merits of both methods. This is actually the basic idea behind the famous *frame transformation* (FT) method originally introduced in the landmark paper by Chang and Fano (1972). Due to the "partitioning" of the space according to the variable r, this form of the frame transformation is known as *radial frame transformation*. Alternative approaches based on partitioning according to the angular momentum l of the incident electron have been also reported (Collins and Norcross, 1978) and are known as *angular frame transformations* (Morrison, 1983). Physical explanation in this case is based on the observation that for large angular momenta l, the electron is effectively repelled from the molecule due to the centrifugal barrier and thus "feels" predominantly only the long range part of the interaction potential. On the other hand, one can expect that for small l the major role is played by the short range interaction. Therefore it might be reasonable to introduce some boundary angular momentum value l_{c} such that for $l < l_{\mathrm{c}}$, the $\mathcal{S}$-matrix elements can be with sufficient accuracy computed in the body frame formalism whereas for $l > l_{\mathrm{c}}$, these elements could be rendered successfully in the laboratory frame approach.

[17] harmonic approximation is presupposed

Frame transformation according to Chang and Fano

In the original treatment (Chang and Fano, 1972), the interaction area is effectively divided into three parts as depicted schematically in Figure 1.1.

1. in region I, *i.e.*, for $r \in [0, r_{\mathrm{v}}]$, where the scattered electron is very close to the molecule, the strongly attractive interaction potential dominates other terms in the Hamiltonian (1.11) washing out the energy dependency of the target states (υ, j). The appropriate set of equations in this situation is therefore (1.24), where one employs the FN approximation, *i.e.*, the rovibrational Hamiltonian is disregarded.

2. in region II, *i.e.*, for $r \in [r_{\mathrm{v}}, r_{\mathrm{r}}]$, the dependence of the interaction potential on the internuclear distance R will be much weaker. As a consequence, the radial equations (1.28) can be considered as approximately decoupled in υ. On the other hand, the upper boundary of region II is chosen in such a way that the rotational Hamiltonian can be still neglected (as compared to the interaction potential)

3. finally, region III, $r \in [r_{\mathrm{r}}, \infty]$, representing the "asymptotic region" requires to take the rotational Hamiltonian fully into account and the appropriate treatment is thus the laboratory frame approach governed by Eq. (1.19).

Transition between regions I→II and II→III is known as *vibrational frame transformation* (VFT) and *rotational frame transformation* (RFT), respectively. Alternatively, one might join regions I and II into one domain by setting $r_{\mathrm{v}} = r_{\mathrm{r}}$ performing thus the VFT and RFT simultaneously.

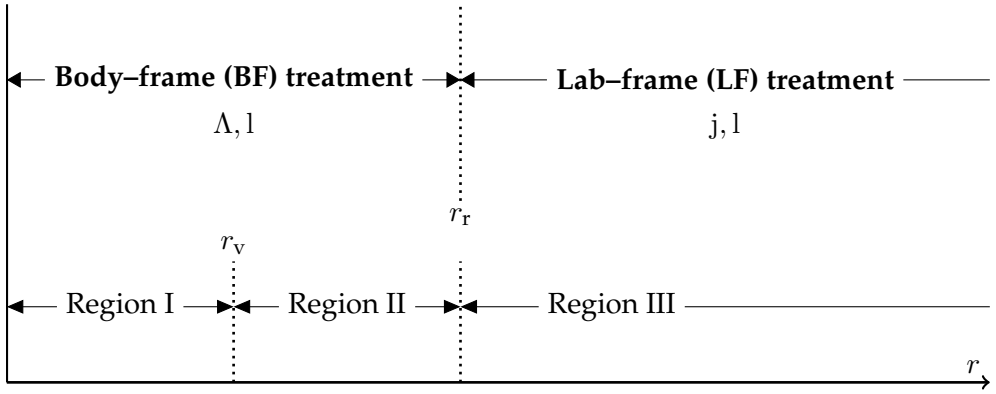

Figure 1.1: Schematic representation of the r-partitioning used in the frame transformation theory. Physical meaning of individual regions is discussed in the text.

Rotational frame transformation (RFT)

The rotational frame transformation melts essentially down to the question how to transform between angular parts of the respective laboratory (1.17) and body frame (1.27) bases. More general derivation applicable also to diatomic molecules in non-Σ electronic states can be found in Appendix of Chang and Fano (1972), nevertheless in

case of Σ electronic states and ignoring parity designation it is possible to proceed as

$$\begin{aligned}
\mathcal{Y}^{J\,M}_{j\,l}\big(\hat{R},\,\hat{r}\big) &\overset{(1.17)}{=} \sum_{m_j,m_l} (jl\,m_j m_l|\;J\,M)\,\mathrm{Y}_{j,\,m_j}\big(\hat{R}\big)\mathrm{Y}_{l,\,m_l}\big(\hat{r}\,\big) = \\
&= \sum_k \sqrt{\frac{2j+1}{4\pi}}\mathrm{Y}_{l,\,k}\big(\hat{r}'\big) \sum_{m_j,m_l} (jl\,m_j m_l|\;J\,M)\;\mathcal{D}^{j}_{m_j,0}\big(\hat{R}\big)\,\mathcal{D}^{l}_{m_l,k}\big(\hat{R}\big) = \\
&= \sum_k \sqrt{\frac{2j+1}{4\pi}}\mathrm{Y}_{l,\,k}\big(\hat{r}'\big) \sum_{m_j,m_l}\sum_{L,\mu} \mathcal{D}^{L}_{\mu,k}\big(\hat{R}\big)\,(jl\,m_j m_l|\;J\,M)\times \\
&\qquad\qquad \times (jl\,m_j m_l|\;L\,\mu)\,(jl\,0k|\;L\,k) = \\
&= \sum_k \sqrt{\frac{2j+1}{4\pi}}\,(jl\,0k|\;L\,k)\,\mathrm{Y}_{l,\,k}\big(\hat{r}'\big)\,\mathcal{D}^{J}_{M,k}\big(\hat{R}\big) \\
&= \sum_k \sqrt{\frac{2j+1}{2J+1}}\,(jl\,0k|\;L\,k)\,\mathrm{Y}_{l,\,k}\big(\hat{r}'\big)\sqrt{\frac{2J+1}{4\pi}}\,\mathcal{D}^{J}_{M,k}\big(\hat{R}\big).
\end{aligned} \tag{1.30}$$

Fleeting glance at (1.30) accompanied by comparison with (1.27) reveals that the transformation coefficients $A^{J\Lambda}_{jl}$ connecting "angular parts" of (1.17) and (1.27) can be identified as

$$\begin{aligned}
A^{J\Lambda}_{jl} \equiv \sqrt{\frac{2j+1}{2J+1}}\,(jl\,0\Lambda|\;J\,\Lambda) &= \sqrt{2j+1}\begin{pmatrix} j & l & J \\ 0 & \Lambda & -\Lambda \end{pmatrix}(-1)^{j-l-\Lambda} \\
&= \sqrt{2j+1}\begin{pmatrix} l & J & j \\ -\Lambda & \Lambda & 0 \end{pmatrix}(-1)^{J-\Lambda},
\end{aligned} \tag{1.31}$$

in agreement with Morrison (1988). It is worth noting that the coefficients $A^{J\Lambda}_{jl}$ as given[18] by Chang and Fano (1972) differ at first sight from (1.31). The culprit is hidden in the fact that Chang and Fano (1972) use slightly different angular laboratory frame basis, namely

$$\mathcal{Y}^{J\,M}_{j\,l}\big(\hat{\rho},\,\hat{r}\big) \leftarrow \sum_{m_j,m_l} (lj\,m_l m_j|\;J\,M)\,\mathrm{Y}_{j,\,m_j}\big(\hat{\rho}\big)\mathrm{Y}_{l,\,m_l}\big(\hat{r}\big),$$

which is seen by employing Eq. (B.1) to differ from (1.17) by a phase factor $(-1)^{j+l+J}$. Multiplying Chang and Fano's coefficients by this factor yields indeed Eq. (1.31). In Fabrikant (1983*a*), the author claims that the Chang and Fano (1972)'s coefficients are mangled by improper inclusion of a $(-1)^j$ factor, nevertheless we haven't found a mistake in the derivation and (1.31) seems to correspond also with transformation prescription used by Chandra (1975); Clark (1979) or Huo and Gianturco (1995).

1.3 Adiabatic approximation

The approach known in the literature as *adiabatic approximation* was adapted for scattering applications originally by Chase in his eminent paper (Chase, 1956), where he investigated approximative description of collisions involving composite targets.

For detailed derivation we refer to the original work (Chase, 1956), nevertheless the basic idea underlying this method is actually very straightforward. One supposes that the target is described by Hamiltonian $\mathbf{H}_\mathrm{T}$ defining a set of energy eigenvalues and corresponding eigenvectors

$$\mathbf{H}_\mathrm{T}\Psi_\Gamma(\omega) = \epsilon_\Gamma\,\Psi_\Gamma(\omega). \tag{1.32}$$

[18] coefficient matrix $U^{(jJ\eta)}_{j\Lambda}$ defined by Eq. (7) in Chang and Fano (1972),matrix $A^{J\Lambda}_{jl}$ with no parity η designation corresponds to $U^{(jJ+)}_{j\Lambda} + U^{(jJ-)}_{j\Lambda}$

For the sake of notation, the target internal coordinates were subsumed into a collective symbol ω. The symbol Γ introduced in (1.32) encompasses all quantum numbers uniquely determining a particular eigenstate.

The collisional process between the incident particle the position of which is denoted by $\vec{r}$ and the target is for fixed value of ω formally equivalent to scattering in a potential $V(\vec{r},\omega)$. The incident particle with momentum $\vec{k}$ is in this case described by a wave function $w_{\vec{k}}(\vec{r};\,\omega)$ parametrically dependent on ω. From asymptotic behavior of $w_{\vec{k}}(\vec{r};\,\omega)$, one can extract information about corresponding scattering amplitude $f(\theta,\phi;\omega)$, which is called by Chase (1956) as "ω-modulated" for its parametric dependence[19] on ω. Since this amplitude is evaluated for fixed target coordinates, it contains of course no information about possible inelastic $\Gamma \to \Gamma'$ transitions of the target. However, if one approximates the total wave function of the system in channel Γ in a product-like form

$$w_{\vec{k}_\Gamma}(\vec{r};\,\omega)\Psi_\Gamma(\omega), \tag{1.33}$$

then an approximation to the exact scattering amplitude $f_{\Gamma\Gamma'}(\theta,\phi)$ corresponding to the $\Gamma \to \Gamma'$ transition can be expressed as

$$f_{\Gamma\Gamma'}(\theta,\phi) \approx -\sqrt{2\pi}\int \mathrm{d}\omega\; \Psi^*_{\Gamma'}\Big(\int \mathrm{d}\vec{r}\,\mathrm{e}^{-\mathrm{i}\vec{k}_{\Gamma'}\cdot\vec{r}}\,V(\vec{r},\omega)\,w_{\vec{k}_\Gamma}(\vec{r};\,\omega)\Big)\Psi_\Gamma(\omega). \tag{1.34}$$

One immediately observes that the integral (1.34) over $\vec{r}$ is apart from a multiplicative factor equal to the ω-modulated amplitude $f(\theta,\phi;\,\omega)$ provided that the channel momentum $\vec{k}_{\Gamma'}$ were replaced by momentum in channel Γ, *i.e.*, $\vec{k}_\Gamma$. The final prescription given by Chase for the approximative $\Gamma \to \Gamma'$ scattering amplitude is thus

$$f_{\Gamma\Gamma'}(\theta,\phi) \approx {}^{\mathrm{ad}}f_{\Gamma\Gamma'}(\theta,\phi) \stackrel{\mathrm{def}}{=} \int \mathrm{d}\omega\; \Psi^*_{\Gamma'}(\omega) f(\theta,\phi;\,\omega)\Psi_\Gamma(\omega). \tag{1.35}$$

In other words, this result is formally equivalent to the statement that the approximative amplitude ${}^{\mathrm{ad}}f$ is rendered by averaging the ω-modulated amplitude $f(\theta,\phi;\,\omega)$ over the space of target coordinates. From the amplitude (1.35), the corresponding differential cross-section results straightforwardly

$$\left.\frac{\mathrm{d}\sigma}{\mathrm{d}\Omega}\right|_{\Gamma\to\Gamma'} = \frac{k_{\Gamma'}}{k_\Gamma}\Big|\,{}^{\mathrm{ad}}f_{\Gamma\Gamma'}(\theta,\phi)\,\Big|^2, \tag{1.36}$$

where the kinematic factor $k_{\Gamma'}/k_\Gamma$ has been appended additionally in order to mimic desired threshold ($k_{\Gamma'} \to 0^+$) behavior of Eq. (1.36).

To sum up, replacement of the exact amplitude $f_{\Gamma\Gamma'}$ by ${}^{\mathrm{ad}}f_{\Gamma\Gamma'}$ is essentially based on two assumptions – expressing the total wave function in a product form (1.33) and the premise of negligible target level spacing $\vec{k}_\Gamma \approx \vec{k}_{\Gamma'}$.

The precise validity conditions of the adiabatic approximation are quite subtle to formulate. However, one feels directly from the derivation above that this procedure could work well if the ω-modulated amplitude is modulated only "weakly", which is in turn equivalent to the rather vague requirement that the characteristic interaction time is much smaller as compared to the typical period of motion of the target.[20] Formally, this condition is a consequence of the replacement of $\vec{k}_{\Gamma'}$ by a vector $\underline{\vec{k}}_{\Gamma'}$ having the same direction as $\vec{k}_{\Gamma'}$ but with magnitude k_Γ in the exponential term in (1.35) to wit

$$\begin{aligned}\mathrm{e}^{-\mathrm{i}\vec{k}_{\Gamma'}\cdot\vec{r}} &= \mathrm{e}^{-\mathrm{i}\underline{\vec{k}}_\Gamma\cdot\vec{r}}\cdot\mathrm{e}^{-\mathrm{i}\left(\vec{k}_{\Gamma'}-\underline{\vec{k}}_\Gamma\right)\cdot\vec{r}}\\ &\approx \mathrm{e}^{-\mathrm{i}\underline{\vec{k}}_\Gamma\cdot\vec{r}}\cdot\Big(1-\mathrm{i}\big(\vec{k}_{\Gamma'}-\underline{\vec{k}}_\Gamma\big)\cdot\vec{r}\Big).\end{aligned} \tag{1.37}$$

[19] this parametric dependence is in $f(\theta,\phi;\,\omega)$ underlined by the convention that ω appears after a semicolon

[20] or equivalently, as pointed out by Chase (1956), that the average width of the colliding particle wave packet is much larger than average target level spacing

A necessary condition is thus $\left|\vec{k}_{\Gamma'} - \underline{\vec{k}}_{\Gamma}\right| R \ll 1$, with R denoting characteristic size of the interaction area. Conservation of the total energy

$$\frac{1}{2}\vec{k}_{\Gamma'}^2 + \epsilon_{\Gamma'} = \frac{1}{2}\underline{\vec{k}}_{\Gamma}^2 + \epsilon_{\Gamma}$$

enables us to rewrite the momentum difference $\left|\vec{k}_{\Gamma'} - \underline{\vec{k}}_{\Gamma}\right|$ as

$$\left|\vec{k}_{\Gamma'} - \underline{\vec{k}}_{\Gamma}\right| = 2\frac{\epsilon_{\Gamma'} - \epsilon_{\Gamma}}{k_{\Gamma'} + k_{\Gamma}},$$

thus rendering the above stated validity condition in the form

$$2R\frac{\epsilon_{\Gamma'} - \epsilon_{\Gamma}}{k_{\Gamma'} + k_{\Gamma}} \ll 1. \tag{1.38}$$

Since the passage time of the incident electron with average momentum k through the interaction area is roughly given as R/k and the target period of motion can be estimated as being inversely proportional to the level spacing, *i.e.*, $1/(\epsilon_{\Gamma'} - \epsilon_{\Gamma})$, one immediately sees that condition (1.38) is indeed equivalent to the adiabatic character of the investigated collision process.

More care has to be taken regarding validity of Eq. (1.38) near excitation threshold, *i.e.*, if the outgoing momentum $k_{\Gamma'}$ is very small. In that case, more relevant criterion is to require the relative error of the approximation introduced in Eq. (1.37) to be small instead of the condition on the absolute error leading to Eq. (1.38). Therefore, Chase (1956) imposes following relation

$$R \cdot \left|\vec{k}_{\Gamma'} - \underline{\vec{k}}_{\Gamma}\right| \ll R \cdot k_{\Gamma}.$$

Employing Eq. (1.38) finally yields

$$2\frac{\epsilon_{\Gamma'} - \epsilon_{\Gamma}}{(k_{\Gamma'} + k_{\Gamma}) \cdot k_{\Gamma'}} \ll 1, \tag{1.39}$$

which reveals explicitly that the adiabatic approximation is expected to break down close to the threshold $k_{\Gamma'} \to 0$.

It is probably hardly viable to obtain generally applicable criterion regarding validity of the adiabatic approximation and its use has to be therefore justified in each particular case separately. However, several numerical studies dealing with this topic have been published in the past. Chang and Temkin (1970) investigated rigid-rotor rotational excitations of H_2 induced by electron impact in the framework of the adiabatic approximation. The authors argue that this approach is justifiable for electron incident energies E satisfying

$$\frac{E}{\Delta\epsilon} \geq 1.65, \tag{1.40}$$

with $\Delta\epsilon$ denoting the excitation energy of particular rotational transition. A comparative numerical study of the adiabatic approximation with close-coupling calculations modeling rovibrational excitations in case of e^-–H_2 scattering has been given by Morrison, Feldt and Austin (1984); Morrison, Feldt and Saha (1984), where the authors find that the percent error of the total scattering cross-section for pure rotational transitions at incident energies close to the lower bound (1.40) is typically around 10-20% as indicated in Figure 1.2. More importantly, results for vibrational excitations indicate that the relative error of the adiabatic approximation is in order of units even for energies exceeding the threshold several times. This behavior is probably closely linked with the fact that "approximating" target vibrational states as being energetically degenerate is far less justifiable than in case of pure rotational excitations.

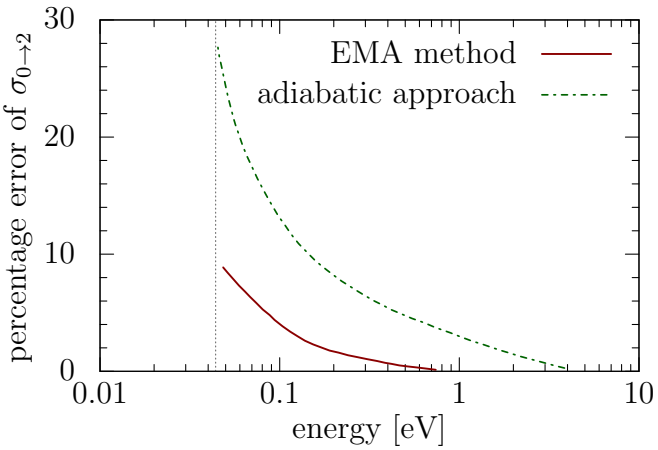

Figure 1.2: Comparison of the adiabatic approach and Energy modified adiabatic method of Nesbet (1979) with laboratory frame static exchange close coupling calculations as reported by Morrison, Feldt and Austin (1984). The percentage error of the excitation cross-section $0 \to 2$ is displayed as a function of the incident energy. Dotted vertical line visualizes the excitation threshold.

1.4 Application to rotational excitations

In the following, the ideas of the preceding two sections are applied to theoretical investigation of electron-molecule scattering processes where we take into account merely rotational excitations of the target molecule, described in the Born-Oppenheimer approximation, confining us thus to low-energy region such that the kinetic energy of the incident electron is below the first vibrational (and therefore of course also electronic) threshold.

1.4.1 Laboratory frame treatment

In order to describe the rotational excitations in the laboratory frame of reference, where the molecule is allowed to rotate freely, we assume the rigid rotor approximation discussed in more detail in Appendix E. In this framework, one is led to a simplified form of the Hamiltonian (1.11), namely

$$\mathbf{H} = -\frac{1}{2}\nabla^2_{\vec{r}} + \mathbf{H}_{\mathrm{rot}} + \mathbf{V}_{\mathrm{int}}\left(r, \theta'\right), \tag{1.41}$$

where $\vec{r}$ specifies location of the incident[21] electron, $\mathbf{H}_{\mathrm{rot}}$ is the rotational Hamiltonian and finally $\mathbf{V}_{\mathrm{int}}$ represents the interaction potential, to the more thorough investigation of which is devoted Chapter 2. Since our computational applications of laboratory frame treatment for description of rotational excitations of small molecules were limited to diatomics, we shall confine ourselves in the following discussion also to this case for which the rotational Hamiltonian $\mathbf{H}_{\mathrm{rot}}$ given by (E.1) is especially simple

$$\mathbf{H}_{\mathrm{rot}}\mathrm{Y}_{j,m_j}\big(\alpha,\,\beta\big) = B\,j(j+1)\mathrm{Y}_{j,m_j}\big(\alpha,\,\beta\big), \tag{1.42}$$

with $\hat{\rho} \equiv (\alpha,\,\beta)$ specifying the orientation of the molecular axis and B standing for the rotational constant of the target molecule. Decomposition of the plane wave representing the incident electron into spherical harmonics allows to label respective channels in this setting by quantum numbers (j, l) with l denoting the angular momentum of the electron.

[21] θ' determines the angle between molecular axis and the vector $\vec{r}$

As proposed already decades ago (Arthurs and Dalgarno, 1960), the wave function corresponding to the total angular momentum J (and its space fixed projection M) can be then chosen as

$$\Psi_{jl}^{JM}(\vec{r},\hat{\rho}) = \frac{1}{r}\sum_{j',l'} {}^{J}u_{j'l'}^{j\,l}(r)\mathcal{Y}_{j'\,l'}^{J\,M}(\hat{r},\,\hat{\rho}). \tag{1.43}$$

The angular part conforming to the LAB-CAM treatment of Subsection 1.2.1 is constructed in order to ensure conservation of the total angular momentum

$$\mathcal{Y}_{j\,l}^{J\,M}(\hat{r},\,\hat{\rho}) = \sum_{m_j,m_l} (jl\,m_j m_l|\;J\,M)\,\mathrm{Y}_{j,\,m_j}(\hat{\rho})\mathrm{Y}_{l,\,m_l}(\hat{r}). \tag{1.44}$$

Substituting (1.43) into the Schrödinger equation and projecting out the angular part (1.44) of the wave function readily yields a coupled set of differential equations for the radial ${}^{J}u_{j'l'}^{j\,l}$ components[22]

$$\left[\frac{\mathrm{d}^2}{\mathrm{d}r^2} - \frac{l'(l'+1)}{r^2} - k_{j'}^2\right] {}^{J}u_{j'l'}^{j\,l}(r) = 2\sum_{j'',l''} \left\langle j''l'';\;JM\right|\mathbf{V}_{\mathrm{int}}\left|j'l';\;JM\right\rangle {}^{J}u_{j''l''}^{j\,l}(r). \tag{1.45}$$

The channel momentum k_j entering (1.45) is determined naturally by conservation of the total energy

$$\frac{1}{2}k_{j'}^2 = E - Bj'(j'+1). \tag{1.46}$$

It is worth noting that the coupling matrix element containing the interaction potential should be understood as a function of r. More explicitly stated, one has

$$\left\langle j'l';\;JM\right|\mathbf{V}_{\mathrm{int}}\left|jl;\;JM\right\rangle = \int \mathrm{d}\hat{r}\mathrm{d}\hat{\rho}\;\mathcal{Y}_{j'\,l'}^{JM*}\mathbf{V}_{\mathrm{int}}\,(r,\hat{r},\hat{\rho})\,\mathcal{Y}_{j\,l}^{J\,M}. \tag{1.47}$$

This form of the potential matrix element automatically reflects the fact – stemming from overall rotational invariance – that the set of equations (1.45) decouples[23] in J and M and can be therefore solved for each J independently offering thus the possibility of an efficient parallel numerical implementation as discussed in Section 1.5.

The solution of (1.45) is uniquely determined by prescribing asymptotic conditions[24] for $r \to \infty$. This is usually done (Arthurs and Dalgarno, 1960; Crawford and Dalgarno, 1971) in complex domain, where one arrives in this way to the $\mathcal{S}$-matrix and consequently the $\mathcal{T}$-matrix. If we restrict ourselves to the discussion of open channels, then from the computational point of view it might be more convenient to formulate the asymptotic behavior in the real domain (Chandra, 1977) as

$${}^{J}u_{j'l'}^{j\,l}(r) \xrightarrow{r\to\infty} \frac{1}{\sqrt{k_{j'}}}\left[\sin\left(k_{j'}r - l'\frac{\pi}{2}\right)\delta_{j'l',jl} + \cos\left(k_{j'}r - l'\frac{\pi}{2}\right){}^{J}\mathcal{K}_{j'l',jl}\right]. \tag{1.48}$$

This equation defines the $\mathcal{K}$-matrix, the connection of which[25] with the $\mathcal{S}$- and $\mathcal{T}$-matrix can be easily deduced

$${}^{J}\mathcal{T} = {}^{J}\mathcal{S} - \mathcal{I} = -2\,{}^{J}\mathcal{K}\cdot\left(i + {}^{J}\mathcal{K}\right)^{-1}. \tag{1.49}$$

[22] in Arthurs and Dalgarno (1960), there is probably a misprint concerning the order of indices in the potential coupling term. Eq. (1.45) is in agreement with Crawford and Dalgarno (1971)

[23] actually it is independent on M

[24] apart from the natural zero boundary condition at the origin

[25] The $\mathcal{T}$-matrix in Chandra (1977) has opposite sign than in Crawford and Dalgarno (1971). We follow the convention of Chandra (1977). For other frequently used conventions in scattering theory and their possible consequences we refer to an excellent overview given by Morrison and Feldt (2007).

The $\mathcal{T}$-matrix contains essentially all information about the scattering process. Some extensive use of Racah algebra based on formulae presented in Appendix B leads finally to the relation for differential cross-section corresponding to the $j \to j'$ rotational transition

$$\left.\frac{\mathrm{d}\sigma}{\mathrm{d}\Omega}\right|_{j\to j'} = \frac{1}{4k_j^2}\sum_{\lambda} \mathrm{A}_\lambda\left(j \to j'\right)\mathrm{P}_\lambda(\cos\theta), \tag{1.50}$$

with

$$\begin{aligned}\mathrm{A}_\lambda\left(j \to j'\right) = \frac{(-1)^{j'-j}}{2j+1}\sum_{J_1,J_2}\sum_{l_1,l_2}\sum_{l_1',l_2'} &\mathcal{Z}\left(l_1J_1,\, l_2J_2;\, jL\right)\cdot \\ &\cdot \mathcal{Z}\left(l_1'J_1,\, l_2'J_2;\, j'L\right)\mathcal{T}^{J_1^*}_{j'l_1',jl_1}\mathcal{T}^{J_2}_{j'l_2',jl_2},\end{aligned} \tag{1.51}$$

containing the algebraic *Persival-Seaton* (Percival and Seaton, 1957) $\mathcal{Z}$-coefficients defined as

$$\begin{aligned}\mathcal{Z}\left(ab,\, cd;\, ef\right) \equiv (-1)^{(f-a+c)/2}(-1)^{b+d}&\left[(2a+1)(2b+1)(2c+1)(2d+1)(2f+1)\right]^{1/2} \\ &\times \begin{pmatrix} a & c & f \\ 0 & 0 & 0 \end{pmatrix}\begin{Bmatrix} a & b & e \\ d & c & f \end{Bmatrix}.\end{aligned} \tag{1.52}$$

For evaluation of the integral cross-section $\sigma_{j\to j'}$, just the coefficient A_0 in (1.51) is needed due to the mutual orthogonality of the Legendre polynomials. One therefore obtains (Crawford and Dalgarno, 1971)

$$\begin{aligned}\sigma_{j\to j'} &= \frac{\pi}{k_j^2}\mathrm{A}_0\left(j \to j'\right) = \\ &= \frac{\pi}{k_j^2(2j+1)}\sum_{J=0}^{\infty}(2J+1)\sum_{l,l'}\left|{}^J\mathcal{T}_{j'l',jl}\right|^2.\end{aligned} \tag{1.53}$$

Note that as regards the backward scattering cross-section discussed extensively in Chapter 4, only A_λ's with odd λ are required since the "angular Jacobian" containing term $\sin\theta$ is itself an odd function of θ.

Potential matrix elements

In practical application, we need to be able to efficiently evaluate the potential matrix elements (1.47). Along the lines of the methods based on *single center expansion* (SCE) (Faisal, 1970) approach, we might therefore try to expand the potential into Legendre polynomials

$$\mathbf{V}_{\mathrm{int}}\left(r, \hat{r}, \hat{\rho}\right) = \sum_{\lambda=0}^{\infty} V_\lambda(r)\mathrm{P}_\lambda(\cos\theta), \tag{1.54}$$

in the variable $\cos\theta \equiv \hat{r}\cdot\hat{\rho}$, *i.e.*, in the cosine of the angle spanned by the molecular axis and unit vector pointing in the direction of the incident electron.

Although (1.54) represents a general form of the interaction potential only for diatomic molecules, we shall assume its validity in the following also in the symmetric top case in order to obtain a direct connection between the formulae obtained in both settings.

By inserting (1.44) and (1.54) into (1.47) and performing some rather lengthy algebra one arrives (Brink and Satchler, 1994; Child, 2010) at the relation[26]

$$\begin{aligned}\left\langle j'l';\, JM\right|\mathbf{V}_{\mathrm{int}}\left|jl;\, JM\right\rangle = \sum_{\lambda=0}^{\infty} V_\lambda(r)(-1)^{J-\lambda}\sqrt{[\,j\,][\,j'\,][\,l\,][\,l'\,]}\cdot \\ \cdot \begin{pmatrix} j & j' & \lambda \\ 0 & 0 & 0 \end{pmatrix}\begin{pmatrix} l & l' & \lambda \\ 0 & 0 & 0 \end{pmatrix}\begin{Bmatrix} j' & l' & J \\ l & j & \lambda \end{Bmatrix}.\end{aligned} \tag{1.55}$$

1.4.2 Born approximation in the laboratory frame

Further insight into the above stated approach can be obtained if one computes the Born approximation to the total (1.53) and differential (1.50) excitation cross-sections directly without employing the partial wave expansion. The incident electron is described by a pure plane wave corresponding to the initial momentum $\vec{k}_i$. In order to specify the rotational state of the target molecule, we shall use slightly more general notation, for the explicit form of the rotational wave function depends on the type of the target rigid rotor. The i^{th} target rotational state will be thus denoted as $\Gamma_i(\omega)$, where $\omega = (\alpha, \beta, \gamma)$ is the set of Euler's angles describing the orientation of the target.[27] The unit vector $\rho = (\alpha, \beta) \equiv (\phi_{\mathrm{m}}, \theta_{\mathrm{m}})$ then determines the orientation of the molecular axis in the laboratory frame of reference. At large collision distance, the dynamics of the electron and the target is not coupled and therefore the wave function of the composite system will be given as a product of individual terms as

$$X_i\big(\omega, \vec{r}\,\big) \equiv \Gamma_i(\omega)\cdot \mathrm{e}^{\mathrm{i}\vec{k}_i\cdot\vec{r}}, \tag{1.56}$$

and we are interested in evaluation of the scattering amplitude corresponding to a transition to the final state

$$X_f\big(\omega, \vec{r}\,\big) \equiv \Gamma_f(\omega)\cdot \mathrm{e}^{\mathrm{i}\vec{k}_f\cdot\vec{r}}. \tag{1.57}$$

Introducing the final momentum $\vec{k}_f$ and momentum transfer

$$\vec{K} \equiv \vec{k}_i - \vec{k}_f,$$

and inserting initial and final states into the well-known (Gell-Mann and Goldberger, 1953) formula for Born scattering amplitude yields

$$f_{i\to f}\big(\vec{k}_i \to \vec{k}_f\big) = -\frac{1}{2\pi}\sum_{\lambda=0}^{\infty}\int \mathrm{d}\vec{r}\,\mathrm{e}^{\mathrm{i}\vec{K}\cdot\vec{r}}\,V_\lambda(r)\int \mathrm{d}\omega\,\Gamma_f^*(\omega)\Gamma_i(\omega)\mathrm{P}_\lambda(\hat{r}\cdot\hat{\rho}), \tag{1.58}$$

where we have already employed the "angular" decomposition of the interaction potential (1.54). Expressing the exponential term containing the momentum transfer $\vec{K}$ in terms of spherical harmonics according to (D.6) and restating $\mathrm{P}_\lambda(\hat{r}\cdot\hat{\rho})$ as a product of two spherical harmonics in $\hat{\rho}$ and $\hat{r}$ via (B.10) furnishes further simplification in the form

$$\begin{aligned}f_{i\to f}\big(\vec{k}_i \to \vec{k}_f\big) = -2\sum_{\lambda=0}^{\infty}\mathrm{i}^\lambda\sum_{\mu=-\lambda}^{\lambda}\Big[\int_0^\infty \mathrm{d}r\,r^2 V_\lambda(r) j_\lambda(Kr)\Big]\mathrm{Y}^*_{\lambda,\,\mu}\big(\hat{K}\big)\frac{4\pi}{2\lambda+1}\times \\ \times\int \mathrm{d}\omega\,\Gamma_f^*(\omega)\mathrm{Y}_{\lambda,\,\mu}\big(\hat{\rho}\big)\Gamma_i(\omega).\end{aligned} \tag{1.59}$$

In order to perform the angular integration over $\mathrm{d}\omega$, we need to know of course the explicit form of Γ_i, Γ_f. In the following, we will discuss two particular cases, namely diatomic and symmetric top molecules considering interaction potential of the form (1.54).

[26] in order to compress slightly the notation we have introduced the symbol $[\,x\,] \equiv 2x+1$

[27] as in the preceding subsection, we are assuming rigid rotor model

Diatomic molecules

The rotational wave functions labeled by quantum numbers j, m of a diatomic molecule coincide with spherical harmonics $\mathrm{Y}_{j,m}$. Thus the initial and final state can be relabeled as $\Gamma_i(\omega) \equiv \mathrm{Y}_{j,m}(\hat{\rho})$ and $\Gamma_f(\omega) \equiv \mathrm{Y}_{j',m'}(\hat{\rho})$, respectively. Inserting these expressions into (1.59) and performing the integration using (B.11), one finally obtains

$$\begin{aligned} f_{jm\to j'm'}(\vec{k}_i \to \vec{k}_f) = -2(-1)^{m'}\sqrt{(2j+1)(2j'+1)}\cdot \\ \cdot \sum_{\lambda=0}^{\infty} \mathrm{i}^{\lambda}\Big[\int_0^{\infty} \mathrm{d}r\, r^2\, V_\lambda(r) j_\lambda(Kr)\Big] \sum_{\mu=-\lambda}^{\lambda} \mathrm{Y}^*_{\lambda,\mu}(\hat{K})\times \\ \times \sqrt{\frac{4\pi}{2\lambda+1}} \begin{pmatrix} j & j' & \lambda \\ m & -m' & \mu \end{pmatrix} \begin{pmatrix} j & j' & \lambda \\ 0 & 0 & 0 \end{pmatrix}. \end{aligned} \tag{1.60}$$

Experimentally measurable quantity is however the differential cross-section corresponding to the $j \to j'$ rotational transition. This is expressible from (1.60) by taking square of the modulus, summing over m' and averaging over m, using (B.7a) to simplify the final result in accordance with Crawford et al. (1967)

$$\begin{aligned} \left.\frac{\mathrm{d}\sigma}{\mathrm{d}\Omega}\right|_{j\to j'} = \frac{4k'}{k}(2j'+1)\sum_{\lambda=0}^{\infty}\left[\int_0^{\infty}\mathrm{d}r\, r^2\, V_\lambda(r) j_\lambda(Kr)\right]^2 \cdot \\ \cdot \frac{1}{2\lambda+1}\begin{pmatrix} j & j' & \lambda \\ 0 & 0 & 0 \end{pmatrix}^2. \end{aligned} \tag{1.61}$$

Symmetric top molecules

The computational procedure is slightly more complicated in this case, since the rotational states of a symmetric top molecule are described by Wigner $\mathcal{D}^j_{m,k}$ functions introduced in (E.2)

$$\Gamma_i(\omega) \equiv \sqrt{\frac{2J+1}{8\pi^2}}\,\mathcal{D}^J_{M,K}(\omega)\,, \tag{1.62a}$$

$$\Gamma_f(\omega) \equiv \sqrt{\frac{2J'+1}{8\pi^2}}\,\mathcal{D}^{J'}_{M',K'}(\omega)\,. \tag{1.62b}$$

However, plugging these Γ_i, Γ_f into (1.59) and simplifying consequently the angular integrals using Eqs. (E.21) and (E.22) yields after some effort the expression

$$\begin{aligned} f^{J'K'M'}_{JKM}(\vec{k}_i \to \vec{k}_f) = -2\sqrt{(2J+1)(2J'+1)}(-1)^{K'-M'}\sum_{\lambda=0}\mathrm{i}^{\lambda}\sqrt{\frac{4\pi}{2\lambda+1}} \\ \sum_{\mu=-\lambda}^{\lambda}\mathrm{Y}^*_{\lambda,\mu}(\hat{K})\cdot\left[\int_0^{\infty}\mathrm{d}r\, r^2\, V_\lambda(r) j_\lambda(Kr)\right]\begin{pmatrix} J & J' & \lambda \\ M & -M' & \mu \end{pmatrix}\begin{pmatrix} J & J' & \lambda \\ K & -K' & 0 \end{pmatrix}, \end{aligned} \tag{1.63}$$

which in the case of a degenerate symmetric top (*i.e.*, in the formal limit $K, K' \to 0$) coincides with the diatomics formula (1.60). Differential cross-section for the $JK \to J'K'$ transition is computed as in the preceding case by taking squared modulus of (1.63), summing over M' and averaging over M

$$\begin{aligned} \left.\frac{\mathrm{d}\sigma}{\mathrm{d}\Omega}\right|_{JK\to J'K'} = \frac{4k'}{k}(2J'+1)\sum_{\lambda=0}^{\infty}\left[\int_0^{\infty}\mathrm{d}r\, r^2 V_\lambda(r) j_\lambda(Kr)\right]^2 \cdot \\ \cdot \frac{1}{2\lambda+1}\begin{pmatrix} J & J' & \lambda \\ K & -K & 0 \end{pmatrix}^2 \delta_{K,K'}. \end{aligned} \tag{1.64}$$

Specialization to the point dipole potential

Especially important is the case of a point dipole interaction, *i.e.*, when the potential expansion (1.54) contains only single term $\lambda = 1$ to wit

$$V_1(r) \approx -\frac{D}{r^2}.$$

Since $\int_0^\infty j_1(Kr)\,\mathrm{d}r = 1/K$, Eqs. (1.61) and (1.64) are amenable to further simplification. With $\epsilon \equiv k'/k \leq 1$ one gets for diatomic molecules

$$\left.\frac{\mathrm{d}\sigma}{\mathrm{d}\Omega}\right|_{j\to j'} = \frac{4D^2}{3k^2}(2j'+1)\begin{pmatrix} j & j' & 1 \\ 0 & 0 & 0 \end{pmatrix}^2 \frac{\epsilon}{1+\epsilon^2-2\epsilon\cos\theta}, \tag{1.65}$$

and for symmetric tops

$$\left.\frac{\mathrm{d}\sigma}{\mathrm{d}\Omega}\right|_{JK\to J'K'} = \frac{4D^2}{3k^2}(2J'+1)\begin{pmatrix} J & J' & 1 \\ K & -K & 0 \end{pmatrix}^2 \frac{\epsilon}{1+\epsilon^2-2\epsilon\cos\theta}\ \delta_{K,K'}. \tag{1.66}$$

In order to obtain the corresponding angular coefficients A_λ introduced in (1.50), it is necessary to expand (1.65) or (1.66) into Legendre polynomials. At first sight, this task might seem quite formidable. As far as we know, a simple derivation is not available in the literature and therefore we would like to present one possible approach based on neat utilization of the Legendre polynomials recurrence properties (Abramowitz and Stegun, 1965, ch. 8).

• **Expansion of $1/K^2$ into Legendre polynomials**

Our problem at hand can be actually reduced to the question how to efficiently find the coefficients in the formal expansion[28]

$$\frac{1}{\alpha-\beta x} = \sum_{n=0}^{\infty} a_n \mathrm{P}_n(x). \tag{1.67}$$

Multiplying Eq. (1.67) by $\mathrm{P}_m(x)$, calling upon the orthogonality of Legendre polynomials and integrating over the domain $x \in [-1,1]$ readily yields

$$a_m = \frac{2m+1}{2}\int_{-1}^{1}\mathrm{d}x\,\frac{\mathrm{P}_m(x)}{\alpha-\beta x} = \frac{2m+1}{2\beta}\int_{-1}^{1}\mathrm{d}x\,\frac{\mathrm{P}_m(x)}{\gamma-x}, \tag{1.68}$$

where $\gamma \equiv \alpha/\beta > 1$. We are thus interested solely in the evaluation of the last integral in (1.68) which we denote as I_m. Using the well-known recurrence relation for Legendre polynomials (Abramowitz and Stegun, 1965, chap. 8) furnishes after some manipulation recurrence relations for $I_{m>1}$, namely

$$\begin{aligned}(m+1)I_{m+1} &= \int_{-1}^{1}\mathrm{d}x\,\frac{m+1}{\gamma-x}\mathrm{P}_m(x) = \\ &= (2m+1)\int_{-1}^{1}\mathrm{d}x\,\frac{x}{\gamma-x}\mathrm{P}_m(x) - m\int_{-1}^{1}\mathrm{d}x\,\frac{\mathrm{P}_{m-1}(x)}{\gamma-x.}\end{aligned} \tag{1.69}$$

Plugging further $x/(\gamma-x) = -1+\gamma/(\gamma-x)$ into (1.69) gives

$$(m+1)I_{m+1} = \gamma(2m+1)I_m - (2m+1)\underbrace{\int_{-1}^{1}\mathrm{d}x\,\mathrm{P}_m(x)}_{0 \text{ for } m>1} - mI_{m-1}. \tag{1.70}$$

[28] we are assuming that α, β are real constants and $\alpha > \beta > 0$

Since the integrals I_m can be computed easily directly for $m \in \{0, 1\}$ as

$$I_0 = \log\left(\frac{\gamma+1}{\gamma-1}\right) \quad \text{and} \quad I_1 = 2\gamma \operatorname{arccoth}\gamma - 2 = 2I_0 - 2, \tag{1.71}$$

the relation (1.70) yields finally the sought prescription how to generate the expansion coefficients in (1.67). Strictly speaking, the coefficients (1.68) can be formally expressed using the Legendre functions of the second kind, Q_m, as

$$a_m = \frac{2m+1}{\beta}\mathrm{Q}_m(\gamma), \tag{1.72}$$

nevertheless the contribution of the derivation above is that it actually furnishes an algorithm intended for a practical numerical implementation. As a side effect we have therefore also obtained an algorithm how to generate the $\mathrm{Q}_l(\gamma)$ functions. In actual numerical tests this approach turned out to be superior to the method `gsl_sf_legendre_Ql` offered by the `GSL` numerical library (Galassi et al., 2009), which is unable to handle arguments γ very close to 1 corresponding to higher incident energy or small rotational constant B. As far as we know, functions $\mathrm{Q}_l(\gamma)$ are not available in the, otherwise very rich, numerical library CERNLIB (2006).

In notation compatible with (1.51) we thus finally obtain[29]

$${}^{\mathrm{FBA}}\mathrm{A}_{\lambda}^{\mathrm{p.d.}}\left(j \to j'\right) = \frac{8}{3}D^2(2j'+1)\begin{pmatrix} j & j' & 1 \\ 0 & 0 & 0 \end{pmatrix}^2 (2\lambda+1)\,\mathrm{Q}_\lambda\left(\frac{1+\epsilon^2}{2\epsilon}\right). \tag{1.73}$$

Formula (1.73) is a theoretical justification of the so-called "quadratic scaling rule" often used (Randell et al., 1996) in the analysis of experimental data stating that the scattering cross-sections are proportional to the square of the dipole moment D.

1.4.3 Analytic Born completion in the laboratory frame

The main drawback of the close coupling approach is the fact that the number of channels (target states) taken into account is limited. Depending on the problem under investigation, convergence issues with respect to this truncation may arise. The method known in the literature as *Analytic Born Completion* (ABC) or *Born closure approximation* constitutes one attempt how to circumvent these issues by clever employment of the Born approximation. The main idea can be formally summarized as follows. Suppose that we need to compute numerically the sum $F = \sum_{n=0}^{\infty} f_n$, where the terms f_n decay slowly to zero with increasing n so in general a lot of terms is needed to assure proper convergence of F. Nevertheless if we can find a similar series $\sum_{n=0}^{\infty} g_n$, the sum G of which is known analytically and whose terms g_n exhibit similar asymptotic (for $n \to \infty$) behavior as f_n, then we can make following approximation

$$F \approx \sum_{n=0}^{N}(f_n - g_n) + G. \tag{1.74}$$

As concerns scattering applications, the quantities g are typically Born approximations of f which explains the name of the method. Ideas along these lines have been used extensively in the past (Clark, 1977; Crawford and Dalgarno, 1971). The original idea dates back probably to Thompson (1966), where the author applied the above discussed technique in description of elastic electron scattering on neon and argon. More recent review with applications can be found, *e.g.*, in Feldt and Morrison (2008*a*); Isaacs and Morrison (1996) or Itikawa (2000*a*,*b*).

[29] superscript p.d. reflects that (1.73) refers to the point dipole potential

Illustration on $e^- - CO$ scattering

In the following we would like to present the simplest possible application of the ABC procedure with some illustrations. For this purpose we chose system used by Crawford and Dalgarno (1971) mimicking the electron interaction with carbon monoxide. The potential expansion (1.54) in this model is considered only for $\lambda \in \{0, 1, 2\}$, therefore we are taking effectively into account contributions stemming from spherical polarizability, dipole, quadrupole and anisotropic polarizability interactions. For explicit form of the potential we refer to Crawford and Dalgarno (1971). Moreover, we shall confine ourselves to the evaluation of the integral scattering cross-section for the inelastic $0 \to 1$ rotational transition. In light of Eq. (1.53), it means that we need to evaluate the A_0 coefficient defined by Eq. (1.51). Explicitly stated

$$\begin{aligned} \sigma_{0\to1} &= \frac{\pi}{k_0^2}\mathrm{A}_0\,(0 \to 1) = \\ &= \frac{\pi}{k_0^2}\sum_{J=0}^{\infty}(2J+1)\sum_{l,l'}\left|{}^J\mathcal{T}_{1l',0l}\right|^2. \end{aligned} \tag{1.75}$$

In numerical implementation, one needs to restrict the channel space by imposing upper limits $J_{\max}, l_{\max}, j_{\max}$ on J, l, j.[30] Some testing revealed in accordance with Garrett (1975) that the final cross-section (1.75) is rather insensitive to the value of $j_{\max}$ if $j_{\max} \gtrsim 3$. Thus according to the requirement 30, we have essentially one free parameter $l_{\max}$, the value of which influences the convergence of the sum in Eq. (1.75). The quantities $\sum_{l,l'}\left|{}^J\mathcal{T}_{1l',0l}\right|^2$ thus play the role of f_n in Eq. (1.74).

By inspection of the Born prediction (1.73), we naturally expect that the main contribution to the $0 \to 1$ transition is caused by the dipole contribution to the potential and we might try to suppose that the $\mathcal{T}$-matrix elements for high J in case of point dipole potential[31] won't differ much from their counterparts resulting from the original potential. Therefore g_n in Eq. (1.74) would be interpreted as Born approximation to the $\mathcal{T}$-matrix elements for a point dipole potential.

However, the integral FBA scattering cross-section in this case can be obtained by quadrature from (1.65). The result is

$${}^{\mathrm{FBA}}\sigma_{0\to1} = \frac{8\pi}{3k_0^2}D^2\log\frac{1+\epsilon}{1-\epsilon} \qquad \epsilon = \frac{k_1}{k_0},\ 0 < \epsilon < 1 \tag{1.76}$$

Next, we need to evaluate the Born $\mathcal{T}$-matrix elements for the dipole potential. The Born $\mathcal{T}$-matrix can be directly obtained from (1.124) by discarding terms $\mathcal{O}(V^2)$. This yields

$${}^{\mathrm{FBA}}\mathcal{K} = -2\int_0^{\infty}\mathrm{J}\cdot\mathrm{V}\cdot\mathrm{J}. \tag{1.77}$$

Plugging this approximative $\mathcal{K}$-matrix into (1.49) and keeping only terms linear in $\mathcal{K}$ (and thus linear in V) gives in turn the desired Born $\mathcal{T}$-matrix in the form

$${}^{\mathrm{FBA}}\mathcal{T} = -4\mathrm{i}\int_0^{\infty}\mathrm{J}\cdot\mathrm{V}\cdot\mathrm{J}. \tag{1.78}$$

The so-called *unitarized Born approximation* as discussed, *e.g.*, by Padial et al. (1981) is obtained by a modification of the second step, where one uses the "exact" prescription for the $\mathcal{T}$-matrix, *i.e.*, even terms of higher order in $\mathcal{K}$ are retained.[32]

[30] we prefer to deal with "complete" J-subspaces, *i.e.*, the value of $J_{\max}$ is connected with $l_{\max}, j_{\max}$ by the requirement $J_{\max} \le |l_{\max} - j_{\max}|$

[31] with the same dipole moment as in the original potential

[32] nevertheless the $\mathcal{K}$-matrix itself is still only linear in V

From Eq. (1.78) we easily calculate (Clark, 1977) individual matrix elements as

$$
{}_{\mathrm{FBA}}{}^{J}\mathcal{T}_{1l',0l} = 4\mathrm{i}(-1)^{J} D\sqrt{k_0 k_1}\left(\int_0^\infty \mathrm{d}r\, j_{l'}(k_1 r)\, j_l(k_0 r)\right)\cdot \\
\cdot\sqrt{2l+1}\sqrt{2l'+1}\begin{pmatrix} l & l' & 1 \\ 0 & 0 & 0 \end{pmatrix}\begin{Bmatrix} 1 & l' & J \\ l & 0 & 1 \end{Bmatrix}. \tag{1.79}
$$

The identity (D.8) allows us to perform the radial integration analytically[33] yielding

$$
{}_{\mathrm{FBA}}{}^{J}\mathcal{T}_{1l',0l} = \mathrm{i}\pi D(-1)^{J}\frac{k_1^{l'+\frac{1}{2}}}{k_0^{l'+\frac{1}{2}}}\sqrt{2l+1}\sqrt{2l'+1}\begin{pmatrix} l & l' & 1 \\ 0 & 0 & 0 \end{pmatrix}\begin{Bmatrix} 1 & l' & J \\ l & 0 & 1 \end{Bmatrix}\cdot \\
\cdot\frac{\Gamma\left(\frac{l+l'+1}{2}\right)}{\Gamma\left(\frac{l-l'+2}{2}\right)\Gamma\left(l'+\frac{3}{2}\right)}\,{}_2F_1\left(\frac{l+l'+1}{2},\,\frac{l'-l}{2},\,l'+\frac{3}{2};\,\frac{k_1^2}{k_0^2}\right). \tag{1.80}
$$

Since the integral cross-section is proportional to the square of the $\mathcal{T}$-matrix elements, as a side product we obtain the prediction $k_1^{2l'+1}$ for the threshold behavior of the J-component of the integral cross-section, where l' is the minimal orbital angular momentum accompanying $j = 1$ for a given value of J.

Putting everything together, the integral excitation cross-section (1.53) can be thus approximated as

$$
\sigma_{0\to1} \approx \frac{\pi}{k_0^2}\sum_{J=0}^{J_{\max}}(2J+1)\left[\sum_{l,l'}\left|{}^{J}\mathcal{T}_{1l',0l}\right|^2 - \sum_{l,l'}\left|{}_{\mathrm{FBA}}{}^{J}\mathcal{T}_{1l',0l}\right|^2\right] + \\
+\frac{8\pi}{3k_0^2}D^2\log\frac{k_0+k_1}{k_0-k_1}, \tag{1.81}
$$

with the last summand originating from Eq. (1.76). Behavior of individual J-components

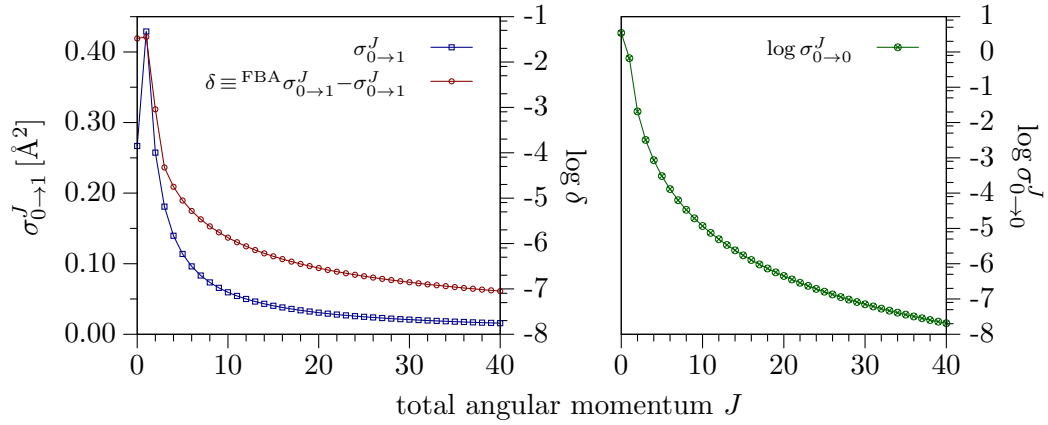

Figure 1.3: Convergence of the excitation $0 \to 1$ (left panel) and elastic $0 \to 0$ (right panel) cross-sections for incident energy of 100 meV. Left panel demonstrates the slow convergence of $\sigma_{0\to1}$ with respect to J and its approaching to the Born approximation results. Calculations were performed with close coupling parameters $J_{\max} = 40$, $l_{\max} = 43$, $j_{\max} = 3$.

[33] for more involved numerical methods intended for evaluation of oscillatory integrals of spherical Bessel functions we refer to Lehman et al. (1981)

of $\sigma_{0\to1}$ is demonstrated in the left panel of Figure 1.3, the results of which were obtained using Volterra propagator method with adaptive grid discussed in more detail in Section 1.5.

Even for $J_{\max} = 40$, straightforward application of Eq. (1.75) for incident energy 100 meV yields value of 2.59 Å^2, whereas the Born closure formula (1.81) predicts 4.09 Å^2 in accordance with Crawford and Dalgarno (1971). At lower energies, this behavior is less pronounced, for example for 10 meV, formula (1.75) yields 25.29 Å^2, whereas the Born closure formula (1.81) predicts 26.89 Å^2. The intuitive reason for this is hidden possibly in the fact that higher partial waves won't contribute due to the centrifugal barrier and therefore also high J-components will be less important, since the minimal angular momentum l in block J is given as $l_{\min} = \max(J - j_{\max}, 0)$.

Note that even within this rather "crude" model, the obtained result (1.81) for 10 meV is thanks to the dominant character of the dipole interaction in acceptable agreement with the value 23.84 Å^2 reported by Randell et al. (1996) and also with results of Chandra (1977); Jain and Norcross (1992).

Finally, we would like to mention slightly different interpretation of the subtraction technique (1.74) as proposed by Norcross and Padial (1982). The authors consider the expression (1.51) for the differential cross-section and re-express it in the first step following Crawford and Dalgarno (1971) as

$$\left.\frac{\mathrm{d}\sigma}{\mathrm{d}\Omega}\right|_{j\to j'} = \left.\frac{\mathrm{d}\sigma}{\mathrm{d}\Omega}\right|^{\mathrm{FBA}}_{j\to j'} + \Delta \left.\frac{\mathrm{d}\sigma}{\mathrm{d}\Omega}\right|_{j\to j'}, \tag{1.82}$$

with

$$\Delta \left.\frac{\mathrm{d}\sigma}{\mathrm{d}\Omega}\right|_{j\to j'} = \frac{1}{4k_j^2}\sum_{\lambda}\Big[A_\lambda - A_\lambda^{\mathrm{FBA}}\Big]\mathrm{P}_\lambda(\cos\theta). \tag{1.83}$$

They key observation rests again in the fact that for large angular momenta l, the $\mathcal{T}$-matrix elements entering coefficients A_λ in (1.83) will ultimately coincide with values calculated in the first Born approximation. Since A_λ does not couple $\mathcal{T}$-matrix elements differing in l by more than λ, the high l contributions effectively cancel in (1.83). Therefore one could interpret the splitting (1.82) in such a way that it separates the cross-section into low and high angular momenta components. Norcross and Padial (1982) also made the observation that the high l cancellation in (1.83) is actually equivalent to the fact that the long range part of the potential does not influence significantly (1.83). The authors consequently argue that exactly because of this reason, the adiabatic treatment might be appropriate for evaluation of (1.83) even if it is inapplicable for evaluation of the original cross-section. Moreover, it is certainly possible to go beyond Born approximation in the sense that one can introduce an approximative (APP) potential provided the $\mathcal{T}$-matrix elements coincide with original $\mathcal{T}$-matrix elements for high l. Then a natural extension of (1.83) reads

$$\left.\frac{\mathrm{d}\sigma}{\mathrm{d}\Omega}\right|_{j\to j'} = \left.\frac{\mathrm{d}\sigma}{\mathrm{d}\Omega}\right|^{\mathrm{APP}}_{j\to j'} + \Delta \left.\frac{\mathrm{d}\sigma}{\mathrm{d}\Omega}\right|_{j\to j'}, \tag{1.84}$$

with

$$\Delta \left.\frac{\mathrm{d}\sigma}{\mathrm{d}\Omega}\right|_{j\to j'} = \frac{1}{4k_{\mathrm{B}}^2}\sum_{\lambda}\Big[B_\lambda - B_\lambda^{\mathrm{APP}}\Big]\mathrm{P}_\lambda(\cos\theta). \tag{1.85}$$

The central difference from the previous approach is however that the expression (1.85) is evaluated in the adiabatic framework whereas (1.84) is *not*. The inherent body frame approach is in Eq. (1.85) also indicated by introduction of the B coefficients (1.97) and the body frame momentum k_{B}. Norcross and Padial (1982) denote resulting

approximation as *Multipole Extracted Adiabatic Nuclei* (MEAN). In the sense that this method treats essentially low and high angular momenta components in substantially different way, it can be considered closely linked to the *Angular Frame Transformation* methods mentioned briefly in Subsection 1.2.2.

1.4.4 Body frame treatment & Rotational frame transformation

An alternative tack to the same problem is based on the body frame formalism which is the subject of Subsection 1.2.1. In the parlance of the frame transformation theory, one essentially works in the region I introduced on p. 14 in the section devoted to the partitioning of the space according to the radial variable r. Since we are interested only in the rotational excitations, we can afford to disregard the vibrational Hamiltonian $\mathbf{H}_{\mathrm{m}}^{(v)}$, which means that the wave function expansion (1.23) is amenable to simplifications described below Eq. (1.23), namely omission of the designation of the initial vibrational state and also the dependence of the radial functions on the internuclear separation R. The coupled equations (1.24) for $\phi^{J v_0}_{l\Lambda,l_0\Lambda_0}(r,R)$ thus reduce into

$$\sum_{l'}\left[\left(\frac{\mathrm{d}^2}{\mathrm{d}r^2}-\frac{l(l+1)}{r^2}+k_{\mathrm{B}}^2\right)\delta_{l,l_0}\quad -2\,V^{\Lambda}_{l,l'}\quad\right]\phi^{\Lambda}_{l',l_0}(r)=0. \tag{1.86}$$

In Eq. (1.86), we have also dropped the (redundant) label J since the potential matrix elements[34] $V^{\Lambda}_{l,l'}$ in the body frame are not dependent on J. The symbol k_{B} denotes the so-called "body frame energy" of the incident electron. By imposing the usual asymptotic behavior on $\phi^{\Lambda}_{l',l}$ as in the laboratory frame treatment discussed previously

$$\phi^{\Lambda}_{l',l}(r)\xrightarrow{r\to\infty}\frac{1}{\sqrt{k_{\mathrm{B}}}}\left[\sin\left(k_{\mathrm{B}}r-l'\frac{\pi}{2}\right)\delta_{l',l}+\cos\left(k_{\mathrm{B}}r-l'\frac{\pi}{2}\right){}^{\mathrm{B}}\mathcal{K}^{\Lambda}_{l',l}\right], \tag{1.87}$$

we can readily obtain the body frame reactance matrix ${}^{\mathrm{B}}\mathcal{K}$-matrix or the closely linked body frame ${}^{\mathrm{B}}\mathcal{T}$-matrix using a relation identical to (1.49)

$${}^{\mathrm{B}}\mathcal{T}^{\Lambda}=2\,{}^{\mathrm{B}}\mathcal{K}^{\Lambda}\left(i+{}^{\mathrm{B}}\mathcal{K}^{\Lambda}\right)^{-1}. \tag{1.88}$$

The first Born approximation (FBA) (1.77) to (1.88) can be derived again by retaining only first order terms in ${}^{\mathrm{B}}\mathcal{K}^{\Lambda}$ yielding

$${}^{\mathrm{B}}_{\mathrm{FBA}}\mathcal{T}^{\Lambda}=-2i\,{}^{\mathrm{B}}\mathcal{K}^{\Lambda}. \tag{1.89}$$

However, this ${}^{\mathrm{B}}\mathcal{T}$-matrix (or its FBA counterpart) still refers to the body frame and as such contains of course no information about the rotational dynamics under investigation. Therefore one needs to perform the transition to the laboratory frame by means of the frame transformation procedure. In the present setting the regions I and II of Subsection 1.2.1 collapse into one and one has to deal just with the rotational frame transformation (1.30) effecting the transition from body frame basis (1.17) to its laboratory counterpart (1.27).

The matrices $A^{J\Lambda}_{jl}$ specified by (1.30) constitute a unitary transformation connecting individual channels in the body and laboratory formalism. Since we work in the real domain, the transformation properties of the wave functions are easily extended to the ${}^{\mathrm{B}}\mathcal{K}$-matrix defined by (1.87). An approximate laboratory frame ${}^{\mathrm{L}}\tilde{\mathcal{K}}$-matrix is then

$${}^{\mathrm{L}}\tilde{\mathcal{K}}^{J}_{j'l',jl}\overset{\mathrm{def}}{=}\sum_{\Lambda}A^{J\Lambda}_{j'l'}\cdot{}^{\mathrm{B}}\mathcal{K}^{\Lambda}_{l',l}\cdot A^{J\Lambda}_{jl}. \tag{1.90}$$

[34] slightly compressed notation has been used in (1.86) as compared to (1.24) – $V^{\Lambda}_{l,l'}$ is just a convenient shorthand to $\langle l\Lambda;\,JM|\mathbf{V}_{\mathrm{int}}|l'\Lambda';\,JM\rangle$ used in (1.86)

The approximate laboratory frame ${}^{\mathrm{L}}\tilde{\mathcal{T}}$-matrix is then rendered analogously to (1.49)

$$\begin{aligned} {}^{\mathrm{L}}\tilde{\mathcal{T}}^{J}_{j'l',jl} &= -2\,{}^{\mathrm{L}}\tilde{\mathcal{K}}^{J}_{j'l',jl}\cdot\left(i+{}^{\mathrm{L}}\tilde{\mathcal{K}}^{J}_{j'l',jl}\right)^{-1} \\ &= -2\,{}^{\mathrm{L}}\tilde{\mathcal{K}}^{J}_{j'l',jl}\cdot\left(1+{}^{\mathrm{L}}\tilde{\mathcal{K}}^{J\ 2}_{j'l',jl}\right)^{-1} + 2\mathrm{i}\,{}^{\mathrm{L}}\tilde{\mathcal{K}}^{J}_{j'l',jl}\cdot\left(1+{}^{\mathrm{L}}\tilde{\mathcal{K}}^{J\ 2}_{j'l',jl}\right)^{-1}. \end{aligned} \tag{1.91}$$

It has been shown (Chandra, 1975) that due to the unitarity of the transformation $A^{J\Lambda}_{jl}$, one can equivalently transform the body frame ${}^{\mathrm{B}}\mathcal{T}$-matrix using prescription analogous to (1.90), where one formally replaces all occurrences of "K by corresponding T", arriving at the same result as by using the "indirect" procedure *via* the ${}^{\mathrm{B}}\mathcal{K}$-matrix.

Having obtained an approximation to the laboratory frame transition matrix, we can formally follow the procedure outlined in the section devoted to the laboratory frame treatment. Thus the individual (rotational) state-to-state cross-sections are

$$\tilde{\sigma}_{j\to j'} = \frac{\pi}{k^2_{\mathrm{B}}(2j+1)}\sum_{J=0}^{\infty}(2J+1)\sum_{l,l'}\left|{}^{\mathrm{L}}\tilde{\mathcal{T}}^{J}_{j'l',jl}\right|^2. \tag{1.92}$$

Analogously, the differential cross-section is given by relation (1.50) with ${}^{\mathrm{L}}\tilde{\mathcal{T}}^{J}_{j'l',jl}$ being substituted for the ${}^{\mathrm{L}}\mathcal{T}$-matrix.

Alternatively, one may be tempted to calculate the total scattering (body frame) cross-section directly from the body frame ${}^{\mathrm{B}}\mathcal{T}$-matrix according to Huo and Gianturco (1995) *via*

$$\sigma_{\mathrm{B}} = \sum_{\Lambda}\sigma^{\Lambda}, \tag{1.93}$$

with

$$\sigma^{\Lambda} = \frac{\pi}{k^2_{\mathrm{B}}}\sum_{l=0}^{l_{\max}}\sum_{l'=0}^{l_{\max}}\left|{}^{\mathrm{B}}\mathcal{T}^{\Lambda}_{l',l}\right|^2. \tag{1.94}$$

It has been shown (Chan et al., 1968; Temkin et al., 1969) that[35] the quantity (1.93) is, apart from possible kinematic factors, equal to

$$\sigma_{j\to} = \sum_{j'}\tilde{\sigma}_{j\to j'} \tag{1.95}$$

and the sum on r.h.s. of Eq. (1.95) does not depend on the initial rotational state j. Because of this summation over the final rotational states, the body frame total cross-section σ_{B} in (1.93) is often termed as "rotationally-summed". Finally, the body frame equivalent to relation (1.50) can be written in quite similar form as

$$\left.\frac{\mathrm{d}\sigma}{\mathrm{d}\Omega}\right|_{\mathrm{B}} = \frac{1}{4k^2_B}\sum_{L}(2L+1)\,\mathrm{B}_L\,\mathrm{P}_L(\cos\theta), \tag{1.96}$$

where

$$\mathrm{B}_L = \sum_{\substack{\Lambda_1,\Lambda_2\\ l_1,l'_1,l_2,l'_2}} i^{l'_1-l_1-l'_2+l_2}\left[(2l'_1+1)(2l_1+1)(2l'_2+1)(2l_2+1)\right]^{1/2} d_L\big(l_1,\,l_2,\,l'_1,\,l'_2\big)\mathcal{T}^{\Lambda_1}_{l'_1,l_1}\mathcal{T}^{\Lambda^*_2}_{l'_2,l_2}, \tag{1.97}$$

[35] in light of results presented in Chandra (1975) regarding the equivalence of the adiabatic approximation and the RFT, this statement is actually explicitly proved by reasoning mentioned in Subsection 1.4.5

with coupling[36] terms d_L (Sun et al., 1995, p. 4)

$$d_L\left(l_1,\, l_2,\, l_1',\, l_2'\right) \equiv \begin{pmatrix} l_1 & l_2 & L \\ 0 & 0 & 0 \end{pmatrix} \begin{pmatrix} l_1' & l_2' & L \\ 0 & 0 & 0 \end{pmatrix} \begin{pmatrix} l_1 & l_2 & L \\ -\Lambda_1 & \Lambda_2 & \bullet \end{pmatrix} \begin{pmatrix} l_1' & l_2' & L \\ -\Lambda_1 & \Lambda_2 & \bullet \end{pmatrix}. \tag{1.98}$$

1.4.5 Adiabatic approximation

Section 1.3 shows that the central ingredient to the adiabatic approximation is the elastic body frame "modulated" scattering amplitude. According to the Chase (1956)'s prescription, the approximate laboratory frame (in principle inelastic) amplitude is consequently rendered as a single matrix element of the transformed body frame amplitude sandwiched by respective rotational states of the target molecule. In this sense, the approach based on adiabatic approximation (AA) thus resembles quite closely the body frame approach accompanied by rotational frame transformation discussed in the preceding section. One therefore expects that there must be some specific relation between these two approaches and it has been indeed shown (Chandra, 1975) that these methods in their original form actually furnish identical cross-sections. Nevertheless because of the different theoretical background, we have devoted a separate section to the AA method.

Formalism of the adiabatic approximation

The subsequent analysis is most easily performed in the partial wave expansion which finds a natural generalization in case of polar molecules as elaborated in more detail in Chapter 4. The body frame elastic scattering amplitude is thus expressed[37] as

$$f(\vec{k}_f',\, \vec{k}_i') = \frac{2\pi}{\mathrm{i}k} \sum_{\substack{m,m' \\ l,l'}} \mathrm{i}^{l-l'} \cdot \underbrace{\left\{ -\delta_{l,l'}\delta_{m,m'} + \mathbb{S}_{l'm',lm} \right\}}_{\mathbb{T}_{l'm',lm}} \cdot \mathrm{Y}^*_{l,\,m}\big(\hat{k}_i'\big)\mathrm{Y}_{l',\,m'}\big(\hat{k}_f'\big), \qquad \text{with } k \equiv k_f = k_i \tag{1.99}$$

with the term in curly braces $\mathbb{T}_{l'm',lm}$ being known as the partial wave transition matrix. Consequently, it is necessary to transform this amplitude to the laboratory frame obtaining in this way the "ω-modulated" scattering amplitude required by the central equation (1.35) of the adiabatic approximation. To this end, we conveniently employ the Wigner $\mathcal{D}^j_{m,k}$ functions (the most important algebraic properties of which are summarized by Appendix E) to transform spherical harmonics in (1.99) using relations (E.5). The resulting (transformed) scattering amplitude takes the form

$$f(\vec{k}_f,\, \vec{k}_i;\, \omega) = \frac{2\pi}{\mathrm{i}k} \sum_{\substack{m \\ l,l'}} \mathrm{i}^{l-l'} \sqrt{\frac{2l+1}{4\pi}}\, \mathbb{T}^m_{l',l} \sum_{k'} \mathrm{Y}_{l',\,k'}\big(\hat{k}_f\big)\, \mathcal{D}^l_{0,m}(\omega)\; \mathcal{D}^{l'\,*}_{k',m}(\omega)\,, \tag{1.100}$$

where we put the incident momentum $\vec{k}_i$ into coincidence with the fixed laboratory frame z-axis and the Euler angles specifying the orientation of the molecule have been subsumed into a collective label ω. As already mentioned above, the amplitude (1.100) is consequently sandwiched by rotational states of the molecule and resulting expression is integrated over ω (*i.e.*, averaged over possible molecular orientations). The result of course depends on the explicit form of the rotational states. Since we have applied this

[36] notation of Appendix B has been used in (1.97), namely that the symbol $\bullet$ appearing in the individual $3j$-symbols represents the unique value for which the respective symbol doesn't vanish

[37] in accordance with the convention introduced in Section 1.2, primed vectors refer to the body frame of reference

approach for studying rotational excitations of polar symmetric top molecules, we shall confine ourselves in the following to this particular case. The approximative laboratory frame amplitude rendered in the adiabatic approximation is thus

$$ {}^{\mathrm{LF}}_{\mathrm{ad.}} f^{J'K'M'}_{JKM}(\hat{k}_f) = \left\langle J'K'M' \right| f(\vec{k}_f, \vec{k}_i; \omega) \left| JKM \right\rangle , \tag{1.101} $$

with $|JKM\rangle$ representing the symmetric top rotational states introduced in Subsection E.1.1. Performing the integration over ω in Eq. (1.101) and utilizing composition (E.24) and orthogonality (E.18) properties of the $\mathcal{D}^{j}_{m,k}$ functions yields after some algebraic effort the final result

$$ \begin{aligned} {}^{\mathrm{LF}}_{\mathrm{ad.}} f^{J'K'M'}_{JKM}(\hat{k}_f) = \frac{2\pi}{ik}\sqrt{\frac{(2J+1)(2J'+1)}{4\pi}}(-1)^{K-M'}\delta_{K,K'}\sum_{\substack{m\\ l,l'}}(-1)^m\sqrt{2l+1} \\ \times \mathrm{i}^{l-l'}\mathbb{T}^m_{l',l}\sum_L (2L+1)\begin{pmatrix} J & J' & L \\ M & -M' & \Delta M \end{pmatrix}\begin{pmatrix} J & J' & L \\ K & -K & 0 \end{pmatrix}. \\ \Delta M = M' - M \qquad \cdot \begin{pmatrix} l & l' & L \\ 0 & \Delta M & -\Delta M \end{pmatrix}\begin{pmatrix} l & l' & L \\ m & -m & 0 \end{pmatrix} \mathrm{Y}_{l',\bar{M}}(\hat{k}_f). \\ \bar{M} = M - M' \end{aligned} \tag{1.102} $$

The form (1.102) is in agreement with expression given by Fabrikant (1983*b*), where the author presents similar formula for diatomic molecules obtainable from Eq. (1.102) in the formal limit $K, K' \to 0$.

Having obtained the scattering amplitude in (1.102), it is then straightforward to evaluate the differential scattering cross-section *via* standard formula

$$ \mathrm{d}\sigma_{\Gamma',\Gamma} = \frac{k_{\Gamma'}}{k_{\Gamma}} \left| {}^{\mathrm{LF}}_{\mathrm{ad.}} f_{\Gamma',\Gamma}(\hat{k}_f) \right|^2 \mathrm{d}\Omega, \tag{1.103} $$

where Γ and Γ' were introduced as shorthands for rotational quantum numbers JKM and $J'K'M'$, respectively.

The cross-section corresponding to all possible rotational transitions from an initial energetically non-degenerate subspace evaluated in the adiabatic approximation has the interesting property that it is independent on this initial subspace. The explicit analysis for diatomic molecules has been carried out long time ago by Chang and Temkin (1969) and Temkin et al. (1969). The underlying idea is quite simple and the proof can be compressed just into a few lines as outlined below, where we extend the treatment also to symmetric top molecules.

• Diatomic molecules

The energetically non-degenerate subspaces regarding diatomic molecules are labeled just by the rotational quantum number j. Thus the physical quantity (cross-section $\sigma_{j\to}$) of interest as described above is

$$ \sigma_{j\to} \equiv \frac{1}{2j+1}\sum_m \sum_{j',m'} \sigma_{j,m\to j',m'}. \tag{1.104} $$

The first sum over m in (1.104) corresponds to averaging over initial energetically degenerate states[38] and the second sum over j', m' reflects summing over all possible final rotational states. Expressing the individual cross-sections in Eq. (1.104) in terms

[38] the initial subspace is of dimension $2j+1$

of adiabatically approximated scattering amplitude (1.101) yields

$$\begin{aligned}
\sigma_j &= \frac{1}{2j+1}\sum_m\sum_{j',m'}\left|\left\langle j'm'\right|f(\vec{k}_f,\,\vec{k}_i;\,\omega)\left|jm\right\rangle\right|^2 = \\
&= \frac{1}{2j+1}\sum_m\sum_{j',m'}\left\langle jm\right|f(\vec{k}_f,\,\vec{k}_i;\,\omega)^*\left|j'm'\right\rangle\left\langle j'm'\right|f(\vec{k}_f,\,\vec{k}_i;\,\omega)\left|jm\right\rangle = \\
&= \frac{1}{2j+1}\sum_m\sum_{j',m'}\left\langle jm\right|\left|f(\vec{k}_f,\,\vec{k}_i;\,\omega)\right|^2\left|jm\right\rangle = \\
&= \frac{1}{2j+1}\sum_m\sum_{j',m'}\int\mathrm{d}\omega\left|f(\vec{k}_f,\,\vec{k}_i;\,\omega)\right|^2\mathrm{Y}_{j,\,m}(\omega)\mathrm{Y}^*_{j,\,m}(\omega) = \frac{1}{4\pi}\int\left|f(\vec{k}_f,\,\vec{k}_i;\,\omega)\right|^2\mathrm{d}\omega,
\end{aligned} \tag{1.105}$$

where we have utilized the closure property of the $|j'm'\rangle$ states in the second row and the well-known relation $4\pi\sum_m \mathrm{Y}_{j,\,m}(\omega)\mathrm{Y}^*_{j,\,m}(\omega) = 2j+1$ in the final algebraic manipulation. In other words, the result obtained in Eq. (1.105) can be also interpreted as that the cross-section (1.104) is simply an angular average of the squared modulus of the body-frame scattering amplitude transformed into the laboratory frame.

In the derivation (1.105), we have tacitly assumed that the target diatomic molecule finds itself in a Σ electronic state. Therefore the expectation values of the operators $\mathbf{J}_{z'}$ and $\mathbf{l}_{z'}$ coincide and the rotational wave functions are simply spherical harmonics. For generalization to non-Σ states we refer to Temkin and Faisal (1971). Since a diatomic molecule in a non-Σ state is, roughly speaking, almost a symmetrical top (as far as angular momentum is concerned), it is not too surprising that the formalism quite resembles the one given below.

• Symmetric top molecules

For symmetric top molecules, the rotational energy is determined by quantum numbers J, K. Therefore one obtains the relevant cross-section σ_{JK} by summing over final states and averaging over the $(2J+1)$-fold degenerate initial quantum number M

$$\sigma_{JK} \equiv \frac{1}{2J+1}\sum_M\sum_{J'K'M'}\sigma_{JKM\to J'K'M'}. \tag{1.106}$$

Consequently, one can proceed along very similar lines as for diatomic molecules to wit

$$\begin{aligned}
\sigma_{JK} &= \frac{1}{2J+1}\sum_M\sum_{J'K'M'}\left|\left\langle J'K'M'\right|f(\vec{k}_f,\,\vec{k}_i;\,\omega)\left|JKM\right\rangle\right|^2 = \\
&= \frac{1}{2J+1}\sum_{\substack{J'K'M'\\M}}\left\langle JKM\right|f(\vec{k}_f,\,\vec{k}_i;\,\omega)^*\left|J'K'M'\right\rangle\left\langle J'K'M'\right|f(\vec{k}_f,\,\vec{k}_i;\,\omega)\left|JKM\right\rangle = \\
&= \frac{1}{2J+1}\sum_M\sum_{J'K'M'}\left\langle JKM\right|\left|f(\vec{k}_f,\,\vec{k}_i;\,\omega)\right|^2\left|JKM\right\rangle = \\
&= \frac{1}{8\pi^2}\sum_M\sum_{J'K'M'}\int\mathrm{d}\omega\left|f(\vec{k}_f,\,\vec{k}_i;\,\omega)\right|^2\cdot\left|\,\mathcal{D}^J_{K,M}(\omega)\right|^2 = \frac{1}{8\pi^2}\int\left|f(\vec{k}_f,\,\vec{k}_i;\,\omega)\right|^2\mathrm{d}\omega.
\end{aligned} \tag{1.107}$$

The essential algebraic simplification is again based on the closure property of the $\mathcal{D}^{J'}_{K',M'}$ functions and the orthogonality property (E.18) enabling to carry out the summation over M. The interpretation of Eq. (1.107) is almost identical as in the previous case. The only distinction is present in the factor $8\pi^2$ which is due to the fact that the orientation of a symmetric top is specified by all three Euler angles and therefore the "angular space" size is correspondingly $2\pi\times$ larger than in Eq. (1.105).

Analytic Born completion in the body frame

The ideas outlined in Subsection 1.4.3 regarding the analytic Born closure techniques are easily extended also to the framework of the body frame treatment facilitating significantly numerical calculations especially in case of polar molecules as discussed in Chapter 4. Following the procedure introduced in Subsection 1.4.3, we need first to identify the dominant part of the electron-molecule interaction. In the following we shall suppose that the dipole contribution does the job. For the subtraction technique (1.74), it is again not necessary to consider exact form of the dipole potential since one can assume that for high partial waves, the difference between point dipole and the actual potential will be effectively washed out.

• **Born point dipole amplitude**

From the formal point of view, two main ingredients are required. Firstly, we need to compute the Born approximation to the body frame elastic point dipole scattering amplitude in the partial wave expansion obtaining thus the corresponding body frame Born partial wave T-matrix (1.99). To this end we employ plane wave resolution (D.6) in the standard expression for the Born amplitude obtaining[39]

$$\begin{aligned} f(\vec{k}_f,\,\vec{k}_i) &= 4\pi^2 \left\langle \vec{k}_f \right| \frac{\vec{D}\cdot\vec{r}}{r^3} \left| \vec{k}_i \right\rangle = \frac{1}{2\pi}\int \mathrm{d}\vec{r}\,\frac{\vec{D}\cdot\vec{r}}{r^3}\mathrm{e}^{\mathrm{i}(\vec{k}_i-\vec{k}_f)\cdot\vec{r}} = \\ &= 8\pi D \sum_{\substack{l,l'\\ m,m'}} \mathrm{i}^{l-l'}\mathrm{Y}^*_{l,\,m}\big(\hat{k}_i\big)\mathrm{Y}_{l',\,m'}\big(\hat{k}_f\big)\cdot\int_0^\infty \mathrm{d}r\; j_l(k_i r)\, j_{l'}(k_f r)\cdot \\ &\qquad\qquad \cdot\int \mathrm{d}\Omega_{\hat{x}}\;\mathrm{Y}_{l,\,m}\big(\hat{x}\big)\cos\theta\,\mathrm{Y}^*_{l',\,m'}\big(\hat{x}\big) \\ &= \frac{2\pi}{ik}\sum_{\substack{m\\ l,l'}} \mathrm{i}^{l-l'}\cdot {}^{\mathrm{FBA}}_{\mathrm{pd}}\rho^m_{l',l}\cdot\mathrm{Y}^*_{l,\,m}\big(\hat{k}_i\big)\mathrm{Y}_{l',\,m'}\big(\hat{k}_f\big), \end{aligned} \tag{1.108}$$

with ${}^{\mathrm{FBA}}_{\mathrm{pd}}\rho^m_{l',l}$ representing the mentioned Born point dipole partial wave T-matrix

$${}^{\mathrm{FBA}}_{\mathrm{pd}}\rho^m_{l',l} \equiv 2\mathrm{i}D\left[\frac{\delta_{l',l+1}}{l+1}\sqrt{\frac{l'^2-m^2}{4l'^2-1}} + \frac{\delta_{l'+1,l}}{l'+1}\sqrt{\frac{l^2-m^2}{4l^2-1}}\right], \tag{1.109}$$

the elements of which are immediately seen to decay only as $1/l$ confirming thus the expected slow convergence of the resulting cross-sections with respect to the angular momentum basis. Nevertheless if the dipole interaction dominates in the collisional process under investigation, it is not completely unreasonable to expect that the "exact" partial wave T-matrix elements will exhibit similar behavior for large l. One might be thus tempted to subtract the matrix elements (1.109) from T-matrix elements (1.99) computed in the body frame by solving the corresponding radial equations (1.24). Consequently, we need something which we would add in the laboratory frame in order to compensate for this subtraction. To this end, we evaluate in a straightforward way the FBA body frame scattering amplitude in the plane wave basis to wit

$$\begin{aligned} f(\vec{k}'_f,\,\vec{k}'_i) &= 4\pi^2 \left\langle \vec{k}'_f \right| \frac{\vec{D}\cdot\vec{r}}{r^3} \left| \vec{k}'_i \right\rangle = \\ &= -2\mathrm{i}\frac{\vec{D}'\cdot\vec{K}'}{K^2} \text{ with } \vec{K}' \equiv \vec{k}'_f - \vec{k}'_i. \end{aligned} \tag{1.110}$$

[39] superscript FBA stands for *First Born Approximation*

Now, it is necessary to transform the expression (1.110) to the laboratory frame. To this end, it is convenient to rewrite the dot product $\vec{D}' \cdot \vec{K}'$ in terms of spherical harmonics and consequently employ the transformation rules (E.17)

$$\begin{aligned} \frac{\vec{D}' \cdot \vec{K}'}{D\,K} = \mathrm{P}_1(\hat{D}' \cdot \hat{K}') &= \frac{4\pi}{3} \sum_{m=-1}^{1} \mathrm{Y}^*_{1,\,m}\big(\hat{K}'\big)\mathrm{Y}_{1,\,m}\big(\hat{D}'\big) \\ &= \sqrt{\frac{4\pi}{3}}\mathrm{Y}^*_{1,\,0}\big(\hat{K}'\big) = \sqrt{\frac{4\pi}{3}} \sum_{k=-1}^{1} \mathcal{D}^1_{k,0}(\omega)\,\mathrm{Y}_{1,\,k}\big(\hat{K}\,\big). \end{aligned} \tag{1.111}$$

Thus the body frame scattering amplitude (1.110) transformed into the laboratory frame is

$$f(\vec{k}_f,\,\vec{k}_i) = -2\mathrm{i}\frac{D}{K}\sqrt{\frac{4\pi}{3}} \sum_{k=-1}^{1} \mathcal{D}^1_{k,0}(\omega)\,\mathrm{Y}_{1,\,k}\big(\hat{K}\,\big). \tag{1.112}$$

Inserting this result into Eq. (1.100) and performing the angular integration using relation (E.21) yields

$$\begin{aligned} {}^{\text{LF-FBA}}_{\text{ad.}}f^{J'K'M'}_{JKM}(\hat{K}) = -\frac{2\mathrm{i}D}{K}\sqrt{\frac{4\pi}{3}}\sqrt{[\,J\,][\,J'\,]}\,(-1)^{M'-K}\delta_{K,K'}\times \\ \begin{pmatrix} J & J' & 1 \\ M & -M' & \bullet \end{pmatrix} \begin{pmatrix} J & J' & 1 \\ K & -K & 0 \end{pmatrix} \mathrm{Y}_{1,\,M'-M}\big(\hat{K}\,\big). \end{aligned} \tag{1.113}$$

Note that (1.113) is in contrast to (1.102) expressed in terms of the laboratory frame transfer momentum $\vec{K}$. Nevertheless the appropriate workaround is quite easy. Assuming that the laboratory frame is chosen so that the incident electron momentum $\vec{k}_i$ lies in coincidence with the laboratory z-axis and denoting the polar (scattering) angles of $\vec{k}_f$ as $\theta_\mathrm{f}, \phi_\mathrm{f}$, the magnitude of the momentum transfer is $K^2 = 2k_i^2(1 - \cos\theta_\mathrm{f})$ and the corresponding polar angles $\theta_\mathrm{K}, \phi_\mathrm{K}$ obey

$$\cos\phi_\mathrm{K} = -\frac{k_i}{K}\big(1 - \cos\theta_\mathrm{f}\big) \text{ and } \phi_\mathrm{K} = \phi_\mathrm{f}.$$

Strictly speaking, the final momentum expressed in the laboratory frame $\vec{k}_f$ violates energy conservation for it differs from $\vec{k}_i$ only in the direction. This nuisance is closely linked with our starting point, the body frame *elastic* amplitude (1.99). On the other hand, from the formal point of view, this is not of much importance, since (1.113) is used solely to compensate for the subtraction of the FBA partial wave T-matrix (1.109).

Finally, a natural question might be what is the connection between the FBA amplitude (1.113) obtained by digression to the body frame and the Born differential cross-section (1.66) calculated directly in the laboratory frame. Taking squared modulus of (1.113), summing over final and averaging over initial energetically degenerate states readily provides

$$\begin{aligned} {}^{\text{LF-FBA}}_{\text{ad.}}\frac{\mathrm{d}\sigma}{\mathrm{d}\Omega}\bigg|_{JK\to J'K'} &= \frac{1}{2J+1}\sum_{M,M'}\Big|{}^{\text{LF-FBA}}_{\text{ad.}}f^{J'K'M'}_{JKM}(\hat{K})\Big|^2 \\ &= 4\pi\frac{4D^2}{3K^2}(2J'+1)\begin{pmatrix} J & J' & 1 \\ K & -K & 0 \end{pmatrix}^2 \sum_{M,M'} \mathrm{Y}^*_{1,\,M'-M}\big(\hat{K}\,\big)\times \\ &\quad \times \mathrm{Y}_{1,\,M'-M}\big(\hat{K}\,\big)\begin{pmatrix} J & J' & 1 \\ M & -M' & \bullet \end{pmatrix}^2. \end{aligned} \tag{1.114}$$

The sums in (1.114) over M, M' are easily evaluated by introducing temporary variable $\Delta = M' - M$ so that one has

$$\underbrace{\sum_{\Delta} \mathrm{Y}^{*}_{1,\Delta}(\hat{K})\mathrm{Y}_{1,\Delta}(\hat{K})}_{\frac{3}{4\pi}\mathrm{P}_1(\hat{K}\cdot\hat{K})=\frac{3}{4\pi}} \underbrace{\sum_{M} \begin{pmatrix} J & J' & 1 \\ M & \bullet & \Delta \end{pmatrix}^2}_{\frac{1}{3}}. \tag{1.115}$$

We thus immediately see that (1.114) reduces to (1.66) with $\epsilon = 1$ reflecting the above mentioned fact that the amplitude (1.113) is "artificially elastic".

1.5 Radial equations

Vast majority of computational methods intended for description of electron-molecule scattering lead in the end to a set of coupled second order differential equations for the radial wave function components of the scattered electron. Quite generally, these equations can be written in the following form

$$\left[\frac{\mathrm{d}^2}{\mathrm{d}r^2} - \frac{l_\alpha(l_\alpha+1)}{r^2} + k_\alpha^2\right]\psi_{\alpha\beta}(r) = 2\sum_{\gamma} V(r)_{\alpha\gamma}\psi_{\gamma\beta}(r). \tag{1.116}$$

Greek subscripts $\alpha, \beta, \ldots$ distinguish individual channels and in the following they are used as a compressed notation for all relevant channel quantum numbers. These depend of course on the problem under investigation, nevertheless we shall assume that the angular momentum of the incident electron l is always included. This proviso is already explicitly present in Eq. (1.116), where the symbol l_α stands for the angular momentum l in channel α. Similarly, k_α denotes channel momentum given by energy conservation

$$k_\alpha^2 = 2(E - E_\alpha), \tag{1.117}$$

with E being the total initial energy of the system[40] and E_α representing the energy of the target in channel α. Finally, two subscripts on the wave function $\psi_{\alpha\beta}$ are used in order to distinguish outgoing (α) and ingoing (β) channels.

In the absence of the coupling potential term V, the real solutions[41] of Eq. (1.116) can be chosen as the *Ricatti-Bessel* functions introduced in Appendix D

$$\widehat{\mathrm{j}}_{l_\alpha}(k_\alpha r) \equiv \frac{1}{\sqrt{k_\alpha}}\widehat{j}_{l_\alpha}(k_\alpha r) \quad \widehat{\mathrm{n}}_{l_\alpha}(k_\alpha r) \equiv \frac{1}{\sqrt{k_\alpha}}\widehat{n}_{l_\alpha}(k_\alpha r)\,. \tag{1.118}$$

In (1.118), we have chosen slightly different normalization[42] of the free solutions as compared, *e.g.*, to Huo and Gianturco (1995, chap. 6) in order to ensure unit Wronskian and thus to eliminate kinematic factors in the real asymptotic form of the solution of (1.116) as mentioned in Appendix D.

To determine the solutions of (1.116) uniquely, one further imposes scattering boundary conditions, namely

$$\psi_{\alpha\beta}(0) = 0, \tag{1.119a}$$

$$\psi_{\alpha\beta}(r) \xrightarrow{r\to\infty} \delta_{\alpha\beta}\,\widehat{\mathrm{j}}_{l_\beta}(k_\beta r) + \mathcal{K}_{\alpha,\beta}\,\widehat{\mathrm{n}}_{l_\beta}(k_\beta r)\,. \tag{1.119b}$$

Condition (1.119a) has to be satisfied in order to ensure finite solutions of the three-dimensional Schrödinger equation at the origin and condition (1.119b) can be understood as a defining relation for the so-called $\mathcal{K}$-matrix. Strictly speaking, condition

[40] energy of the incident electron + target

[41] in the following we shall refer to these functions as *free solutions*

[42] and therefore also different symbols j and n

(1.119b) applies only for energetically accessible channels.[43] The role of closed channels in all applications presented in this thesis seemed to be marginal. Therefore we shall omit discussion of these topics and for additional details we refer to Norcross and Seaton (1973).

Equations (1.116) can be interpreted as a set of equations with nonzero r.h.s., where the r.h.s. contains the solution itself. At least from the theoretical point of view, the Green's function approach is specifically tailored for these situations. The particular (channel α) Green's function $g_{l_\alpha}(r, r')$ extensively used in Subsection 1.5.1 and vanishing identically[44] for $r' > r$ is

$$g_{l_\alpha}(r, r') = \theta\left(r - r'\right)\left\{\widehat{\mathrm{j}}_{l_\alpha}(k_\alpha r)\,\widehat{\mathrm{n}}_{l_\alpha}\left(k_\alpha r'\right) - \widehat{\mathrm{n}}_{l_\alpha}(k_\alpha r)\,\widehat{\mathrm{j}}_{l_\alpha}\left(k_\alpha r'\right)\right\}. \tag{1.120}$$

1.5.1 Numerical solution of the radial equations

In order to tackle equations (1.116) numerically, we have employed a technique based on the possibility to reformulate the original set of differential equations into a set of Volterra equations of the second kind, originally proposed and successfully applied in a series of papers (Sams and Kouri, 1969*a*,*b*, 1970*a*,*b*; White and Hayes, 1972). This approach yields an efficient and easily implementable iterative procedure as opposed to standard methods based on discretization of the differential operator. The applicability of the latter methods to quantum scattering problems has been investigated very extensively in the past (Allison, 1989; Blatt, 1967; Sullivan and Temkin, 1982). Approaches have been also reported, which are based on conversion of the second order to first order equations amenable to treatment by exponential techniques (Chan et al., 1968). Gordon (1969) has used a different strategy consisting in a piecewise linear approximation of the potential on several sectors. The solution on each sector can be then constructed analytically and consequently matched at the sector boundaries to supply an approximative wave function. For a recent overview of these and related methods we refer to Anastassi and Simos (2009) and references therein.

Another possibility consists in restating the Schrödinger equation into a first order differential equation for the log-derivative matrix of the solution. However, standard discretization methods are not especially practical in this case due to the possible pole singularities of the log-derivative matrix. An efficient numerical algorithm (although without derivation) has been proposed in Johnson (1973) and later put on more rigorous grounds by Manolopoulos et al. (1993). Mrugala (1985) has shown how to extend this algorithm also to handle Schrödinger equation with inhomogeneous terms. From the formal point of view, these methods are closely related to the *Variable Phase Approach* of Calogero (1967). Adaptation of the approximative method of Gordon (1969) to the framework of log-derivative methods can be found in Alexander and Manolopoulos (1987).

Although closed channels in the close coupling approach don't play a dominant role in the presented applications, an elaboration on propagation under these circumstances is contained, *e.g.*, in Norcross and Seaton (1973).

Volterra integral method

Set of N equations (1.116) being of second order has in general $2N$ solutions. The condition (1.119a) reduces this number to N. It turns out to be convenient to arrange individual solutions $\psi_{\alpha\beta}$ distinguished by the ingoing channel β into a square matrix

[43] *i.e.*, channels α for which $k_\alpha^2 > 0$

[44] $\theta(x)$ represents Heaviside step function

$\Psi_{\alpha\beta}$. In the same spirit we introduce following diagonal square matrices

$$\mathsf{J}_{\alpha,\beta} \equiv \widehat{\mathrm{j}}_{l_\alpha}(k_\alpha r)\,\delta_{\alpha,\beta} \qquad \mathsf{N}_{\alpha,\beta} \equiv \widehat{\mathrm{n}}_{l_\alpha}(k_\alpha r)\,\delta_{\alpha,\beta}, \tag{1.121}$$

representing the free solutions of Eq. (1.116). Taking into account the Green's function (1.120), the original set of equations can be easily restated into matrix form as

$$\Psi_{\alpha,\,\beta}(r) = \sum_{\gamma} \left(\mathsf{J}_{\alpha,\gamma}(r)\mathsf{Q}_{\gamma,\beta}(r) - \mathsf{N}_{\alpha,\gamma}(r)\mathsf{P}_{\gamma,\beta}(r)\right), \tag{1.122}$$

where the matrices Q and P depend on r and are given as[45]

$$\mathsf{Q}(r) \equiv \mathrm{I} + 2\int_0^r \mathrm{d}r'\ \mathsf{N}\cdot\mathsf{V}\cdot\Psi \tag{1.123a}$$

$$\mathsf{P}(r) \equiv 2\int_0^r \mathrm{d}r'\ \mathsf{J}\cdot\mathsf{V}\cdot\Psi \tag{1.123b}$$

Combining the boundary conditions (1.119) and Eq. (1.123) yields directly a relation for the $\mathcal{K}$-matrix

$$\mathcal{K} = -\lim_{r\to\infty} \mathsf{P}(r)\cdot\mathsf{Q}(r)^{-1}. \tag{1.124}$$

Discretization of Eq. (1.123)

To obtain the numerical solution of Eq. (1.121), one follows typically these steps

- the radial variable r is confined into some prescribed interval $[0, r_{\max}]$,
- radial grid $\{r_n\}_{n=0}^{N}$ is introduced, where n labels the individual grid points and $r_0 = 0$, $r_N = r_{\max}$,
- the integrals in Eq. (1.123) are replaced by suitable numerical quadrature scheme.

The issues regarding the choice of particular quadrature and its influence on the numerical properties of the resulting algorithm are discussed in more detail in Appendix A. In light of the material presented there, an acceptable compromise between precision and computational demands seems to be the *Simpson's method 2* with adaptive grid spacing. In practical calculations it turned out that it is quite satisfactory to use just simple trapezoidal rule with adaptive grid or "truncated" Simpson's method introduced in Section A.3.

This behavior is mainly due to the fact that the major error in the computed scattering quantities stems from the truncation of the close coupling target expansion and the error caused by the inaccuracy of the integrator can be remedied by increasing the density of the grid. This is accompanied by linear increase of the computational costs, whereas the scaling with respect to the number of target states is typically of third order. In the following, we shall therefore assume that the integration weights w_i^n given by (A.3) don't depend on n.

We thus readily obtain discretized versions of Eq. (1.123) as

$$\mathsf{Q}_n \equiv \mathrm{I} + 2\sum_{i=0}^{n} w_i\,\mathsf{N}_i\cdot\mathsf{V}_i\cdot\Psi_i \tag{1.125a}$$

$$\mathsf{P}_n \equiv 2\sum_{i=0}^{n} w_i\,\mathsf{J}_i\cdot\mathsf{V}_i\cdot\Psi_i \tag{1.125b}$$

[45] indices are dropped and symbol $\cdot$ denotes matrix-matrix multiplication

Subscript i indicates that the matrices $\mathsf{Q}, \mathsf{P}, \ldots$ are referred to the i^{th} grid point. Plugging (1.125) into Eq. (1.122) furnishes the final relation for propagating the solution

$$\Psi_{n+1} = \mathsf{J}_{n+1} \cdot \mathsf{Q}_n - \mathsf{N}_{n+1} \cdot \mathsf{P}_n, \tag{1.126}$$

which is a consequence of the fact that the contributions at the n^{th} grid point from Q and P cancel. Eq. (1.126) is thus a prescription how to generate the solution at grid point $n+1$ using the knowledge of the solution at grid point n.

Initial conditions

Eq. (1.126) has to be of course accompanied with proper boundary conditions at the origin. These can be obtained by direct inspection of Eq. (1.123), namely

$$\mathsf{Q}(0) = \mathrm{I} \qquad \mathsf{P}(0) = 0. \tag{1.127}$$

It is worth to note that the use of Green's function (1.120) actually already fixes the normalization of the resulting wave function and we are therefore not free to prescribe the matrices Q, P at the second grid point r_1, as it is usually done in, *e.g.*, Numerov type methods (Anastassi and Simos, 2009).

Numerical stabilization

The numerical errors arising in practical implementations of (1.126) are unavoidable. Probably the main consequence is the fact that the linear independence of individual solutions (*i.e.*, columns of Ψ) degrades during the propagation. Several techniques how to circumvent this nuisance have been proposed (Morrison et al., 1977; Rescigno and Orel, 1981, 1982). The main idea is based on the observation that all columns of Ψ are solutions of the original linear equation (1.116) and therefore Ψ post-multiplied by some regular matrix A will be also a solution. From the mathematical point of view, this approach essentially corresponds to a change of the initial conditions. The matrices Q, P will be transformed into $\tilde{\mathsf{Q}}, \tilde{\mathsf{P}}$, given as

$$\tilde{\mathsf{Q}} \leftarrow \mathsf{Q} \cdot \mathrm{A} \quad \text{and} \quad \tilde{\mathsf{P}} \leftarrow \mathsf{P} \cdot \mathrm{A}.$$

However, the key element of scattering calculations, the $\mathcal{K}$-matrix, is invariant under this transformation as can be immediately seen from (1.124)

$$\tilde{\mathcal{K}} = -\lim_{r\to\infty} \tilde{\mathsf{P}}(r) \cdot \tilde{\mathsf{Q}}(r)^{-1} = -\lim_{r\to\infty} \mathsf{P}(r) \cdot \mathrm{A} \cdot \mathrm{A}^{-1} \cdot \mathsf{Q}(r)^{-1} = \mathcal{K}.$$

Various methods then differ in the choice of the matrix A. Rescigno and Orel (1982) use in place of A the inverse of Q, *i.e.*, Q^{-1}. This yields the transformation

$$\tilde{\mathsf{Q}} \leftarrow \mathrm{I} \quad \text{and} \quad \tilde{\mathsf{P}} \leftarrow \mathsf{P} \cdot \mathsf{Q}^{-1}.$$

Another choice consists (Čurík et al., 2000) in employing the inverse of the solution matrix Ψ, although it might seem strange to multiply by Ψ^{-1} in this case since the matrix Ψ is close to singular. Therefore the stabilization procedure has to be performed "soon enough" to prevent numerical deterioration of Ψ.

On the other hand, as pointed out by Huo and Gianturco (1995), this approach suffers from the fact that it is not suitable for reproducing the wave function itself, for it would be necessary to store all transformation matrices and finally undo all matrix multiplications in order to return to the original initial conditions. But since we are usually interested solely in the $\mathcal{K}$-matrix, this poses no serious restriction.

1.6 R-matrix formalism for potential scattering

As a part of the presented thesis, we have investigated computational methods for determination of scattering lengths in case of long range potentials[46] emerging, *e.g.*, in theoretical description of Cs_2 or $^4He_2$ dimer ground states. Our interest concerning this topic was motivated mainly by theoretical significance of the scattering length quantity in the low-temperature physics of molecular dimers for which the point of Bose-Einstein condensation is experimentally attainable (Motovilov et al., 2001).

In this regard, we have proposed an alternative method which is based on combination of the R-matrix approach and the celebrated Schwinger-Lanczos (SL) variational principle. Details concerning this approach can be found in Šulc et al. (2010) comprising also the Attachment A of this thesis. Briefly stated, the basic idea consists in decomposing the interaction potential into a local V and non-local (possibly energy dependent) W part. Solution of the Lippmann-Schwinger (LS) equation for the potential $V+W$ is then in turn rendered by means of the so-called "two-potential" formula (Taylor, 2006, ch. 14), *i.e.*, one first solves the local problem taking into account only the potential V, the solution of which is then employed as a "source term" for an equation of the LS type but with potential W only. For handling the local part of the potential, we have employed Green's function technique along the lines of the R-matrix method as suggested in Mil'nikov et al. (2001). Finally, the non-local problem W is solved by application of the SL variational principle following the implementation of Meyer et al. (1991).

The purpose of this section is to merely summarize the basic principles and formalism of the R-matrix framework constituting a common denominator to a vast amount of methods in modern electron-molecule scattering theory. Originally, this approach was proposed by Wigner and Eisenbud (1947) in the context of nuclear physics and later adapted for scattering calculations by many authors (Burke et al., 1971, 1977; Shimamura, 1977).

1.6.1 Non-variational derivation

In the simplest possible setting of one-channel s-wave potential scattering, the relevant problematics is essentially reduced to solving the radial Schrödinger equation

$$\Big[-\frac{1}{2}\frac{\mathrm{d}^2}{\mathrm{d}r^2}+V(r)-\frac{1}{2}k_0^2\Big]\psi(r)=0, \tag{1.128}$$

with $V(r)$ and k_0 representing the interaction and incident momentum, respectively. In the usual R-matrix derivation (Burke and Robb, 1976), one fixes a radius $r=r_0$ and introduces a set $\{\phi_n\}$ of radial functions being comprised of solutions of

$$\Big[-\frac{1}{2}\frac{\mathrm{d}^2}{\mathrm{d}r^2}+V(r)-\frac{1}{2}k_n^2\Big]\phi_n(r)=0, \tag{1.129}$$

satisfying moreover boundary conditions

$$\phi_n(0)=0, \tag{1.130a}$$

$$\frac{1}{\phi_n(r_0)}\frac{\mathrm{d}\phi_n}{\mathrm{d}r}\bigg|_{r_0}=\frac{b}{r_0}. \tag{1.130b}$$

Following Lane and Thomas (1958), simple algebraic manipulations readily reveal that functions ϕ_n corresponding to different k_n are mutually orthogonal (and thus linearly

[46] decaying as some inverse power of r for $r\to\infty$

independent) on the interval $[0, r_0]$.[47] Consequently, the sought original solution of Eq. (1.128) can be expanded into this basis. Formally, one has

$$\psi(r) = \sum_{n=1}^{\infty} c_n \phi_n(r) \text{ for } 0 \leq r \leq r_0. \tag{1.131}$$

Multiplying (1.128) by ϕ_n and (1.129) by ψ, integrating from 0 to r_0 and finally subtracting both equations yields

$$\int_0^{r_0} \left[\phi_n \psi'' - \psi \phi_n''\right] \mathrm{d}r = \left(k_n^2 - k_0^2\right) \int_0^{r_0} \phi_n \psi \, \mathrm{d}r. \tag{1.132}$$

Left hand side of (1.132) is simplified by employing Green's theorem and taking into account the boundary conditions (1.130). This procedure renders directly the expansion coefficients c_n in (1.131) as

$$c_n = \frac{1}{r_0} \frac{\phi_n(r_0)}{k_n^2 - k_0^2} \left[r \frac{\mathrm{d}\psi}{\mathrm{d}r} - b\psi \right]_{r_0}. \tag{1.133}$$

Having obtained c_n and introducing the *R-matrix via*

$$R_b \equiv \frac{1}{r_0} \sum_{n=1}^{\infty} \frac{\phi_n^2(r_0)}{k_n^2 - k_0^2} \tag{1.134}$$

one can restate (1.131) into a form

$$R_b = \psi(r_0) \left(r_0 \left. \frac{\mathrm{d}\psi}{\mathrm{d}r} \right|_{r_0} - b\, \psi(r_0) \right)^{-1}, \tag{1.135}$$

where the R-matrix R_b manifests itself as a dimensionless quantity directly relating the value of ψ and its derivative at the boundary $r = r_0$. Knowledge of the logarithmic derivative of the solution of (1.128) enables us then in turn either to continue in the radial propagation by means of some other method or to extract relevant scattering quantities such as the reactance matrix provided the potential $V(r)$ is already negligible at $r = r_0$, the latter situation being abundant in the originally proposed nuclear physics applications where the interactions are typically of short range.

However, from the practical point of view, this approach is of limited use since to obtain the expansion basis ϕ_n by solving (1.129) is actually almost equivalent to solving the original problem (1.128) directly. On the other hand, we can introduce some approximative potential $V_0(r)$ and introduce functions φ_n^0 being solutions of

$$\left[-\frac{1}{2} \frac{\mathrm{d}^2}{\mathrm{d}r^2} + V_0(r) - \frac{1}{2}\kappa_n^2 \right] \varphi_n^0(r) = 0 \tag{1.136}$$

obeying the same boundary conditions (1.130) as before. The original functions ϕ_n can be then approximated by linear combinations of φ_n^0 as

$$\phi_i \approx \varphi^{(N)} \equiv \sum_{j=1}^{N} \alpha_{ji}^{(N)} \varphi_j^0 \qquad i = 1, \ldots, N\,, \tag{1.137}$$

where the coefficients $\alpha_{ji}^{(N)}$ are obtained by diagonalizing the differential operator

$$-\frac{1}{2} \frac{\mathrm{d}^2}{\mathrm{d}r^2} + V(r) \tag{1.138}$$

[47] without loss of generality we can therefore assume that ϕ_n comprise an orthonormal set

in the basis φ_n^0. Resulting eigenvalues are denoted as $k_j^{(N)}$ for $j = 1, \ldots, N$. In order to ensure completeness, this set of N functions and eigenvalues is for $k \geq N+1$ augmented by φ_k^0 and κ_k^2, respectively. For the sake of clarity, the notation $\varphi_j^{(N)}$ is used for the entire basis with the proviso that $\varphi_j^{(N)} = \varphi_j^0$ for $j > N$. An N-term approximation $\psi^{(N)}(r)$ to the solution of (1.128) is then analogically to (1.131) sought in the form

$$\psi^{(N)}(r) = \sum_{j=1}^{\infty} c_j^{(N)} \varphi_j^{(N)}(r) \text{ for } 0 \leq r \leq r_0. \tag{1.139}$$

Assuming that the differential operator (1.138) is diagonal also in the augmented basis and that $\psi^{(N)}(r)$ represents its eigenfunction corresponding to k_0^2 one can perform similar manipulations as leading to (1.133) obtaining a relation for the coefficients $c_j^{(N)}$ to wit

$$c_j^{(N)} = \frac{1}{r_0} \frac{\phi_j^{(N)}(r_0)}{\kappa_n^2 - k_0^2} \Big[r \frac{\mathrm{d}\psi^{(N)}}{\mathrm{d}r} - b\, \psi^{(N)} \Big]_{r_0}. \tag{1.140}$$

Thus the approximative R-matrix expression is now

$$R_b^{(N)} \equiv \frac{1}{r_0} \sum_{n=1}^{\infty} \frac{\phi_n^{(N)}(r_0)^2}{{k_n^{(N)}}^2 - k_0^2}. \tag{1.141}$$

Of course in practical applications, the infinite summation in (1.141) has to be somehow truncated. However, it turns out that naive omission of terms with $n > N$ leads to very slow convergence due to the inherent discontinuity of the derivative of $\phi^{(N)}$ at r_0. An alternative tack has been proposed by Buttle (1967), in the spirit of which the author considers the part of the summation (1.141) for $n > N$, *i.e.*,

$$\Delta R_b^{(N)} \equiv \frac{1}{r_0} \sum_{n=N+1}^{\infty} \frac{\phi_n^{(N)}(r_0)^2}{{k_n^{(N)}}^2 - k_0^2} = \frac{1}{r_0} \sum_{n=N+1}^{\infty} \frac{\varphi_n^0(r_0)^2}{\kappa_n^2 - k_0^2}. \tag{1.142}$$

The key observation rests then in the fact that (1.142) is actually equivalent to

$$\left(\frac{r_0}{\chi_0(r_0)} \left. \frac{\mathrm{d}\chi_0}{\mathrm{d}r} \right|_{r_0} - b\, \chi_0(r_0) \right)^{-1} - \frac{1}{r_0} \sum_{n=1}^{N} \frac{\varphi_n^0(r_0)^2}{\kappa_n^2 - k_0^2}. \tag{1.143}$$

The first term is linked with the logarithmic derivative of the solution of (1.136) corresponding to the considered incident energy $k_0^2/2$. Inserting (1.143) into (1.141) yields "Buttle–corrected" expression for the approximate R-matrix, namely

$$R_b^{(N)} \equiv \frac{1}{r_0} \sum_{n=1}^{N} \frac{\phi_n^{(N)}(r_0)^2}{{k_n^{(N)}}^2 - k_0^2} - \frac{1}{r_0} \sum_{n=1}^{N} \frac{\varphi_n^0(r_0)^2}{\kappa_n^2 - k_0^2} + \left[\frac{r_0}{\chi_0(r_0)} \left. \frac{\mathrm{d}\chi_0}{\mathrm{d}r} \right|_{r_0} - b\, \chi_0(r_0) \right]^{-1}. \tag{1.144}$$

Explicit form of analogical corrections to the constructed wave function are discussed in terms of projection formalism by Zvijac et al. (1975).

Although it might seem that the introduction of the approximative potential $V_0(r)$ in (1.136) for potential scattering calculations brings no computational merits since the original problem (1.128) could be in principle attacked directly, the real "power" of the approach (1.144) reveals itself in more complicated settings such as, *e.g.*, in description of electron molecule collisions for which it can be naturally generalized and has proven to be quite powerful. For conceptual details as well as an overview of possible applications of this approach we refer to Burke and Robb (1976); Lane and Thomas (1958) or Aymar et al. (1996); Burke and Tennyson (2005) and references therein.

From the usual derivation adumbrated above, it might seem that the R-matrix method suffers by an internal inconsistency. To be more specific, the possible culprit is hidden in the fact that in practical applications, the expansion sum (1.131) contains a finite number of terms each of which satisfies the prescribed boundary conditions (1.130). Therefore the logarithmic derivative of the constructed solution (1.131) being a linear combination of ϕ_n will be also equal to b.[48] From the mathematical point of view, this is equivalent to the statement that the sum (1.131) converges uniformly only for $r < r_0$.

The actual value of the logarithmic derivative of the solution ψ is of course *a priori* unknown and therefore the approximative solution will be in general discontinuous in its first derivative. One possible way how to cope with this nuisance is to employ the above mentioned *Buttle's correction*. Techniques have been also proposed where the parameter b is adjusted iteratively in order to conform with the actual logarithmic derivative of ψ as elaborated by Fano and Lee (1973).

1.6.2 Variational approach

Alternatively, it turns out to be convenient to relax the requirements on the basis (1.131) as demonstrated by Kohn (1948) in terms of variational reformulation of the R-matrix approach, the extension of which for multichannel case is discussed by Jackson (1951) or Oberoi and Nesbet (1973). Elucidating overview of the underlying ideas has been summarized by Nesbet (2004, ch. 8).

In his milestone paper, Kohn (1948) introduces following functional

$$\begin{aligned}\Xi_\lambda[\phi] &\equiv \int_0^{r_0} \mathrm{d}r\, \phi(r) \left(-\frac{1}{2}\frac{\mathrm{d}^2}{\mathrm{d}r^2} + V(r) - \frac{1}{2}k_0^2\right) \phi(r) = \\ &= \int_0^{r_0} \mathrm{d}r\, \left[\frac{1}{2}\left(\phi'(r)\right)^2 + \left(V - \frac{1}{2}k_0^2\right)\phi^2(r)\right] - \frac{1}{2}\lambda\phi^2(r_0).\end{aligned} \tag{1.145}$$

The second equality in (1.145) follows after performing integration by parts and denoting the logarithmic derivative of ϕ at r_0 as λ. Kohn (1948) further emphasizes that for fixed energy, the value of λ as calculated from (1.145) is stationary.[49] Corresponding variation of the functional (1.145) with λ held fixed reads

$$\delta\Xi_\lambda = 2\int_0^{r_0} \mathrm{d}r\, \delta\phi\big[-\frac{1}{2}\frac{\mathrm{d}^2}{\mathrm{d}r^2} + V(r) - \frac{1}{2}k_0^2\big] + \delta\phi(r_0)\big[\phi'(r_0) - \lambda\varphi(r_0)\big] \tag{1.146}$$

vanishing identically if and only if

$$\begin{gathered}\big[-\frac{1}{2}\frac{\mathrm{d}^2}{\mathrm{d}r^2} + V(r) - \frac{1}{2}k_0^2\big]\varphi(r) = 0 \text{ for } 0 \le r \le r_0, \text{ and} \\ \lambda = \frac{\phi'(r_0)}{\phi(r_0)}.\end{gathered} \tag{1.147}$$

The sought solution ψ is now expanded into a basis η_i the elements of which are solely required to obey the zero boundary condition at the origin (1.130a) and be linearly independent. The functional (1.145) can be consequently varied with respect to the expansion coefficients c_i yielding a matrix equation of the form

$$\sum_j A_{ij}c_j = \lambda\eta_i(r_0)\psi(r_0) \tag{1.148}$$

[48] logarithmic derivative of a linear combination of terms each of which has logarithmic derivative λ is again equal to λ

[49] this observation is actually closely linked with similar approach in bound state calculations where one utilizes the stationarity property of k for fixed λ

with

$$A_{ij} \equiv \int_0^{r_0} \left[\eta_i' \eta_j' + \eta_i \left(2V - k_0^2 \right) \eta_j \right] \mathrm{d}r. \tag{1.149}$$

It can be shown that solution of (1.148) exists only for one particular value of λ which is thus in this way uniquely determined.[50] Solving formally for the coefficients c_j in (1.148), expressing the wave function ψ as corresponding linear combination and bearing in mind that the one channel R-matrix is related to λ as $R = (r_0\lambda)^{-1}$ furnishes the final expression

$$R = \frac{1}{r_0 \lambda} = \sum_{i,j} \eta_i(r_0) \left[A^{-1} \right]_{i,j} \eta_j(r_0). \tag{1.150}$$

An interesting connection between the variational approach and the original Wigner-Eisenbud (Wigner and Eisenbud, 1947) treatment has been presented in Robicheaux (1991), although essentially similar ideas can be found already in Jackson (1951). The key step is to explicitly exclude from the matrix A in (1.149) its dependence on the incident energy. By introducing the overlap matrix $S_{ij} = \int_0^{r_0} \eta_i \eta_j$, we can restate (1.149) as

$$\begin{aligned} A_{ij} =& \equiv \int_0^{r_0} \eta_i' \eta_j' + 2\eta_i V \eta_j \, \mathrm{d}r - k_0^2 \int_0^{r_0} \eta_i \eta_j \, \mathrm{d}r = \\ &= 2G_{ij} - k_0^2 S_{i,j}. \end{aligned} \tag{1.151}$$

Diagonalizing the symmetric matrix $\mathcal{G}$ in the (nonorthogonal) basis $\{\eta_i\}$ and storing its eigenvectors in the columns of a matrix $\mathcal{V}$ yields the relation $\mathcal{G}\mathcal{V} = \mathcal{S}\mathcal{V}$. Matrix $\mathcal{V}$ links two linearly independent bases so it is certainly regular. Moreover, the overlap matrix $\mathcal{S}$ turns out to be positive-definite (Szabo and Ostlund, 1996, p. 143). Since the eigenvectors are supposed to be normalized, one has by definition that $\mathcal{V}^\dagger \mathcal{S} \mathcal{V}$ is an identity matrix. Expressing $\mathcal{G}$ as $\mathcal{G} = \mathcal{S}\mathcal{V}\mathcal{V}^{-1}$ and substituting $\mathcal{V}^\dagger \mathcal{S}$ for $\mathcal{V}^{-1}$ yields finally the spectral decomposition

$$\mathcal{G} = \mathcal{S}\mathcal{V} \cdot \epsilon \mathcal{V}^\dagger \mathcal{S}.$$

Plugging this result into (1.149) and taking into account that $\mathcal{S}$ is identical with the inverse of $\mathcal{V}\mathcal{V}^\dagger$ enables to invert the matrix $\mathcal{A}$ explicitly

$$\mathcal{A}^{-1} = \left(2\mathcal{G} - k_0^2 \mathcal{S} \right)^{-1} = \mathcal{V} \cdot \left(2\epsilon - k_0^2 \right) \cdot \mathcal{V}^\dagger. \tag{1.152}$$

In combination with (1.150) this recovers the usual expression for the R-matrix, namely

$$R = \frac{1}{2r_0} \sum_i \frac{\varphi_i(r_0)^2}{E_0 - \epsilon_i} \quad \text{, with} \quad \varphi_i(r_0) = \sum_j V_{ji} \eta_j(r_0). \tag{1.153}$$

The functions φ_i represent the eigenfunctions of $\mathcal{G}$ and are in the literature also known as *surface amplitudes*.

Finally, we find interesting that a connection between the "classical" approach (Burke and Robb, 1976) and the variational treatment (Nesbet, 2004) can be also achieved by calculating explicitly the variational R-matrix expression (1.150) in a basis with fixed logarithmic derivative at the boundary r_0. Since we haven't found this derivation in other sources, we would like to present it briefly below. To this end, we

[50] this has been proven already in Kohn (1948) by means of the *matrix-determinant lemma* (Ding and Zhou, 2007) intended for evaluation of determinant of a rank-one updated matrix in terms of the original determinant

consider an orthogonal basis $\{\eta_i\}$ comprised of eigenfunctions of (1.129) obeying moreover the boundary conditions (1.130). Matrix elements of the matrix $\mathcal{A}$ in this basis are then easily expressible

$$A_{ij} = \frac{b}{r_0}\eta_i(r_0)\eta_j(r_0) + \left(k_i^2 - k_0^2\right)\delta_{i,j}. \tag{1.154}$$

This follows by employing integration by parts in (1.149) and taking into account the boundary conditions (1.130) together with the orthogonality property of the basis $\{\eta_i\}$. Now we need to evaluate the inverse of this matrix. This is probably most easily done by utilizing the Sherman-Morrison formula (Bartlett, 1951)

$$\left(\mathcal{C} + |u\rangle\,|v\rangle\right)^{-1} = \mathcal{C}^{-1} - \frac{\mathcal{C}^{-1}\,|u\rangle\,\langle v|\,\mathcal{C}^{-1}}{1 + \langle v|C^{-1}|u\rangle} \tag{1.155}$$

applicable for any regular matrix $\mathcal{C}$. In the present notation, we have that $C_{i,j} = (k_i^2 - k_0^2)\delta_{i,j}$ and $|u\rangle_i = |v\rangle_i = \sqrt{b/r_0}\eta_i(r_0)$. Thus the matrix elements of the inverse matrix are given as

$$\left(A^{-1}\right)_{ij} = \frac{1}{k_i^2 - k_0^2}\delta_{i,j} - \frac{b}{r_0}\frac{\frac{1}{k_i^2-k_0^2}\eta_i(r_0)\eta_j(r_0)\frac{1}{k_j^2-k_0^2}}{1 + \frac{b}{r_0}\sum_l \frac{\eta_l(r_0)\eta_l(r_0)}{k_l^2-k_0^2}} \tag{1.156}$$

Substituting into (1.150) and calling upon the definition of R_b in (1.134) yields a relation between R and R_b

$$R = R_b - \frac{R_b^2}{1 + bR_b} = \frac{R_b}{1 + bR_b}, \tag{1.157}$$

which essentially recovers Eq. (1.135).

CHAPTER
TWO

INTERACTIONS

2.1 Static Exchange approximation

The derivation of the static exchange approximation as given by Huo and Gianturco (1995) contains several misprints and therefore we would like to present detailed sketch of the entire procedure along very similar lines instead of just referring to this source.

The considered system comprised of the incident electron and target molecule is expected to be described by a wave function Ψ that depends[1] on the coordinates $\vec{x}_1, \ldots, \vec{x}_N$ of the bound electrons and $\vec{x}_{N+1}$ representing the scattered electron. Wave function Ψ is of course sought as an eigenfunction of the total Hamiltonian $\mathbf{H}$ corresponding to the total energy E to wit[2]

$$\mathbf{H}\Psi(1,\ldots,N+1) = E\Psi(1,\ldots,N+1), \tag{2.1}$$

where the Hamiltonian $\mathbf{H}$ takes the usual well-known form[3]

$$\mathbf{H} = \mathbf{H}_{\mathrm{m}}(1,\ldots,N) + \mathbf{V}_{\mathrm{int}}(1,\ldots,N+1) + \mathbf{T}_{N+1}, \text{ with} \tag{2.2a}$$

$$\mathbf{V}_{\mathrm{int}} = -\sum_{i=1}^{N} \frac{1}{\left|\vec{r}_{N+1} - \vec{r}_i\right|} + \sum_{i=1}^{M} \frac{Z_j}{\left|\vec{r}_{N+1} - \vec{R}_j\right|}. \tag{2.2b}$$

The "molecular Hamiltonian" denoted as $\mathbf{H}_{\mathrm{m}}$ in (2.2a) is just a shorthand for the corresponding sum of one-electron Hamiltonians and electron-electron repulsion (within the molecule) terms. The operator $\mathbf{H}_{\mathrm{m}}(1,\ldots,N)$ defines a set of eigenvalues and eigenfunctions

$$\mathbf{H}_{\mathrm{m}}(1,\ldots,N)\Phi_{\mathrm{m}}(1,\ldots,N) = E_{\mathrm{m}}\Phi_{\mathrm{m}}(1,\ldots,N), \tag{2.3}$$

approximating the electronic levels of the target molecule rendered at the considered fixed nuclear geometry. The wave function Ψ is a function of $N+1$ electron variables and as such can be expanded into (presumably) complete basis (2.3) comprised of the functions Φ_{m} of N variables with expansion coefficients F_{m} depending thus on the remaining variable

$$\Psi = \mathcal{A}\sum_{\mathrm{m}} \Phi_{\mathrm{m}} F_{\mathrm{m}}, \tag{2.4}$$

where the Pauli exclusion principle reflects itself in the presence of the $(N+1)$-electron antisymmetrizer $\mathcal{A}$.

[1] the molecule (disposing of N electrons and M nuclei witch charges $\{Z_j\}_{j=1}^{M}$) is assumed to be rigid therefore the nuclear positions specified by $\{\vec{R}_j\}_{j=1}^{M}$ are constant

[2] the independent variables of the i^{th} electron entering Ψ have been subsumed into a label i

[3] symbol $(1,\ldots,j)$ underlines explicitly that the corresponding quantity is dependent on the coordinates of electrons $1,\ldots,j$

The basic idea of *static exchange* (SE) approximation is then closely connected with the product-like expansion (2.4), for which one can hope that keeping explicitly just the first term $m = 0$ will furnish reasonable results. Approximate incorporation of molecular terms $m > 0$ is in the literature known usually as *static exchange + polarization* method.

Taking into account that Ψ_0 is already antisymmetrized in its variables, a little juggling with permutations reveals quickly that one can obtain normalized[4] SE–approximation to Ψ in the form[5]

$$\Psi_{\mathrm{SE}} = \frac{1}{\sqrt{N+1}} \sum_{i=1}^{N+1} (-1)^{N+i-1} \Phi_{\mathrm{m}}\big(\{1,\ldots,N+1\}\backslash\{i\}\big) F_0(i), \tag{2.5}$$

where we have employed the notation $\big(\{1,\ldots,N+1\}\backslash\{i\}\big)$ for specifying the coordinates of all $N+1$ electrons excluding the i^{th}. In order to obtain an equation for F_0, it is necessary to project the Schrödinger equation (2.1) onto the first target state Φ_0. Exploiting permutation symmetry and antisymmetry of $\mathbf{H}$ and Φ_0, respectively, it is quite straightforward to show that this projection procedure yields following condition

$$\begin{aligned} \int \Phi_0^*(1,\ldots,N)\big[\mathbf{H}(1,\ldots,N) - E\big]\big[\Phi_0\big(\{1,\ldots,N+1\}\backslash\{N+1\}\big) F_0(N+1) \\ - N\Phi_0\big(\{1,\ldots,N+1\}\backslash\{N\}\big) F_0(N)\big]\,\mathrm{d}\tau = 0. \end{aligned} \tag{2.6}$$

Equation (2.6) admits further significant simplification provided one assumes that Φ_0 corresponds to Hartree-Fock ground state of a closed shell molecule. In that case, since Ψ_{SE} is presupposed in a form of a single determinant, the Pauli exclusion principle reflects itself in the requirement that the one-electron continuum function F_0 be orthogonal to all bound orbitals with the same symmetry comprising Ψ_0. Employing Slater rules (Szabo and Ostlund, 1996) for evaluation of the matrix elements between functions in determinantal form readily furnishes sought integro-differential equation for F_0, namely

$$\Big[-\frac{1}{2}\Delta_{\vec{r}} - \underbrace{(E - E_0)}_{-\frac{1}{2}k^2} + V_{\mathrm{st.}}(\vec{r})\Big] F_0(\vec{r}) = \int \mathrm{d}\vec{s}\; V_{\mathrm{ex.}}\big(\vec{r},\vec{s}\big) F_0(\vec{s}). \tag{2.7}$$

The *static* potential $V_{\mathrm{st.}}$ is rendered *via* Coulombic repulsion terms

$$V_{\mathrm{st.}}(\vec{r}) = \sum_{i=1}^{N} \int \mathrm{d}\vec{s}\, \frac{\phi_i^*(\vec{s})\phi_i(\vec{s})}{\big|\vec{r}-\vec{s}\big|} + \sum_{j=1}^{M} \frac{Z_j}{\big|\vec{r}-\vec{R}_j\big|}, \tag{2.8}$$

whereas the kernel $V_{\mathrm{ex.}}$ of the integral *exchange* operator is slightly more complicated

$$V_{\mathrm{ex.}}(\vec{r},\vec{s}) = \sum_{i=1}^{N} \frac{\phi_i^*(\vec{s})\phi_i(\vec{r})}{\big|\vec{r}-\vec{s}\big|}. \tag{2.9}$$

2.2 Exchange potential

In the preceding section, it has been shown how the incorporation of the Pauli exclusion principle manifests itself in nonlocal potential terms which in turn complicate significantly numerical treatment of the resulting Schrödinger equation (2.7) for the

[4] at least as long as Ψ_0 is a single determinant and F_0 is orthogonal to all orbitals entering Φ_0

[5] the factor $(-1)^N$ is merely an overall phase and can be thus dropped with impunity, nevertheless its presence is in accordance with Eq. (2.5) in Morrison and Collins (1978)

"continuum orbital", the function F_0, introduced in Eq. (2.5). In principle, it is possible to handle the nonlocal term in Eq. (2.7) directly and such methods are known in the literature as *Exact Static Exchange* (ESE). In this regard, one typically employs some iterative approach (Collins et al., 1980) with possible incorporation of the celebrated Schwinger variational principle [*e.g.*, (Lucchese and McKoy, 1979; Takatsuka and McKoy, 1981) or (Winstead and McKoy, 2007) and references therein]. As regards the direct methods, adaptation of the Volterra propagator method of Section 1.5 for the ESE treatment is discussed by Collins and Schneider (1981) in the framework of their *Linear-Algebraic* (LA) method. More recently, Feng et al. (2009) have incorporated the exchange term in their study of vibrational excitations of N_2 induced by low-energy electrons by considering the exchange kernel (2.9) *per se*, expanding the bound orbitals (parametrically depending on the internuclear distance R) using single center expansion techniques, sandwiching resulting expression between initial and final vibrational states, performing the integration over R and working in the partial wave formalism. However, these methods are not subject of this section and for a concise overview we refer to Huo and Gianturco (1995, ch. 4).

From the computational point view, much more tractable tack consists in replacing the nonlocal potential part by some local approximation, the energy dependence of which is practically unavoidable. Common denominator of a broad class of methods is to use the *free electron gas* approximation for the bound electrons of the target, *i.e.*, to treat them as noninteracting fermions occupying some prescribed volume V. Corresponding one-electron wave functions are just simple plane waves[6] (normalized to V) $\mathrm{e}^{\mathrm{i}\vec{k}_j\cdot\vec{r}}/\sqrt{V}$. Moreover, for the purposes of evaluation of the exchange term, one might suppose that the incident electron is not influenced significantly and therefore invoke the first Born approximation, *i.e.*, approximate $F_0(r)$ by a term proportional to $\mathrm{e}^{\mathrm{i}\vec{k}\cdot\vec{r}}$, with $\vec{k}$ being related to the incident energy E_i as $|\vec{k}| = \sqrt{2E_i}$. Following the derivation neatly delineated by Morrison and Collins (1978) one can plug these assumptions into Eq. (2.7). By performing integration over the volume V and summing over bound orbitals using techniques summarized in Slater (1960, Appendix 22), one obtains the *Free Electron Gas* (FEG) approximation to the exchange potential

$$V_{\mathrm{FEG}}(\vec{r}) \equiv -\frac{2}{\pi} k_{\mathrm{F}} F(\eta), \tag{2.10}$$

with

$$F(\eta) \stackrel{\mathrm{def}}{=} \frac{1}{2} + \frac{1-\eta^2}{4\eta} \log\left|\frac{1+\eta}{1-\eta}\right| \text{ and } \eta \equiv \frac{k}{k_{\mathrm{F}}}. \tag{2.11}$$

The symbol k_{F} denotes the Fermi momentum expressible in terms of the target charge density ρ by well-known formula

$$k_{\mathrm{F}} = \left(3\pi^2\rho\right)^{\frac{1}{3}}. \tag{2.12}$$

The potential (2.10) is directly connected with a class of so-called $X\alpha$ potentials $V_{X\alpha}(\vec{r})$ approximating exchange terms as

$$V_{X\alpha}(\vec{r}) = -\left(\frac{3\alpha}{2\pi}\right)\left(3\pi^2\rho\right)^{\frac{1}{3}}. \tag{2.13}$$

Bearing in mind the definition of the Fermi momentum (2.12) and comparing (2.13) with (2.10) immediately reveals that the $X\alpha$ potential can be actually obtained from (2.10) by imposing further approximation on the $F(\eta)$ term. The tack proposed by

[6] subscript j numbers individual bound orbitals

Slater (1960) is equivalent to replacing $F(\eta)$ in (2.10) by its average[7] over the Fermi sphere yielding thus $\alpha = 1$. On the other hand, Gáspár (1954) and later Kohn and Sham (1965) have shown that considerations based on utilization of the variational principle result in smaller value of $\alpha = 2/3$. Although the potential (2.13) has found its practical use in the past (see, *e.g.*, Tully and Berry (1969) or Riley and Truhlar (1975) and references therein), its use for scattering calculations is rather limited as pointed out by O'Connell and Lane (1983).

However, potential (2.10) is amenable to further modifications which make it in turn much more satisfactory as has been observed[8] by Hara (1967). First of all, the charge density in (2.12) is of course not constant. In this sense, the Fermi momentum and consequently also the parameter η can be made position dependent by assuming that (2.12) holds for all $\vec{r}$ to wit

$$k_{\mathrm{F}}(\vec{r}) = \left(3\pi^2\rho(\vec{r})\right)^{\frac{1}{3}}. \tag{2.14}$$

Second step (Morrison and Collins, 1978) consists in replacing the momentum k in the definition (2.11) by a "local momentum" $\kappa(\vec{r})$, the value of which is fixed naturally by energy conservation

$$\frac{1}{2}\kappa(\vec{r})^2 + V(\vec{r}) = E_i, \tag{2.15}$$

where V denotes the potential governing the motion of the impinging electron. Further, the outermost bound electron (its momentum being equal to the Fermi momentum k_{F}) can be approximatively considered as moving in the same potential V. Since its energy is (apart from the sign) equal to the ionization potential I, energy conservation yields

$$\frac{1}{2}k_{\mathrm{F}}(\vec{r})^2 + V(\vec{r}) = -I. \tag{2.16}$$

Solving (2.16) and (2.15) for κ readily gives

$$\kappa(\vec{r})^2 = 2(E_i + I) + k_{\mathrm{F}}(\vec{r})^2, \tag{2.17}$$

which reflects itself in a modified formula for η

$$\eta(\vec{r})^2 = 1 + 2\frac{(E_i + I)}{k_{\mathrm{F}}(\vec{r})^2}. \tag{2.18}$$

From the formal point of view, the local momentum $\kappa(\vec{r})$ should far from the target molecule correspond just to the incident energy E_i, *i.e.*, $\kappa(\vec{r}) \to 2E_i$. However, this natural requirement is not compatible with (2.17) due to the presence of the ionization potential I. Therefore, it has been suggested by Riley and Truhlar (1975) to disregard I in (2.17). Riley and Truhlar (1975) call resultant approximation as *Asymptotically Adjusted Free Electron Gas Exchange* (AAFEGE). The authors also introduce another approximative treatment, the *Second Order Free Electron Gas Exchange* (SOFEGE), the idea of which is to employ instead of (2.17) a prescription of the form

$$\frac{1}{2}\kappa(\vec{r})^2 = E_i - V_{\mathrm{st.}}(\vec{r}), \tag{2.19}$$

where $V_{\mathrm{st.}}$ represents the static potential of Section 2.1. It is clear that (2.19) exhibits proper asymptotic behavior in the sense mentioned above.

[7] being equal to 3/4

[8] by comparing formulae from various sources, one should be take into account that this paper contains several misprints as pointed out by Riley and Truhlar (1975)

Rather than disregarding the ionization potential I altogether, it turned out to be much more convenient to treat I as a freely adjustable parameter the value of which is numerically tuned in order to reproduce some chosen property of a particular quantity of the scattering calculations. Because of this tunning, this modified method is known as *Tuned Free Electron Gas* (TFEGE) approximation. Although I should be considered as a "global" parameter characterizing the target molecule, Sun et al. (1995) in their body-frame FNO e^-–N_2 scattering calculations have tuned I for the Σ and Π symmetries independently in order to obtain better agreement with the experiment.

An interesting alternative to the former approach has been proposed by Riley and Truhlar (1975). The authors approximate the exchange term on the right hand side of (2.7) in an energy dependent local formal $-L(\vec{r}, E_0)F_0(\vec{r})$. In this notation, they restate Eq. (2.7) as

$$\left[\Delta_{\vec{r}} + \kappa_0^2(\vec{r})\right] F_0(\vec{r}) = 0, \text{ with } \frac{1}{2}\kappa_0^2(\vec{r}) = E_0 - V_{\text{st.}} - L(\vec{r}, E_0) \tag{2.20}$$

The original individual contributions to the exchange integral

$$M_i(\vec{r}) = \int \mathrm{d}\vec{s}\, \frac{\phi_i^*(\vec{s})F_0(\vec{s})}{\left|\vec{r} - \vec{s}\right|}, \tag{2.21}$$

understood as functions of $\vec{r}$ can be without loss of generality expressed as a product of a presumably slowly varying amplitude $A_i(\vec{r})$ and (rapidly oscillating) function F_0. Acting by Δ on (2.21), plugging in the definition of the local momentum κ_0 and rearranging terms yields an expansion for A_i in inverse powers of κ_0^2, the lowest order term of which is

$$M_i(\vec{r}) \approx 4\pi \frac{\phi_i^*(\vec{r})}{\kappa_0^2(\vec{r})} + \dots . \tag{2.22}$$

At this level of approximation, the exchange contribution thus reads

$$\sum_{i=1}^{N} \left|\phi_i(\vec{r})\right|^2 \frac{2\pi}{E_0 - V_{\text{st.}}(\vec{r}) - L(\vec{r}, E_0)} F_0(\vec{r}). \tag{2.23}$$

Compatibility requirement with the original local approximative form $-L(\vec{r}, E_0)F_0(\vec{r})$ furnishes quadratic equation for the function $L(\vec{r}, E_0)$, the admissible[9] solution of which is[10]

$$2L(\vec{r}, E_0) = \left(E_0 - V_{\text{st.}}\right) - \left[\left(E_0 - V_{\text{st.}}(\vec{r})\right)^2 + 4\pi\rho(\vec{r})\right]^{\frac{1}{2}}. \tag{2.24}$$

Riley and Truhlar (1975) call the approximation obtained in this way as *Semiclassical Exchange approximation* (SCE). In the limit of high energy E_0, it is possible to expand the square root term in (2.24) by obtaining the *High Energy Exchange* (HEE) approximation

$$L(\vec{r}, E_0) \approx -\frac{\pi\rho(\vec{r})}{E_0 - V_{\text{st.}}(\vec{r})} + \mathcal{O}\left(\rho^2\right). \tag{2.25}$$

All these methods approximating the ESE approach are in the literature usually collectively denoted as *Static Model Exchange* (SME). One of their serious drawbacks is that in general, the orthogonality condition (mentioned below Eq. (2.6)) of the continuum orbital F_0 to the bound target orbitals is not guaranteed. On benchmark $e^- - Li$ scattering calculations, it has been demonstrated (Collins et al., 1980) that omission of this property can lead to spurious resonant features in the $\mathcal{K}$-matrix eigenphase sums

[9] *i.e.*, the solution vanishing for $E_0 \to \infty$

[10] closed shell molecule is assumed for which the sum $\sum_{i=1}^{N} \left|\phi_i(\vec{r})\right|^2$ reduces to the charge density $\rho(\vec{r})$

understood as functions of energy which are not at all present in the ESE treatment. Therefore the authors suggest additional enforcement of the orthogonality requirement along the lines of the ideas described in Burke and Chandra (1972). Due to this "added" orthogonality constraint, Salvini and Thompson (1981) call modified versions of the methods presented above as OFEGE and OAAFEGE.

2.3 Correlation–polarization potential

The Static Exchange approximation adumbrated briefly in Section 2.1 disregards one important feature of the electron–molecule interaction. More specifically, the culprit is hidden in the fact that in this framework, one does not take into account the distortion (polarization) of the target charge density induced by the electric field of the impinging electron. This effect can be qualitatively understood in a semi-classical picture (Lane, 1980) in which the slowly incoming electron causes redistribution of the target charge density resulting in an induced dipole moment. This dipole moment can be consequently thought of as "acting" back on the electron giving rise to an attractive *polarization* contribution to the interaction potential. However, this simple picture is unacceptable in the vicinity of the nuclei, where the bound and the incoming electrons should be treated on the same footing. In other words, indistinguishability of the electrons and the inherent many-body character of the electron-target system in this region of space reflect in *correlation* effects.

From the (formal) quantum mechanical point of view, these flaws of the SE approximation are closely linked with the fact that only one (ground) target state contributes to the total wave function (2.4). In this sense, incorporation of these polarization effects is usually attributed to virtual electronic excitations of the target (Castillejo et al., 1960). However, direct inclusion of more electronic terms is far beyond the SE approximation and would drastically increase the computational demands. Therefore in order to stay within the SE framework, one seeks some compromise in terms of an approximative optical potential, which is for reasons mentioned in the previous paragraph denoted usually as *correlation-polarization* potential $\mathbf{V}_{\mathrm{cp}}$.

The situation is far more simple for the long range part of the correlation-polarization potential where only the polarization effects come into play. The corresponding asymptotic form has been shown (Almbladh and von Barth, 1985) to exhibit following behavior

$$-\frac{1}{2r^6}\sum_{i,j=1}^{3}\alpha_{ij}x_i x_j, \tag{2.26}$$

with α_{ij} representing the molecular polarizability tensor. For diatomic molecules, being the subject of the following discussion, only two components of α_{ij} are independent due to the cylindrical symmetry. The polarizability in the direction of the molecular axis α_{zz} is denoted usually as *parallel*, $\alpha_{||}$, whereas the component corresponding to the perpendicular direction $\alpha_{xx} = \alpha_{yy}$ is known as *perpendicular* polarizability $\alpha_{\perp}$. In this case, only two spherical irreducible components of the polarizability tensor are nonvanishing. Namely $(0,0)$ and $(2,0)$ being given in terms of Cartesian components (Edmonds, 1996) as $-\mathrm{Tr}\,\alpha/\sqrt{3}$ and $(3\alpha_{zz} - \mathrm{Tr}\,\alpha)/\sqrt{6}$, respectively. Utilizing the fact that the position unit vector $\hat{r}$ can be interpreted as a tensor operator with rank 1 corresponding to $\sqrt{4\pi/3}\mathbb{Y}$, where $\mathbb{Y}$ has spherical components $\mathrm{Y}_{1,q}, q = -1,\ldots,1$, forming the scalar product of the tensors α_{ij}, $x_i x_j$ implied by (2.26) in terms of spherical components and taking into account that only $(0,0)$ and $(2,0)$ components contribute yields after some manipulations a simplified form (Dalgarno and Lewis, 1956) of the

potential

$$\mathbf{V}_{\rm cp}(\vec{r}) \xrightarrow{r\to\infty} -\frac{\alpha_0}{2r^4} - \frac{\alpha_2}{2r^4}\mathrm{P}_2(\cos\theta), \tag{2.27}$$

where the *spherical* $\alpha_0 = (\alpha_{||}+2\alpha_\perp)/3$ and *non-spherical* $\alpha_2 = 2(\alpha_{||}-\alpha_\perp)/3$ polarizabilities have been introduced. In (2.27), one formally requires that $r \to \infty$, nevertheless the "asymptotic region" is for small diatomic molecules reached already for $r \gtrsim 10$ a.u. (Morrison and Hay, 1979).

Pioneering approaches to the problem of determination of the correlation-polarization potential were based on the knowledge of this asymptotic form. It might be tempting to suppose that (2.27) holds for all r. However, in the vicinity of the nuclei, the electron gains large local kinetic energy and the target charge density is not able to adjust instantly. It turns then out that the potential (2.27) overestimates the actual interaction for small r. For this reason, a simple phenomenological rectification consists in multiplying the potential (2.27) by an cut-off function $C(r)$ containing typically some adjustable parameters which can be in turn fitted to reproduce some particular feature in the experimental cross-section data. Typical form of $C(r)$ which has been used in the past reads

$$C(r) = 1 - \exp\Big[-\Big(\frac{r}{r_c}\Big)^p\Big], \tag{2.28}$$

with r_c representing the cut-off radius (*i.e.*, radius of the sphere from which one tries to effectively "remove" the polarization interaction) and exponent p. This approach can be traced back to the work of Biermann (1943), where the authors use (2.28) with $p = 5$ for investigation of atomic polarizabilities. For an overview of other possible choices of the cut-off function $C(r)$ we refer to Breig and Lin (1965) or Truhlar and Brandt (1976); Truhlar and Rice (1970) and references therein.[11]

The semiclassical picture of the incident electron at intermediate and large distances from the target molecule is quantum mechanically equivalent to an *adiabatic* description in which the scattered electron is supposed to be held fixed in space at location $\vec{r}_e$ and the target charge density is allowed to relax under its influence. More explicitly, the adiabatic Hamiltonian ${}^{\rm A}\mathbf{H}$ for the target plus the incident electron takes the form

$${}^{\rm A}\mathbf{H}(\vec{r}_{\rm e}, \vec{r}_i, \vec{R}_j) = \mathbf{H}_{\rm m}^{(e)}(\vec{r}_i, \vec{R}_j) + \mathbf{V}_{\rm int}(\vec{r}_{\rm e}, \vec{r}_i, \vec{R}_j) \tag{2.29}$$

where the $\mathbf{H}_{\rm m}^{(e)}$ is the electronic Hamiltonian (1.11) and the Coulombic perturbation $\mathbf{V}_{\rm int}$ reads

$$\mathbf{V}_{\rm int}(\vec{r}_{\rm e}, \vec{r}_i, \vec{R}_j) = \sum_{i=1}^{N} \frac{1}{|\vec{r}_{\rm e} - \vec{r}_i|} - \sum_{j=1}^{M} \frac{Z_j}{|\vec{r}_{\rm e} - \vec{R}_j|}. \tag{2.30}$$

An essential step in the calculation of the polarization potential is to determine the ground state wave function $\psi_0^{(\rm p)}(\vec{r}_{\rm i};\, \vec{r}_{\rm e}, \vec{R}_j)$ of the "polarized" Hamiltonian (2.29). Corresponding "polarized" energy is then naturally given as[12]

$$E_0^{(\rm p)}(\vec{r}_{\rm e};\, \vec{R}_j) = \big\langle \psi_0^{(\rm p)}(\vec{r}_{\rm i};\, \vec{r}_{\rm e}, \vec{R}_j)\big|\, {}^{\rm A}\mathbf{H}(\vec{r}_{\rm e}, \vec{r}_i, \vec{R}_j)\big|\psi_0^{(\rm p)}(\vec{r}_{\rm i};\, \vec{r}_{\rm e}, \vec{R}_j)\big\rangle_{\vec{r}_{\rm i}}. \tag{2.31}$$

Since the target density is allowed to relax, this quantity is expected to be lower as

[11] *e.g.*, Truhlar and Brandt (1976) suggest that the cut-off function (2.28) (for a diatomic molecule) should be chosen in such a way that the polarization effect is attenuated not for $r \to 0$ but in the vicinity of the nuclei. Therefore the authors choose $C(r)$ in the form $g(r_+)g(r_-)$, where $g(r) = 1-\exp(-r^3/b^3)$ and r_+, r_- represent distance of the incident electron from the respective nuclei.

[12] semicolon in (2.31) suggests parametric dependence on the nuclear geometry $\{\vec{R}_j\}$ and the subscript $\vec{r}_{\rm i}$ symbolizes integration over the electronic coordinates

compared to the ground state energy[13] of the undistorted system[14]

$$E_0(\vec{r}_{\rm e};\,\vec{R}_j) = \big\langle \psi_0(\vec{r}_{\rm i};\,\vec{R}_j)\big|{}^{\rm A}\mathbf{H}(\vec{r}_{\rm e},\vec{r}_i,\vec{R}_j)\big|\psi_0(\vec{r}_{\rm i};\,\vec{R}_j)\big\rangle_{\vec{r}_{\rm i}}, \tag{2.32}$$

when no distortion of the target is possible giving thus rise to an attractive potential as has been already mentioned above. The *adiabatic polarization potential* is then simply defined as the difference of (2.31) and (2.32)

$$\mathbf{V}^{\rm A}_{\rm cp}(\vec{r}_{\rm e};\,\vec{R}_j) \equiv E_0^{\rm (p)}(\vec{r}_{\rm e};\,\vec{R}_j) - E_0(\vec{r}_{\rm e};\,\vec{R}_j). \tag{2.33}$$

This gambit has been extensively studied in the past among others by Morrison and Hay (1979) and Dixon et al. (1979); Truhlar et al. (1979) where the authors used this approach in their calculations regarding electron scattering off H_2 and Li_2 molecules. However, potential (2.33) suffers of course from the fact that the adiabatic picture breaks down near the nuclei. Probably the simplest tack how to rectify this nuisance is the so-called *Non-Penetrating Approximation* (NP) Henry and Lane (1969); Temkin (1957); Temkin and Lamkin (1961). Roughly speaking, in the NP framework, one simply multiplies the adiabatic Hamiltonian (2.29) by a step-function which essentially "switches off the interaction for target density outside the radial position of the projectile" (Morrison et al., 1987). Following Gibson and Morrison (1984), one can express the Coulombic term $1/|\vec{r}_{\rm e}-\vec{r}_i|$ in (2.30) *via* modified multipole expansion

$$\frac{1}{\big|\vec{r}_{\rm e}-\vec{r}_i\big|} = \begin{cases} \dfrac{1}{r_{\rm e}}\displaystyle\sum_{\lambda=0}^{\infty}\sum_{\mu=-\lambda}^{\lambda}\frac{4\pi}{2\lambda+1},\Big(\frac{r}{r_{\rm e}}\Big)^{\lambda}\mathrm{Y}^{*}_{\lambda,\,\mu}\big(\hat{r}_i\big)\mathrm{Y}_{\lambda,\,\mu}\big(\hat{r}_{\rm e}\big). & r_i < r_{\rm e} \\ 0 & r_i > r_{\rm e} \end{cases} \tag{2.34}$$

This expression is consequently used in all calculations leading to the potential (2.33) which is now designated as *non-adiabatic*. For reasons discussed by Gibson and Morrison (1984); Lane and Henry (1968) the monopole $\lambda = 0$ term in (2.34) is usually disregarded. In their study of $e^- - N_2$ scattering, Morrison et al. (1987) have employed further approximation to (2.34), namely they retained just the dipole ($\lambda = 1$) term. The resulting approximation is then called by Morrison et al. (1987) as *Better Than Adiabatic Dipole* (BTAD) potential. Their approach closely resembles the *Polarized Orbital* (PO) method proposed thirty years earlier by Temkin (1957); Temkin and Lamkin (1961). However, the Temkin (1957)'s PO treatment differs from the BTAD approximation of Morrison et al. (1987) in several important aspects. Similarly to the BTAD approach, it employs the non-penetrating approximation retaining only the dipole term in (2.34). Unlike BTAD, in the PO method one then computes the polarized wave function of the system (2.29) in the first order perturbation theory. Original PO approach has been used, *e.g.*, in Onda and Temkin (1983) in combination with the FEGE exchange model potential for study of $e^- - N_2$ collisions.

An alternative way how to incorporate the non-adiabatic effects in the theoretical description has been proposed by Bouferguene et al. (1999) and later extended by Feng et al. (2003). In this innovative procedure, the incident electron is described as a continuous normalized Gaussian charge density

$$\rho(\vec{r}) \equiv -\left(\frac{2\xi}{\pi}\right)^{\frac{3}{2}}\mathrm{e}^{-2\xi|\vec{r}-\vec{r}_e|^2}, \tag{2.35}$$

[13] being equal to the sum of the Born-Oppenheimer electronic energy of the target and the static potential (2.8)

[14] Gibson and Morrison (1984) speak about the undistorted system as being described in "frozen-core" approximation, *i.e.*, the system is not allowed to relax

where the parameter[15] ξ depends on the radial distance of the impinging electron as

$$\xi = \beta\, r_{\mathrm{e}}, \tag{2.36}$$

ensuring that for $r_{\mathrm{e}} \to 0^{+}$ the density (2.35) tends to be more diffuse while in the opposite limit $r_{\mathrm{e}} \to \infty$ this density becomes essentially localized around r_{e}. The Coulombic contributions to the Hamiltonian (2.29) are then in turn converted to integrals over the charge density (2.35)

$$\mathbf{V}_{\mathrm{int}}(\vec{r}_{\mathrm{e}}, \vec{r}_i, \vec{R}_j) = \sum_{i=1}^{N} \int \mathrm{d}\vec{x}\, \frac{\rho(\vec{x}\,)}{\left|\vec{x} - \vec{r}_i\right|} - \sum_{j=1}^{M} \int \mathrm{d}\vec{x}\, Z_j \frac{\rho(\vec{x}\,)}{\left|\vec{x} - \vec{R}_j\right|}. \tag{2.37}$$

Due to the spreading indicated in (2.36) of the "incoming charge density" for $r_{\mathrm{e}} \to 0$, these expressions give rise to weaker polarization potential than in the adiabatic case[16] reflecting thus the desired behavior. From the formal point of view, this method is actually equivalent to the adiabatic approach in the formal limit of $\xi \to \infty$, *i.e.*, also for $r_{\mathrm{e}} \to \infty$.

Moreover, presence of the Gaussian charge density (2.35) facilitates significantly numerical evaluation of the matrix elements of (2.37) sandwiched by target molecular orbitals in (2.31) since these are typically given also in a Gaussian basis and very efficient numerical algorithms for this class of problems are known (Helgaker et al., 2000, ch. 9).

Feng et al. (2003) have further modified the approach of Bouferguene et al. (1999) by arguing that the parameter β introduced in (2.36) should in general depend on the internuclear separation R (in case of diatomic molecules) and also on the "approach angle" θ_{e} of the incident electron. Therefore whereas Bouferguene et al. (1999) consider β as an adjustable parameter, Feng et al. (2003) suggested following form[17]

$$\beta\big(\theta_{\mathrm{e}}, R\big) \equiv \frac{1}{R R_0^2}\left(1 + \cos\theta_{\mathrm{e}}\right), \tag{2.38}$$

reflecting the expected behavior that the polarization potential should be stronger for greater R and also for the parallel approach, *i.e.*, small θ_{e}.

Finally, following Callaway et al. (1968), the non-adiabatic effects can be also accounted for by calculating explicitly a correction to the adiabatic potential (2.33) in terms of

$$\Delta V(\vec{r}_{\mathrm{e}};\, \vec{R}_j) \equiv -\frac{1}{2} \sum_{k=1}^{N} \left\langle \psi_0^{(\mathrm{p})}(\vec{r}_{\mathrm{i}};\, \vec{r}_{\mathrm{e}}, \vec{R}_j) \middle| \Delta_{\vec{r}_k} \middle| \psi_0^{(\mathrm{p})}(\vec{r}_{\mathrm{i}};\, \vec{r}_{\mathrm{e}}, \vec{R}_j) \right\rangle_{\vec{r}_{\mathrm{i}}}. \tag{2.39}$$

Callaway et al. (1968) call this term as *distortion potential*. It can be shown that it is positive and falls off as $1/r^6$ (Dalgarno and Lewis, 1956) weakening thus the polarization potential at small distances.

A conceptually different approach allowing to go beyond the adiabatic approximation consists in employing the *Density Functional Theory* (DFT) for determination of the short-range part of the correlation-polarization potential. This methodology has been originally proposed for scattering calculation purposes in O'Connell and Lane (1983); Padial and Norcross (1984) where the authors utilize the *Local Density Approximation* (LDA) originating from the local spin density (LSD) approximation well-known in the field of solid state physics (Perdew and Zunger, 1981). In order to obtain the

[15] being of dimension inverse length cubed

[16] moreover, the potential terms (2.37) are not singular in the vicinity of the nuclei or bound electrons, *i.e.*, for $r_{\mathrm{e}} \to R_j$ or $r_{\mathrm{e}} \to r_i$

[17] R_0 represents the equilibrium internuclear separation

correlation-polarization potential, O'Connell and Lane (1983) and Padial and Norcross (1984) consider model calculations of the free electron gas correlation energy [for details we refer to, *e.g.*, Fetter and Walecka (2003, ch. 1) or Carr et al. (1961); Gordon and Kim (1972) and references therein] being functionally dependent on the charge density. The correlation energy is not obtainable analytically even at the free electron gas level, nevertheless approximative fits[18] are available (Cohen and Pack, 1974). O'Connell and Lane (1983) consequently argue that the correlation energy density $\mathcal{E}_c[\rho(\vec{r})]$ is directly related to the correlation potential as

$$\mathbf{V}_{\mathrm{c}}(\vec{r}) \equiv 2\,\mathcal{E}_c[\rho(\vec{r})]. \tag{2.40}$$

In (2.40), the subscript c instead of cp has been used for $\mathbf{V}$ in order to emphasize that (2.40) describes only the short-range correlation effects. Among other reasons, this is a direct consequence of the free electron gas model which can not be hoped to describe the interaction adequately when the incident electron is "beyond the outer edge" of the target molecule since this model contains the inherent limitation that it doesn't allow for polarization of the target by the impinging electron (O'Connell and Lane, 1983). On the other hand, Padial and Norcross (1984) interpret the correlation energy density differently. Along the lines of the Hohenberg-Kohn method, they define the correlation potential by means of functional derivative of the correlation energy to wit[19]

$$\mathbf{V}'_{\mathrm{c}}(\vec{r}) \equiv \frac{\delta}{\delta\rho}\rho\,\mathcal{E}_c[\rho(\vec{r})]. \tag{2.41}$$

Similar approach has been later followed in Perdew and Zunger (1981) employing more precise calculations of the free electron gas correlation energy based on numerical Monte Carlo simulations (Ceperley and Alder, 1980). Corresponding fitted form of $\mathcal{E}_c[\rho]$ may be found in Perdew and Zunger (1981) or in Conclusions of Padial and Norcross (1984). Slightly modified (more precise) fit was later proposed in Perdew and Wang (1992). According to Gianturco and Rodriguez-Ruiz (1992), this fit results generally in weaker polarization potential near the origin, nevertheless in practical scattering calculations in case of small hydrocarbon molecules (C_3H_6, C_3H_8), the difference turns out to be rather negligible (Čurík and Šulc, 2010).

Colle and Salvetti (1975) computed the correlation energy density in an approximative manner by multiplying the Hartree-Fock wave function by an explicit "correlation factor" $\prod_{i>j}\big(1-\varphi(\vec{r}_i,\vec{r}_j)\big)$ with a suitably chosen function φ. For details of this procedure we refer to Colle and Salvetti (1975). Their chief result is a formula for the correlation energy density expressed in terms of the electron density and Laplacian of the second order Hartree-Fock density matrix, which was later restated into a DFT form by Lee et al. (1988), where the authors establish in this way the well-known LYP functional.

Alternative gradient based corrections to the LDA were suggested by Perdew et al. (1992) in their *Generalized Gradient Approximation*. The resulting functional is known in the literature as PW91.

As already discussed above, a common drawback of the DFT approaches introduced above is that they are unable to furnish the long-range part (2.26) of the correlation-polarization potential. A heuristic reason in the free electron gas framework is mentioned above, nevertheless in the general case the correlation energy/potential exhibits exponential decay following similar behavior of the target charge density.

[18] the procedure usually applied in practice is to use known expansions of the correlation energy in the limits of low and high charge densities ρ in terms of the variable $r_{\mathrm{s}} \equiv (3/4\pi\rho)^{1/3}$ and consequently "smoothly" join these two forms. For details we refer to Padial and Norcross (1984).

[19] this approach would actually reduce to (2.40) provided that $\mathcal{E}_c[\rho(\vec{r})]$ depends on ρ linearly

O'Connell and Lane (1983) and Padial and Norcross (1984) therefore suggest for linear molecules to augment the model by polarizabilities α_0, α_2 entering (2.27) determined by other means and consequently join individual Legendre λ components of the short-range correlation potential with their asymptotic counterparts at some crossing point r_c. Since for homonuclear diatomic molecules (2.26) simplifies to (2.27), only two terms $\lambda \in 0, 2$ come into play. The correlation potential components with $\lambda > 2$ can be thus either disregarded or retained in the model with their exponential decay. For example, Padial and Norcross (1984) neglect these components in description of electron scattering off small molecules (H_2, HCl, N_2, CO, ...) arguing they are negligible as compared to corresponding components of the static exchange potential.

A modified "joining" procedure has been proposed in Gianturco et al. (1993); Telega et al. (2004). First step in this tack is to find a "matching point" r_m where the short- and long-range spherically symmetric components intersect. The long-range part of the potential is then augmented by additional terms $\sum_{lm} C_{lm} r^{-\lambda} \mathrm{Y}_{l,\,m}(\hat{r}\,)$ where the coefficients C_{lm} are determined by the requirement of the overall smoothness of the potential.[20]

Čurík and Šulc (2010) used in a study of electron scattering on small hydrocarbons molecules employing the DMR method (introduced in Section 1.1) a different approach consisting in expanding the long-range polarization potential (2.26) analytically into partial-wave components

$$V_\mathrm{p}(\vec{r}\,) = \sum_{l=0}^{2} \sum_{m=-l}^{l} v_{lm}(r) \mathrm{Y}_{l,\,m}(\hat{r}\,). \tag{2.42}$$

The short-range correlation potential is accordingly decomposed into two mutually orthogonal angular components

$$V_\mathrm{c}(\vec{r}\,) = \sum_{l=0}^{2} \sum_{m=-l}^{l} w_{lm}(r) \mathrm{Y}_{l,\,m}(\hat{r}\,) + W(\vec{r}\,), \tag{2.43}$$

where the higher angular components are contained in $W(\vec{r}\,)$. One can then join the radial functions in (2.42) and (2.43) independently. This results in a correlation-polarization potential which is smooth in all partial-wave components up to $l \leq 2$. Components with $l > 2$ decay exponentially, nevertheless they are retained in the model.

The DFT approach for incorporation of non-adiabatic effects into the correlation-polarization potential has been quite popular. Among vast amount of relevant studies we refer to Gianturco and Rodriguez-Ruiz (1992, 1993) or Čurík and Gianturco (2002*a*,*b*); Čurík and Šulc (2010); Telega et al. (2004) and references therein.

[20] the exponent λ depends on l and for each l it corresponds to the first neglected term in the long-range part of the polarization potential, *i.e.*, $\lambda(l) = 6, 5, 6$ for $l = 0, 1, 2$ and $\lambda = l + 2$ for $l > 2$

CHAPTER
THREE

ANALYSIS OF THE EXPERIMENTAL DATA

3.1 Experimental setup

The theoretical ideas presented in Sections 4.1 and 4.2 were originally motivated by an attempt to fully utilise and also explain the precise experimental data gathered at the *Institute for Storage Ring Facilities*[1] at the University of Århus by the group of Prof. D. Field.

Crucial property of any apparatus intended for measuring low-energy scattering is the requirement of high energy resolution of the resulting electron beam. On the other hand, it is necessary to ensure also a sufficient current density. Technical details concerning the Århus setup can be found in Field et al. (2001); Hoffmann et al. (2002).

In this apparatus, the electrons are generated by threshold photo-ionisation of Ar at 15.75 eV using synchrotron radiation supplied by the ASTRID storage ring. Typical energy resolution of the emerging electrons is approximately 1.6 meV. The electrons are then focused by a zoom lens and enter the scattering chamber filled with the gas under investigation, the density of which is assumed to be low enough so that multiple scattering processes can be safely neglected. Unscattered electrons are in turn allowed to leave the chamber *via* the exit slit. The *total integral cross-section* σ_{T} is measured by examining the beam attenuation. The designation "total" underlines explicitly the fact that σ_{T} includes elastic as well as inelastic processes, whereas "integral" refers to integration over the full 4π sr.

Moreover, whole apparatus can be immersed in an axial magnetic field of typical strength of 2 mT. For incident energies up to roughly 0.7 eV, the electrons scattered into the forward hemisphere exhibit a spiral trajectory with radius smaller than the radius of the exit slit (1.5 mm) and leave thus the chamber without being detected. It is elementary to show that the necessary magnitude B of the magnetic field[2] ensuring that electrons with energy $\leq E_{\max}$ scattered into the forward hemisphere leave the chamber through the exit slit with radius r can be estimated as

$$B \leq \frac{1}{er}\sqrt{2E_{\max}}.$$

For $E_{\max} = 1$ meV we readily obtain $B \approx 2.25$ mT.

On the basis of the facts mentioned in the preceding paragraph, we can thus assume that only the electrons scattered into the rear hemisphere contribute to the measured *total backward cross-section* σ_{B} in this case. These ideas are schematically presented in a pictorial form in Figure 3.1. In the following we will also drop the designation "total"

[1] `http://www.isa.au.dk/`

[2] the conversion factor from atomic units to T is $\hbar/ea_0^2 \approx 2.35 \cdot 10^5$

unless stated otherwise and simply refer to the total integral and total backward cross-section as σ_{T} and σ_{B}, respectively.

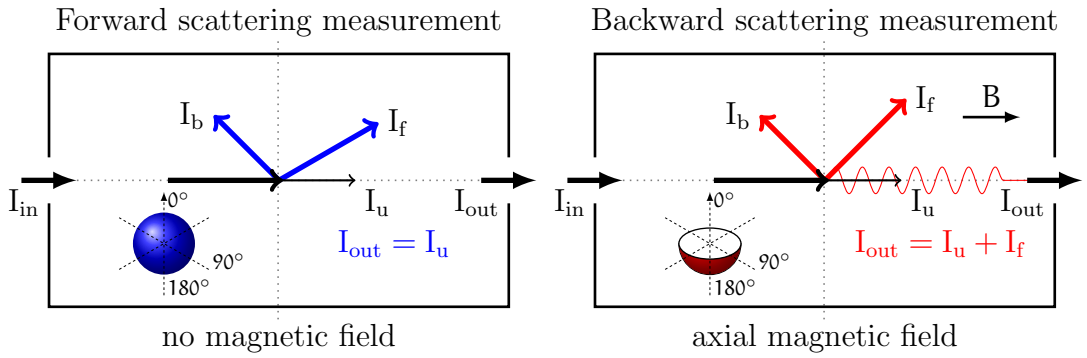

Figure 3.1: Schema of the experimental apparatus: I_{in} and I_{out} stand for the ingoing and outgoing flux, respectively. Intensity of the unscattered electrons is denoted as I_{u} and finally $I_{\mathrm{f}}/I_{\mathrm{b}}$ represent intensities corresponding to scattering into the forward/rear hemisphere.

Finally, we would like to make a comment on the interpretation of the total scattering cross-section σ_{T}. The gas in the experimental chamber is sufficiently diluted so that multiple scattering events can be disregarded from our consideration with impunity. Nevertheless from Figure 3.1, it is immediately obvious that the minimum scattering angle θ_{min} contributing to σ_{T} is closely linked with the position on the chamber axis where the collisional event occurred as schematically represented by Figure 3.2. If d represents location of the collision, L denotes length of the scattering chamber and h stands for the width of the exit slit, then θ_{min} is easily determined by the conditions

$$\theta_{\mathrm{min}} = \arctan \frac{1}{2} \frac{h}{L-d} \text{ and } \theta_{\mathrm{min}} \in [0, \pi].$$

The resulting total "integral" cross-section thus corresponds to scattering into angular range $\theta \in [\theta_{\mathrm{min}}, \pi]$. In order to obtain theoretical quantity conforming to the experiment in computations described in Chapter 4, we are therefore forced to average the calculated cross-sections over the scattering chamber.

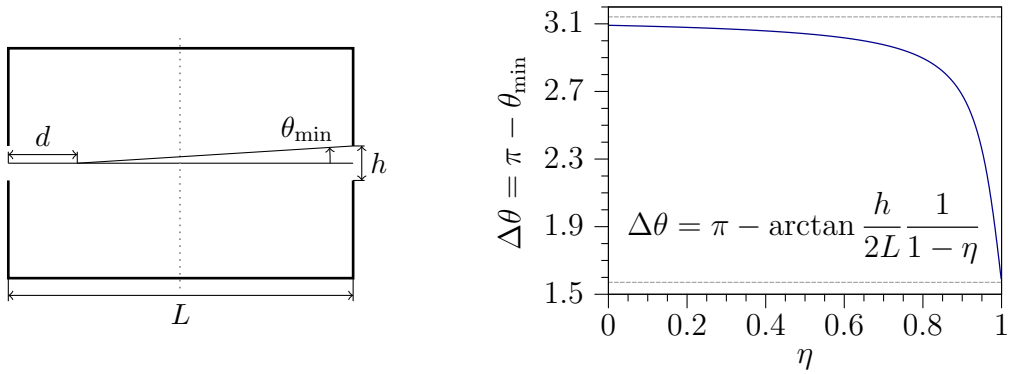

Figure 3.2: The dependence of the minimum scattering angle θ_{min} contributing to the total cross-section σ_{T} on the location d of the scattering event in a chamber of length L with an exit slit of width h. The location of the event is characterized by a dimensionless parameter $\eta = d/L$ which for the actual experimental setup attains the value of 0.1.

3.2 Phase-shifts fitting

The energy dependence of the generalized phase shifts introduced in Subsection 4.1.2 by Eq. (4.6) is determined via a numerical fitting procedure. In this way we thus obtain a "bridge" between theoretical considerations and direct experimental measurement. This short section should provide a more detailed explanation of the method itself.

In the following, we will confine ourselves on two generalized phase shifts η_0, η_1 and denote their energy dependence explicitly as $\eta_0(E)$, $\eta_1(E)$. Then the integral σ_{T} and backward σ_{B} cross-sections – being functions of η_0, η_1 – depend on the energy through these two quantities (apart from possible kinematic factors). The experiment furnishes us for given collision energy E_0 with two numbers – $\sigma_{\mathrm{T}}^{\mathrm{e}}$ and $\sigma_{\mathrm{B}}^{\mathrm{e}}$ – representing the observed values of the integral and backward cross-section, respectively.[3] One is then naturally interested in finding the numerical values of $\eta_0(E_0)$ and $\eta_1(E_0)$ which give the best[4] agreement with the experiment. To this end, we introduce an auxiliary function χ^2 of two variables x, y according to the following relation

$$\chi^2(x,y) \equiv \left(\frac{\sigma_{\mathrm{T}}^{\mathrm{e}} - \sigma_{\mathrm{T}}(x,y)}{\sigma_{\mathrm{T}}^{\mathrm{e}}}\right)^2 + \left(\frac{\sigma_{\mathrm{B}} - \sigma_{\mathrm{B}}(x,y)}{\sigma_{\mathrm{B}}}\right)^2. \tag{3.1}$$

The original question can now be thought of as an minimisation problem, where we are looking for the (preferably global) minimum of the function (3.1) in an open set containing some specified initial point (x_0, y_0).

Unfortunately, there is of course no guarantee that the physical values of η_0, η_1 will coincide with the (presumably existing) global minimum of χ^2. Another issue is then also connected with the dilemma which minimum (probably one of many in general) of χ^2 should we choose. Although it is tempting to argue that when we have two experimental quantities σ_{T}, σ_{B} and two fitting parameters η_0, η_1, there should be a bijective mapping, the situation is actually not so clearly cut. On the other hand, it is essential to take into account that also the experimental values are "contaminated" by systematical errors – the upper bound estimate on this error (Hoffmann et al., 2002) is in our case approximately 8%.

Figure 3.3 supports the ideas of the preceding paragraph in a pictorial form. It depicts a contour plot of the function χ^2 interpreted as a function of η_0, η_1 on given domain for two collisional energies, namely 20 meV (left panel) and 150 meV (right panel). As can be readily observed, even for 20 meV we experience two comparable minima. The 4%– and 8%–"trust-areas"[5] are denoted by solid black and dashed white lines, respectively. With increasing collisional energy, these domains tend to "evolve" in the η_0, η_1–space.

In order to approach this issue more systematically, we employed following procedure

1. for the considered energy range $[E_{\min}, E_{\max}]$ construct discrete grid

$$\{E_i\}_{i=0}^{N}, \text{ where } E_0 = E_{\min} \text{ and } E_N = E_{\max},$$

2. for $i = 0$ set the initial guess on $\eta_0(E_0), \eta_1(E_0)$ to zero which is an approximation to the assumed threshold behavior provided that E_0 is sufficiently "small"

3. *via* minimizing the expression (3.1) find the appropriate values of η_0^0, η_1^0 in the vicinity of the starting point

[3] superscript $^{\mathrm{e}}$ denotes that these quantities are obtained by experiment

[4] This formulation is rather vague. However, a slightly more precise definition is given below Eq. (3.1)

[5] *i.e.*, values of η_0, η_1 for which $\chi^2 \leq 32 \cdot 10^{-4}$. That in turn corresponds to 4% relative errors in σ_{T} and σ_{B}. Similarly, condition $\chi^2 \leq 128 \cdot 10^{-4}$ is compatible with the relative error being less than 8%.

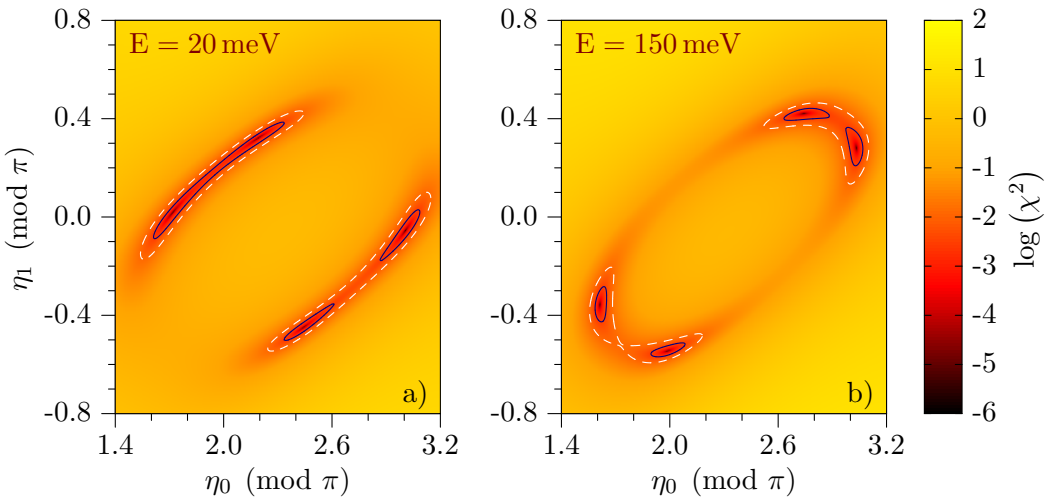

Figure 3.3: Dependence of χ^2 defined in Eq. (3.1) as a function of two generalized phase shifts η_0, η_1 for collision energy of 20 meV (left panel) and 150 meV (right panel). Experimental data for CH_3Cl molecule recorded in the right panel of Figure 4.1 are assumed.

4. then proceed recursively:

   - for energy point $k+1$ use as the initial guess the phase shifts from previous step, *i.e.*, η_0^k, η_1^k and repeat the procedure

Heuristically, this approach should ensure smoothness of the resulting phase shifts in the considered energy range provided that the grid spacing is not too large and the experimental values are also sufficiently smooth. To guarantee the latter, we have approximated the $\sigma_{\mathrm{T}}^{\mathrm{e}}$ and $\sigma_{\mathrm{B}}^{\mathrm{e}}$ with piece-wise spline fit prior to the entire procedure.

Alternative modification to this method is to use for each energy grid point E_k directly the experimental values in the role of the initial guess. However, in practical computations it turned out that this doesn't make any significant difference.

As concerns the minimisation procedure itself, our implementation for polar molecules relied on standard gradient based *Fletcher-Powell* (Press et al., 2007, p. 521) algorithm, where we have conveniently utilised the fact that it is very cheap to compute the derivatives of χ^2 analytically since the scattering amplitude (4.5) depends on the short-range $\mathcal{S}$-matrix (4.6) linearly.

The entire approach can be easily extended to more phase shifts than just two, *i.e.*, in general we would deal with a set of fitting parameters of η_j for $j = 1, \ldots, N$, nevertheless the physical meaning of the obtained phase shifts certainly decreases with increasing k.

3.2.1 Uniqueness of the phase shifts

The fact that the obtained generalized phase shifts are not guaranteed to be unique has been demonstrated in Figure 3.3. In this regard, we think that it is worth to mention a very similar problem consisting in the question, originally posed by Crichton (1966), whether the knowledge of the differential cross-section for one particular energy uniquely determines the phase shifts (assuming spherically symmetric potential). This resembles our situation, for the quantities σ_{T}, σ_{B} can be naturally understood as functionals of the differential cross-section. Crichton (1966) considered one particular differential cross-section taking into account s-,p- and d- partial waves ($l \leq 2$) and

found two sets of phase shifts yielding the same angular dependence of the cross-section. The same question for a general spd- cross section was later studied by Atkinson et al. (1973). The authors show that if one considers only partial waves with $l \leq 2$ then for a given set of phase shifts δ_0, δ_1, δ_2 and for certain intervals of δ_2, there exists another set $\delta_0' = \delta_0 - \epsilon_0$, $\delta_1' = \delta_1 - \epsilon_1$, $\delta_2' = \delta_2$ which yields exactly the same differential cross-section, where the ϵ_0, ϵ_1 are defined in terms of

$$\begin{aligned} 2\Delta \cos\epsilon_0 &= \kappa^2 - \Delta^2 - 1 \\ 2\Delta\kappa \cos\epsilon_1 &= \kappa^2 + \Delta^2 - 1, \end{aligned} \tag{3.2}$$

with constants κ, Δ being given by

$$\begin{aligned} \kappa &= -3\frac{\sin\alpha_1}{\sin\alpha_0} & \alpha_1 &= \delta_2 - \frac{\pi}{2} \\ \Delta &= -2\frac{\sin\alpha_1}{\sin(\alpha_0 - \alpha_1)} & \tan\alpha_0 &= \frac{\sin 2\delta_2}{\cos 2\delta_2 - \frac{3}{5}}. \end{aligned} \tag{3.3}$$

Similar analysis was later extended for $l \leq 3$ (Berends and Ruijsenaars, 1973) and $l \leq 4$ (Cornille and Drouffe, 1974). Case of an arbitrary finite number of contributing partial waves has been discussed in Berends and Van Reisen (1976) and a more general study for infinitely many partial waves was provided later by Atkinson et al. (1978).

In the light of the arguments presented above, it seems thus necessary to amend the fitting procedure by some additional physical information such as low-energy threshold behavior of the phase shifts, which could in principle help to remove unphysical "branches" of the resulting phase shifts.

CHAPTER
FOUR

APPLICATIONS

The following sections should present several applications of the theoretical concepts discussed previously. Special attention is devoted predominantly to the content of Chapter 1 and Chapter 3. Since the theoretical treatment of electron-molecule scattering in case of polar molecular is markedly different as opposite to the non-polar case, the discussion is divided accordingly.

An explanatory intuitive argument explaining the reason why molecules without a permanent dipole moment exhibit much smaller cross-sections at low incident energies has been given by Gerjuoy and Stein (1955). The reasoning is as follows. To induce a rotational transition of the target molecule, the incident electron has also to experience a change in its angular momentum l for the total angular momentum is conserved. However, at low energies only $l = 0$ electrons can penetrate the (missing) centrifugal barrier to the vicinity of the molecule. Electrons with $l > 0$ capable of rotational excitation are thus found far from the molecule and the resulting cross-section is therefore small. On the other hand, the situation is drastically changed in case of dipolar potential, the strength of which is comparable with the centrifugal barrier and the preceding argument is thus invalid as had been already observed decades ago (Massey, 1932).

These arguments are supported in pictorial form by Figure 4.1 depicting the energy dependence of the total integral and backward scattering cross-sections as introduced in Chapter 3. By comparing the experimental data for a polar [CH_3Cl (Field and Jones, n.d.) in the right panel] and non-polar [N_2 (Hoffmann et al., 2002) in the left panel] molecule, one immediately observes the marked qualitative difference at lower incident energies.

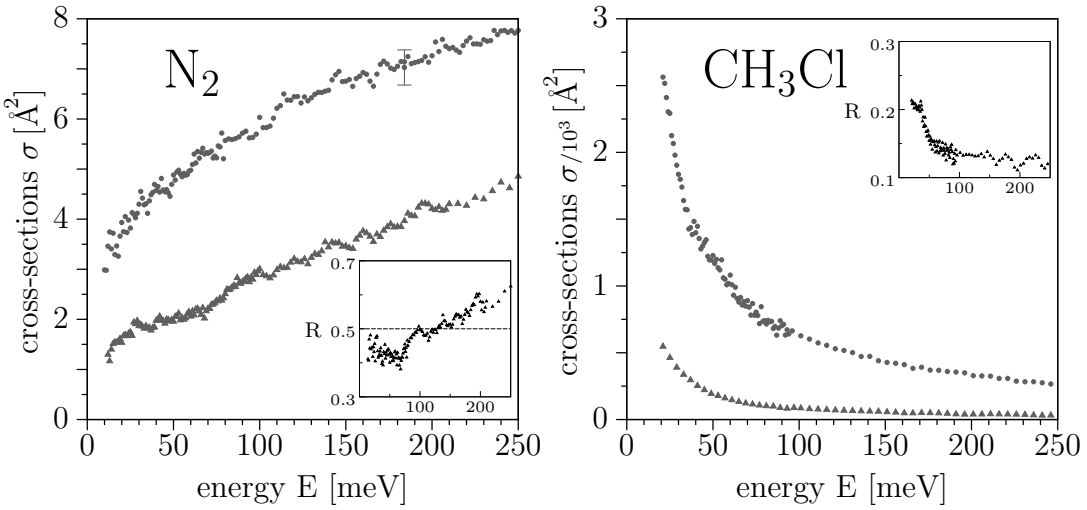

Figure 4.1: Typical experimental data of integral and backward cross-sections in case of a nonpolar (N_2 – left panel) and polar (CH_3Cl – right panel) molecule demonstrating the marked difference at low incident energies. Insets show the ratio R of the backward and integral cross-sections as a function of the incident energy. This quantity is discussed in more detail in Section 4.2.

4.1 Polar molecules

When the dominant long-range dipole potential is present, it seems that instead of fighting this fact it is more natural to take advantage of it. In this regard, one could try to express the scattering matrix, as formulated neatly by Clark (1984), to "describe the state of the system relative to what it would be if all other, short-range, interactions were absent". This idea has been actually known for a long time and stems originally from the description of electron-ion scattering (Burgess et al., 1970).

4.1.1 Short-range S matrix

Along these lines, one can try to re-express the body frame scattering amplitude not with respect to the usual angular basis comprised of spherical harmonics but with respect to the eigenfunctions (C.5) of the dipole operator (C.3). Following almost identical procedure as in basis comprised of spherical harmonics, one finally arrives (Fabrikant, 1976) at the expression

$$f(\vec{k}_f,\,\vec{k}_i) = \frac{2\pi}{\mathrm{i}k}\sum_{\substack{m,m'\\ \lambda,\lambda'}} \mathrm{Z}_{\lambda',\,m'}(\hat{k}_f)\Big[-\delta_{\lambda,\lambda'}\delta_{m,m'}\mathrm{Z}^{*}_{\lambda,\,m}(\hat{k}_i) + \\ + \frac{1}{\mathrm{i}^{\Re\lambda' + \,\Re\lambda}}\check{\mathbb{S}}_{\lambda' m',\lambda m}\mathrm{Z}^{*}_{\lambda,\,m}(-\hat{k}_i)\Big], \tag{4.1}$$

which in the limit of zero dipole moment $D \to 0$ naturally coincides with the well-known partial wave decomposition (1.99). The symbol $\check{\mathbb{S}}$ introduced in (4.1) denotes so-called *short-range $\mathcal{S}$-matrix*, which reflects effects of the short-range perturbations to the dipole potential and in this sense describes the scattering state relative to the dipole interaction.

Matrix elements of $\check{\mathbb{S}}$ are easily expressible in terms of ordinary partial wave $\mathcal{S}$-matrix. Utilizing transformation relations (C.5) between angular bases $\mathrm{Y}_{l,\,m}$ and $\mathrm{Z}_{\lambda,\,m}$ readily

furnishes the desired transformation together with its inversion as

$$\frac{1}{\mathrm{i}^{l'+\,l}}\mathbb{S}_{l'm',lm} = \sum_{\lambda,\lambda'} \mathcal{A}^{m'}_{l'\lambda'} \cdot \frac{1}{\mathrm{i}^{\Re\lambda'+\,\Re\lambda}}\check{\mathbb{S}}_{\lambda'm',\lambda m} \cdot \mathcal{A}^{m*}_{l\lambda}, \tag{4.2a}$$

$$\frac{1}{\mathrm{i}^{\Re\lambda'+\,\Re\lambda}}\check{\mathbb{S}}_{\lambda'm',\lambda m} = \sum_{l,l'} \mathcal{A}^{m'*}_{l'\lambda'} \cdot \frac{1}{\mathrm{i}^{l'+\,l}}\mathbb{S}_{l'm',lm} \cdot \mathcal{A}^{m}_{l\lambda}. \tag{4.2b}$$

It is worth noting that this transformation is *not* unitary for overcritical[1] dipole moments due to the renormalization (D.5) of the radial solutions ensuring unit ingoing and outgoing fluxes.

If we further suppose that the short-range interaction preserves the symmetry of the potential, then it follows that the short-range $\mathcal{S}$-matrix will be diagonal in m so that formulae (4.1) and (4.2) simplify to

$$f(\vec{k}_f,\,\vec{k}_i) = \frac{2\pi}{\mathrm{i}k}\sum_{\substack{m\\ \lambda,\lambda'}} \mathrm{Z}_{\lambda',\,m}(\hat{k}_f)\Big[-\delta_{\lambda,\lambda'}\mathrm{Z}^{*}_{\lambda,\,m}(\hat{k}_i) + \\ + \frac{1}{\mathrm{i}^{\Re\lambda'+\,\Re\lambda}}\check{\mathbb{S}}^{m}_{\lambda',\lambda}\mathrm{Z}^{*}_{\lambda,\,m}\big(-\hat{k}_i\big)\Big], \tag{4.3}$$

and

$$\frac{1}{\mathrm{i}^{l'+\,l}}\mathbb{S}^{m}_{l',l} = \sum_{\lambda,\lambda'} \mathcal{A}^{m}_{l'\lambda'} \cdot \frac{1}{\mathrm{i}^{\Re\lambda'+\,\Re\lambda}}\check{\mathbb{S}}^{m}_{\lambda',\lambda} \cdot \mathcal{A}^{m*}_{l\lambda}, \tag{4.4a}$$

$$\frac{1}{\mathrm{i}^{\Re\lambda'+\,\Re\lambda}}\check{\mathbb{S}}^{m}_{\lambda',\lambda} = \sum_{l,l'} \mathcal{A}^{m*}_{l'\lambda'} \cdot \frac{1}{\mathrm{i}^{l'+\,l}}\mathbb{S}^{m}_{l',l} \cdot \mathcal{A}^{m}_{l\lambda}. \tag{4.4b}$$

Spherical symmetry of the short-range perturbation to the dipole potential ensures the short-range $\mathbb{S}$-matrix being diagonal in λ. In this case, more insight into the structure of Eq. (4.3) is gained if one substitutes into it the transformation relations (C.5) directly. Performing this substitution, taking into account that $\mathrm{Y}_{l,\,m}\big(-\hat{n}\big) = (-1)^{l}\mathrm{Y}_{l,\,m}\big(\hat{n}\big)$ and rearranging terms finally yields[2]

$$f(\vec{k}_f,\,\vec{k}_i) = \frac{2\pi}{\mathrm{i}k}\sum_{\substack{m\\ l,l'}} \mathrm{Y}_{l',\,m}(\hat{k}_f)\mathrm{Y}^{*}_{l,\,m}(\hat{k}_i)\sum_{\lambda}\Big[-\mathcal{A}^{m}_{l'\lambda}\cdot\mathcal{A}^{m*}_{l\lambda} + \mathcal{A}^{m}_{l'\lambda}\cdot(-1)^{\Re\lambda}\,\check{\mathbb{S}}^{m}_{\lambda,\lambda}\cdot\mathcal{A}^{m*}_{l\lambda}(-1)^{l}\Big]. \tag{4.5}$$

4.1.2 Parametrization of the short-range S matrix

Popular technique in the field of low-energy electron-molecule scattering in case of short-range potentials is parametrization of the phase shifts since for sufficiently low energy only a few partial l-waves will be significant. In the very same spirit, one might assume that for sufficiently low energy, the electron scattered in dipole potential modified by some presumably unknown short-range perturbation will be reasonably described by just a few λ-components, *i.e.*, by just a few "dipole waves". Assuming spherical symmetry of the short-range interaction, one might be then tempted to use following *Ansatz* for the short-range $\mathcal{S}$-matrix

$$\check{\mathbb{S}} = \mathrm{diag}\Big(\check{\mathbb{S}}^{0},\,\check{\mathbb{S}}^{1},\,\ldots\Big),\ \text{where}\ \check{\mathbb{S}}^{j} = \begin{pmatrix} \mathrm{e}^{\mathrm{i}2\eta_j} & & \\ & \mathrm{e}^{\mathrm{i}2\eta_{j+1}} & \\ & & \ddots \end{pmatrix}. \tag{4.6}$$

[1] explanation of the overcritical dipole moment concept can be found in Appendix C

[2] the term $\mathcal{A}^{m}_{l'\lambda}\cdot\mathcal{A}^{m*}_{l\lambda}$ summed over λ is equal to $\delta_{l,l'}$ provided that one doesn't perform truncation of the matrices $\mathcal{A}^{m}_{l'\lambda}$ to achieve better numerical precision of the eigenvalues (C.5) – in actual numerical implementation, we keep the form as indicated by (4.5)

Individual steps of the subsequent procedure are consequently as follows

- the short-range $\mathcal{S}$-matrix is parametrized by two generalized (short-range) phase shifts η_0, η_1 as implied by Eq. (4.6)
- using the transformation relations (4.4a), one obtains the partial wave components of the ordinary $\mathcal{S}$-matrix which are central for construction of the body frame scattering amplitude (1.99) in the $\mathrm{Y}_{l,m}$ angular basis
- having done so, one can consequently transform (1.99) into the laboratory frame *via* (1.100) obtaining thus the Chase's "ω-modulated" amplitude
- this expression is then finally the essential ingredient for the *adiabatic approximation* discussed in Section 1.3, which provides an approximative laboratory frame amplitude (1.101) in the form of a single matrix element between respective rotational states. Based on the knowledge of this quantity, we can easily calculate differential cross-sections for individual rotational transitions.

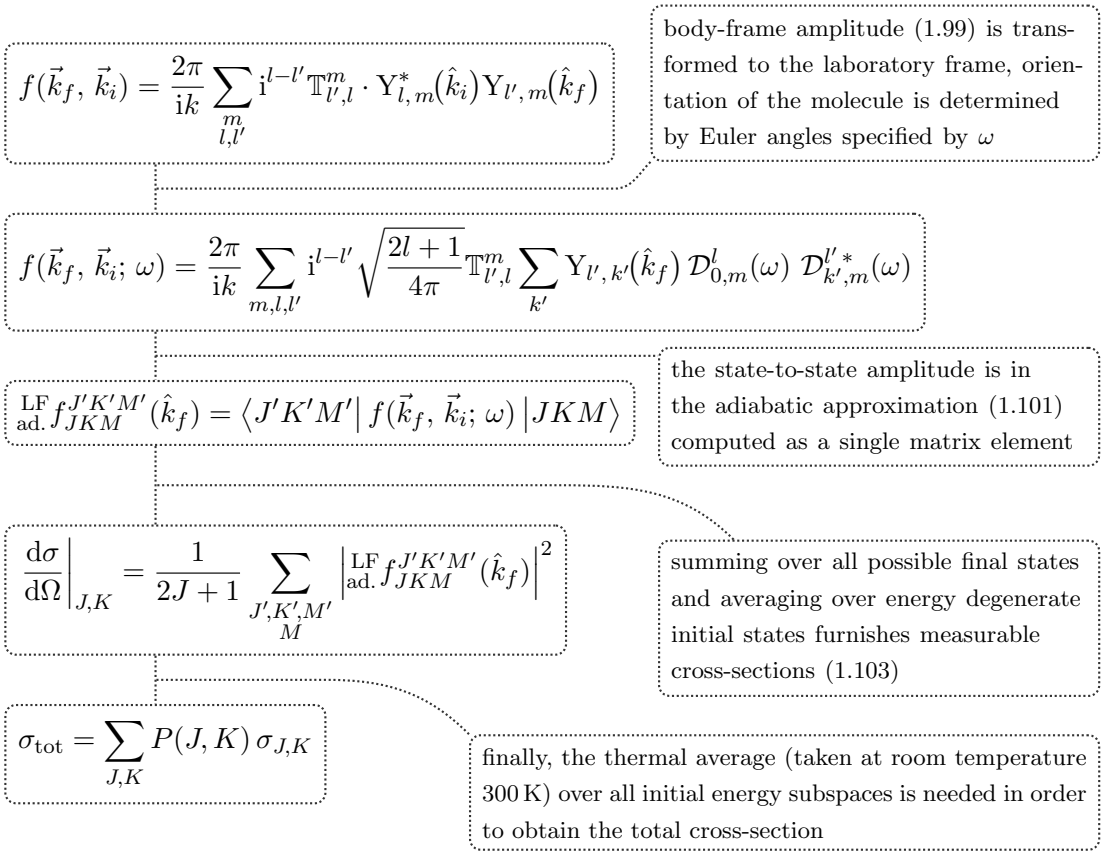

Figure 4.2: Schematic summary of individual steps in the description of rotational excitations of polar molecules in the framework of the adiabatic approximation discussed in Section 1.3

At this point, we would like to make a few comments regarding the connection of the theoretical values with the experimental data generated by the setup discussed in Section 3.1. First of all, the resulting cross-sections should be thermally averaged. To this end, it is necessary to introduce corresponding partition function $\mathcal{Z}$ which takes

the form

$$\mathcal{Z} = \sum_{J=0}^{\infty} \sum_{K=-J}^{J} g_{J,K}\, \mathrm{e}^{-\beta\, E_{JK}}, \tag{4.7}$$

with $\beta = 1/kT$ denoting the usual Boltzmann factor[3] and $g_{J,K}$ representing *statistical weights* of individual levels as elaborated in more detail in Section E.4. Thus in evaluation of the total cross-section, contribution from level J, K are weighted by

$$P(J,K) = \frac{1}{\mathcal{Z}} g_{J,K}\, \mathrm{e}^{-\beta\, E_{JK}}. \tag{4.8}$$

The total cross-section σ_{tot} of the last step in Figure 4.2 is therefore expressible *via*

$$\sigma_{\mathrm{tot}} = \frac{1}{\mathcal{Z}} \sum_{J,K} g_{J,K}\, \sigma_{J,K}\, \mathrm{e}^{-\beta\, E_{JK}}. \tag{4.9}$$

It might seem that evaluation of the total cross-section is accompanied by significant computational demands since at the room temperature of $\sim 300\,\mathrm{K}$, tens of rotational states contribute typically to the partition function (4.7). However, an approximative value can be easily obtained in light of the result (1.107) stating that the cross-sections $\sigma_{J,K}$ are in the adiabatic approximation independent on the initial J, K state designation. The only dependence is introduced by the kinematic factor $k_{\Gamma'}/k_{\Gamma}$ in (1.36). If the incident energy is therefore not too low, one might assume that $k_{\Gamma'}/k_{\Gamma} \approx 1$. Consequently, the terms $\sigma_{J,K}$ can be taken out of the sum (4.9) which in turn reduces by definition to one. For evaluation of σ_{tot}, it is then permissible to choose arbitrary values of J, K and since $\sigma_{0,0}$ is the most easily computable quantity, one obtains an interesting approximation

$$\sigma_{\mathrm{tot}} \approx \sigma_{0,0}. \tag{4.10}$$

4.1.3 Connection with the experiment

Following the above described procedure, we thus introduce two generalized phase shifts η_0, η_1 in order to parametrize the short-range $\mathcal{S}$-matrix. We might hope that these two quantities will be in 1-1 correspondence with the two values furnished by the experiment, namely the total σ_{T} and backward σ_{B} cross-section. Equipped with the experimental energy dependence of σ_{T}, σ_{B}, we perform consequently the fitting procedure described in detail in Chapter 3 obtaining thus corresponding energy dependence of η_0, η_1 denoted as $\eta_0(E), \eta_1(E)$.

Using $\eta_0(E), \eta_1(E)$ and plugging it back into the model we can, in turn, easily calculate individual state-to-state cross-sections. In this way, it is therefore possible to separate the total cross-section σ_{T} into its elastic and inelastic components.

This approach has been used in the past to study rotational excitations of water molecules induced by electron impact (Čurík et al., 2006). The authors report energy dependence of various state-to-state cross-sections for incident energies up to 200 meV and above 100 meV, where other data are available, they find quite good agreement with *ab initio* prediction based on the R-matrix theory (Faure et al., 2004).

Following similar treatment, we have employed the procedure of Subsection 4.1.2 in case of two polar molecules, namely CH_3Cl and SO_2, for which accurate experimental data regarding total integral and backward scattering cross-sections are available (Field and Jones, n.d.). The results for both molecules are summarized in graphical form below.

[3] Boltzmann constant k expressed in atomic units per Kelvin attains approximately the numerical value of $3.1668 \cdot 10^{-6}$

The agreement of the theoretical prediction with the experimental data of another group (Gulley and Buckman, 1994) regarding differential cross-sections in case of the SO_2 molecule presented in Figure 4.6(b) is remarkable. On the other hand, this model is apparently less successful for CH_3Cl as can be seen in Figure 4.4(b). We think that the principal culprit could be hidden in the inherent assumption present in the model concerning the spherical symmetry of the short-range perturbation to the dipole potential disregarding thus the significantly prolate character of CH_3Cl. To remedy this, one would be forced to consider also the non-diagonal terms in the parametrization of the short-range $\mathcal{S}$-matrix in (4.6). On the other hand, this would spoil the 1-1 correspondence between the elements of the short-range $\mathcal{S}$-matrix and directly available experimental data turning thus the entire approach to a mere fitting procedure.

CH_3Cl

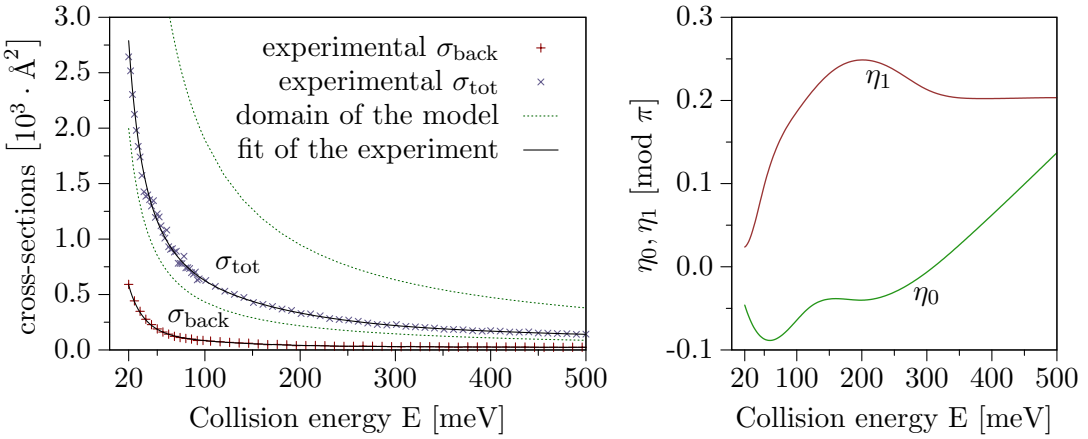

(a) Total cross-sections

(b) Fitted generalized phase shifts η_0, η_1

Figure 4.3: Experimental data of the total integral and total backward scattering cross-sections for CH_3Cl. Black solid line represent fit of the experimental values by the η_0, η_1-model described above. Dashed green line denotes range of cross-sections achievable with two generalized phase shifts η_0, η_1 independently ranging over $[0, 2\pi]$.

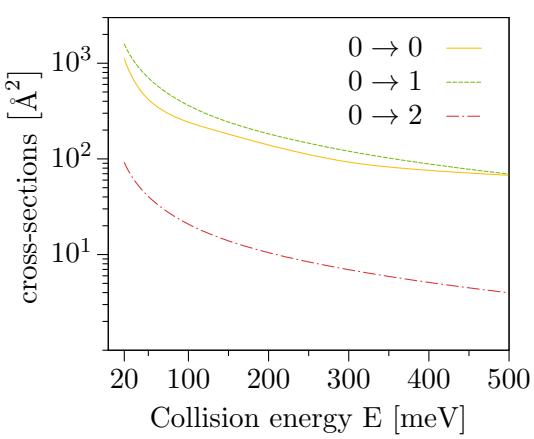

(a) Rotationally resolved cross-sections

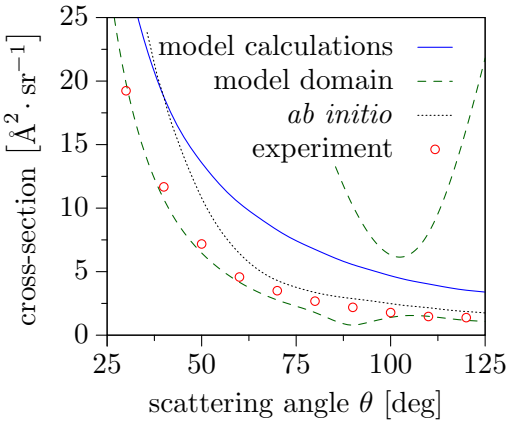

(b) Rotationally summed DCS for 500 meV

Figure 4.4: Left panel: predicted rotational cross-sections for various $J \to J'$ transitions, Right panel: rotationally summed DCS for 500 meV as calculated on the basis of fitted η_0, η_1 [blue solid line – (4.3(b))], compared with the experimental values [red circles – (Shi et al., 1996)] and *ab initio* calculations [dotted black line – (Rescigno et al., 1997)]. Dashed green lines show attainable DCS range on the basis of the considered two-parametric model as in Figure 4.3(a).

SO_2

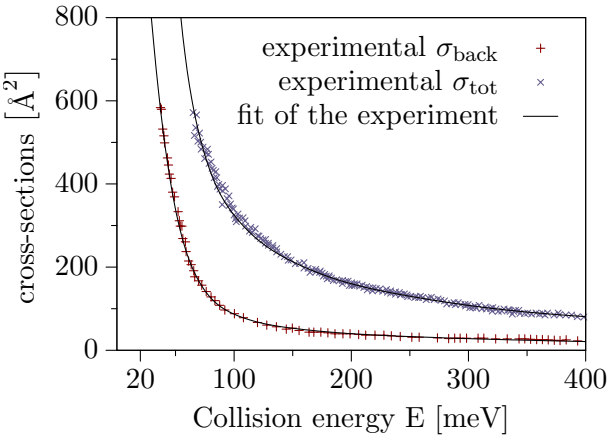

(a) Experimental data for SO_2

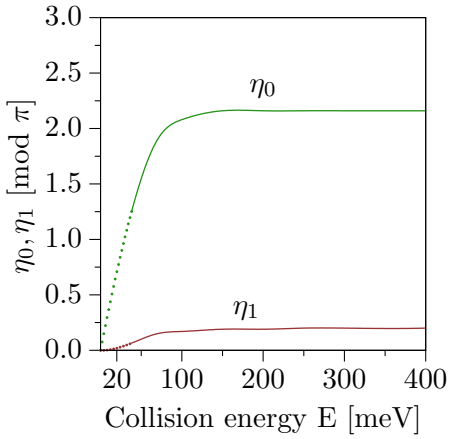

(b) Fitted phase shifts η_0, η_1 reproducing the experimental data in the left panel

Figure 4.5: Experimental data of the total integral and total backward scattering cross-sections for SO_2. Black solid line represents fit of the experimental data by two generalized phase shifts η_0, η_1 depicted in Figure 4.5(b). Dotted part of their energy dependence shows extrapolation to "zero" energy.

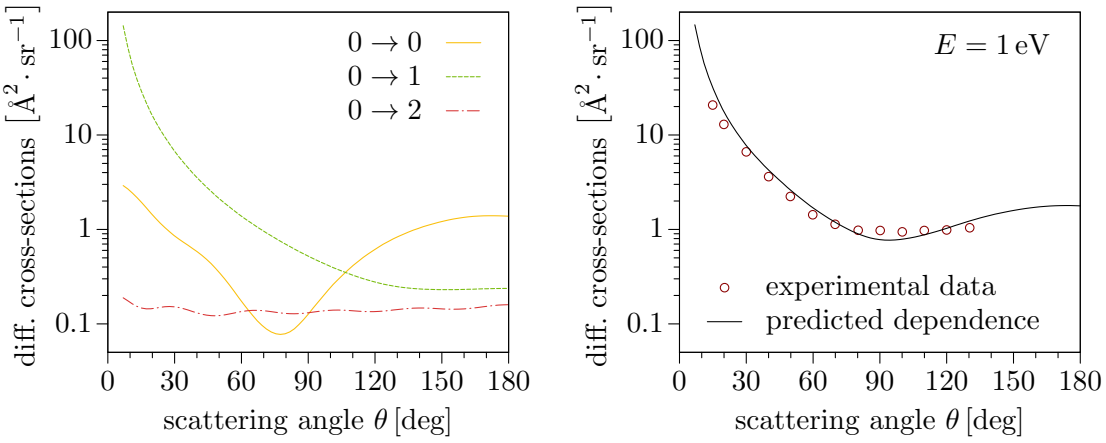

(a) Rotationally resolved differential cross-section

(b) Rotationally summed differential cross-section

Figure 4.6: Rotationally resolved (4.6(a)) and summed (4.6(b)) differential cross-section for SO_2 at incident energy of 1 eV as calculated using phases in Figure 4.5(b) extrapolated constantly up to 1 eV by their values for 400 meV. Experimental data in Figure 4.6(b) are taken from Gulley and Buckman (1994).

4.2 Non-polar molecules

As an representative example of a non-polar molecule, we have chosen molecular nitrogen N_2 since (possibly apart from H_2) it represents one of the most studied systems in the field of electron-molecule scattering (see Itikawa and Mason (2005) and references therein) and the experimental data for total integral σ_T and backward σ_B cross-sections are also available (Hoffmann et al., 2002).

The experimental energy dependence of σ_T and σ_B from various sources up to 250 meV is depicted in Fig. 1 of Attachment B. A fleeting glance reveals the anomalous behavior of the backward scattering cross-section σ_B for incident energies around 80 meV exhibiting a significant dip in value which is not at all present in the integral cross-section data. This behavior is even more pronounced in the inset of the left panel of Figure 4.1 showing the ratio R being equal to σ_B/σ_T as a function of the incident energy. Since we are not aware of any theoretical study dealing with this phenomenon, we have investigated the possible causes of the backward scattering cross-section suppression in this energy region coming consequently to the conclusion that it can be satisfactory explained by destructive p-wave interference.

The relevant details regarding the theoretical treatment can be found in the Attachment B of the presented work in the form of a standalone paper and we will thus confine ourselves in the following just to the principal ideas.

In order to gain a notion about the most important features of the system under consideration, we have employed an *ab initio* theory exploiting the material presented in Chapter 2. Briefly stated, the calculations were done in the fixed nuclei approximation (see Section 1.2) with the interaction between the incident electron and the target N_2 molecule being described in the framework of the static exchange plus polarization approximation. The static part (2.8) of the potential was rendered using the Hartree-Fock wave function for the N_2 ground state. As concerns the approximative treatment of the exchange component (2.9), we have utilized the TFEGE method described in more detail in Section 2.2. The free TFEGE parameter in (2.16) was tuned in order to reproduce the position of the Π_g resonance in the integral cross-section.

In this regard, the results reported in Telega and Gianturco (2006) and shown in

Fig. 3 of Attachment B, were obtained in a similar fashion, whereas for the calculation of the simultaneously displayed "SCME" data (Telega et al., 2004), the authors used a semiclassical exchange description elaborated in Section 2.2.

Finally, the correlation-polarization part of the interaction potential was determined at the local density approximation level (Gianturco and Rodriguez-Ruiz, 1993) in the DFT framework as adumbrated in Section 2.3. For adjusting the long-range part of the potential, we have used experimental values of the polarizabilities (see Morrison et al. (1997) and references therein).

The fixed nuclei body frame radial equations were solved using the Volterra integral propagator of Section 1.5, the details about the use of which can be found in the attached paper.

The main outcome of the fixed nuclei calculations are the converged body frame $\mathcal{K}$-matrices. Fig. 2 of Attachemnt B records the energy dependence of selected $\mathcal{K}$-matrix elements as compared to the results of Morrison et al. (1997). Another important result stemming from the *ab initio* calculations is the observation that the influence of the $l > 1$ partial waves is insignificant for incident energies up to 250 meV.

Therefore to connect the *ab initio* calculations with the experiment, we have employed a truncated $\mathcal{K}$-matrix presented in Figure 4.7 excluding thus the partial waves with $l > 1$. The body frame $\mathcal{K}$-matrix in Figure 4.7 is directly related, *via* Eq. (1.88), to the $\mathcal{T}$-matrix, from which one can readily evaluate the rotationally summed integral σ_{T} and backward σ_{B} cross-sections by means of Eq. (1.96). Although it is possible to

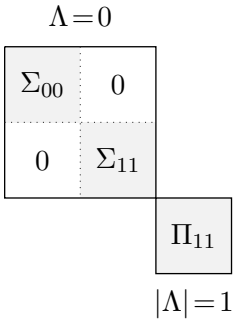

Figure 4.7: Reduced $\mathcal{K}$-matrix used in the fitting procedure described in the text. Since Σ_{00} is the only nonzero element in the $\Lambda = 0$ block with gerade symmetry, we adhere to the notation Σ_{g}. With the same proviso, the symbols Σ_{u} and Π_{u} are used instead of Σ_{11} and Π_{11}, respectively.

obtain the expression for σ_{T},σ_{B} understood as functions of Σ_{g}, Σ_{u}, Π_{u} in closed form, it is instructive to consider the case of small energies E since then the $\mathcal{T}$-matrix is actually directly proportional to the $\mathcal{K}$-matrix as $\mathcal{T} = -2\mathrm{i}\mathcal{K}$. Evaluating the cross-sections σ_{T}, σ_{B} with this proviso yields

$$\sigma_{\mathrm{tot}} = \frac{4\pi}{k^2}\left(\Sigma_{\mathrm{g}}^2 + \Sigma_{\mathrm{u}}^2 + 2\Pi_{\mathrm{u}}^2\right), \tag{4.11a}$$

$$\sigma_{\mathrm{back}} = \frac{1}{2}\sigma_{\mathrm{tot}} - \frac{2\pi}{k^2}\Sigma_{\mathrm{g}}\left(\Sigma_{\mathrm{u}} + 2\Pi_{\mathrm{u}}\right). \tag{4.11b}$$

We thus immediately recognize that the departure from the backward/forward symmetry for low energies reflecting itself in R differing from 0.5 is mainly on behalf of the interplay between the Σ_{u} and Π_{u} phases. Since the Σ_{g} phase is rather dominant we fix its energy dependence according to the *ab initio* prediction and consider the phases Σ_{u}, Π_{u} as free parameters which can be in turn fitted to the experimental data of σ_{T}, σ_{B} in a very similar fashion as we have employed for the polar molecules and described in Chapter 3.

In case of quadrupole potential, it can be actually shown analytically (Fabrikant, 1984; Isaacs and Morrison, 1992) that the power expansion of the $\mathcal{K}$-matrix elements Σ_u, Π_u in the incident momentum k attains the form

$$\Sigma_u \xrightarrow{k\to 0} +\frac{Q}{5}k + \mathcal{O}\big(k^2\big)\,, \tag{4.12a}$$

$$\Pi_u \xrightarrow{k\to 0} -\frac{Q}{10}k + \mathcal{O}\big(k^2\big)\,, \tag{4.12b}$$

confirming thus the expected result that $R \to 0.5$ for $k \to 0^+$.

The results of the fitting procedure are summarized in Fig. 5 of Attachment B, the main message of which is that the employed *ab initio* model seems to greatly underestimate the Σ_u component of the $\mathcal{K}$-matrix. Moreover, for incident energies around 90 meV, the phases Σ_u and Π_u act indeed in opposite rendering thus the desired behavior. For physical arguments supporting this observed behavior we refer again to the attached paper.

CONCLUSIONS

In the first part of the presented thesis we have proposed a numerical method based on the R-matrix framework (Mil'nikov et al., 2001) adapted for potential scattering in case of long range potentials. Moreover, combination with Schwinger-Lanzcos method (Meyer et al., 1991) turned out to represent an efficient extension of this approach for handling nonlocal interactions. We have studied the numerical behavior of the resulting numerical procedure Šulc et al. (2010) and performed several tests on simple (benchmark) systems, namely ground state potentials of Cs_2 and $^4He_2$ dimers. Comparison with relevant results available in the literature demonstrates that the robustness of the R-matrix renders an efficient and computationally effective algorithm superior to standard treatments usually employed for this class of problems.

In the second project we diverted our interest to the development of the correlation-polarization potential component in the static exchange + polarization approximation as discussed in Section 2.1 and Section 2.3. Following ideas of Gianturco et al. (1993) we profited from the possibility to construct the short-range part of the correlation potential by means of the local density approximation within the density functional theory framework. The long range polarization component obeying known asymptotic behavior specified in (2.26) is subsequently added by means of a joining procedure elaborated in Section 2.3. Complete SEP potential is then implemented into the DMR method reviewed in Section 1.1. Practical applications in case of electron scattering off small hydrocarbon molecules (propane, cyclopropane) indicate good agreement with other theoretical methods as well as experimental measurements. Further details and relevant references can be found in the Attachment C of the presented thesis.

The main contribution to this work was however comprised by investigation of mechanisms of rotational excitations of small molecules in the gas phase induced by electron impact. Since the necessary theoretical treatment exhibits significant difference in case of polar molecules as compared to nonpolar species, we have divided our approach accordingly. In the former case, it has turned out to be convenient to work in the dipole asymptotic formalism (Fabrikant, 1976), introduce generalized phase shifts and interpret these quantities as free parameters of the model. These are in turn fitted to the experimental data of integral and backward cross-sections. Their knowledge enables us then to compute other scattering quantities, notably the differential and individual state-to-state cross-sections resolving thus actually the total integral cross-sections into elastic and inelastic components. In the light of the encouraging results for water molecules (Čurík et al., 2006), we have adapted this approach for symmetric tops and tested on the experimental data for CH_3Cl molecule. Obtained results are discussed in Section 4.1. To our knowledge, there is only one relevant independent experimental source (Shi et al., 1996) of low energy differential data for CH_3Cl. The agreement is not that impressive as in the H_2O or (so far) unpublished SO_2 case also presented in Section 4.1. The culprit could be hidden in the inherent assumption

of diagonal short-range $\mathcal{S}$-matrix. This is actually equivalent to assuming a spherical symmetric perturbation to the dipole potential. This limitation is probably much more pronounced for strongly prolate CH_3Cl than for the SO_2 molecule. Unfortunately, lack of usable experimental data didn't allow us to resolve this issue in some systematic manner.

For nonpolar molecular species, the dominant dipole contribution is clearly missing and therefore we had to identify other crucial parameters which could be employed in a similar fashion as the generalized phase shifts for polar molecules. Several attempts to obtain converged laboratory frame SEP cross-sections turned out to be rather unrealistic in case of N_2 molecule and we have therefore digressed to the body frame and employed rotational frame transformation as explained in Subsection 1.4.4. Since the number of relevant channels is significantly reduced, the resulting cross-sections exhibited much more favorable numerical behavior. Comparison of these *ab initio* results with available literature (Morrison et al., 1997) enabled us to identify the body frame $\mathcal{K}$-matrix elements dominant for the prediction of the measured quantities as recorded by Figure 4.7. In notation of Section 4.2, we have fixed the Σ_g phase and employed Σ_u, Π_u as fitting parameters in a similar fashion as in the polar case. This gambit has turned out not only to be compatible with the measured data of integral and backward cross-sections but it furnished also an explanation for the observed suppression of the backward cross-section below 95 meV apparent from Figure 4.1. Succinct elaboration on these topics comprises Section 4.2 and is also included as Attachment B. Corresponding publication is currently in the submission process.

APPENDIX

A

VOLTERRA EQUATIONS OF THE 2nd KIND

In connection with their use in Section 1.5 this appendix intends to summarize essential descriptive ideas concerning Volterra integral equations of the second kind. The attention is especially devoted to the topics regarding numerical discretisation.

The scattering theory is usually formulated in multichannel formalism, nevertheless for the economy of notation we shall confine ourselves to the simplest setting of the one-dimensional case. Formally, the general equation of interest can be then written as

$$\psi(x) = \phi(x) + \int_0^x K(x, y, \psi(y))\,\mathrm{d}y, \text{ for } 0 \le x \le R, \tag{A.1}$$

where the range of the independent variable x is restricted to the interval $[0, R]$. Standard result (Linz, 1985) concerning the existence and uniqueness of possible solutions of Eq. (A.1) is summarized by

Theorem 1
Equation (A.1) has an unique (continuous) solution provided that

1. $\phi(x)$ is continuous in $[0, R]$,
2. the kernel $K(x, y, z)$ is continuous for $0 \le y \le x \le R$, $-\infty < z < \infty$,
3. $K(x, y, z)$ satisfies further the *Lipschitz condition*

$$|K(x, y, z_1) - K(x, y, z_2)| \le L\,|z_1 - z_2|\,.$$

In applications connected with this work we shall always assume that the kernel K of Eq. (A.1) is a linear function[1] in the third variable z and therefore fulfills the Lipschitz condition automatically.

Alternatively, existence and uniqueness of an $L^2\,(0, R)$ solution is guaranteed by the following assumptions

- $\phi(x)$ belongs to $L^2\,(0, R)$,
- the kernel fulfills

$$\int_0^R \int_0^R |K(x, y)|^2\,\mathrm{d}x\,\mathrm{d}y < \infty. \tag{A.2}$$

[1] we will use the same symbol K also for the "rest" of the kernel, *i.e.*, $K(x, y, z) = K(x, y)z$

A.1 Numerical methods of solution

What we are most interested in is the numerical solution of Eq. (A.1) for given kernel[2] which is determined by the particular potential under investigation. In this regard, it is practical to introduce discrete grid x_k, where in the simplest case $x_k = k \cdot h$ with h denoting the grid spacing.[3] The numerical integration rule is then assumed in the standard form

$$\int_0^{nh} \phi(x)\,\mathrm{d}x \approx h \sum_{i=0}^{n} w_i^n \phi(x_i), \tag{A.3}$$

where the quantities w_i^n represent the *integration weights*. Approximating integrals in Eq. (A.1) *via*Eq. (A.3) yields directly a numerical method of the form

$$\psi_n = \phi_n + h \sum_{i=0}^{n} w_i^n K\left(x_n, x_i, \psi_i\right) \text{ for } n \geq r, \tag{A.4}$$

with $\phi_n = \phi(x_n)$ and ψ_n representing the value of the numerical solution at grid point n. The restriction on n stems from the fact that higher order integration rules require some minimum number of points and therefore it is necessary to supply these "starting" values $\psi_0, \ldots, \psi_{r-1}$ in some other way. Typical candidate for the underlying integration scheme would be probably a rule of the Newton-Cotes type. However, these rules pose some restrictions on the number of grid points – *e.g.*, the well-known Simpson's rule is applicable only for even n. Nevertheless it is quite easy to circumvent this nuisance by combining rules of even and odd orders. For example, we can apply the 3/8-rule for the first 4 grid points and the Simpson's rule for the rest of the interval. Another possibility is to employ the 3/8-rule at the end of the interval (*i.e.*, for the last 4 points). The former and latter approach is by Linz (1985) denoted as *Simpson's method 1* and *Simpson's method 2*, respectively. For both methods we need to supply somehow the "starting" values ψ_0, ψ_1. Corresponding weights (A.3) obtainable by straightforward calculation are summarized in Table A.1.

A.1.1 Discretization and local-consistency errors

In order to investigate the numerical accuracy of general numerical method of the type (A.4) in more detail it is practical to establish some more formalism and notation.

If the exact analytical solution of Eq. (A.1) is denoted as $\psi(x)$ then the *discretisation error* ϵ is defined as

$$\epsilon_i = \psi_i - \psi(x_i). \tag{A.5}$$

The properties of a particular numerical method (A.4) reflect itself directly in the behavior of ϵ_i for $h \to 0$. The method of the type (A.4) is said to be (on a grid $\{x_i\}_{i=1}^N$) of order p if

$$\max_{0 \leq i \leq N} |\epsilon_i| = \mathcal{O}(h^p). \tag{A.6}$$

It is natural to expect that this order of convergence will be directly connected with the accuracy of the employed numerical integration, the precision of which can be quantified by

[2] the employment of the Green's function of Section 1.5 actually fixes the non-homogeneous term as the regular Bessel function

[3] More generally, the grid can be made of course adaptive in the sense that the spacing h can vary according to the local behavior of the potential. However, the necessary modifications of subsequent discussion in this regard are straightforward.

Definition 1 – local consistency error

$$\delta(h, x_i) = \int_0^{x_i} K(x_i, z, \psi(z))\,\mathrm{d}z - h\sum_{j=0}^{i} w_j^i K(x_i, x_j, \psi(x_j)). \tag{A.7}$$

If δ satisfies the condition

$$\max_{0\le i\le N} |\delta(h, x_i)| = \mathcal{O}\left(h^p\right), \tag{A.8}$$

then the numerical method (A.4) is said to be *consistent of order p* with Eq. (A.1). Basic theorem (Linz, 1985, chap. 7) connecting the conception of consistency and convergence can be stated as follows

Theorem 2 – consistency vs. convergence
Assume that

- the solution $\psi(x)$ of Eq. (A.1) and the kernel K are such that the numerical method (A.4) is consistent of order p with (A.1),
- the weights w_i^n satisfy
$$\sup_{n,i} |w_i^n| < \infty,$$
- the errors of the "starting" values satisfy
$$|\psi_i - \psi(x_i)| = \mathcal{O}\left(h^{p-1}\right).$$

Then the numerical method (A.4) is convergent of order p.

The important message of this theorem is that the "starting" values can be of lower order without decreasing the order of the method itself.

A.2 Numerical stability

Apart from the concept of numerical discretization errors, the issues regarding numerical stability are also important in actual computations. The reason is that even with a high order method the error for given h can in general grow (with x) much faster than the actual solution which makes the method essentially unusable.

For the sake of further analysis, the discretization error (A.5) is usually decomposed into two parts as

$$\epsilon = \epsilon_{\mathrm{S}} + \epsilon_{\mathrm{C}},$$

where ϵ_{S} stems from the propagation of "starting" errors and ϵ_{C} originates in the consistency error (A.7).

Definition 2 – stability
A method of the type (A.4) is said to be *numerically stable* with respect to an error component ϵ_i if this error can be expressed as

$$\epsilon_i = h^p e(x_i) + \mathcal{O}\left(h^q\right) \text{ with } q > p > 0,$$

where $e(x)$ is the solution of

$$e(x) = Q(x) + \int_0^x k(x, y)e(y)\,\mathrm{d}y, \tag{A.9}$$

for some function $Q(x)$.

This definition can be understood as follows. If we denote the difference of the inhomogeneous terms in Eq. (A.9) and Eq. (A.1) by $\Delta Q(x)$ and assume that this function is bounded, *i.e.*, $|\Delta Q(x)| \leq \Delta Q$, then the solutions to Eq. (A.9) and Eq. (A.1) will behave in a "similar way", more precisely their difference will be bounded as $\mathcal{O}(\Delta Q)$.

Definition 3 – repetition factor
If ρ is the smallest integer such that

$$w_i^{n+\rho} = w_i^n, \tag{A.10}$$

then the numerical method in Eq. (A.4) is said to have *repetition factor* ρ.

The main conclusions of a theorem about regarding numerical stability of methods of the type (A.4) are as follows

- all methods (A.4) are stable with respect to the consistency error
- methods (A.4) with repetition factor (A.10) equal to 1 are also stable with respect to the starting errors

For the precise formulation of this statement we refer to (Linz, 1985, p. 106), where it is also proven that the *Simpson's method 1* has repetition factor 2, whereas the *Simpson's method 2* exhibits repetition factor 1 an should be thus preferred in actual numerical applications.

A.3 Integration weights for particular discretization schemes

A.3.1 Simpson's 1/2 methods

Simpson 1			Simpson 2		
$n = 2k$	$w_0^n = w_n^n$	$1/3$	$n = 2k$	$w_0^n = w_n^n$	$1/3$
	w_{2i}^n	$2/3^\dagger$		w_{2i}^n	$2/3^\dagger$
	w_{2i+1}^n	$4/3^\dagger$		w_{2i+1}^n	$4/3^\dagger$
	$^\dagger i \in \{0, \ldots, k-1\}$			$^\dagger i \in \{0, \ldots, k-1\}$	
$n = 2k+1$	w_0^n	$3/8$	$n = 2k+1$	w_0^n	$1/3^\dagger$
	$w_1^n = w_2^n$	$9/8$		w_{2i}^n	$2/3^\dagger$
	w_3^n	$\frac{17}{24} - \frac{1}{3}\delta_{n,3}$		w_{2i+1}^n	$4/3^\dagger$
	w_{2i}^n	$4/3^\dagger$		w_{n-3}^n	$\frac{17}{24} - \frac{1}{3}\delta_{n,3}$
	w_{2i+1}^n	$2/3^\dagger$		$w_{n-1}^n = w_{n-2}^n$	$9/8$
	w_n^n	$1/3^\dagger$		w_n^n	$3/8$
	$^\dagger n \geq 5,\ i \in \{2, \ldots, k\}$			$^\dagger n \geq 5,\ i \in \{2, \ldots, k\}$	

Table A.1: Integration weights (A.3) for *Simpson's 1/2 methods*

A.3.2 Trapezoidal & "Truncated" Simpson's methods

The "truncated" Simpson's method, the integration weights of which are summarized by Table A.2, is actually formally equivalent to constructing an "infinite" grid using ordinary composite Simpson's rule and consequently truncating the grid points as well as the integration weights at the upper limit of integration. A practical advantage is that the weights in Table A.2 don't depend on n and therefore it is very straightforward to advance repeatedly the numerical solution in (A.4). On the other hand, these method are of lower order. Trapezoidal method exhibits second order behavior, whereas "truncated" Simpson's method is supposed to be just of first order due to the truncation at the end of the integration interval. This procedure introduces a quadrature error of order $\mathcal{O}(h)$ into the propagated solution and thus the overall accuracy can't be remedied by higher accuracy of the Simpson's integration itself.

trapezoidal		"truncated" Simpson's		
$n \geq 1$	$w_{n,i} = 1/(1 + \delta_{i,0} + \delta_{i,n})$	$n \geq 1$	$w_{n,2i}$	$\frac{2}{3} - \delta_{i,0}\frac{1}{3}$
			$w_{n,2i+1}$	$4/3^{\dagger}$
				$^{\dagger} i \in \{1, \ldots, n-1\}$

Table A.2: Integration weights (A.3) for trapezoidal and "truncated" Simpson's methods

APPENDIX

B

ANGULAR MOMENTUM

The purpose of this appendix is by no means to be a cheap substitute to the existing rich collection of literature covering the angular momentum topics. Instead, it should merely provide a condensed overview of angular momentum algebra identities collected from various sources and converted to a form suitable for direct application for the algebraic manipulations regarding the body/laboratory frame treatments discussed in previous chapters. Apart from the standard book sources (Brink and Satchler, 1994; Edmonds, 1996; Rose, 1995; Thompson, 2004), we would like also to mention a well-written older overview by Biedenharn et al. (1952) dealing with this subject.

B.1 Symmetries of the Clebsch-Gordan coefficients

$$\begin{aligned}(j_1 j_2\, m_1 m_2|\, j\, m) &= (-1)^{j_1-m_1}\sqrt{\frac{2j+1}{2j_2+1}}\,(j_1 j\, m_1 - m|\, j_2\, -m_2)\\ &= (-1)^{j_2+m_2}\sqrt{\frac{2j+1}{2j_1+1}}\,(j j_2\, -m m_2|\, j_1\, -m_1)\\ &= (-1)^{j_1+j_2-j_3}\,(j_1 j_2\, -m_1 - m_2|\, j\, -m)\\ &= (-1)^{j_1+j_2-j_3}\,(j_2 j_1\, m_2 m_1|\, j\, m)\\ &= (j_2 j_1\, -m_2 - m_1|\, j\, -m)\end{aligned} \tag{B.1}$$

B.2 $3j$-, $6j$-, Racah $\mathcal{W}$- and $\mathcal{Z}$- coefficients

$3j$-symbol

$$\begin{pmatrix} j_1 & j_2 & j_3\\ m_1 & m_2 & m_3\end{pmatrix} = (-1)^{j_1-j_2-m_3}\frac{(j_1 j_2\, m_1 m_2|\, j_3\, -m_3)}{\sqrt{2j_3+1}} \tag{B.2}$$

$6j$-symbol[1]

$$\begin{aligned}\begin{Bmatrix} j_1 & j_2 & j_3\\ j_4 & j_5 & j_6\end{Bmatrix} = \frac{(-1)^{j_1+j_2+j_4+j_5}}{\sqrt{2j_3+1}\sqrt{2j_6+1}}\sum_{m_1,m_2}\\ (j_1 j_2\, m_1 m_2|\, j_3\, \bullet)\,(j_3 j_4\, m_1+m_2\, \bullet\,|\, j_5\, M)\\ (j_1 j_6\, m_1\, \bullet\,|\, j_5\, M)\,(j_2 j_4\, m_2\, \bullet\,|\, j_6\, M-m_1)\end{aligned} \tag{B.3}$$

[1] symbol $\bullet$ denotes the uniquely determined value for which the corresponding Clebsch-Gordan coefficient has nonzero value

Racah $\mathcal{W}$-coefficients

$$\begin{Bmatrix} a & b & e \\ d & c & f \end{Bmatrix} = (-1)^{a+b+c+d}\, \mathcal{W}(abcd;\, ef) \tag{B.4}$$

From the various symmetries of the $3j$- and $6j$- symbols, especially the following are very useful in formal manipulations:

1. $3j$- symbols
   - interchange of any two columns of the $3j$- symbol (B.2) is equivalent to a multiplication of its value by $(-1)^{j_1+j_2+j_3}$
   - sign reversal of the second row in (B.2) is governed also by the previous rule
2. $6j$- symbols
   - the value of the $6j$-symbol (B.3) is invariant under interchange of any two columns (*i.e.*, under any column permutation)
   - the value is also unaltered by interchanging the upper and lower arguments in each of any two columns

From these properties, the symmetries of the Racah coefficients can be easily deduced

$$\begin{aligned} \mathcal{W}(abcd;\, ef) = \mathcal{W}(cdab;\, ef) = \mathcal{W}(badc;\, ef) = \\ = \mathcal{W}(acbd;\, fe) = \mathcal{W}(dbca;\, fe) = \\ = \mathcal{W}(aefd;\, bc) = \mathcal{W}(ebcf;\, ad)\,. \end{aligned} \tag{B.5}$$

Especially in the laboratory frame treatment (Arthurs and Dalgarno, 1960) of rotational excitations of rigid rotor[2] it turns out to be convenient to introduce additional algebraic *Percival-Seaton* (Percival and Seaton, 1957) $\mathcal{Z}$**-coefficients** defined as

$$\begin{aligned} \mathcal{Z}\,(ab,\, cd;\, ef) \equiv (-1)^{(f-a+c)/2}(-1)^{b+d}\,[(2a+1)(2b+1)(2c+1)(2d+1)(2f+1)]^{1/2} \\ \times \begin{pmatrix} a & c & f \\ 0 & 0 & 0 \end{pmatrix} \begin{Bmatrix} a & b & e \\ d & c & f \end{Bmatrix}. \end{aligned} \tag{B.6}$$

B.3 Orthogonality relations

$$(2j_3+1) \sum_{m_1,m_2} \begin{pmatrix} j_1 & j_2 & j_3 \\ m_1 & m_2 & m_3 \end{pmatrix} \begin{pmatrix} j_1 & j_2 & j'_3 \\ m_1 & m_2 & m'_3 \end{pmatrix} = \delta_{j_3,j'_3}\delta_{m_3,m'_3}\delta_{j_1,j_2,j_3} \tag{B.7a}$$

$$\sum_{j_3,m_3} (2j_3+1) \begin{pmatrix} j_1 & j_2 & j_3 \\ m_1 & m_2 & m_3 \end{pmatrix} \begin{pmatrix} j_1 & j_2 & j_3 \\ m'_1 & m'_2 & m_3 \end{pmatrix} = \delta_{m_1,m'_1}\delta_{m_2,m'_2} \tag{B.7b}$$

B.4 Relations between $6j$- and $3j$- symbols

Using the defining and orthogonality relations regarding $3j$- and $6j$- symbols stemming from their relation to unitary transformations between various bases in angular mo-

[2] the essential theoretical framework was actually introduced earlier by Blatt and Biedenharn (1952) although in this work the authors deal just with two particle collisions

mentum recoupling schemes, it is possible to derive a plethora of identities. Let us just mention two of them, which turned out to be most useful for our purposes.

Defining relation of the $6j$-symbol using the $3j$- symbols

$$\frac{\delta_{\gamma_1,\gamma_{1'}}\delta_{c,c_1}}{2c+1}\begin{Bmatrix} a & b & c \\ A & B & C \end{Bmatrix} = \sum_{\alpha,\beta,\gamma,\alpha',\beta'} (-1)^{A+B+C+\alpha+\beta+\gamma} \begin{pmatrix} A & B & c \\ \alpha & -\beta & \gamma' \end{pmatrix} \begin{pmatrix} B & C & a \\ \beta & -\gamma & \alpha' \end{pmatrix} \begin{pmatrix} C & A & b \\ \gamma & -\alpha & \beta' \end{pmatrix} \begin{pmatrix} a & b & c_1 \\ \alpha' & \beta' & \gamma_1' \end{pmatrix} \tag{B.8}$$

Sum over three Clebsch-Gordan coefficients

$$\sqrt{(2e+1)(2f+1)}\,(af\,\alpha M_3|\,c\,\gamma)\;\mathcal{W}(abcd;\,ef) = \sum_{\beta} (ab\,\alpha\beta|\,e\,M_1)\,(ed\,M_1M_2|\,c\,\gamma)\,(bd\,\beta M_2|\,f\,M_3) \tag{B.9}$$

B.5 Other relations

Although following identities are not directly connected with the properties of the $3j$- and/or $6j$- symbols, we found useful to include them also in this appendix mainly because of the fact that in the context of this work, they were typically used in connection with formulae mentioned above.

Composition of spherical harmonics

$$\mathrm{P}_l(\vec{n_1}\cdot\vec{n_2}) = \frac{4\pi}{2l+1}\sum_{m=-l}^{l} Y^*_{l,m}\,(\vec{n_1})\,Y_{l,m}\,(\vec{n_2}) \tag{B.10}$$

Integration of a product of three spherical harmonics

Gaunt's formula

$$\int \mathrm{d}^2\vec{n}\,Y^*_{j,m_j}\,(\vec{n})\,Y_{l,m}\,(\vec{n})\,Y_{j',m_{j'}}\,(\vec{n}) = (-1)^{m_j}\sqrt{\frac{(2j+1)(2j'+1)(2l+1)}{4\pi}}\begin{pmatrix} j & j' & l \\ 0 & 0 & 0 \end{pmatrix}\begin{pmatrix} j & j' & l \\ -m_j & m_{j'} & m \end{pmatrix} \tag{B.11}$$

Product of spherical harmonics with the same argument

$$Y^*_{l_1,m_1}\,(\vec{n})\,Y_{l_2,m_2}\,(\vec{n}) = (-1)^{m_1}\frac{1}{4\pi}\sum_{l,m}\frac{(2l_1+1)(2l_2+1)}{(2l+1)}\,\delta_{m,m_2-m_1} \times (l_1l_2\,00|\,l\,0)\,(l_1l_2\,-m_1m_2|\,l\,m)\cdot Y_{l,m}\,(\vec{n}) \tag{B.12}$$

APPENDIX

C

DIPOLE POTENTIAL

Classically, the interaction between an electrical dipole $\vec{D}$ and a particle with charge q, mass m is naturally given as

$$q\frac{\vec{D}\cdot\vec{r}}{r^3}, \tag{C.1}$$

where the vector $\vec{r}$ specifies the position of the particle. Utilizing the correspondence principle, the relevant Hamiltonian for an electron can be[1] written in the following form

$$\mathbf{H} = -\frac{1}{2}\left[\frac{1}{r^2}\frac{\partial}{\partial r}\left(r^2\frac{\partial}{\partial r}\right) - \frac{1}{r^2}\mathbf{L}^2\right] + q\frac{\vec{D}\cdot\vec{r}}{r^3}, \tag{C.2}$$

with $\mathbf{L}^2$ representing the square of the angular momentum. This Hamiltonian clearly resembles the free particle Hamiltonian, nevertheless in the dipole case, its part acting on the angular variables

$$\mathbf{L}^2 - 2\vec{D}\cdot\hat{r} \tag{C.3}$$

is modified by a term proportional linearly to D representing the magnitude of the dipole moment $\vec{D}$.

C.1 Fixed point dipole

In the simplest possible setting, we can assume that the orientation of the dipole moment $\vec{D}$ is fixed and choose the laboratory frame of reference so as the quantization $\hat{z}$-axis coincides with $\vec{D}$. In order to explore the properties of the operator (C.3) it turns out to be convenient to evaluate its matrix elements using a basis $|l\,m\rangle$ comprised of the eigenstates of $\mathbf{L}^2$ and $\mathbf{L}_z$. The resulting matrix will be diagonal in the quantum number m with each block being in turn tridiagonal in l. This observation immediately results from the Wigner-Eckart theorem. Thus we obtain

$$\begin{aligned}\mathcal{G}^m_{l',l} &\equiv \left\langle l'\,m'\right|\mathbf{L}^2 - 2D\hat{z}\cdot\hat{r}\,\left|l\,m\right\rangle = \\ &= l(l+1)\delta_{l,l'}\delta_{m',m} - 2D\delta_{m',m}\left[\delta_{l',l+1}\sqrt{\frac{l'^2-m^2}{4l'^2-1}} + \delta_{l'+1,l}\sqrt{\frac{l^2-m^2}{4l^2-1}}\right].\end{aligned} \tag{C.4}$$

From this equation we see that the matrix elements do not depend on the sign of m as a direct consequence of the axial symmetry. Of course, the eigenvalues of $\mathcal{G}^m$ will reduce to the well-known eigenvalues of $\mathbf{L}^2$, *i.e.*, $0, 2, 6, \cdots$, for zero dipole moment. On the other hand, for $D \neq 0$, the off-diagonal elements of $\mathcal{G}^m$, *i.e.*, $\mathcal{G}^m_{l,l+1}$, are nonzero and

[1] atomic units are presumed

the matrix is itself symmetric. Arguments based on the *Minimax theorem* (Wilkinson, 1988, p. 299) and Sturm sequence properties lead to the interesting conclusion that such matrices have non-degenerate eigenvalues.

C.1.1 Dipole harmonics

The spectrum and corresponding eigenvectors of the matrix $\mathcal{G}^m$ defined in (C.4) can be for practical purposes obtained most easily by a numerical procedure. To this end, one restricts[2] the quantum number l to $0, 1, \ldots l_{\max}$, evaluates corresponding matrix elements and performs then the diagonalization numerically.

Along the lines of the standard approach, one could try to express the eigenvalues of (C.3) as $\lambda(\lambda+1)$ for non-integer λ being function of l, m and the magnitude of the dipole moment D. In a more pedantic notation following Lévy-Leblond and Provost (1967), the eigenvalues should be therefore labeled as $\lambda_{l,m}(D)$ nevertheless for the sakes of brevity, we shall omit this cumbersome designation. With this proviso, we will call the eigenfunction of the operator (C.3) as *dipole harmonics* – $\mathrm{Z}_{\lambda,\,m}$ – in analogy with spherical harmonics $Y_{l,m}$. Transformation between these two angular bases is established by means of a transformation $\mathcal{A}^m$, namely

$$\mathrm{Z}_{\lambda,\,m} \equiv |\lambda\, m\rangle = \sum_l \langle l\, m|\, \lambda\, m\rangle\, |l\, m\rangle \stackrel{\text{def}}{=} \sum_l \mathcal{A}^m_{l\lambda} Y_{l,m}, \tag{C.5}$$

the matrices $\mathcal{A}^m$ being unitary[3], *i.e.*,

$$\sum_\lambda \mathcal{A}^m_{l\lambda}\mathcal{A}^{m*}_{l'\lambda} = \delta_{l,l'} \qquad \sum_l \mathcal{A}^{m*}_{l\lambda}\mathcal{A}^m_{l\lambda'} = \delta_{\lambda,\lambda'}. \tag{C.6}$$

Momentum normalized eigenfunctions ($k = \sqrt{2E}$) of the Hamiltonian (C.2) can be consequently specified according to the following formula

$$\psi_{klm}(\vec{r}) = \sqrt{\frac{2}{\pi}} k j_\lambda(kr) \mathrm{Z}_{\lambda,\,m}\left(\hat{r}\right), \tag{C.7}$$

with $j_\lambda(z)$ representing regular spherical Bessel function of order λ (Watson, 2008). Alternative approach to the solution of the radial Schrödinger equation for pure point dipole potential based on an expansion into Laguerre and Gegenbauer polynomials has been given by Alhaidari and Bahlouli (2008).

The dependence of the eigenvalues on the magnitude D of the dipole moment is depicted in Figure C.1. Each eigenvalue $l(l+1)$ of $\mathbf{L}^2$ is split into $l+1$ components due to the above mentioned symmetry in $|m|$. Although an analytic expression for the eigenvalues is probably not available, it is possible to derive (Lévy-Leblond, 1967) a continued fraction expansion of $\lambda_{l,m}(D)$ from which one can easily obtain the power expansion of these quantities in the variable $\alpha = 2D$. For example the lowest eigenvalue for $m = 0$ is given as

$$\lambda_{00}(D) \approx -\frac{\alpha^2}{6} + \frac{11}{30}\left(\frac{\alpha^2}{6}\right)^2 - \frac{133}{450}\left(\frac{\alpha^2}{6}\right)^3 + \mathcal{O}\big(\alpha^8\big)\,. \tag{C.8}$$

[2] each matrix $\mathcal{G}^m$ will be of order $l_{\max} - |m| + 1$

[3] in an actual numerical implementation, the truncation in l causes typically some error in the highest eigenvalues. One countermeasure is to increase slightly $l_{\max}$ and crop the vector of eigenvalues and also the transformation matrices after the diagonalization to correspond with the original $l_{\max}$. This technique produces more precise eigenvalues, on the other hand it can compromise the unitary property in (C.6).

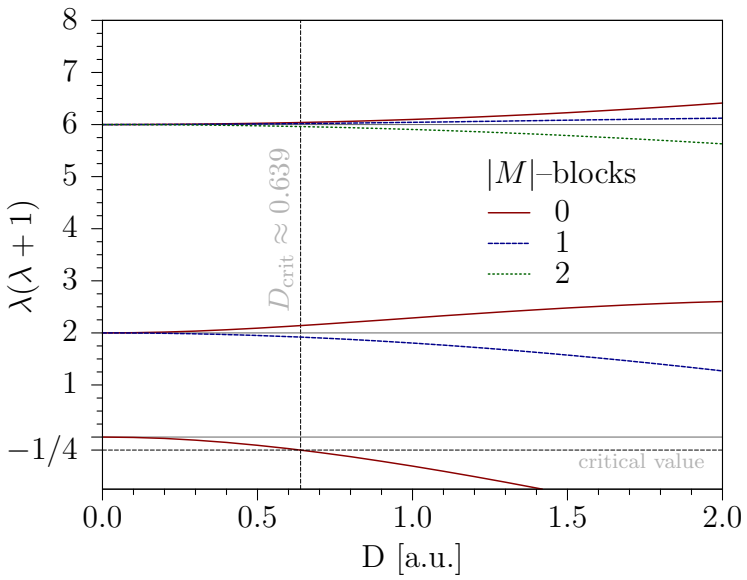

Figure C.1: Dependence of the eigenvalues of the angular operator (C.3) on the magnitude of the dipole moment

For large l one can alternatively consider the dipole term as a perturbation to $\mathbf{L}^2$ and in that case it is possible (Clark, 1984) to derive an approximation to $\lambda_{l,m}(D)$ as

$$\lambda_{l,m}(D) \approx l + \frac{D^2}{4l^3} + \mathcal{O}\left(l^{-4}\right).$$

The dipole harmonics also naturally transform to spherical harmonics in the limit $D \to 0^+$. Figure C.2 depicts the square of the absolute value of three selected $|\lambda, m\rangle$'s understood as functions of the angular variables θ, ϕ for fixed[4] angle $\phi = 0$.

C.1.2 Critical dipole

The operators $\mathbf{L}^2$ and $-2D\cos\theta$ are certainly bounded from below by 0 and $-2D$, respectively. This means that also the operator (C.3), being their sum, is bounded from below by $-2D$. Its lowest eigenvalue is thus greater than $-2D$. If we insist on the eigenvalue parametrization as $\lambda(\lambda+1)$, we immediately see that λ has to be complex for eigenvalues smaller than $-1/4$ (highlighted in Figure C.1). This situation may (and indeed does) thus occur for $D \gtrsim 1/2$ and is directly connected with the question concerning the existence of possible bound states of the electron in the dipole field as discussed in the following section. To avoid unnecessary confusion, it should be noted that each eigenvalue $\lambda_{l,m}(D)$ has its own "critical value" of D. The *critical dipole moment* usually mentioned in the literature refers to the lowest eigenvalue $\lambda_{0,0}$.

To numerically render these critical values forcing λ to be complex can be done using standard methods for root searching (Press et al., 2007, p. 442). To this end, we interpret the eigenvalue $\lambda_{l,m}(D)$ as a function of D and define $f(x) = \lambda_{l,m}(x) + 1/4$. The critical value of D then coincides with roots of f and even the simplest *bisection method* yields very satisfactory results. Table C.1 contains the critical values for several eigenvalues $\lambda_{l,m}$ localized by means of this procedure as compared to Crawford (1967).

[4] because of the axial symmetry, the three dimensional shape would be obtained by rotating the slice depicted in Figure C.2 around the z-axis

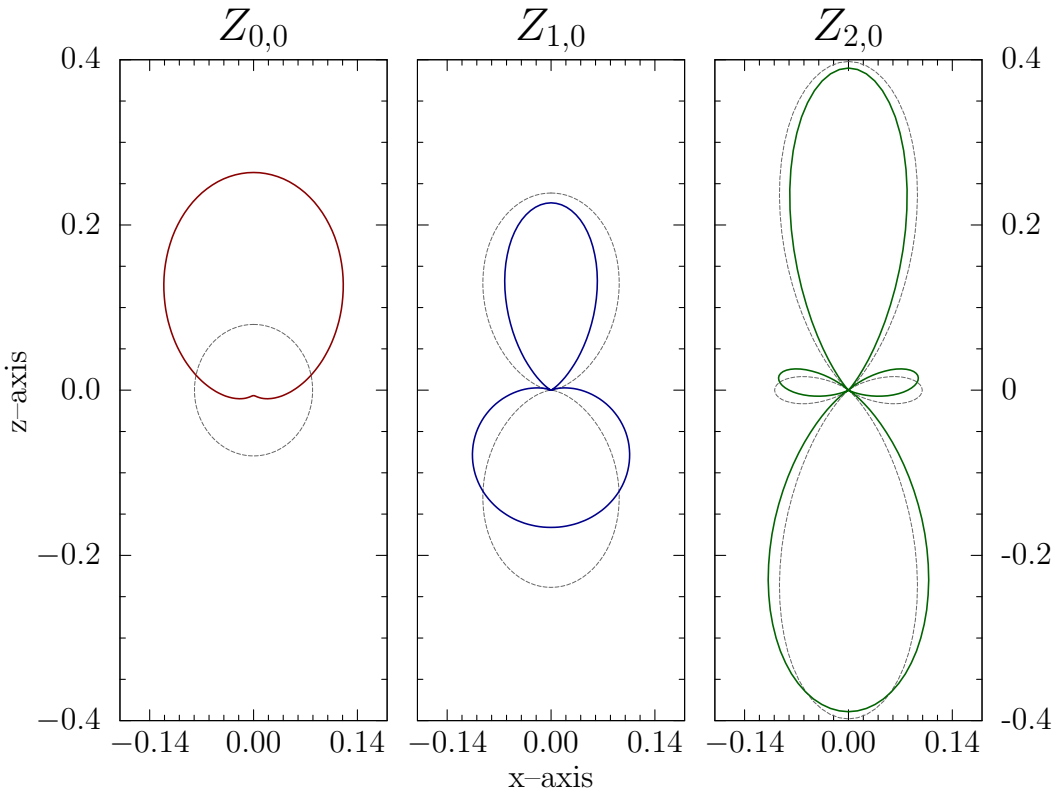

Figure C.2: Selected dipole harmonics for $D = 1.0$ a.u. and $\phi = 0$ – gray lines represent corresponding spherical harmonics (*i.e.*, limiting case for $D \to 0^+$), axial symmetry of the dipole harmonics is preserved, nevertheless the overall shape is deformed.

m	l	$D^{\dagger}_{\mathrm{crit}}$ [a.u.]	D_{crit} [a.u.]
0	0	0.63928	0.639314877
0	1	7.5463	7.546955713
0	2	21.299	21.30090331
1	1	3.7916	3.791967926

Table C.1: Magnitude of the critical dipole moment D_{crit} for several eigenvalues $\lambda_{l,m}$. Values $D^{\dagger}_{\mathrm{crit}}$ in the second column are taken from Crawford (1967). More accurate results can be found in Alhaidari and Bahlouli (2008).

C.2 Other forms of the dipole potential

The dipole interaction model presented in the preceding section is clearly the most simple. In the literature, three additional cases are usually distinguished:

- **fixed finite dipole** – in this case, it is assumed that the electrical field is generated by two point particles fixed in space with opposite charges q separated by a distance R. For $r \to \infty$ the form of the potential coincides naturally with Eq. (C.1).
- **point dipole rotor** – the direction of the dipole moment $\vec{D}$ in Eq. (C.1) can in general depend on time. A crude model of a polar molecule would consist in fixing the dipole moment in the frame of reference of the molecule. The vector $\vec{D}$ will consequently depend on the Euler angles specifying the orientation of the molecule in space.
- **finite dipole rotor** – the last case is a combination of the preceding two schemes, *i.e.*, the dipole is assumed to be finite as well as free to rotate.

C.3 Existence of electron bound states in a dipole field

The question whether and under which conditions can a dipole field bind an electron has aroused the attention of many investigators in the past few decades. Lucid overview regarding this topic can be found in Turner (1977) or in Appendix B of Itikawa (1978). In this section we would like to provide a short summary of the relevant results.

The analysis in the framework of classical mechanics is much simpler as shown by Fox (1968); Turner and Fox (1968). Their conclusions can be summarized as follows:

- fixed finite dipole supports electron bound states for arbitrarily small dipole moment D (Turner and Fox, 1968),
- in the case of a point dipole, the only stable electron orbits are such that $r = \text{const.}$ and total energy $E = 0$. Moreover, a necessary condition is $D > 3\sqrt{3}/4p_\phi^2$, where p_ϕ^2 is the electron's angular momentum along the dipole axis (Fox, 1968).

The notion of quantum mechanical critical dipole can be dated back to the work by Fermi and Teller (1947) almost sixty years ago. Nevertheless as pointed out by Turner (1977), their results didn't attract sufficient attention at that time and thus the existence of the minimal dipole moment required to bind an electron was rediscovered twenty years later by several authors as discussed below. On the other hand, it should be noted that the principal ideas applicable also in the general case are mentioned already in the book by Landau and Lifschitz (1977), the first edition of which is dated to 1958. Landau and Lifschitz (1977) analyze the radial differential equation for an electron in a *spherically symmetric* fixed point dipole field

$$V(r) \sim \beta/r^2. \tag{C.9}$$

The form of the potential (C.9) poses actually no restriction, since the Schrödinger equation for the "proper" dipole potential (C.1) is separable in radial/angular variables. The eigenvalues of (C.3) will then only reflect itself in a particular value of the parameter β. Arguments based on the *oscillation theorem* lead to the following conclusions, for the concise statement of which it is convenient to introduce a parameter γ as

$$\gamma = 2\beta - l(l+1), \tag{C.10}$$

where l is the orbital angular momentum of the electron.

- If the potential is of the form (C.9) in the entire space then
  1. $\gamma > 1/4$ – the particle is said[5] to "fall to the centre",
  2. $\gamma < 1/4$ – the dipole field supports no bound states.
- If the potential (C.9) is modified by some short-range perturbation[6] to mitigate the singular behavior at the origin, then
  1. $\gamma > 1/4$ – there are infinitely many negative energy states for the zero energy radial wave function has infinitely many nodes (*i.e.*, its ordinal number is infinite),
  2. $\gamma < 1/4$ – only a finite number of bound states can exist in this case, depending on the form of the short range perturbation.

In the following discussion, let us distinguish two cases according to the fact whether the rotational degrees of freedom of the dipole moment are taken into account or not. We shall also confine ourselves only on the discussion of negative energy states. For implications of the properties of the dipole potential for scattering calculations we refer to Section 4.1.

C.3.1 Fixed dipole

The bound state problem for a fixed finite dipole was first studied probably by Wallis et al. (1960) who separated the Schrödinger equation in spheroidal coordinates (ξ, η), expressed the sought negative energy wave function in a basis comprised of associated Laguerre (ξ) and Legendre (η) polynomials and thus converted the differential equation into an algebraic problem. These equations were solved for dipole moments in the interval 0.84 - 30.0 a.u. Later, the same problem was variationally solved by Turner et al. (1968) with a basis composed of functions of the type $\exp\{-1/2\alpha(\xi+\eta)\}\xi^p\eta^q$. Resulting energies for the lowest bound state are given in Table C.2 for a few values of the dipole moment D. The theoretical dependence of the binding energies on D has been investigated by Abramov and Komarov (1972). Analogical calculations to Turner et al. (1968) were performed by Garrett et al. (1969) in spherical coordinates. As opposed to Wallis et al. (1960), Turner et al. (1968) present not only the energies but also the form of corresponding eigenfunctions for a much wider range of the dipole moment, namely 0.639 - 400.0 a.u. A very similar numerical approach as in Turner et al. (1968) led Turner and Fox (1966) to the conclusion that fixed finite dipole doesn't support bound electron states for $D < D_{\mathrm{crit}} \approx 0.6393$ a.u. In this work, the variation principle was applied to D for fixed energy $E = 0$ – this corresponds to the fact that we seek the smallest value of D which is compatible with zero energy bound state (critical binding). A surprisingly simple argument can be made to verify this claim (Crawford and Dalgarno, 1967). The reasoning goes as follows. The potential for a fixed finite dipole $q\vec{d}$ is given by

$$V(\vec{r}) = q\left(\frac{1}{\left|\vec{r}-\vec{d}\right|} - \frac{1}{\left|\vec{r}\right|}\right).$$

This expression is everywhere less negative than the lower bound $-q/r^2$, for which we can apply the results of Landau and Lifschitz (1977) and therefore confirm the

[5] This is an interpretation of the fact that the radial part of the wave function can be shown to exhibit infinite number of zeros for any finite energy E. On the other hand, the ground state with energy E_0 has no radial nodes and one is then forced to the conclusion that $E_0 \to -\infty$. This in turn leads to the closure that the electron should be confined to an infinitesimal vicinity of the origin $r = 0$.

[6] short-range meaning that the perturbation decays faster than $1/r^2$ for $r \to \infty$

numerical results of Turner and Fox (1966). The independence of the lower bound on the size or direction of $\vec{q}$ enables us to extend this result also to the case of a fixed/freely rotating finite/point dipole.

Recently, Giri et al. (2008) claimed to prove that the fixed point dipole does support bound states even for undercritical dipole moments. Their argument is based on the statement that the radial Hamiltonian is actually not self-adjoint, nevertheless by direct computation of its deficiency indices they prove that it admits self-adjoint extension. Giri et al. (2008) then aver that this extension (parametrized by ω) posses a bound state, which is in contradiction with previous works. On one hand, Giri et al. (2008) claim that their results are incompatible with older findings, on the other hand, on p. 3 the authors state that "ω encodes the effect of the boundary conditions arising from the short range physics of the system". If this should be understood as a result of particular short range modification to the point dipole potential, then their conclusions essentially reduce to the findings in Crawford (1967), who generalized the analysis of Landau and Lifschitz (1977) to the case of anisotropic dipole potential (C.1) modified by a short-range perturbation.

It could seem tempting to apply the Crawford's results also to the class of potentials modeling rotating polar molecules. Nevertheless, as pointed out in Crawford (1967), this would require the incorporation of the Born-Oppenheimer approximation. However, the predicted discrete spectrum has an accumulation point for $E = 0$, which in turn means that the Born-Oppenheimer approach is itself questionable.

C.3.2 Rotating dipole

If the dipole moment is allowed to freely rotate in space, one would naturally expect that the strength of the dipole potential could be "averaged out" thus altering the conditions for electron binding. From the formal point of view, the incorporation of the rotational degrees of freedom means that we are forced to include additional terms into Eq. (C.2), typically rigid rotor Hamiltonian as introduced in Appendix E.

In the simplest possible setting of a diatomic polar molecule, the radial components of the electron's wave function $U^J_{j,l}$ in the laboratory frame close coupling treatment will satisfy a set of coupled differential equations (Bottcher, 1969; Garrett, 1971*b*), namely

$$\left[\frac{1}{2}\frac{\mathrm{d}^2}{\mathrm{d}r^2} - \frac{l(l+1)}{2r^2} + \left(E - \frac{j(j+1)}{2I}\right)\right] U^J_{j,l}(r) = \\ = \sum_{j',l'} \left\langle jl,\, J\right| V \left|j'l',\, J\right\rangle U^J_{j',l'}(r), \tag{C.11}$$

where j, l are the channel quantum numbers, I stands for the moment of inertia of the molecule and J represents the total angular momentum. In the past, it has been argued

D [a.u.]	E [eV]	D [a.u.]	E [eV]
0.667	$1.2208{\cdot}10^{-18}$	1.000	$2.7882{\cdot}10^{-2}$
0.693	$1.1340{\cdot}10^{-10}$	2.000	$2.3982{\cdot}10^{0}$
0.741	$9.9116{\cdot}10^{-7}$	4.000	$7.0285{\cdot}10^{0}$
0.797	$8.5596{\cdot}10^{-5}$	8.000	$1.0219{\cdot}10^{1}$

Table C.2: Lowest bound state energies for a fixed finite dipole with magnitude D as given by Turner et al. (1968)

that the critical binding properties of an electron in a field of rotating dipole should be identical to the fixed case (Bottcher, 1970), nevertheless as pointed out by Garrett (1971*a*), this argument is flawed by the omission of the difference in the electron's channel momenta. Garrett (1980*a*) showed later that the arguments of Bottcher (1970) are actually valid in the (purely mathematical) limit of point dipole rotor.

The system of a rotating finite dipole moment was thoroughly studied by Garrett (Garrett, 1970, 1971*b*, 1980*a*,*b*). He investigated the radial laboratory frame close-coupling equations for the presumably bound electron. His findings are as follows

- the number of bound states is finite (Garrett, 1971*b*, p. 966),
- the critical dipole moment D_{crit} required to bind an electron depends on I (Garrett, 1970) and decreases monotonically with $I \to \infty$. Moreover, D_{crit} converges in this limit to the value for the fixed point dipole as depicted in Figure C.3

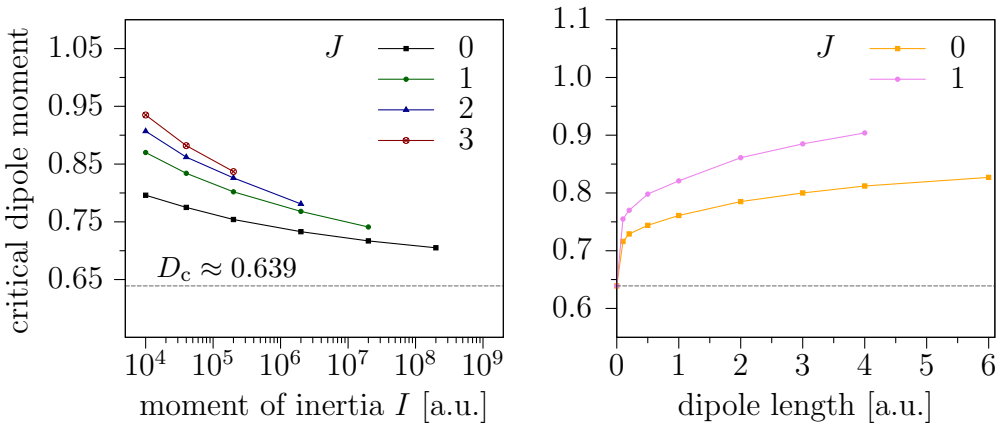

Figure C.3: Dependence of the critical dipole moment on the moment of inertia I and the charge separation in case of rotating finite dipole. Value of D_{crit} is influenced by total angular momentum J. Data taken from Garrett (1970) and Garrett (1980*a*).

- for fixed moment of inertia I and dipole length, D_{crit} is an increasing function of the total angular momentum J
- with decreasing charge separation in the finite dipole rotor model, D_{crit} converges to the value for the point dipole case as demonstrated graphically in the right panel of Figure C.3

Generalization to "real" molecules

Because the binding properties are mainly attributed to the long range behavior of the dipole potential, the finite dipole rotor model could furnish in principle a reliable approximation. However, exact treatment is hardly possible. Employing Rayleigh-Ritz variational principle, Crawford (1971) showed that in the framework of Born-Oppenheimer approximation, all polar molecules with dipole moment higher than the point dipole value 0.693 do support electron bound states. His generalization to freely rotating molecules based on an analysis of critical dipole moments calculated by Garrett (1970) and by using arguments about presumably small influence of the short-range interaction is nonetheless little bit vague – "the facts strongly suggest that any real gas phase molecule or radical with $D > 0.79$ a.u. probably can bind an extra electron, and almost certainly can if $D > 0.98$ a.u.".

Ab initio studies regarding electron affinities of simple polar molecules have been also reported (Jordan and Luken, 1976). Their theoretical value of the affinity for LiCl 0.54 eV is in good agreement with experimental value 0.61 eV (Carlsten et al., 1976). Calculations performed on other small polar molecules suggest that the electron affinity increases with increasing dipole moment and the binding energies are very small as compared to values predicted by finite dipole rotor model. Also no "multiple" bound states have been observed.

In connection with the question about the role of the Born-Oppenheimer approximation in Crawford's results, Crawford and Garrett (1977) have shown for typical values of I, R (only spherical rotors are considered) that the negative ion is still stable provided that the Born-Oppenheimer electron affinity is larger than roughly 1/10 of the rotational constant of the molecule (and thus the energy increase by adding positive semidefinite rotational term $j(j+1)/2I$ to the Hamiltonian is still compatible with the bound character of the respective state).

APPENDIX
D

SPHERICAL BESSEL FUNCTIONS

The purpose of this short appendix is to furnish a concise overview of the normalization (and other possible definition related) conventions regarding the use of various special functions appearing in the presented work in order to avoid confusion with the plethora of other sources in the available literature.

D.1 Spherical & Ricatti-Bessel functions

Spherical Bessel functions naturally enter the stage of quantum mechanics as solutions of the radial Schrödinger equation and are defined in terms of Bessel J, N functions of fractional (Abramowitz and Stegun, 1965, ch. 10) order as

$$j_l(z) \equiv \sqrt{\frac{\pi}{2z}} J_{l+\frac{1}{2}}(z) \qquad j_l(z) \equiv \sqrt{\frac{\pi}{2z}} N_{l+\frac{1}{2}}(z). \tag{D.1}$$

Standard substitution $R \leftarrow \frac{1}{r}\xi$ in the radial Schrödinger equation eliminates the first derivative term and yields thus a simpler differential equation for ξ, the two independent solutions of which are the so-called *Ricatti-Bessel* functions

$$\widehat{j}_l(z) \equiv z j_l(z) \qquad \widehat{n}_l(z) \equiv -z j_l(z)\,. \tag{D.2}$$

Two particular linear combinations of (D.2) turn out to be especially useful, namely the *Ricatti-Hankel* functions given by

$$\widehat{h}_l^+(z) \equiv i\widehat{j}_l(z) + \widehat{n}_l(z) \qquad \widehat{h}_l^-(z) \equiv -i\widehat{j}_l(z) + \widehat{n}_l(z)\,. \tag{D.3}$$

In multichannel scattering formalism, to each channel a with channel momentum k_a, there correspond two radial functions f_a, g_a (regular and irregular solution) which are just conveniently chosen linear combinations of (D.2). However, as discussed by Zemach (1964), the necessary condition ensuring symmetry of the resulting $\mathcal{K}$-matrix is that the absolute value of the Wronskian of these f_a, g_a is 1.

D.1.1 Extension to complex orders

In connection with the radial Schrödinger equation in dipole potential, it turns out to be convenient to define functions (D.1) and (D.2) also for complex orders. In order to distinguish this case we shall denote the order as λ instead of l. Bessel functions are analytic functions of their order in the entire complex plane (possibly except the origin) – for details we refer to an excellent overview by Watson (2008). The well-known

(Taylor, 2006, ch. 11) asymptotic behavior of (D.2) can be thus directly extended for complex orders λ as

$$\widehat{h}_l^{\pm}(z) \approx \mathrm{e}^{\pm\Im\lambda\frac{\pi}{2}}\mathrm{e}^{\pm\mathrm{i}\left(z-\Re\lambda\frac{\pi}{2}\right)}\left(1+\mathcal{O}\left(z^{-1}\right)\right) \qquad \text{for } z\to\infty. \tag{D.4}$$

However, in scattering applications, one prefers radial solutions yielding unit ingoing and outgoing flux. To ensure this, it is necessary to renormalize (Clark, 1984) functions (D.4) as

$$\widehat{\widehat{h}}_\lambda^{\pm}(z) \overset{\text{def}}{=} \widehat{h}_l^{\pm}(z)\cdot\mathrm{e}^{\mp\Im\lambda\frac{\pi}{2}} \approx \mathrm{e}^{\pm\mathrm{i}\left(z-\Re\lambda\frac{\pi}{2}\right)}\left(1+\mathcal{O}\left(z^{-1}\right)\right) \qquad \text{for } z\to\infty. \tag{D.5}$$

D.2 Scattering integrals

Finally, following set of relations entails an overview of integrals, which appear frequently in the first Born approximation framework in computations of scattering amplitudes and transition operator matrix elements. The formal mathematical reason is that in this approximation, the radial wave function is typically described by a regular spherical Bessel function of corresponding order. Another possible use is for integrals the integrand of which contains plane wave terms $\exp(i\vec{k}\cdot\vec{r})$. This expression can be expanded into spherical harmonics as

$$\mathrm{e}^{\mathrm{i}\vec{k}\cdot\vec{r}} = 4\pi\sum_{l=0}^{\infty}\sum_{m=-l}^{l} i^l j_l(kr)\,\mathrm{Y}^*_{l,\,m}\big(\hat{k}\big)\mathrm{Y}_{l,\,m}\big(\hat{r}\big), \tag{D.6}$$

where the radial term is again given by a regular spherical Bessel function so the integration over r or k can in principle benefit from formulae presented below. For other useful properties and relations we refer to Gradshteyn and Ryzhik (2007) or Erdélyi (1954).

Combination of j_l and power[1] of r

$$\eta > 1, \Re\lambda > \eta - 3$$

$$\int_0^\infty j_\lambda(kr)\,r^{2-\eta}\,\mathrm{d}r = \sqrt{\pi}\,2^{1-\eta}k^{\eta-3}\frac{\Gamma\left(\frac{3}{2}+\frac{\lambda}{2}-\frac{\eta}{2}\right)}{\Gamma\left(\frac{\lambda}{2}+\frac{\eta}{2}\right)} \tag{D.7}$$

Combination of two j_l's with different k and power of r

$$0 < k_0 < k,\ \eta > 0,\ \Re\lambda + \Re\lambda_0 > \eta - 3$$

$$\int_0^\infty j_\lambda(kr)\,j_{\lambda_0}(k_0 r)\,r^{2-\eta}\,\mathrm{d}r = \left(\frac{\pi}{2^\eta}\right)\frac{k_0^{\lambda_0}}{k^{3+\lambda_0-\eta}}\frac{\Gamma\left(\frac{\lambda+\lambda_0-\eta+3}{2}\right)}{\Gamma\left(\lambda_0+\frac{3}{2}\right)\Gamma\left(\frac{\lambda-\lambda_0+\eta}{2}\right)}\cdot \\ \cdot\,{}_2F_1\left(\frac{\lambda+\lambda_0-\eta+3}{2},\,\frac{\lambda_0-\lambda-\eta+2}{2},\,\lambda_0+\frac{3}{2};\,\frac{k_0^2}{k^2}\right) \tag{D.8}$$

The symbol ${}_2\mathrm{F}_1$ denotes the standard hypergeometric function (Abramowitz and Stegun, 1965, ch. 15). Although at first sight it might seem that Eq. (D.8) should be symmetrical under simultaneous exchange of $\lambda \leftrightarrow \lambda_0$ and $k \leftrightarrow k_0$, the situation is

[1] in Feldt and Morrison (2008*b*), there is probably a misprint concerning the validity conditions of this formula

slightly more complicated by the fact that the right hand side of Eq. (D.8) is not analytic in the variable k_0/k (Gradshteyn and Ryzhik, 2007, p. 683).

Combination of two j_l's with the same k and power of r

$$0 < k,\ \eta > 1,\ \Re\lambda + \Re\lambda_0 > \eta - 2$$

$$\int_0^\infty j_\lambda(kr)\, j_{\lambda_0}(kr)\, r^{2-\eta}\,\mathrm{d}r = \left(\frac{\pi}{2^\eta}\right) \frac{\Gamma(\eta-1)\,\Gamma\left(\frac{\lambda+\lambda_0-\eta+3}{2}\right)}{\Gamma\left(\frac{\lambda_0-\lambda+\eta}{2}\right)\Gamma\left(\frac{\lambda+\lambda_0+\eta+1}{2}\right)\Gamma\left(\frac{\lambda-\lambda_0+\eta}{2}\right)} \cdot k^{\eta-3} \tag{D.9}$$

A noteworthy special case of Eq. (D.9) is obtained for $\eta = 2$ since then the radial term $r^{2-\eta}$ vanishes. Using a slightly modified *Euler's reflection formula* for $\Gamma(z)$

$$\Gamma(1+z)\Gamma(1-z) = z\Gamma(z)\Gamma(1-z) = \frac{\pi z}{\sin \pi z} \tag{D.10}$$

readily yields for $\Re\lambda + \Re\lambda_0 > 0, k > 0$

$$\int_0^\infty j_\lambda(kr)\, j_{\lambda_0}(kr)\ \mathrm{d}r = \frac{\sin\left((\lambda_0-\lambda)\frac{\pi}{2}\right)}{(\lambda_0-\lambda)(\lambda+\lambda_0+1)} \cdot k^{-1}. \tag{D.11}$$

More specifically, Eq. (D.11) reduces for $\lambda_0 = \lambda \pm 1$ to

$$\int_0^\infty j_\lambda(kr)\, j_{\lambda\pm1}(kr)\ \mathrm{d}r = \frac{1}{2\lambda+1\pm1} \cdot k^{-1}. \tag{D.12}$$

Combination of two j_l's of order λ with different k and power of r

$$k > 0,\ k_0 > 0,\ \Re\eta > 0,\ \Re\lambda > -1$$

$$\begin{aligned}\int_0^\infty j_\lambda(kr)\, j_\lambda(k_0 r)\, r^{2-\eta}\,\mathrm{d}r = \left(\frac{\pi}{2^\eta}\right) &\frac{(kk_0)^\lambda\,\Gamma\left(\lambda+\frac{3}{2}-\frac{\eta}{2}\right)}{(k+k_0)^{2\lambda+3-\eta}\,\Gamma\left(\lambda+\frac{3}{2}\right)\Gamma\left(\frac{\eta}{2}\right)} \\ &\cdot {}^2F_1\left(\lambda+\frac{3}{2}-\frac{\eta}{2},\ \lambda+1,\ 2\lambda+2;\ \frac{4kk_0}{(k+k_0)^2}\right)\end{aligned} \tag{D.13}$$

APPENDIX

E

RIGID ROTOR APPROXIMATION

In the standard treatment of molecular vibrations/rotations, the electronic structure of the molecule is usually disregarded and the molecule is simply modeled by charged point particles representing the nuclei. In order to obtain (Watson, 1970; Wilson et al., 1980) the quantum-mechanical Hamiltonian, it is necessary to perform several steps. Firstly, the translational motion is separated by coordinate transformation into a frame of reference "moving" with the molecule determined by *Eckart conditions*. Consequently, normal coordinates are introduced and the (actually still classical) Hamiltonian is restated in terms of angular momenta and momenta conjugate to the normal coordinates. In order to utilize the correspondence principle, it is further essential to determine the relation between the angular momenta and momenta conjugated to the Euler angles and finally apply a procedure, originally proposed in the early days of quantum mechanics by Podolsky (1928), which yields the "exact" rovibronic Hamiltonian. However, if the coupling between rotations and vibrations is neglected, the total energy separates into the energy of a rotating rigid molecule plus vibrational energy of a non-rotating body and one speaks then about *rigid rotor* approximation.

E.1 Symmetric tops

The rotational Hamiltonian takes in the rigid rotor approximation the following form

$$\mathbf{H}_{\mathrm{r}} = \frac{1}{2}\left[\frac{\mathbf{L}_{\mathrm{A}}}{I_{\mathrm{A}}} + \frac{\mathbf{L}_{\mathrm{B}}}{I_{\mathrm{B}}} + \frac{\mathbf{L}_{\mathrm{C}}}{I_{\mathrm{C}}}\right], \tag{E.1}$$

where the subscripts A, B, C identify body fixed coordinate axes and the $\mathbf{L}_{\_}$ represent corresponding angular momentum projections. The *rotational constants* A, B, C are then defined by means of the moments of inertia I as, *e.g.*, $A = 1/2I_A$ *etc.* By convention $I_A \leq I_B \leq I_C$ and therefore $A \geq B \geq C$. It may happen that $A > B = C$ or $A = B > C$. In that case, the molecule is denoted as a *symmetric top*. This relation is automatically satisfied if the molecule exhibits an n-fold symmetry axis with $n \geq 3$. On the other hand, it may happen that even if the molecule is not itself symmetric, its rotational behavior is close to a symmetric top. This case is denoted as an *accidental symmetric top* (Winnewisser, 1972).

Two cases are distinguished:

prolate top	$A > B = C$	*e.g.*, CH_3Cl, CH_3Br, CF_3Cl
oblate top	$A = B > C$	*e.g.*, NH_3

E.1.1 Rotational eigenfunctions

It can be shown that in the Euler angles representation, the normalized (E.20) rotational eigenstates $|j\,k\,m\rangle$ of a symmetric top are rendered as

$$|j\,k\,m\rangle = \sqrt{\frac{2j+1}{8\pi^2}}\,\mathcal{D}^{j}_{m,k}(\alpha,\,\beta,\,\gamma)\,. \tag{E.2}$$

Each ket $|j\,k\,m\rangle$ is an eigenstate of the total angular momentum, projection of the angular momentum onto the space fixed z-axis and also of the projection of the angular momentum onto the (rotating) molecular z'-axis of symmetry with eigenvalues $j(j+1)$, m and k, respectively. The Euler angles (α,β,γ) are defined in the y-convention as discussed in length, *e.g.*, in Goldstein et al. (2001, p. 154) and determine the orientation of the principal axes frame of reference fixed in the molecule. More importantly, the symbol $\mathcal{D}^{j}_{m,k}$ represents a *Wigner function*[1] the properties of which are concisely summarized in Section E.3.

When comparing relations from various sources in the available literature, proper care has to be taken as concerns the variety of possible conventions regarding Euler angles, Wigner $\mathcal{D}^{j}_{m,k}$ functions and active/passive interpretation of rotation operators. We adhere to the convection used by Davydov (1965), where the $\mathcal{D}^{j}_{m,k}$ functions are defined as matrix elements of the rotation operator expressed in the *passive convention*, *i.e.*, the set of Euler angles (α,β,γ) defines a sequence of three successive rotations applied to the original space fixed coordinate system (x,y,z) ending up with the molecule-fixed reference frame $(\xi,\,\eta,\,\zeta)$ coinciding with the principal axes of inertia. Explicitly written, one has

$$\mathcal{D}^{j}_{m,m'}(\alpha,\,\beta,\,\gamma) \equiv \big\langle jm'\big|\,\mathbf{R}\,(\alpha,\beta,\gamma)\,\big|jm\big\rangle\,, \tag{E.3}$$

with the rotation operator $\mathbf{R}$ being given by

$$\mathbf{R}\,(\alpha,\beta,\gamma) = \mathrm{e}^{\frac{\mathrm{i}}{\hbar}\gamma\mathbf{J}_z}\mathrm{e}^{\frac{\mathrm{i}}{\hbar}\beta\mathbf{J}_y}\mathrm{e}^{\frac{\mathrm{i}}{\hbar}\alpha\mathbf{J}_z}.$$

Simplifying (E.3) and appending a subscript D for Davydov, one obtains

$${}_{\mathrm{D}}\mathcal{D}^{j}_{m,m'}(\alpha,\,\beta,\,\gamma) = \mathrm{e}^{\mathrm{i}m\alpha}\left\langle jm'\right|\mathrm{e}^{\frac{\mathrm{i}}{\hbar}\beta\mathbf{J}_y}\left|jm\right\rangle\mathrm{e}^{\mathrm{i}m'\gamma}, \tag{E.4}$$

where the states $|jm\rangle$,$|jm'\rangle$ can be considered as referring to the space-fixed frame of reference. Davydov consequently obtains the transformation relation of spherical harmonics resulting from the definition (E.3) as

$$\mathrm{Y}_{l,\,m}\big(\theta,\,\phi\big) = \sum_{k} {}_{\mathrm{D}}\mathcal{D}^{l}_{m,k}(\alpha,\,\beta,\,\gamma)\,\mathrm{Y}_{j,\,k}\big(\theta',\,\phi'\big), \tag{E.5a}$$

$$\mathrm{Y}_{l,\,k}\big(\theta',\,\phi'\big) = \sum_{m} {}_{\mathrm{D}}\mathcal{D}^{l\,*}_{m,k}(\alpha,\,\beta,\,\gamma)\,\mathrm{Y}_{j,\,m}\big(\theta,\,\phi\big), \tag{E.5b}$$

where the angular variables θ,ϕ and θ', ϕ' refer to the space fixed (laboratory) and rotated (fixed in the molecule) frame of reference, respectively.

On the other hand, Brink and Satchler (1994) use the same convention regarding Euler angles $(\alpha,\,\beta,\,\gamma)$ but works in the active convention, *i.e.*, they consider the frame of reference as being fixed in space and rotate the physical states. Their D-matrices

[1] also known as *generalized spherical function* or alternatively *D-function*

(distinguished by subscript B) are thus rendered as matrix elements of the rotation operator in active convention to wit

$$\begin{aligned} {}_{\mathrm{B}}\mathcal{D}^{j}_{m,m'}(\alpha,\,\beta,\,\gamma) &= \left\langle jm \right| \mathrm{e}^{-\frac{\mathrm{i}}{\hbar}\alpha\mathbf{J}_z}\mathrm{e}^{-\frac{\mathrm{i}}{\hbar}\beta\mathbf{J}_y}\mathrm{e}^{-\frac{\mathrm{i}}{\hbar}\gamma\mathbf{J}_z} \left| jm' \right\rangle \\ &= \mathrm{e}^{-\mathrm{i}m\gamma} \left\langle jm \right| \mathrm{e}^{-\frac{\mathrm{i}}{\hbar}\beta\mathbf{J}_y} \left| jm' \right\rangle \mathrm{e}^{-\mathrm{i}m'\alpha}. \end{aligned} \tag{E.6}$$

Quick simultaneous glance at Eqs. (E.4) and (E.6) reveals that D-matrices given by Brink and Satchler (1994) are just complex conjugated D-matrices of the D-matrices of Davydov (1965)

$${}_{\mathrm{D}}\mathcal{D}^{j}_{m,m'}(\alpha,\,\beta,\,\gamma) = {}_{\mathrm{B}}\mathcal{D}^{j\,*}_{m,m'}(\alpha,\,\beta,\,\gamma)\,. \tag{E.7}$$

In the active convention, if one rotates a state $|jm\rangle$ by $(\alpha,\,\beta,\,\gamma)$, the resulting state $|jm\rangle' \equiv \mathbf{R}\,|jm\rangle$ is naturally an eigenstate (with the same eigenvalue m) of the angular momentum projection onto the z'-axis, *i.e.*, the rotated z-axis. Expanding $|jm\rangle'$ in the original basis $|jm\rangle$ yields

$$|jm\rangle' \equiv \mathbf{R}\,|jm\rangle = \sum_k |jk\rangle\,\langle jk|\,\mathbf{R}\,|jm\rangle\,, \tag{E.8}$$

with $\langle jk|\,\mathbf{R}\,|jm\rangle$ being identical to Brink's D-matrix (E.6). In coordinate $(\theta,\,\phi)$ representation, Eq. (E.8) is equivalent to

$$\mathrm{Y}_{l,\,m}\big(\theta',\,\phi'\big) = \sum_k {}_{\mathrm{B}}\mathcal{D}^{l}_{k,m}(\alpha,\,\beta,\,\gamma)\,\mathrm{Y}_{j,\,k}\big(\theta,\,\phi\big). \tag{E.9}$$

Taking into account the "compatibility" relation (E.7) recovers Davydov's result (E.5b). Other books preferring the active convention such as Inui et al. (1996) or Bohr and Mottelson (1998) are fortunately in accordance with the results stated previously.

Another heavily cited source on angular momentum, the book by Edmonds (1996), also chooses the passive view point and consequently avers to define the D-matrices as matrix elements of the rotation operator in passive convention as it is done also by Davydov (1965). The defining relation (Eq. 4.1.10 in Edmonds (1996)) is[2]

$$\begin{aligned} {}_{\mathrm{E}}\mathcal{D}^{j}_{m,m'}(\alpha,\,\beta,\,\gamma) &= \left\langle jm \right| \mathrm{e}^{\frac{\mathrm{i}}{\hbar}\alpha\mathbf{J}_z}\mathrm{e}^{\frac{\mathrm{i}}{\hbar}\beta\mathbf{J}_y}\mathrm{e}^{\frac{\mathrm{i}}{\hbar}\gamma\mathbf{J}_z} \left| jm' \right\rangle \\ &= \mathrm{e}^{\mathrm{i}m\gamma} \left\langle jm \right| \mathrm{e}^{\frac{\mathrm{i}}{\hbar}\beta\mathbf{J}_y} \left| jm' \right\rangle \mathrm{e}^{\mathrm{i}m'\alpha} \end{aligned} \tag{E.10}$$

and a discrepancy with Davydov's results is apparent. The nasty culprit is deeply hidden in the fact that the rotation operator in passive convention used by Edmonds (1996) is seriously flawed for reasons discussed thoroughly in Bouten (1969). One of the immediate consequences is the violation of the group-property which can be easily shown (Bouten, 1969) as follows. Let's suppose that that the correct form of the passive rotation operator $\mathbf{R}_{\mathrm{P}}(\alpha,\,\beta,\,\gamma)$ is as considered by Edmonds (1996), namely

$$\mathbf{R}_{\mathrm{P}}(\alpha,\beta,\gamma) = \mathrm{e}^{\frac{\mathrm{i}}{\hbar}\alpha\mathbf{J}_z}\mathrm{e}^{\frac{\mathrm{i}}{\hbar}\beta\mathbf{J}_y}\mathrm{e}^{\frac{\mathrm{i}}{\hbar}\gamma\mathbf{J}_z}.$$

To a composition of two rotations, there should correspond a product of the respective rotation operators. Now let's consider two particular rotations $(\alpha,0,0)$ and $(0,\beta,\gamma)$ in the passive view point. It is easily verified that their composition is $(\alpha,0,0)\circ(0,\beta,\gamma) = (0,\beta,\alpha+\gamma)$, nevertheless corresponding relation for the rotation operators is clearly invalid

$$\mathbf{R}_{\mathrm{P}}(\alpha,0,0)\cdot\mathbf{R}_{\mathrm{P}}(0,\beta,\gamma) = \mathrm{e}^{\frac{\mathrm{i}}{\hbar}\alpha\mathbf{J}_z}\cdot\mathrm{e}^{\frac{\mathrm{i}}{\hbar}\beta\mathbf{J}_y}\mathrm{e}^{\frac{\mathrm{i}}{\hbar}\gamma\mathbf{J}_z} \neq \mathrm{e}^{\frac{\mathrm{i}}{\hbar}\beta\mathbf{J}_y}\mathrm{e}^{\frac{\mathrm{i}}{\hbar}(\alpha+\gamma)\mathbf{J}_z} = \mathbf{R}_{\mathrm{P}}(0,\beta,\alpha+\gamma).$$

[2] subscript E should distinguish Edmonds's notation from two previously discussed cases

We would like to note that the same misconception has unfortunately penetrated also into the, otherwise very elucidating, work by Morrison and Parker (1987). Correct form of the passive rotation operator is on the other hand used, *e.g.*, by Davydov (1965) or Fano and Racah (1959). Discussion regarding these topics found in Rose (1995) is even more confusing in the sense that the author claims to work in the passive viewpoint, nevertheless his rotation operators are actually active as pointed out by Morrison and Parker (1987) and Bouten (1969).

In order to remedy the error in Edmonds's approach one has two possibilities. Either it is possible to interpret his D-matrices as describing an *active* rotation by angles $(-\alpha, -\beta, -\gamma)$ or to formally interchange the Euler angles α and γ.[3]. The former approach is mentioned (but without discussing the reasons) in Brink and Satchler (1994, p. 21). On the other hand, the latter tack might be the reason that Chang and Fano (1972) who adhere to the Edmonds's notation for the D-functions, interchange the Euler angles $\xi \equiv \gamma$ and $\phi \equiv \alpha$, *i.e.*, the orientation of the molecular frame of reference is specified by Euler angles $(\phi, \theta, \xi = 0)$ but the authors use Edmonds's D-matrices in the form $\mathcal{D}^{j}_{m,k}(0, \theta, \phi)$, which makes the relation (A3) of Chang and Fano (1972) compatible with equation (43.9) in Davydov (1965).

> *There are several possibilities how to proceed in order to obtain the eigenfunctions of a symmetrical top. More thorough analysis based on the investigation of the properties of the body-fixed angular momentum components (especially their action on Wigner functions $\mathcal{D}$) is given by Davydov (1965, § 43). Nevertheless, it is possible to arrive to the same conclusion more straightforward way as discussed, e.g., by Brink and Satchler (1994, p. 25) or Landau and Lifschitz (1977). The reasoning is as follows. Suppose that the rigid rotor eigenfunction is $\phi(R)$, where R specifies the orientation of the rotor. If we now rotate the function ϕ by an amount R_1, the transformed function ϕ' will be given by*
>
> $$\phi'(R) = D(R_1)\phi(R) = \phi(R'),$$
>
> *where R' is transformed to R by rotation R_1. Without loss of generality, one can now assume that ϕ is an eigenfunction of $\mathbf{L}^2$, $\mathbf{L}_z$ and $\mathbf{H}$ with eigenvalues $J(J+1)$, N and E, respectively. Consequently, ϕ' will be also an eigenfunction of $\mathbf{L}^2$, $\mathbf{H}$ with the same eigenvalues. Moreover, if the energy level E is only rotationally degenerated, we can expand ϕ' into $\phi_{JM}(R)$ as*
>
> $$\phi'(R) = \phi_{JN}(R') = \sum_M \phi_{JM}(R) \left\langle JM \right| D(R_1) \left| JN \right\rangle .$$
>
> *For the particular choice $R_1 = R$, it follows that $R' = (0)$, i.e., R_1 is an identity transformation. Therefore the preceding equation can be restated into the following form*
>
> $$\phi_{JM}(R) = \sum_N \left\langle JN \right| D^{\dagger}(R) \left| JM \right\rangle \phi_{JN}(0). \qquad \text{(E.11)}$$
>
> *In other words, the eigenfunction is determined in all space just by its value for $R = (0)$. The symmetry around the body fixed z'-axis then requires that only one term in the sum in* (E.11) *can be nonzero.*[4]*. Thus the sought wave function will be indeed proportional to the matrix element of the rotational operator.*

[3] Landau and Lifschitz (1977) actually mention in § 58 that Edmonds interchanges angles α and γ but no detailed comment is given

[4] N will be then equal to the corresponding eigenvalue of $\mathbf{L}_{z'}$

E.1.2 Rotational energy levels

The rotational energy corresponding to (E.2) can be expressed as

$$\begin{aligned} \textit{prolate top} \quad A > B = C \quad E_{JKM} &= BJ(J+1) + (A-B)K^2 \\ \textit{oblate top} \quad A = B > C \quad E_{JKM} &= BJ(J+1) + (C-B)K^2 \end{aligned}$$

and is clearly independent on the quantum number M as well as the sign of K due to the inherent rotational symmetry. Rotational constants together with a graphical depiction of rotational levels for one particular example of a prolate symmetrical top molecule (CH_3Cl) are displayed in Figure E.1. Values for other molecules can be found in Appendix F.

E.2 Asymmetric tops

If $A > B > C$, the body fixed angular momentum projection $\mathbf{L}_{z'}$ does not represent a good quantum number. However, $\mathbf{L}^2$ and $\mathbf{L}_z$ is still conserved and the rotational eigenfunctions of an asymmetric top can be expressed as linear combinations of symmetrical top states $|JKM\rangle$ introduced in (E.2). It is convenient (Kroto, 1975; Winter, 1954) to express the rotational Hamiltonian (E.1) in a slightly more general form as

$$\begin{aligned} \mathbf{H}_\mathrm{r} &= \frac{1}{2}(a+b)\left(\mathbf{L}_a^2 + \mathbf{L}_b^2\right) + c\mathbf{L}_c^2 + \frac{1}{2}(a-b)\left(\mathbf{L}_a^2 - \mathbf{L}_b^2\right) \\ &= \alpha\mathbf{L}^2 + \beta\mathbf{L}_c + \gamma\left(\mathbf{J}^{+2} + \mathbf{J}^{-2}\right). \end{aligned} \qquad \begin{aligned} \alpha &= (a+b)/2 \\ \beta &= c - (a+b)/2 \\ \gamma &= (a-b)/4 \end{aligned} \tag{E.12}$$

The body fixed axes are in (E.12) labeled as a, b, c. It is worth noting that in (E.12), there is no connection between this designation and the rotational constants A, B, C. Actually, the only assumption requires the axis c to be the quantization axis of the symmetric top eigenfunctions but otherwise one is free to "distribute" A, B, C onto the a, b, c axes in any manner. There are in principle six (Kroto, 1975) such possible mappings. The right-handed versions are summarized in Table E.1. If a molecule is

	I	II	III
a	B	C	A
b	C	A	B
c	A	B	C

Table E.1: Axes mapping in the asymmetric rotor problem

a near prolate top then it is convenient to use mapping I for in this case the quantization axis c nearly coincides with the "prefered" axis A. Analogically, mapping III is suitable for a near oblate top.

For practical calculations, another form of the rotational Hamiltonian turns out to be profitable

$$\begin{aligned} \mathbf{H}_\mathrm{r} &= \frac{1}{2}(A+C)\mathbf{L}^2 + \frac{1}{2}(A-C)\mathbf{H}(\kappa) \\ \mathbf{H}(\kappa) &= \mathbf{L}_A^2 + \kappa\mathbf{L}_B^2 + \mathbf{L}_C \end{aligned} \qquad \kappa = \frac{2B - A - C}{A - C}, \tag{E.13}$$

Rotational constants		
A	$0.4806 \cdot 10^{-4}$ a.u.	1.307 meV
B	$0.4055 \cdot 10^{-5}$ a.u.	0.110 meV
Dipole moment		
D	0.7461 a.u.	1.895 D

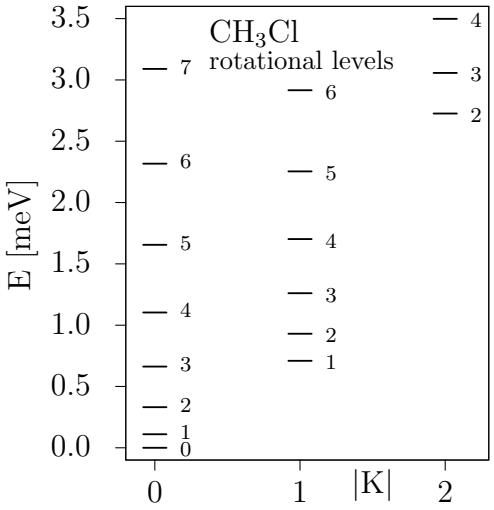

Figure E.1: Rotational constants and dipole moment for CH_3Cl, a symmetric prolate top molecule, together with graphical depiction of the rotational levels specified by quantum numbers J, K. Levels in each "K-stack" are labeled by J.

with $-1 \leq \kappa \leq 1$ being the *Ray's asymmetry parameter*. Prolate top ($B = C$) corresponds to $\kappa = -1$ whereas the oblate top limiting case ($A = B$) is equivalent to $\kappa = 1$. The matrix elements of $H(\kappa)$ are easily determined

$$\begin{aligned} \langle JK|\, H(\kappa)\, |JK\rangle &= FJ(J+1) + (G-F)K^2, \\ \langle JK|\, H(\kappa)\, |JK \pm 2\rangle &= H\, g(J,\, K). \end{aligned} \tag{E.14}$$

Specific form of the function $g(J, K)$ is for our purposes not important and can be found in Kroto (1975, p. 41). The values F, G, H in (E.14) depend on the chosen mapping according to Table E.1. Direct evaluation yields expressions given in Table E.2. Eigenvalues and eigenvectors of the matrix $\mathbf{H}(\kappa)$ are usually denoted as $|J\tau\rangle$ and $E_{J\tau}(\kappa)$

	I	II	III
F	$\frac{1}{2}(\kappa - 1)$	0	$\frac{1}{2}(\kappa + 1)$
G	1	κ	-1
H	$-\frac{1}{2}(\kappa + 1)$	1	$\frac{1}{2}(\kappa - 1)$

Table E.2: Factors appearing in matrix elements of $\mathbf{H}(\kappa)$ in (E.14)

respectively where τ numbers the eigenvalues in order of increasing magnitude. It is often stated without proof in the literature that there are exactly $2J + 1$ *distinct* energy levels $E_{J\tau}(\kappa)$ for $-1 < \kappa < 1$ and that for fixed τ and $-1 < \kappa_1 < \kappa_2 < 1$ the corresponding energies satisfy $E_{J\tau}(\kappa_1) < E_{J\tau}(\kappa_2)$.

However, if we consider the mapping II, it is not difficult to see where these properties originate. In this case, the off-diagonal part of ${}^{II}\mathcal{H}(\kappa)$ is independent on κ and the diagonal part is reduced just to κK^2. The set of eigenvalues of the matrix $-{}^{II}\mathcal{H}(\kappa)$ will be apart from the sign identical to eigenvalues of ${}^{II}\mathcal{H}(\kappa)$. Because change of sign in the off-diagonal elements does not affect the spectrum of a Hermitian matrix, the spectrum of $-{}^{II}\mathcal{H}(\kappa)$ coincides with the spectrum of ${}^{II}\mathcal{H}(-\kappa)$, therefore we obtain following relation

$$E_{J\tau}(\kappa) = -E_{J-\tau}(-\kappa). \tag{E.15}$$

Further, a direct application of the minimax principle (Golub and Loan, 1996, p. 395) yields

$$E_{J\tau}(\kappa) + \mathrm{d}\kappa \cdot 0 \leq E_{J\tau}(\kappa + \mathrm{d}\kappa) \leq E_{J\tau}(\kappa) + \mathrm{d}\kappa \cdot J^2,$$

so that the energy levels are not decreasing with κ. The terms on left/right hand side of this inequality are the smallest/largest eigenvalues of the perturbation $\mathrm{d}\kappa K^2 \delta_{K,K'}$ between $\mathcal{H}(\kappa + \mathrm{d}\kappa)$ and $\mathcal{H}(\kappa)$. Numerical values for one particular case of $J = 3$ are recorded in Figure E.2.

E.2.1 Symmetry classification of asymmetric rotor states

Although the molecule itself doesn't need to be geometrically symmetric, its rotational Hamiltonian (E.1) is invariant under the point group D_2 and therefore the rotational states of an asymmetric rotor can be classified according to the four one-dimensional irreducible representations of this group. Bases of these representations can be constructed by considering proper linear combinations of the states in Eq. (E.2), namely

$$|J\, K\, M\, \gamma\rangle \stackrel{\text{def}}{=} \frac{1}{\sqrt{2}}\Big[\, |J\, K\, M\rangle + (-1)^{\gamma}\, |J\, -K\, M\rangle \,\Big] \tag{E.16}$$

The matrix (E.14) decomposes in this basis into four blocks, designated in the notation of King et al. (1943) as E^+, E^-, O^+, O^-, where $+/-$ denotes the sign of γ in (E.16) and E/O specifies whether the corresponding block is comprised by functions (E.16) with even/odd K only.[5]

The transition from an oblate to a prolate rotor can be understood as a continuous transformation in κ. Because the "incremental" perturbation $\kappa \mathbf{L}_B$ is also invariant in D_2, the symmetry classification of the asymmetric rotor states is independent on κ. These states, however, coincide with rotational states of prolate or oblate symmetric top for $\kappa = -1$ or $\kappa = 1$. Therefore, their symmetry properties are uniquely determined by two numbers – K_{-1}, K_1 – which specify the angular momentum projection onto the symmetry axis in the prolate/oblate limit.

Easily deduced (Townes and Schalow, 1975) transformation properties[6] of the symmetrical top wave functions (E.2) lead directly to the classification[7] summarized in Table E.3.

Symmetry designation		C_A	C_B	C_C	
K_{-1}	K_1				
e	e	+	+	+	A
e	o	+	−	−	B_A
o	o	−	+	−	B_B
o	e	−	−	+	B_C

Table E.3: Symmetry classification of the asymmetric rotor rotational wave functions (E.16) under the operations of the point group D_2.

[5] this formally follows from the fact that only states with $\Delta K = 0$ or $|\Delta K| = 2$ are coupled in (E.16)

[6] strictly speaking, rules for transformation of the symmetric top wave functions furnish directly only symmetry labels for the C_A and C_C rotations, nevertheless $\mathrm{C}_\mathrm{B} = \mathrm{C}_\mathrm{A} \circ \mathrm{C}_\mathrm{C}$ so the middle column in Table E.3 is also easily obtained.

[7] a slightly different convention is used by Herzberg (1956, p. 52) regarding the $+/-$ symmetry labels

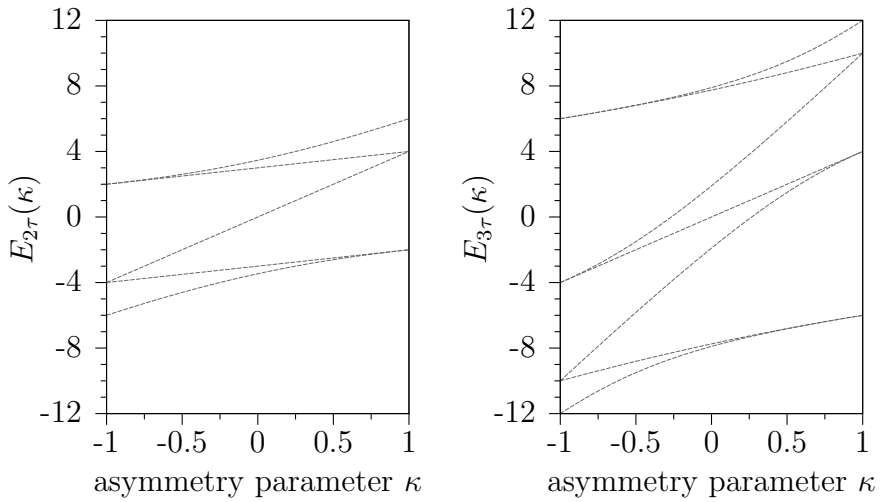

Figure E.2: Eigenvalues of the matrix $\mathcal{H}(\kappa)$ defined in (E.13) as a function of κ for $J = 2$ (left panel) and $J = 3$ (right panel).

E.3 Wigner function properties

Transformation properties

$$\mathrm{Y}_{l,\,m}\big(\theta,\,\phi\big) = \sum_{k} \mathcal{D}^{l}_{m,k}(\alpha,\,\beta,\,\gamma)\,\mathrm{Y}_{j,\,k}\big(\theta',\,\phi'\big) \tag{E.17}$$

In this useful formula, the angle variables θ, ϕ refer to the fixed laboratory frame of reference whereas θ', ϕ' are connected with the rotating body frame.

Orthogonality relations

$$\sum_{m} \mathcal{D}^{j\,*}_{m,k}\,\mathcal{D}^{j}_{m,k'} = \sum_{m} \mathcal{D}^{j\,*}_{k,m}\,\mathcal{D}^{j}_{k',m} = \delta_{k,k'} \tag{E.18}$$

$$\mathcal{D}^{j}_{m,k}(\theta) = \sum_{m_1,k_1} (j_1 j_2\, m_1 m_2|\; j\, m)\;\mathcal{D}^{j_1}_{m_1,k_1}(\theta)\;\mathcal{D}^{j_2}_{m_2,k_2}(\theta)\,(j_1 j_2\, k_1 k_2|\; j\, m) \tag{E.19}$$

$$\begin{aligned}\int \mathcal{D}^{j\,*}_{m,k}(\theta)\;\mathcal{D}^{j'}_{m',k'}(\theta)\;\mathrm{d}\theta = (-1)^{k-m}\int \mathcal{D}^{j}_{-m,-k}(\theta)\;\mathcal{D}^{j'}_{m',k'}(\theta)\;\mathrm{d}\theta = \\ = \frac{8\pi^2}{2j+1}\delta_{j\,j'}\delta_{m\,m'}\delta_{k\,k'}\end{aligned} \tag{E.20}$$

This relation holds only for integer angular momenta j, j'. For detailed discussion and possible generalisations of relation (E.20), we refer to Jonker and Vries (1967).

$$\begin{aligned}\int \mathcal{D}^{j_3\,*}_{m_3,k_3}(\theta)\;\mathcal{D}^{j_2}_{m_2,k_2}(\theta)\;\mathcal{D}^{j_1}_{m_1,k_1}(\theta)\;\mathrm{d}\theta = \frac{8\pi^2}{2j_3+1}\,(j_1 j_2\, m_1 m_2|\; j_3\, m_3) \\ \times\,(j_1 j_2\, k_1 k_2|\; j_3\, k_3)\end{aligned} \tag{E.21}$$

Special cases – relation to spherical harmonics

$$\mathcal{D}^L_{0,0}(0,\,\beta,\,0) = \mathrm{P}_L(\cos\beta) \tag{E.22a}$$

$$\mathcal{D}^L_{m,0}(\alpha,\,\beta,\,0) = \sqrt{\frac{4\pi}{2l+1}}\mathrm{Y}_{l,\,m}\big(\beta,\,\alpha\big) \tag{E.22b}$$

$$\mathcal{D}^L_{0,k}(0,\,\beta,\,\gamma) = (-1)^k\sqrt{\frac{4\pi}{2l+1}}\mathrm{Y}_{l,\,k}\big(\beta,\,\gamma\big) \tag{E.22c}$$

Composition properties

$$\sum_m \mathcal{D}^j_{m,k}(\theta_2)\;\mathcal{D}^j_{m,k'}(\theta_1) = \sum_m \mathcal{D}^j_{k',m}(\theta_2\circ\theta_1) \tag{E.23}$$

$$\mathcal{D}^{j_1}_{m_1,k_1}(\theta)\;\mathcal{D}^{j_2}_{m_2,k_2}(\theta) = \sum_{j=|j_1-j_2|}^{j_1+j_2}(j_1j_2\,m_1m_2|\;j\,m)\;\mathcal{D}^j_{m,k}(\theta)\,(j_1j_2\,k_1k_2|\;j\,k) \tag{E.24}$$

E.4 Statistical weights

The rigid rotor complete wave function ψ is typically approximated as a product of several terms, each of which corresponds to different type of degrees of freedom. In this sense, we can schematically write

$$\psi \approx \psi_{\mathrm{E}}\psi_{\mathrm{V}}\psi_{\mathrm{R}}\psi_{\mathrm{ns}}, \tag{E.25}$$

where the individual subscripts E, V, R and ns represent electronic, vibrational, rotational and nuclear spin parts of the complete wave function, respectively. To fully utilize the Pauli exclusion principle, it is necessary to take properly into account symmetry properties of the individual parts of the complete approximate wave function (E.25). To this end, it is essential to identify the convenient group, the irreducible representations of which will furnish the appropriate symmetry labels.

The analysis is more complicated for molecules with several alternative "configurations"[8] as discussed originally by Longuet-Higgins (1962) and Hougen (1962, 1963). Nevertheless, it may happen that transitions between these configurations are in the considered model not energetically possible. In that case, we say that the molecule is *rigid*, following Bunker and Jensen (2004).

Regardless of the geometrical configuration of the molecule, the molecular Hamiltonian is invariant under operations belonging to the so-called **CNPI group**[9] comprised of all permutations of identical nuclei present in the molecule together with spatial inversion of all coordinates. If one removes from this group all elements which interchange individual energetically inaccessible configurations[10], one obtains the so-called **MS group**.[11] Each operation from this MS group will affect vibronic, rotational and nuclear spin coordinate in a different way. The key observation is that for rigid molecules, its effect on the vibronic variables is identical to the effect of molecular

[8] by two distinct configurations of a given molecule we mean two specific permutations of identical particles which are not interchangeable by a simple rotation of the molecule as a whole

[9] CNPI meaning "complete nuclear permutation group + inversion"

[10] in the terminology of Hougen (1962), these operations are said to be not "feasible"

[11] MS stands for "molecular symmetry"

point group defined in the usual way.[12] Thus in the case of rigid molecules, the analysis reduces actually to that given much earlier by Wilson (1935) for spherical and symmetrical top molecules. Similar treatment for asymmetric tops has been presented by Mulliken (1941).

For symmetry classification of the entire wave function (E.25), Wilson (1935) considers only the rotational subgroup $\mathcal{G}_{\mathrm{R}}$ (having σ elements) of the full molecular point group $\mathcal{G}_{\mathrm{P}}$ (of order N). This stems from the fact that the effect of improper operations in $\mathcal{G}_{\mathrm{P}}$ on the rotational variables (Euler angles) is not clearly defined. Wilson (1935) further assumes that each rotationally configuration of the molecule can be described by a wave function ψ_i of the type (E.25). Since $\mathcal{G}_{\mathrm{P}}$ can be decomposed into N/σ cosets, one has precisely N/σ such functions. However, ψ_i have good transformation properties only under operations belonging to $\mathcal{G}_{\mathrm{R}}$. The total wave function Ψ obeying the Pauli principle for all operations in $\mathcal{G}_{\mathrm{P}}$ can be expressed as an linear combination of ψ_i's. The question at hand is now how many of such Ψ's it is possible to construct. Simple argument leads to the conclusion that there is only one such Ψ.

Let's consider the reducible representation of $\mathcal{G}_{\mathrm{P}}$ generated by functions ψ_i. Number of Ψ's is then the same as the multiplicity of the totally symmetric representation A of $\mathcal{G}_{\mathrm{P}}$ in the aforementioned reducible representation. On the other hand, there are exactly σ elements of $\mathcal{G}_{\mathrm{P}}$ which leave each of the ψ_i's invariant. Their contribution into the expression $\sum_j \chi_j$, where j runs over all elements of $\mathcal{G}_{\mathrm{P}}$ will be then just σ. But there are N/σ such functions, therefore one has in total that $\sum_j \chi_j = N$. The multiplicity of the totally symmetric representation is then according to the character orthogonality formula (Inui et al., 1996) equal[13] to $\frac{1}{N}\sum_j \chi_j \cdot 1 = 1$.

The symmetry of the complete wave function will be finally given as a product of the symmetries of its individual components. For low energy electron molecule scattering it is usually justifiable to consider the molecule in its ground electronic and vibrational state, each of which are supposed to be totally symmetric. In that case, it is sufficient to investigate just ψ_{R} and ψ_{ns}.

E.4.1 Application to symmetric tops

In connection with the results presented in Chapter 4 we would like to mention one particular application of the above mentioned procedure to a class of symmetric top molecules with point group symmetry C_{3v}, *i.e.*, molecules having threefold symmetry axis[14] and three vertical mirror planes – typical representatives of this class are for example molecules such as CH_3Cl or NH_3. In the following we shall discuss the former case.

CH_3X molecules

For the sake of brevity, let's suppose that spin S_{X} of the nucleus X is zero. If this is not the case, it is sufficient just to multiply the final statistical weights by $2S_{\mathrm{X}} + 1$. For example in the case[15] of CH_3Cl/CH_3Br and CH_3I, $S_{\mathrm{X}} = 3/2$ and $S_{\mathrm{X}} = 5/2$, respectively. Because spin of the hydrogen nuclei is 1/2, we have in total 8 nuclear spin functions ψ_i. These functions form an eight dimensional reducible representation of the rotational subgroup C_3 of the full point group C_{3v}. It is easily deduced that this representation will decompose into irreducible representations of C_3 as

$$4A \oplus 2E. \tag{E.26}$$

[12] in this sense, these two groups are therefore isomorphic

[13] the one-dimensional totally symmetric representation has all characters equal to 1

[14] in case of polar molecules this axis coincides with the dipole moment

[15] these values are valid for stable isotopes, *e.g.*, ^{36}Cl and ^{129}I have nuclear spin 2 and 7/2, respectively

Moreover for $S_X = 0$, the value of the total spin can attain only 1/2 or 3/2, where the doublet and quadruplet states transform according to the E and A representation, respectively. Transformation properties of the rotational functions can be demonstrated in a similar way.[16] Results are summarized in the first two columns of Table E.4. Third column contains symmetry classification of the vibrational normal modes together with corresponding energies (Shimanouchi, 1972). Finally, employing decomposition rules regarding direct product of two irreducible representations, one readily obtains the resulting statistical weights recorded in Table E.5.

ψ_{ns}		ψ_{rot}		ψ_{vib}			
$S = 3/2$	A	$K = 0$	A	C-Cl stretch	ν_3	A	90.9
$S = \frac{1}{2}$	E	$\lvert K\rvert = 3n$	$2A$	C-Cl rocking	ν_6	E	126.1
		$\lvert K\rvert \neq 3n$	E	C-H sym. bending	ν_2	A	168.3
				C-H asym. bending	ν_5	E	180.7
				C-H sym. stretch	ν_1	A	368.4
				C-H asym. stretch	ν_4	E	377.8

Table E.4: Symmetry properties of nuclear-spin ψ_{ns}, rotational ψ_{rot} and vibrational ψ_{vib} functions of a CH_3X molecule with respect to the rotational subgroup of C_{3v}. In the first column it is assumed that nuclei X has zero spin. Vibrational energies (Shimanouchi, 1972) of the normal modes are given in meV.

ψ_{EV}	A	E
$K = 0$	4	4
$\lvert K\rvert = 3n$	8	8
$\lvert K\rvert \neq 3n$	4	12

Table E.5: Nuclear-spin statistical weights for a molecule of the type CH_3X. All weights should be multiplied by $2J+1$ due to the rotational degeneracy and by $2S_X+1$, where S_X stands for the spin of the nuclei X. The columns of the table distinguish two possible symmetry species of the vibronic part of the wave function (E.25).

Selection rules consequences

In all electron-molecule collision models considered in this work, the incident electron can not change the value of the total spin. In case of $S_X = 0$, to each value of S, there exists uniquely determined rotational state with symmetry given by Table E.5. For example the rotational states $|K| \neq 3n$ correspond to $S = 1/2$ and states with $|K| = 3n$[17] correspond on the other hand to $S = 3/2$. Therefore rotational transitions between these two sets of states induced by electron collisions are not allowed. However, this analysis is not applicable in case of $S_X > 0$. For example if $S_X = 3/2$ as in CH_3Cl then the total spin can attain values 0, 1, 2, 3. The $S = 0$, 3 states are of A symmetry, nevertheless the $S = 1$, 2 states can be of A as well as E symmetry. On the other hand, it should be noted that in the framework of the adiabatic approximation, only $\Delta K = 0$ transitions are allowed due to the inherent body frame formulation and the anticipated symmetry around the body fixed z'-axis.

[16] functions with $K = 0$ and $K > 0$ span one and two dimensional representations, respectively

[17] including the case $n = 0$

In low energy electron-molecule collisions, the assumption that the molecule is in its ground electronic state is typically well justified, nevertheless the assumption concerning vibrations is by no means so clear as can be observed by considering the energies in Table E.4. Symmetry difference between initial and final states could in principle render some of the $\Delta K = 0$ transitions to be forbidden. Then it would be necessary to incorporate these additional selection rules into the model by hand. On the other hand, these effects should play a considerable role only in the case that the corresponding vibrational excitation (VE) cross-section is comparable to the rotational cross-sections under investigations. Theoretical predictions concerning VE for CH_3Cl suggest that in the energy range considered in this work, the VE cross-sections are much smaller as compared to rotational excitation (Fabrikant, 1991).

E.4.2 Application to asymmetric tops

The procedure briefly outlined in Section E.4 can be directly applied also to the asymmetric top case. As regards asymmetric tops in our scattering calculations, we have dealt only with water H_2O and sulfur dioxide SO_2 molecules and therefore in the following we will confine our attention to these two particular cases. The symmetry point group of interest is now C_{2v} having 4 one-dimensional irreducible representations. Because these molecules are planar, the moment of inertia around the axis parallel to

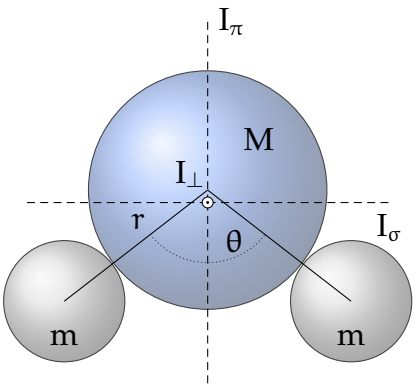

$$\begin{aligned} \mathrm{I}_\pi &= 2mr^2 \sin^2 \theta/2 \\ \mathrm{I}_\sigma &= 2mr^2 \frac{M}{M+2m} \cos^2 \theta/2 \\ \mathrm{I}_\perp &= \mathrm{I}_\pi + \mathrm{I}_\sigma \end{aligned} \qquad \text{(E.27)}$$

Figure E.3: Configuration of a planar triatomic molecule with two identical nuclei of mass m and center nuclei with mass M. Quantities r and θ denote the bond length and angle, respectively. "Classical" expressions for principal moments of inertia are summarized in Eq. (E.27).

this plane $\mathrm{I}_\perp$ is just sum of the other two principal moments of inertia and this axis is thus in notation employed above denoted as C. Relation between I_σ and I_π introduced in Figure E.3 depends on the particular geometry and masses of the nuclei, nevertheless $\mathrm{I}_\pi > \mathrm{I}_\sigma$ for H_2O as well as SO_2. The C_2 symmetry axis is thus axis B (middle moment of inertia). If the moments of inertia are computed from Figure E.3 "classicaly", one obtains quite reasonable values. For example in H_2O, the experimental (Hall and Dowling, 1967) value of $1/2\mathrm{I}_\pi$ is 1.799 meV, whereas corresponding formula in Figure E.3 yields for the equilibrium geometry the value of 1.807 meV.

H_2O

Oxygen and hydrogen nuclei in H_2O have spin 0 and 1/2, respectively. We thus have 4 nuclear spin functions which generate 4-dimensional reducible representation of the rotational subgroup C_2 of C_{2v}. Point group C_2 has just two one dimensional irreducible representations A, B. Direct calculation reveals that the mentioned representation

reduces as

$$3\mathrm{A} \oplus \mathrm{B}. \tag{E.28}$$

Finally, we need to determine the symmetries of the rotational states labeled by K_{-1}, K_1 as introduced in Subsection E.2.1. Because the C_2 axis is the axis B, the sought symmetry labels are directly contained in the middle column of Table E.3. Therefore e, e or o, o and e, o or o, e states transform according to the A and B representation of C_2, respectively. Combination with decomposition (E.28) immediately yields the corresponding weights summarized in the left part of Table E.6.

SO_2

The situation for SO_2 is slightly different than in the H_2O case in the sense that sulfur and also oxygen nuclei have zero spin. The nuclear spin wave function is thus totally symmetric and therefore only rotational states transforming according to the A representation of the point group C_2 are allowed. In other words, the effective statistical weights of e, o and o, e states are zero as indicated in the right part of Table E.6.

H_2O		
K_{-1}	K_1	weight
even	even	3
even	odd	1
odd	even	1
odd	odd	3

SO_2		
K_{-1}	K_1	weight
even	even	1
even	odd	0
odd	even	0
odd	odd	1

Table E.6: Statistical weights for the H_2O (left panel) and SO_2 (right panel) asymmetric rotor states classified by the parity of K_{-1}, K_1.

APPENDIX

F

UNITS, DIPOLE MOMENTS & ROTATIONAL CONSTANTS

F.1 Energy units

	a.u.	meV	cm^{-1}	MHz
a.u.	1	$27.2114 \cdot 10^{3}$ $\{m_e c^2 \alpha^2 / e\} \cdot 10^{3}$	$2.1947 \cdot 10^{5}$ $\{m_e c \alpha^2 / h\} \cdot 10^{-2}$	$6.5797 \cdot 10^{9}$ $\{m_e c^2 \alpha^2 / h\} \cdot 10^{-6}$
meV	$3.6749 \cdot 10^{-5}$ $\{e / m_e c^2 \alpha^2\} \cdot 10^{-3}$	1	8.0655 $\{e/hc\} \cdot 10^{-5}$	$2.4180 \cdot 10^{5}$ $\{e/h\} \cdot 10^{-9}$
cm^{-1}	$4.5563 \cdot 10^{-6}$ $\{h / m_e c \alpha^2\} \cdot 10^{2}$	$1.2398 \cdot 10^{-1}$ $\{hc/e\} \cdot 10^{5}$	1	$2.9979 \cdot 10^{4}$ $\{c\} \cdot 10^{-4}$
MHz	$1.5198 \cdot 10^{-10}$ $\{h / m_e c^2 \alpha^2\} \cdot 10^{6}$	$4.1357 \cdot 10^{-6}$ $\{h/e\} \cdot 10^{9}$	$3.3356 \cdot 10^{-5}$ $\{1/c\} \cdot 10^{4}$	1

Table F.1: Conversion factors for various energy units – displayed numerical values are merely informational, full available precision can be found, *e.g.*, in National Institute of Standars and Technology (2008). Quantities enclosed in curly braces are to be evaluated numerically in SI units.

F.2 Dipole moment units

	a.u.	D	esu·cm	esu·Å
a.u.	1	2.5417 $\{cea_0\} \cdot 10^{21}$	$2.5417 \cdot 10^{-18}$ $\{cea_0\} \cdot 10^{3}$	$2.5417 \cdot 10^{-10}$ $\{cea_0\} \cdot 10^{11}$
D	0.3934 $\{1/cea_0\} \cdot 10^{-21}$	1	10^{-18}	10^{-10}
esu·cm	$0.3934 \cdot 10^{18}$ $\{1/cea_0\} \cdot 10^{-3}$	10^{18}	1	10^{8}
esu·Å	$0.3934 \cdot 10^{10}$ $\{1/cea_0\} \cdot 10^{-11}$	10^{10}	10^{-8}	1

Table F.2: Conversion factors for various dipole moment units – displayed numerical values are merely informational, full available precision is listed, *e.g.*, by National Institute of Standars and Technology (2008).

F.3 Rotational constants & Dipole moments

Asymmetric top molecules

	D [D]	A [meV]	B [meV]	C [meV]
H_2O	1.855	3.456757(4)	1.800470(4)	1.150289(4)
SO_2	1.633	0.25135988(2)	0.042671452(4)	0.036392429(4)

Table F.3: Dipole moments (Debye) and rotational constants (meV) of H_2O and SO_2 being representative examples of polar asymmetric top molecules. Values of dipole moments taken from Lide (2009), rotational constants of water and sulfur dioxide adopted from DeLucia et al. (1974) and Lovas (1978), respectively.

Symmetric top molecules

	D [D]	A [meV]	B [meV]
CH_3Cl	1.896	0.630	0.061
CH_3I	1.641	0.628	0.035

Table F.4: Dipole moments (Debye) and rotational constants (meV) of CH_3Cl and CH_3I being representative examples of polar symmetric top molecules. Dipole moment and rotational constants values adopted from Lide (2009) and Herzberg (1991), respectively.

Spherical top molecules

	B [meV]	Q [a.u.]	α_0 [a.u.]	α_2 [a.u.]
N_2	$0.247750^{\dagger}$	-1.09 ± 0.07^{a}	11.744 ± 0.004^{a}	3.080 ± 0.002^{a}
H_2	$7.5448^{\dagger}$	0.474 ± 0.034^{b}	5.179^{c}	1.202^{c}

† adopted from Lide (2009)
^{a} experimental values – (Morrison et al., 1997) and references therein
^{b} experimental values – (Morrison, Feldt and Austin, 1984) and references therein
^{c} accurate CI (equilibrium) values – (Kołos and Wolniewicz, 1965)

Table F.5: Rotational constants (meV), quadrupole moments (a.u.), spherical and nonspherical polarizabilities of H_2 and N_2 – homonuclear spherical top molecules. The dipole moment vanishes due to the symmetry reasons.

APPENDIX
G

LIST OF PUBLICATIONS

- Šulc, M., Kolorenč, P., Tarana, M. and Horáček, J. (2008), 'Fast and Efficient Solution of Scattering Integral Equations', *AIP Conf. Proc.* **1046**(1), 142–145.
- Šulc, M. and Horáček, J. (2009), 'Application of the R-matrix theory to low-energy potential scattering', *AIP Conf. Proc.* **1168**(1), 531–534.
- Šulc, M. and Čurík, R. (2010), 'Numerical solution of Volterra equations applied in electron-molecule collision calculations', *AIP Conf. Proc.* **1281**(1), 2107–2110.
- Šulc, M., Čurík, R. and Horáček, J. (2010), 'Efficient solution of scattering equations by combination of R-matrix and Lanczos methods', *Eur. Phys. J. D* **57**, 187–196.
- Čurík, R. and Šulc, M. (2010), 'Towards efficient *ab initio* calculations of electron scattering by polyatomic molecules: III. Modelling correlation–polarization interactions', *J. Phys. B* **43**(17), 175205.
- Wehrle, M., Šulc, M. and Vaníček, J. (2011), 'Time-Resolved Electronic Spectra with Efficient Quantum Dynamics Methods', *Chimia* **65**, 334–338.
- Šulc, M., Čurík, R., Ziesel, J.-P., Jones, N. C. and Field, D. (2011), 'A new type of interference phenomenon in cold collisions of electrons with N_2', *submitted to J. Phys. B*

LIST OF ABBREVIATIONS

AA	adiabatic approximation	Section 1.3
AFT	angular frame transformation	Subsection 1.4.4
BF	body frame	Subsection 1.4.4
CP	Correlation-Polarization (potential)	Section 2.3
DFT	Density Functional Theory	Section 2.3
DMR	Discrete momentum representation method	Section 1.1
FBA	First Born approximation	Subsection 1.4.1
FN	fixed nuclei approximation	Section 1.2
FNO	fixed nuclei orientation approximation	Section 1.2
FT	frame transformation	Subsection 1.4.4
LDA	local density approximation	Section 2.3
LF	laboratory frame	Subsection 1.4.1
LFCC	laboratory frame close coupling	Section 1.5
LS	Lippmann-Schwinger (equation)	Section 1.1
RFT	rotational frame transformation	Subsection 1.4.4
RR	rigid rotor (approximation)	Appendix E
SE	Static Exchange (approximation)	Section 2.1
SEP	Static Exchange + Polarization (approximation)	Section 2.1
SL	Schwinger-Lanczos (method)	Section 1.6

Eur. Phys. J. D **57**, 187–196 (2010)
DOI: 10.1140/epjd/e2010-00028-5

THE EUROPEAN PHYSICAL JOURNAL D

Regular Article

Efficient solution of scattering equations by combination of R-matrix and Lanczos methods

M. Šulc[1,2,a], R. Čurík[2], and J. Horáček[1]

[1] Institute of Theoretical Physics, V Holešovičkách 2, 180 00 Prague 8, Czech Republic
[2] J. Heyrovský Institute of Physical Chemistry of the ASCR, v. v. i., Dolejškova 3, 182 23 Prague 8, Czech Republic

Received 25 November 2009 / Received in final form 15 January 2010
Published online 16 February 2010 –

Abstract. We propose a fast and economical computational method for solving scattering Lippmann-Schwinger integral equation. Our approach benefits from the accurate construction of the Green's function based on the R-matrix theory combined with the Schwinger-Lanczos variational principle. No principal restrictions on the form of the potential are assumed. Theoretical description of our method in the first part of this paper is then followed by numerical examples. In particular we demonstrate how to adapt our method for computation of partial wave phase-shifts in the case of electron-hydrogen atom scattering. Then we also investigate the properties of a family of long-range potentials (emerging e.g. in the theoretical description of the Cs_2 or $^4He_2$ dimer ground state interaction). As demonstrated on these particular cases, our approach turns out to be very accurate in comparison with other computational methods.

1 Introduction

In the last decades there has been expended great deal of effort to study the collisions of slow electrons and positrons with atoms and molecules as well as collisions of cold atoms [1–3]. This subject is appealing not only from the theoretical point of view the main reason being that these scattering processes find an application in a wide variety of problems as in atmospheric or plasma physics, astrophysics, radiative processes etc.

The theoretical description usually leads to Fredholm type integral equations of the second kind which can be hardly solved analytically except in a few simple cases. Therefore it turns out to be important to have a numerical method which would be accurate and robust in the sense that its implementation should be essentially independent of the interaction under investigation.

Our aim in this paper is to propose one such approach. In the following we restrict ourselves to the one dimensional case (utilizing the standard partial-wave decomposition) and assume the interaction being given in the form $V(r) + W(r, r')$, where V and W represent the local and nonlocal part of the potential respectively.

As is well known [4], the scattering wave function is then governed by the Lippmann-Schwinger equation

$$|\phi\rangle = |u\rangle + G_0(E)(V + W)\,|\phi\rangle\,, \tag{1}$$

where $|u\rangle$ describes the incident plane wave and $G_0(E) = (E - H_0)^{-1}$ stands for the free propagator. Simple algebraic manipulations furnish another insight onto this equation. Explicitly written

$$\begin{aligned}|\phi\rangle &= (1 - G_0(E)V)^{-1}\,|u\rangle + (1 - G_0(E)V)^{-1}\,G_0(E)W\,|\phi\rangle \\ &\equiv |\overline{u}\rangle + G(E)W\,|\phi\rangle\,,\end{aligned} \tag{2}$$

where we have introduced the symbol $|\overline{u}\rangle$ for the "distorted" wave obeying an equation of the same structure as equation (1), namely

$$|\overline{u}\rangle = |u\rangle + G_0(E)V\,|\overline{u}\rangle\,. \tag{3}$$

Having solved equation (2) we are consequently in position to evaluate the quantity $\langle u|\,V + W\,|\phi\rangle$ which can be shown to be directly related to the tangent of the scattering phase shift. According to the two-potential formula [5], p. 271 this matrix element can be equivalently computed as a sum $\langle u|\,V\,|\overline{u}\rangle + \langle\overline{u}|\,W\,|\phi\rangle$. We exploit the latter approach in our method – the first term is computed using the R-matrix framework and the second summand is rendered as a byproduct of the Schwinger-Lanczos iterative algorithm described below.

The numerical section of this paper is divided into two parts. In the first one we focus on the application of our method to electron-hydrogen atom scattering in the static exchange approximation [6], p. 412. In this case both local V and nonlocal terms W have to be taken into account. In the second part we consider long-range spherically symmetric potentials which decay as $\mathcal{O}(1/r^n)$ for large r. Due to this symmetry we are allowed to exploit, in the standard manner, the partial wave decomposition of the radial Schrödinger equation and study consequently the low-energy behavior of each partial wave phase shift δ_l independently.

[a] e-mail: miroslav.sulc@jh-inst.cas.cz

However, we are particularly interested in the s-wave (i.e. in the properties of δ_0 understood as a function of the wave number k). We can assume that under usual circumstances and for sufficiently small k only this wave yields significant contribution to the total scattering cross-section due to the absence of the centrifugal barrier in the zero angular momentum case.

It is well known [7] that the quantity $k^{2l+1}\cot\delta_l$ is an even function of k and for potentials decaying fast enough (typically exponentially or of finite range) it is even analytic in the complex plane in some neighborhood of the origin $k=0$. The leading terms of the expansion in k are then given by the *effective range theory* (ERT for future reference), namely

$$k^{2l+1}\cot\delta_l \approx -\frac{1}{a_l}+\frac{1}{2}r_0k^2+\ldots, \tag{4}$$

where the parameter a_0 has (for $l=0$) the dimension of length and is called the *scattering length* whereas the quantity r_0 is known [7] as the *effective range*.

For long-range potentials (decaying as r^{-n}), these nice analytic properties are unfortunately violated, nevertheless $k^{2l+1}\cot\delta_l$ is still an even function of k and it is essentially again possible to find an expansion in k similar to equation (4) termed usually MERT (*modified effective range theory*) [8,9]. It is an interesting question to determine the lower bound which needs to be imposed on n in order to guarantee the existence of a_l ([8], p. 492) and r_l as introduced in equation (4). Following simple arguments given in [10], p. 546 one can show that the corresponding condition as regards a_l is $n\geq 2l+3$. For more thorough discussion extending these arguments see e.g. [8], where it is also shown that $n\geq 6$ is required for the existence of the effective range r_0.

The $n=4$ case, i.e. the r^{-4} interaction, describing polarizability effects deserves particular interest. An elaborate review can be found in the pioneering works [8,11]. Unfortunately for a general interaction of the type r^{-n}, the investigation has to be carried through for each n separately. In the second part of this paper we are concerned with the "van der Waals"-like $\approx 1/r^6$ terms. Relevant analysis regarding the applicability of MERT in this case is given in [12] including a formula similar to equation (4) for the s-wave

$$\frac{1}{k}\tan\delta_0 = -A_0-\frac{1}{2}r_0A_0^2k^2+\frac{1}{15}\pi\gamma^4k^4 + \frac{4}{15}A_0\gamma^4k^5\ln|2kd|+\mathcal{O}\left(k^5,\gamma^5\right), \tag{5}$$

where the leading term of the potential is assumed to be of the form $-\gamma^4/r^6$ [2]. Higher partial waves are then discussed in [13]. It is of particular interest that even an analytic solution of the full Schrödinger equation is known for this interaction [14].

[2] RHS of equation (5) seems to violate the statement that $\tan\delta_0/k$ is odd function of k, nevertheless as discussed on p. 496 in [8], for $k<0$ an alternative derivation of equation (5) is necessary having as result the need to replace all occurrences of k by $-k$.

2 Theoretical background

In this section we introduce concisely the main theoretical concepts used in our method. For details we refer to original papers. Consequently we show how to adapt these general procedures for our particular needs.

2.1 R-matrix method

The theory behind R-matrix approach is described elaborately in the original work [15] so we present only a short summary below.

In general we can restate the LS-equation as a second order differential equation supplemented with proper boundary conditions, actually an equation of Schrödinger type with nonzero right hand side. R-matrix method is in the simplest possible case devised just for solving this class of problems, i.e.

$$-\frac{1}{2\mu}\frac{d^2\Psi(r)}{dr^2}+\left(V_{\text{eff}}(r)-E\right)\Psi(r)=\chi(r), \tag{6}$$

where Ψ is required to satisfy

$$\Psi(0)=0, \text{ and} \tag{7a}$$

$$\left(A-\frac{d}{dr}\right)\Psi(r)\Big|_{r_{\text{f}}}=0. \tag{7b}$$

The cutoff radius r_{f} is required to lie in the asymptotic region where the interaction can be neglected in comparison with the electron energy. Main idea of this method is to divide the radial range $[0,\,r_{\text{f}}]$ into several sectors, expanding on each sector the sought wave function into basis formed by the eigenfunctions of the homogeneous Schrödinger equation supplemented by the so-called *Bloch term* [16] (ensuring actually hermiticity of the resulting differential operator). The expansion coefficients are then determined by the natural requirement of continuity of the logarithmic derivative at the respective sector boundaries. For the sake of simplicity we describe this technique in the simplest case of just one sector. For more details and general discussion also in the three dimensional case see [15].

As already mentioned above, in the first step we need to construct a basis comprised of the eigenfunctions of the operator $\tilde{K}+V_{\text{eff}}(r)$, i.e.

$$\tilde{K}\Psi_n(r)+\left(V_{\text{eff}}(r)-E_n\right)\Psi_n(r)=0, \tag{8}$$

where $\tilde{K}$ is the operator of "modified kinetic energy" and is usually written in the form $\tilde{K}\equiv-\frac{1}{2\mu}\frac{d^2}{dr^2}+L$, where L stands for the Bloch operator, the matrix elements of which are in the respective basis given as

$$L_{ij}=\frac{1}{2\mu}\Psi_i(r_{\text{f}})\left.\frac{d\Psi_j(r)}{dr}\right|_{r_{\text{f}}}. \tag{9}$$

Its domain of definition is the space of square integrable functions satisfying the boundary condition (7a). Integration per-partes and using the boundary condition gives for

the matrix elements of the modified kinetic energy following relation

$$\tilde{K}_{ij} = \frac{1}{2\mu}\int_0^{r_f} \frac{d\Psi_i(r)}{dr}\frac{d\Psi_j(r)}{dr}dr. \tag{10}$$

We see that the operator $\tilde{K} + V_{\text{eff}}(r)$ is indeed symmetric thus has real eigenvalues E_n and its eigenvectors $\Psi_n(r)$ build basis of the corresponding function space. Incorporating the Bloch operator into equation (6) yields

$$\tilde{K}\Psi(r) + (V_{\text{eff}}(r) - E)\Psi(r) = \chi(r) + L\Psi(r). \tag{11}$$

By expanding $\Psi(r)$ into basis $\Psi_n(r)$ as $\Psi(r) = \sum_n C_n\Psi_n(r)$ and plugging into equation (11) we obtain a relation for the coefficients C_n,

$$C_n = \frac{1}{E_n - E}\left[\chi_n + \frac{1}{2\mu}\Psi_n\left(r_f\right)\lambda\right], \tag{12}$$

where

$$\chi_n = \int_0^{r_f} \Psi_n(r)\chi(r)dr$$

and the parameter λ is equal to the ordinary derivative of the complete wave function $\Psi(r)$ at $r = r_{\text{f}}$, i.e.

$$\lambda = \left.\frac{d\Psi(r)}{dr}\right|_{r_{\text{f}}}.$$

It can be related to the parameter A introduced in equation (7b) by using equation (12), namely

$$\lambda = \frac{A}{1 - A\mathcal{R}}\sum_k \frac{\chi_k\Psi_k(r_{\text{f}})}{E_k - E}, \tag{13}$$

where $\mathcal{R}$ stands for

$$\mathcal{R} = \frac{1}{2\mu}\sum_n \frac{\Psi_n(r_{\text{f}})\Psi_n(r_{\text{f}})}{E_n - E}.$$

This expression understood as a function of r_{f} has a direct physical meaning. It can be shown to be equal to the inverse logarithmic derivative of the complete wave function at $r = r_{\text{f}}$. Its knowledge is in the one dimensional case equivalent to the information contained in $\langle\chi|\,V\,|\Psi\rangle$.

At this point, equation (6) is solved completely because the coefficients C_n are known. However, according to [15], the solution can be expressed in a slightly different form more suitable for computational needs. Namely

$$\Psi(r) = \int_0^{r_{\text{f}}} G(E, r, r')\chi(r')dr', \tag{14}$$

where $G(E, r, r')$ is indeed the Green's function of the original equation (6) being the solution of this equation for the special source term $\chi(r) = \delta(r - r')$. Explicit expression (unimportant for our purposes) can be found again in [15], p. 4.

2.2 Schwinger-Lanczos variational method

Schwinger-Lanczos method is an iterative approach to the problem of T-matrix elements calculation. Its use is practical especially in the presence of nonlocal interactions and relies on the complex Schwinger variational principle as described in the fundamental work [17]. According to this principle the desired T-matrix element

$$T_{\beta\alpha} = \langle\phi_\beta|\,V\left(V - VG_0V\right)^{-1}V\,|\phi_\alpha\rangle$$

is given as the stationary value of the following functional

$$\begin{aligned} T\left[\psi_-, \psi_+\right] = {} & \langle\phi_\beta|\,W\,|\psi_+\rangle + \langle\psi_-|\,W\,|\phi_\alpha\rangle \\ & - \langle\psi_-|\,W - WG_0W\,|\psi_+\rangle, \end{aligned}$$

which can be shown to attain its stationary value for ψ_-, ψ_+ being the corresponding solutions of the associated Lippmann-Schwinger equations. The Schwinger-Lanczos method expands the sought solution into a properly chosen basis and solves consequently for these expansion coefficients.

If we denote the basis under consideration as $\{|g_k\rangle\}_{k=1}^N$ and the variational coefficients as $c_k^{(\pm)}$, then we can write

$$|\psi_\pm\rangle = \sum_{k=1}^N c_k^{(\pm)}\,|g_k\rangle\,.$$

The final T-matrix element is then approximated as

$$T_{\beta\alpha}^N = \sum_{k,l=1}^N \langle\phi_\beta|\,W\,|g_k\rangle\left(M^{-1}\right)_{kl}\langle g_l|\,W\,|\phi_\alpha\rangle\,, \tag{15}$$

where the elements of the matrix M are given as $M_{kl} = \langle g_k|W - WG_0W|g_l\rangle$. Although the choice of the basis seems to be quite arbitrary, it is a fundamental ingredient of this method. In principle, all we need is the matrix M being regular. However, this requirement is only a necessary and not a sufficient condition on the basis to ensure fast convergence of the entire method.

According to [18] it turns out to be convenient to construct the basis so as to be "W-orthogonal", i.e.

$$\langle g_k|W|g_l\rangle = \delta_{kl}. \tag{16}$$

In addition, the matrix WG_0W is required to be tridiagonal, i.e.

$$\begin{aligned} \langle g_{k-1}|\,WG_0W\,|g_k\rangle &= \langle g_k|\,WG_0W\,|g_{k-1}\rangle = \beta_{k-1} \\ \langle g_k|\,WG_0W\,|g_k\rangle &= \alpha_k \\ \langle g_k|\,WG_0W\,|g_l\rangle &= 0, \quad \text{for} \quad |k-l| \geq 2. \end{aligned} \tag{17}$$

The basis that fulfills these conditions is constructed iteratively with the first vector $|g_1\rangle$ chosen in the form $\langle\phi|\,V\,|\phi\rangle^{-1/2}$. Because of the W-orthogonality condition (16) only the matrix element $\left(M^{-1}\right)_{11}$ is required

in equation (15). Some rather tedious calculations furnish this element in the form of a continued fraction, namely

$$T^N = \langle\phi|\, W\, |g_1\rangle \left(M^{-1}\right)_{11} \langle g_1|\, W\, |\phi\rangle = \cfrac{\langle\phi|\, W\, |\phi\rangle}{1-\alpha_1-\cfrac{\beta_1^2}{1-\alpha_2-\cfrac{\beta_2^2}{1-\alpha_3-\cdots\cfrac{\beta_{N-1}^2}{1-\alpha_N}}}}\,. \quad (18)$$

Complete recurrent relations according to [18] are

$$|r_k\rangle = G_0 W\, |g_k\rangle - \beta_{k-1}\, |g_{k-1}\rangle\,, \quad (19a)$$
$$\alpha_k = \langle g_k|\, W\, |r_k\rangle\,,$$
$$|s_k\rangle = |r_k\rangle - \alpha_k\, |g_k\rangle\,, \quad (19b)$$
$$\beta_k = \langle s_k|\, W\, |s_k\rangle^{1/2}\,,$$
$$|g_{k+1}\rangle = \beta_k^{-1}\, |s_k\rangle\,, \quad (19c)$$

where we set $\beta_0 = 0$ and $|g_1\rangle = \langle\phi|\, V\, |\phi\rangle^{-1/2}$.

2.3 RLS algorithm

We have already mentioned partly in the introduction how to adapt the two cornerstones described above for our computational needs so let us now sum up the details. For purposes of future reference we hereafter call our method as the *RLS*-algorithm – *R* standing for R-matrix and *LS* for Lippmann-Schwinger principle. Following the ideas depicted in the previous sections, the overall strategy of the proposed method can be summarized according to the following prescription using the "two-potential" formula.

1. Solve equation (1) with source term $|u\rangle$ considering only the local potential V using the R-matrix technique and obtain the solution $|\overline{u}\rangle$ as:
   (a) write the sought solution $|\overline{u}\rangle$ as a sum of two parts $|\overline{u}\rangle = |u\rangle + |\xi\rangle$, where $|\xi\rangle$ represents a "correction" to the source term $|u\rangle$;
   (b) $|\overline{u}\rangle$ is also an eigenvector (corresponding to the same energy E) of the Hamiltonian $H_V \equiv K_T + V$, where K_T is the operator of free particle's kinetic energy with reduced mass μ. The following relations are thus easily seen to hold

$$(K_T + V)\,\{|u\rangle + |\xi\rangle\} = E\,\{|u\rangle + |\xi\rangle\}\,, \quad (20a)$$
$$V\,|u\rangle + H_V\,|\xi\rangle = E\,|\xi\rangle\,, \quad (20b)$$
$$|\xi\rangle = (E - H_V)^{-1}\, V\,|u\rangle \equiv G(E) V\,|u\rangle\,, \quad (20c)$$

   where the symbol $G(E)$ has been used for $(E - H_V)^{-1}$ in accordance with the former definition given by equation (2). This handy observation can be checked immediately by means of the following operator identity $(\mathrm{A} - \mathrm{B})^{-1} = \mathrm{A}^{-1} + \mathrm{A}^{-1}\mathrm{B}(\mathrm{A} - \mathrm{B})^{-1}$.
2. Obtain the solution $|\overline{u}\rangle$ according to equation (20c) as a sum of the source term $|u\rangle$ and the ket $G(E)V\,|u\rangle$. The Green's function is constructed using the R-matrix method as described above. This approach ensures that the desired boundary condition at the end of the integration interval is correctly incorporated into the Green's function under construction.
3. Solve the LS-equation considering only the nonlocal potential W with source term $|\overline{u}\rangle$ by means of Schwinger-Lanczos iterative algorithm obtaining the final solution $|\phi\rangle$ and also the T-matrix element as a byproduct of the iterative procedure [18].

In the second part of the next section where we apply our method to the local "van der Waals"-like potentials, we merely skip the third step in the previous scheme since no nonlocal interaction W enters the stage in this case.

The most time consuming part of the entire computation is the construction of the R-matrix basis specified by equation (8). But it should be noted that this procedure is energy independent and needs to be carried out only once. Therefore we can render the phase-shift energy dependence for various energies at almost negligible additional cost. This positive feature is profitably employed especially in the computation of the scattering length as we discuss elaborately in Section 3.2.

As concerns the construction of numerical solutions of equation (8), we use a polynomial basis to restate this equation to an algebraic matrix eigenvalue problem. In the case of the first sector $0 \le r \le r_1$, we utilized a set of modified Jacobi polynomials $rP_n^{(0,2)}(2r/r_1 - 1)$, which are orthogonal in $[0, r_1]$ with respect to r and obey naturally the zero boundary condition at the origin, whereas Legendre polynomials adapted for the respective interval were used for the remaining sectors. In order to evaluate the integrals appearing in the R-matrix framework we employed standard Gauss-Legendre or Clenshaw-Curtis (in the case of potentials diverging at the origin) quadrature. In practice, the number of mesh points N in each sector should be set slightly higher than the number of basis functions N_b to assure exact integration of basis functions products.

3 Numerical examples

In this section we demonstrate the use of our method for tackling two different class of problems. Namely determining the phase-shift energy dependence for $\mathrm{e}^- - \mathrm{H}$ scattering in the static exchange approximation and consequently computation of scattering length and effective range for a family of potentials decreasing as $\mathcal{O}\left(1/r^6\right)$ for $r \to \infty$. These model potentials appear e.g. in description of ground state interactions of particular dimers such as Cs_2 or $^4He_2$.

3.1 $\mathrm{e}^- - \mathrm{H}$ scattering

The numerical tests of the presented algorithm consisted in the calculation of the *s*-wave phase shift for electron

scattering off the ground state of hydrogen atom in the presence of exchange terms, both for the spin singlet $\delta^{(+)}$ and triplet $\delta^{(-)}$ state. We have chosen this model as our subject of interest because similar calculations using different approaches can be found in the literature [19] offering the possibility to compare the results.

From the mathematical point of view, we need to solve following integral equation for the radial part $R_0(r)$ of the $l = 0$ wave function. Namely

$$\left(\frac{d^2}{d\,r^2} + k^2\right) R_0(r) = V(r)R_0(r) \pm \int_0^\infty K(r, r')R_0(r')\,dr'. \tag{21}$$

In our particular case we set

$$V(r) = -2re^{-2r}\left(1 + \frac{1}{r}\right) \tag{22}$$

$$K(r,\, r') = 2v(r)u(r') + \gamma u(r)u(r') \text{ for } r' < r \tag{23}$$
$$K(r,\, r') = 2u(r)v(r') + \gamma u(r)u(r') \text{ for } r' > r,$$

where (k denotes incident momentum)

$$\gamma = -k^2 - 1,$$
$$u(r) = 2re^{-r} \text{ and } v(r) = \frac{u(r)}{r} = 2e^{-r}.$$

We compare our results with outcomes of the following alternative methods

- **S–IEM** is an spectral (the convergence with increasing number of mesh points n is under some assumptions faster than $\mathcal{O}\left(n^{-p}\right)$ for $p \in \mathcal{N}$) integral equation method developed by Gonzales et al. by extending the approach outlined originally in [20,21]. In [22] a new method is introduced for solving the LS-equation with local potentials. With a slight generalization [19] it is possible to handle properly also the nonlocal terms in the form (23). The LS-equation for the s-wave wave function can be schematically written in operator form as $(I+K)\psi(x) = \sin(kx)$. The radial integration range is further divided into several subsectors and the restriction of K on the i-th subsector is denoted as K_i. It is shown in [19] that the final solution on each of the subsectors can be found as a linear combination of four functions which are obtained by acting of $(I+K_i)^{-1}$ on four different "source" terms. These do not depend on i and are determined by the particular potential. The original problem is then reduced to solving a sparse set of linear equations for the coefficients of the linear combinations on each subsector. For practical implementation details we refer to [19] and [22].
- **M–IEM** is an iterative method originally introduced by Kim and Udagawa in [23]. The core of this method relies on utilizing of the algebraic Lanczos method for the nonlocal potential W while the local problem (with potential V) is handled in similar manner as in [24]. The authors use some additional computational tweaks in order to improve the convergence properties. Namely an additional term V_0 is subtracted from the nonlocality W and consequently added to V. Nevertheless they do not discuss effects of this approach in detail and we have not investigated this issue further.
- **N–IEM** stands for an older non-iterative integral equation method based on the work [25] of Sams and Kouri. In principle, the final solution ψ of the original one channel LS-equation is expressed as a linear combination of two auxiliary functions ψ_0 and ψ_2. Each function is required to solve a Volterra type integral equation which is easily handled by standard quadrature methods. It turns further out [25] that the two coefficients in the mentioned linear combination are given as a solution of a set of two linear equations the matrix of which depends functionally on $\psi_{0,2}$. The general discussion and a slight generalization of this method can be found in [25].
- **MCFV** is an iterative technique based on series of papers [26–28] by Horáček and Sasakawa. In this approach the local and nonlocal parts of the potential are also handled separately as in the presented RLS method. Nevertheless the Green's function is constructed in this case directly from the two independent solutions of the free Schrödinger equation. This procedure seems to be less numerically accurate than the R-matrix approach especially in the classically forbidden region where the difference in the order of magnitude of the two independent solutions is considerable. The nonlocal part W is then handled iteratively by successive subtractions of separable terms from the potential until it is weak enough so the remaining term can be neglected. Moreover the trapezoidal rule used in this method allows to incorporate e.g. the Romberg extrapolation scheme. The implementation details are given in [29].

Table 1. Accuracy of the calculated singlet phase shift $\delta^{(+)}$ for several reference methods.

Method	$\delta^{(+)}$ (mod π)	Number of m.p.
RLS	1.87015788	64
S–IEM	1.8701579	80
MCFV	1.8701579	128
M–IEM	1.870156	4000
N–IEM	1.87015	4000

Relatively detailed accuracy study of the N–IEM method is contained in [25], so we have decided to test our RLS method for the same set of parameters. Explicit results relevant to the other mentioned approaches for this set of parameters can be found in [19,29]. The case chosen is the singlet phase shift with exchange $-\delta^{(+)}$. The magnitude of the wave number of the incident particle is in atomic units $k = 0.2$ and the maximum radial distance r_f is set to 20.

Obtained results are summarized in Table 1, where the number of significant figures in the second column is determined from the stability of the phase shift value after rounding, when compared to the result corresponding to higher number of mesh points. The overall energy dependence of $\delta^{(\pm)}$ is depicted in Figure 1.

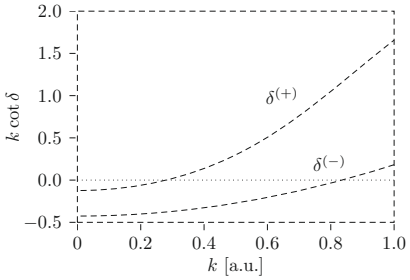

Fig. 1. Energy dependence of the calculated phase shifts $\delta^{(\pm)}$.

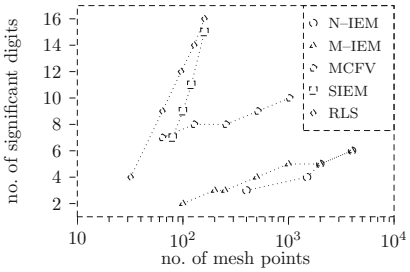

Fig. 2. Comparison of the accuracy of the tested methods. For details see text.

More transparent overview of the convergence properties of the tested methods is contained in Figure 2 in which we are dealing essentially with an "inverse" task. That is with determining the number of mesh points necessary to obtain some prescribed number of significant figures. As can be seen from Figure 2 the proposed RLS method is very stable even for low number of mesh points. We believe that it is primarily ensured by the accurate construction of the Green's function in the R-matrix framework.

3.2 Cs–Cs dimer

We have tested our method on the model potential for the Cs−Cs dimer $^3\Sigma_u$ ground state interaction described according to [30] by potential

$$V_{\mathrm{d}}(r) = \frac{1}{2}Br^{\mu}e^{-\eta r} - \left[\frac{C_6}{r^6} + \frac{C_8}{r^8} + \frac{C_{10}}{r^{10}}\right] \times \left\{\theta(r - R_{\mathrm{c}}) + \theta(R_{\mathrm{c}} - r)e^{-\left(\frac{R_{\mathrm{c}}}{r}-1\right)^2}\right\}, \quad (24)$$

where θ represents the Heaviside step-function. The first term in equation (24) is related to the exchange repulsion of the valence electrons whereas the remaining part in the form of a sum of van der Waals terms corresponds to the long-range interaction. Suitable cutoff function (term in the curly braces) is introduced to cancel the divergent behavior of $1/r^n$ at the origin. For $r \to 0$ the potential tends

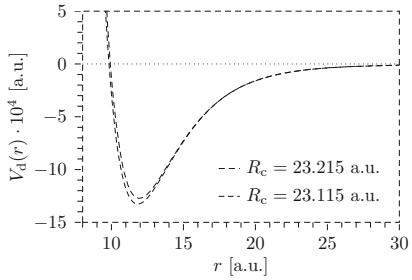

Fig. 3. Model potential for the Cs–Cs ground state interaction as given by equation (24).

Table 2. Parameters of the local potential $V_{\mathrm{d}}(r)$ introduced in equation (24).

μ	η	B	C_6	C_8	C_{10}
5.53	1.072	1.6×10^{-3}	7.02×10^3	1.10×10^6	1.70×10^8

erroneously (the exchange repulsion should increase exponentially) to zero but this discrepancy is physically irrelevant because the wave function vanishes rapidly in this classically forbidden region (especially for low energy).

The numerical values of the constants μ, η, B and $C_{6,8,10}$ that enter equation (24) are listed in Table 2 and the Cs reduced mass was set to $m_{\mathrm{Cs}} = 2.422 \times 10^5$. The cutoff radius R_{c} is considered as a free parameter. Comparing the potential curve with ab-initio results in the radial range from 7 to 20 a.u. shows [31] that best fit is obtained by $R_{\mathrm{c}} = 23.615$. However, since the potential is by no means exact, we have performed the calculations for several values of R_{c} to partly reveal its influence on the scattering length. Typical behavior of $V_{\mathrm{d}}(r)$ is depicted in Figure 3 for two values of R_{c}.

In connection with the formula (24), we would like to point out, that this function dependence is not smooth in the vicinity of $r = R_{\mathrm{c}}$ (actually, already the second derivative exhibits a jump discontinuity). This poses some subtle complications in our R-matrix approach based on polynomial approximation and Gaussian quadrature and we are forced to set one sector boundary precisely at R_{c}.

3.2.1 Bound states of $V_{\mathrm{d}}(r)$

As a first practical application of our method in this case we demonstrate its use on the determination of the number of s-wave bound states of the potential (24) with R_{c} set to 23.215 by calculating the zero energy solution of the full Schrödinger equation using the R-matrix machinery. We postpone the stability and convergence questions for further discussion and merely show the shape of the full zero energy solution in Figure 4.

We see that the wave function attains slowly its asymptotic behavior approximately at $r \approx 400$. According to the well-known oscillation theorem [10], the number of bound

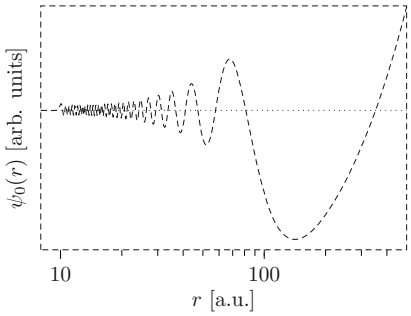

Fig. 4. The zero-energy solution of the Schrödinger equation with the potential (24) for $R_c = 23.215$ a.u.

states should be no less than 58 (total count of the nodes) in this case. However, equipped only with the results of the numerical computation, we can be hardly sure that the potential is not strong enough to bend the wave function once (or perhaps several times) again even for $r > 400$.

We shall show now that this is actually not the case and we have exactly 58 bound states. Our argument is based on the *Bargmann condition* [32,33] – stating that the number of bound states n_l in the partial wave l is bounded from above by

$$n_l \leq \frac{1}{2l+1} \int_0^\infty r|V(r)|\, dr.$$

According to Figure 4, the last found node of ψ_0 is located at $r_0 \approx 350$. Using the Bargmann condition, it is easy to see that the number of s-wave nodes in the interval (r_0, ∞) is bounded by the quantity

$$I(r_0) \stackrel{\text{def}}{=} \frac{1}{2 \cdot 0 + 1} \int_{r_0}^\infty (r - r_0)\, |V_\mathrm{d}(r)|\, dr.$$

Straightforward inspection of this integral yields that $I(r_0)$ is non-increasing function of r_0 for $r_0 > r_{\min}$, where $r_{\min} \approx 12$ a.u. locates the minimum of $V_\mathrm{d}(r)$, and that $I(r_0) < 1$ for $r_0 \gtrsim 100$ a.u., i.e. the wave function has no additional nodes for $r \geq r_0$.

3.2.2 Computation of the scattering length a_0 and effective range r_e

We have devoted our main computational effort to the evaluation of the scattering length a_0 and effective range r_0. Although it is mathematically possible to apply the R-matrix method directly for zero energy, we have used different approach based on extrapolation of the phase-shift towards zero energy according to the modified ERT formula (5). Because for zero energy the scattered particle can never be considered as free for an infinite-range potential we need to propagate the wave-function theoretically to $r \to \infty$. Moreover, if we denote the maximal distance of propagation as $r_{\max}$, then the inverse logarithmic derivative $\mathcal{R}$ (supplied by R-matrix calculations) diverges as $r_{\max}$. The scattering length can be further shown to be equal to $(r_{\max} - \mathcal{R})$ for zero energy. But in this expression we would subtract large numbers comparable in magnitude and the numerical precision will be probably significantly decreased.

Table 3. Accuracy of the calculated quantity $k \cot \delta_0$ vs. increasing grid density (together with the number of basis functions).

No. of basis functions	24	26	28	30	34
No. of significant digits	5	6	8	9	11

On the other hand, for non-zero k it is sufficient to propagate until the energy dominates the potential by several orders of magnitude.

Quick glance at Figure 4 reveals that the full wave function is almost identically equal to zero in the radial range $r \in \langle 0, 10 \rangle$, rapidly oscillates in $\langle 10, 30 \rangle$ and for $r \gtrsim 30$ the oscillations slow down attaining gradually the asymptotic behavior.

As concerns the numerical stability and convergence properties of our method, two important factors enter the stage. Firstly, it is the structure and density of the grid in the oscillatory region and secondly the particular value of maximal propagation distance $r_{\max}$.

1. In order to gain insight onto the influence of the first factor we have tested our method with several grids for $r_{\max} = 30$ a.u. (this corresponds to phase shift computation for the potential given by (24) for $r \leq r_{\max}$ and zero elsewhere). We have used equisized sectors (2 a.u. wide) with increasing grid density together with the basis functions count and observed consequently the influence on the quantity $k \cot \delta_0$. Results are summarized in Table 3.
   We always assume that the number of grid points in each sector is set approximately slightly higher than the number of basis functions to ensure exact numerical integration of basis functions products. It seems that for more basis functions no further refinement is achieved – we account this to the non-smoothness of the potential at $r = R_c$.
2. Equipped with a stabilized "short-range" grid obtained in the previous step we have investigated consequently the influence of $r_{\max}$ on $k \cot \delta_0$. Because it is not especially convenient nor desirable to have too many sectors for large r, we have used for the grid density for $r > r_0$ the following rule of thumb. We have found out that 10 significant digits of $k \cot \delta_0$ are retained in the considered energy region when we use approximately 18−20 mesh points per local wave length given by
$$\lambda = \frac{2\pi}{\sqrt{k^2 - 2\mu V_\mathrm{d}(r)}}.$$

This enables us to fix the grid for small r while expanding the last sector by increasing the corresponding number of mesh points resp. basis functions in it and observing the convergence properties of our method. Of course we

Table 4. Dependence of the scattering length a_0 and the effective range r_e on the "cutoff" parameter R_c.

	I	II	III		IV	
R_c [*a.u.*]	a_0 [1]	a_0 [2]	a_0 [3]	r_e [3]	a_0	r_e
23.215	376	352.5	350.6305	169.9843	350.6305570	169.9
23.190	140	144.2	145.4336	157.5894	145.4335866	157.2
23.165	65	68.0	68.21596	624.5533	68.21596735	622.7
23.140	-69	-67.7	-72.24305	2069.113	-72.24304633	2067.4
23.115	467	485.3	477.1465	1916.246	477.1465226	191.6

[1] Extrapolation procedure [30]; [2] semi-classical WKB based method [30]; [3] results taken from [34] – the last value of r_e is probably a misprint.

can take only those decimal places seriously which were guaranteed by the stabilization of the "short-range" grid because further propagation introduces additional numerical error so we can hardly expect to gain higher accuracy.

As concerns the MERT extrapolation procedure, comparison with independent sources [30,34] revealed that best the fit is obtained for wave numbers k from 10^{-8} to 10^{-5}. This interval was chosen mostly by trial and error since for lower energies the method starts to exhibit convergence problems similar to the zero energy case while for higher k the use of the modified effective range theory (5) could be dubious.

In connection with this question we would like to mention an alternative approach developed in the work of Sasakawa and Horáček [35], and Nowak et al. [36] based on rational approximation of $k \cot \delta_0$ in k which is supposed to be convergent in larger domain of k as well as being able to cope with possible Ramsauer-like effects accompanied by zeros of δ_0 for certain values of k where the standard power expansion breaks down completely ([35], p. 169).

The typical behavior regarding the convergence with respect to increasing $r_{\max}$ is shown for two distinct energies in Figure 5, where we display the behavior of the relative error of $k \cot \delta_0$ understood as a function of $r_{\max}$ with respect to its "limiting" value obtained for $r_{\max} = 50{\times}10^4$.

We see that in order to ensure ten-eleven significant decimal places, we need to propagate up to ca. $r \approx 150 \times 10^3$. For determination of the scattering length a_0 we use this "asymptotic value", while the effective range r_e is computed via standard Levenberg-Marquardt fit of $k \cot \delta_0$ understood as a function of energy determined by (5). An important advantage of the presented method is the ease of repetitive calculations for several energy values because the most time consuming (≈95% of total running time) part is the construction of the *energy independent* basis. We haven't performed thorough time complexity benchmarks of our computations nevertheless the typical running time for calculating $k \cot \delta_0$ for 500 energy points is on a today's low-end computer (Intel P4 3 GHz, 2 GB RAM) in order of seconds.

Using the presented method and following [34], we have computed the quantities a_0, r_e for several values of the cutoff parameter R_c. The relevant numerical values are listed in the column IV of Table 4. In this table we also show results of other authors for comparison.

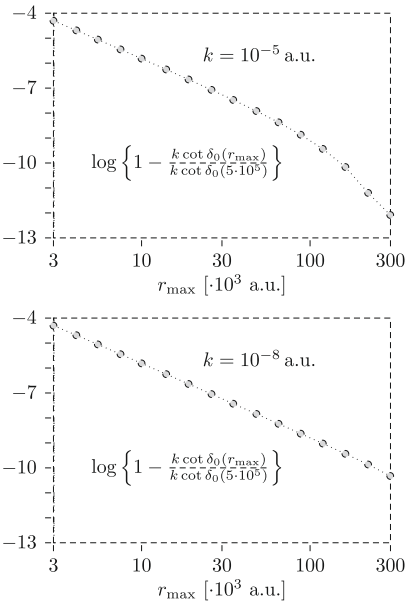

Fig. 5. Number of significant digits in the quantity $k \cot \delta_0$ as a function of $r_{\max}$ for $k = 10^{-5}$ (in the upper panel) and $k = 10^{-8}$ (lower panel).

Details of these alternative methods can be found in corresponding papers so let us only briefly mention the essential basic ideas.

Col. I The first column of Table 4 contains values of scattering length computed by direct extrapolation of the s-wave phase shift δ_0 for k tending to 0, where δ_0 is determined simply via integration of the Schrödinger equation starting at the origin with zero boundary condition and comparing the obtained wave function at some large r with its presumed asymptotic form $\sin(kr + \delta_0)$ [30].

Col. II These results adopted also from [30] were gained using the WKB approximation. The radial range is divided by some R into an asymptotic $r > R$

(where only the long-range part of the potential is supposed to be significant) and inner region part $r \in (0, R)$. In the inner region, the solution of Schrödinger equation for zero-energy is expressed in terms of WKB and then matched at the boundary of these two regions, i.e. at $r = R$, with the known analytic solution for $r > R$.

Col. III The main idea behind the method used in [34] is to express the zero energy solution $U(r)$ of the Schrödinger equation for large r as a sum of two independent free solutions $U(r) = \alpha\epsilon_\alpha(r) + \beta\epsilon_\beta(r)$, where ϵ_α and ϵ_β tend to r and 1 for $r \to \infty$, respectively. Functions $\epsilon_{\alpha,\beta}$ solve the same equation as $U(r)$ but can not be obtained exactly for a general potential. Nevertheless we can try to solve the Schrödinger equation in an iterative manner as it is often done in the theory of integral equations. Sufficient approximation of $\epsilon_{\alpha,\beta}$ is then used in the expression for $U(r)$ and matched at some (set fixed in advance) $r = R_0$ with the numerical solution obtained by integration for $r < R_0$ in order to determine the constants α, β. Scattering length a is then easily evaluated as $-\beta/\alpha$.

Col. IV Finally the last column summarizes our results obtained by means of the presented method denoted as RLS-algorithm.

As demonstrated by Table 4, our results regarding the scattering length are in full accordance with [34], moreover we were able to secure typically 4 additional significant decimal places. As concerns the effective range, our method suffers from the fact that r_e is determined indirectly by fitting because two contradictory requirements are essential here. On one hand we need small k for validity of (5) and on the other hand the change $\Delta_{k\cot\delta_0}$ in $k\cot\delta_0$ induced by a slight variation Δ_{r_e} in r_e is given as (assumed a_0 fixed)

$$\Delta_{k\cot\delta_0} \approx \frac{1}{2}\Delta_{r_e}\, k^2. \tag{25}$$

Using the values from Table 4 we see that e.g. for $k = 10^{-5}$ and $\Delta_{r_e} = 0.1$ we have $\Delta_{k\cot\delta_0} \approx 10^{-11}$ so, since $k\cot\delta_0 \approx 10^{-3}$, it is desirable to compute eight significant decimal places of $k\cot\delta_0$ in order to being able to detect this tilt in r_e.

The effective range in the last row of Table 4 exhibits large discrepancy but we believe that the corresponding value in [34] is merely a misprint.

3.3 $^4He_2$ dimer

We have also tested the presented method with three different forms of $^4He_2$ dimer ground state semiempirical potential by Aziz et al., namely HFDHE2 [37], HFD-B [38] and LM2M2 [39]. For the explicit form of these potentials we refer to [40]. The computational procedure is almost identical as in the previous case of the Cs_2 dimer so we merely state the results in Table 5.

Table 5. The scattering length a_0 and the effective range r_e for various model potentials of the $^4He_2$ dimer ground state.

	I[1]	Present calculations	
	a_0 [Å]	a_0 [Å]	r_e [Å]
HFDHE2	124.65	124.645898672	26.4
HFDB	88.50	88.6009728852	26.0
LM2M2	100.23	100.233913812	26.2

[1] Data taken from [40].

4 Conclusion

In this paper we have proposed a general, practical and very efficient method for handling the basic equation of scattering theory, namely the one-channel Lippmann-Schwinger integral equation containing local as well as nonlocal interactions. Our approach makes use of the R-matrix framework to construct the Green's function of the local problem while the potential nonlocality is handled by the Schwinger-Lanczos iterative algorithm. Comparison with results of other alternative approaches indicates that our technique is superior to all standard methods based on the direct numerical integration of the Schrödinger equation. This was demonstrated on the example of electron scattering with hydrogen atom in the static exchange approximation. This is a standard test for any numerical method designated for solving the scattering equations. The RLS method is so efficient that using only 64 meshpoints in the calculation yields phaseshifts correct to nine significant digits. Using 20 meshpoints we obtain results correct to about four significant digits. This accuracy surpasses the accuracy of any experimental data. In addition, it was shown that, contrary to the previous electron-atom case where all interactions were of short range, excellent numerical accuracy was also obtained for a class of long range local potentials decaying as r^{-n} at infinity. This problem is of great importance in the field of collisions of cold atoms. The precise knowledge of the scattering length is an important factor for understanding the formation of Bose-Einstein condensate. Even in this case we obtain results with an excellent accuracy.

We gratefully appreciate the substantial financial support of the Czech Grant agency (grant no. 202/08/0631), Grant agency of the Academy of Sciences of the Czech Republic (grant no. KJB400400803) and the Grant agency of the Charles university in Prague (grant no. 257718). The author is also greatly indebted to Dr. Michal Tarana and Dr. Přemysl Kolorenč for valuable and inspiring discussions concerning the material of this paper.

References

1. D. Field, S. Lunt, J.P. Ziesel, Acc. Chem. Res. **34**, 291 (2001)
2. J. Weiner, Rev. Mod. Phys. **71**, 1 (1999)

3. N. Lane, Rev. Mod. Phys. **52**, 29 (1980)
4. M. Gell-Mann, M. Goldberger, Phys. Rev. **91**, 398 (1953)
5. J. Taylor, *Scattering theory: The quantum theory on nonrelativistic collisions* (John Wiley & Sons, Inc., 1972)
6. N. Mott, H. Massey, *The theory of atomic collisions* (Oxford Univeristy Press, 1965)
7. P. Roman, *Advanced quantum theory* (Addison-Wesley Publishing Company Inc, 1965)
8. T. O'Malley, L. Spruch, L. Rosenberg, J. Math. Phys. **2**, 491 (1961)
9. M.L. Goldberger, K.M. Watson, *Collision theory* (John Wiley & Sons, Inc., 1967)
10. L.D. Landau, E.M. Lifshitz, *Quantum Mechanics: Non-Relativistic Theory* (Butterworth-Heinemann, 1981)
11. R. Berger, H. Snodgrass, L. Spruch, Phys. Rev. **185**, 113 (1969)
12. O. Hinckelmann, L. Spruch, Phys. Rev. A **3**, 642 (1971)
13. P. Ganas, Phys. Rev. A **5**, 1684 (1972)
14. B. Gao, Phys. Rev. A **58**, 1728 (1998)
15. G.V. Mil'nikov, H. Nakamura, J. Horáček, Comput. Phys. Commun. **135**, 278 (2001)
16. C. Bloch, Nucl. Phys. **4**, 503 (1957)
17. B. Lippmann, J. Schwinger, Phys. Rev. **79**, 469 (1950)
18. H.D. Meyer, J. Horáček, L. Cederbaum, Phys. Rev. A **43**, 3587 (1991)
19. G.H. Rawitscher, S.Y. Kang, I. Koltracht, J. Chem. Phys. **118**, 9149 (2003)
20. L. Greengard, SIAM J. Numer. Anal. **28**, 1071 (1991)
21. L. Greengard, V. Rokhlin, Commun. Pure Appl. Math. **44**, 419 (1991)
22. R. Gonzales, J. Eisert, I. Koltracht, M. Neumann, G. Rawitscher, J. Comput. Phys. **134**, 134 (1997)
23. B. Kim, T. Udagawa, Phys. Rev. C **42**, 1147 (1990)
24. F. Perey, B. Buck, Nucl. Phys. **32**, 353 (1962)
25. W. Sams, D. Kouri, J. Chem. Phys. **51**, 4809 (1969)
26. J. Horáček, T. Sasakawa, Phys. Rev. A **28**, 2151 (1983)
27. J. Horáček, T. Sasakawa, Phys. Rev. A **30**, 2274 (1984)
28. J. Horáček, T. Sasakawa, Phys. Rev. C **32**, 70 (1985)
29. J. Horáček, J. Bok, Comput. Phys. Commun. **59**, 319 (1990)
30. G. Gribakin, V. Flambaum, Phys. Rev. A **48**, 546 (1993)
31. M. Krauss, W. Stevens, J. Chem. Phys. **93**, 4236 (1990)
32. V. Bargmann, Proc. Acad. Sci. USA **38**, 961 (1952)
33. J. Schwinger, Proc. Acad. Sci. USA **47**, 122 (1961)
34. M. Marinescu, Phys. Rev. A **50**, 3177 (1994)
35. T. Sasakawa, J. Horáček, J. Phys. B **15**, L169 (1982)
36. E. Nowak, L. Rosenberg, L. Spruch, J. Phys. B **13**, L599 (1980)
37. R. Aziz, V. Nain, J. Carley, W. Taylor, G. McConville, J. Chem. Phys. **70**, 4330 (1979)
38. R. Aziz, F. McCourt, C. Wong, Molec. Phys. **61**, 1487 (1987)
39. R. Aziz, M. Slaman, J. Chem. Phys. **94**, 8047 (1991)
40. A. Motovilov, W. Sandhas, S. Sofianos, E. Kolganova, Eur. Phys. J. D **13**, 33 (2001)

A new type of interference phenomenon in cold collisions of electrons with N_2

M Šulc[1,2], R Čurík[2], J P Ziesel[3], N C Jones[4] and D Field[4]

[1]Institute of Theoretical Physics, V Holešovičkách 2, 180 00 Prague 8, Czech Republic
[2]J. Heyrovský Institute of Physical Chemistry, Dolejškova 3, 182 23 Prague 8, Czech Republic
[3]Laboratoire Collisions Agrégats Réactivité (CNRS-UPS UMR5589), Université Paul Sabatier, 31062 Toulouse, France
[4]Department of Physics and Astronomy and Institute for Storage Ring Facilities (ISA), Aarhus University, DK-8000 Aarhus C, Denmark

E-mail: `roman.curik@jh-inst.cas.cz`

Abstract. A novel cold collision phenomenon is described which is caused by interference within the manifold of electron waves of unit angular momentum (p-waves). Experimental electron scattering data in N_2, down to energies of 10 meV, reveal this phenomenon through the angular distribution of scattered electrons. *Ab initio* theory, analytical results and a simple physical model illustrate how interference arises through the presence of a quadrupole on the target N_2. The effect is of a general nature and may be found in all systems in which, in the cold regime, charged particles interact with target species with a permanent quadrupole moment.

PACS numbers: 68.35.Bs,61.16.Ch,61.46.+w,82.65.My

Submitted to: *J. Phys. B: At. Mol. Opt. Phys.*

1. Introduction

A new phenomenon in cold scattering is described involving explicit interference effects between the x-, y- and the z-components of unit angular momentum matter waves. Results are relevant to all charged particle interactions with target species where the dominant static pole in the interaction is a quadrupole, for example for homonuclear diatomics and non-polar triatomics. The phenomenon is potentially of interest in the closely related field of cold collisions involving heavy particle scattering (Weiner et al. 1999, Field & Madsen 2003). The Ramsauer-Townsend effect, involving only the s-wave and based on somewhat different physics (e.g. Field & Madsen 2003), is the only other hitherto known quantum interference effect in cold collisions with which this new phenomenon may be compared.

Electron scattering in N_2 is a test-bed of our understanding of electron-molecule collisions and has been studied extensively in the cold regime. Computational studies available in the literature employ different levels of close-coupling schemes. Body-frame fixed-nuclei approach was used in Isaacs & Morrison (1992). The method was later extended by including vibrational dynamics via close-coupling (Morrison et al. 1997). Recently, laboratory-frame calculations with vibrational and rotational close-coupling procedure were reported by Telega & Gianturco (2006). Although the agreement of the calculated integral cross-sections with the experimental data (Sohn et al. 1986, Sun et al. 1995) is quite good, it has been demonstrated (Telega & Gianturco 2006) that computed results strongly depend on the short-range interaction model. In particular, it has been shown (Telega & Gianturco 2006) that different local exchange models may lead to cross-sections that differ by 30% in absolute value.

These findings are in accord with modified effective-range theory (MERT) (Fabrikant 1984) studies by Isaacs & Morrison (1992) and Morrison et al. (1997). In both works authors concluded that in the case of N_2 molecule the original MERT model (Fabrikant 1984) fails to describe integral cross-sections above collision energies of approx. 20 meV. Such a surprising result was attributed to a small value of scattering length A that was determined to the range of 0.36 - 0.44 a.u. (Fabrikant 1984, Isaacs & Morrison 1992, Morrison et al. 1997). Therefore, the leading terms in the MERT expansion may not be dominant and the introduction of higher-order terms (proportional to k^3 and k^4) becomes necessary to describe cross-sections in the range of 20 - 200 meV (Isaacs & Morrison 1992, Morrison et al. 1997). These higher-order contributions are due to forces of a short or intermediate range and predicted cross-sections were found to be sensitive to their presence.

In present analysis of the experimental data we therefore refrain from employing MERT. We instead attempt to determine the absolute value of the phase shifts from the experimental integral and backward cross-sections. Since the full information about the computed values of the phase shifts for all the partial waves with $l \leq 2$ is unavailable in the literature we also decided to carry out body-frame fixed-nuclei calculations. These calculations then serve us as a guide to determine the dominant partial waves necessary

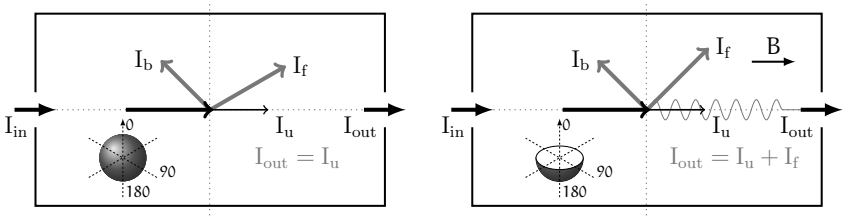

Figure 1. Schematic representation of the experimental apparatus: the ingoing electron beam intensity I_{in} splits into the unscattered component I_u plus the parts I_f and I_b corresponding to the forward and backward scattering, respectively. With no magnetic field (left panel), the outgoing intensity I_{out} is essentially equivalent to I_u and thus the outcome of the experiment is the total integral cross-section σ_T. In presence of an axial magnetic field (right panel), I_f also contributes to I_{out} (see text), therefore the total backward cross-section σ_B is measured in this case.

to describe $e^- - N_2$ collisions in the measured range of 10 - 250 meV. Using an analytic approach we then show how our experimental data may be reproduced using phase shifts as fitting parameters. This yields a graphic physical description of how interference effects arise in the p-manifold.

2. Experimental details

In our experiments (Hoffmann et al. 2002, Field, Lunt & Ziesel 2001), synchrotron radiation from the ASTRID storage ring at Aarhus University provides a high resolution photon source and through threshold photoionization of Argon at 15.75 eV creates photoelectrons with an energy resolution determined by the energy resolution in the photon beam. This is set here to ~ 1.5 meV full-width half-maximum. Electrons, formed into a beam, pass through room temperature target gas (99.999% purity) contained in a collision cell of length 30 mm. The intensity of the electron beam, in the presence and absence of target gas, is recorded as a function of electron energy. This yields the variation of the total integral scattering cross-section, $\sigma_{T,I}$, where "total" refers to all elastic and rotationally inelastic events and "integral" to integration over the full 4π sr. $\sigma_{T,I}$ is given by $(Nl)^{-1}\ln(I_0/I_t)$ where N is the target gas number density, l is the path length in the gas and I_0 and I_t are respectively the intensities of the incident and transmitted electron beams. Absolute values of total integral scattering cross-section at 1 to 4 eV show excellent agreement with those reported by Kennerly (1980). In independent experiments, an axial magnetic field of strength $\sim 2 \times 10^{-3}$ T was introduced. Electrons scattered into the forward hemisphere exhibit a spiral trajectory with radius smaller than the radius of the exit hole of the collision chamber (1.5 mm) and, guided onto the detector, are recorded as unscattered. Thus only electrons scattered into the backward 2π sr are recorded as lost to the incident beam and the cross-section measured is the total backward scattering cross-section σ_B. The absolute electron

energy scale is calibrated to ±1 meV and ±2 meV (Hoffmann et al. 2002, Field, Lunt & Ziesel 2001, Jones et al. 2002) by observing the peak in the N_2^- $^2\Pi_g$ resonance around 2.442 eV (Kennerly 1980). We estimate errors in cross-sections of ±5% to ±8% (2σ), the latter at the lowest energies for integral scattering data. Pictorial scheme of the two independent experimental settings (with and without an axial magnetic field) is presented in Figure 1.

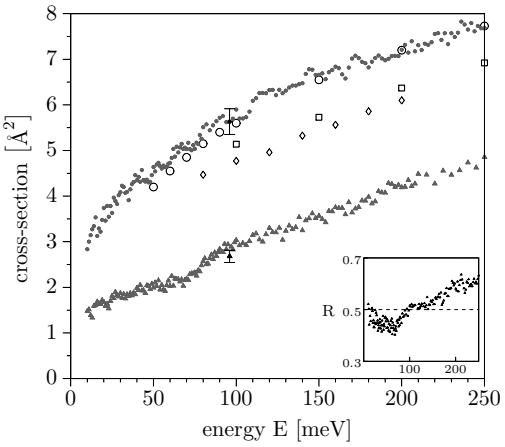

Figure 2. Experimental cross-sections – grey • and ▲ are present integral and backward hemisphere data respectively. ○, □ and ◊ are data of Jost, Ferch and Sun respectively (Brunger & Buckman 2002, Sun et al. 1995). The inset shows the ratio of backward and integral data, R, as a function of energy.

Experimental results for cross-sections for N_2 are shown in Figure 2. The anomalous behaviour of the backward scattering cross-section between 70 and 90 meV is apparent, showing a marked dip in value with no such feature in the integral cross-section. This represents a destructive interference of scattered waves in the backward hemisphere compensated by a rise in the forward hemisphere. Discussion of the data of other groups, shown in Figure 2 may be found in Itikawa (2006) or Sun et al. (1995). There are no data suitable for comparison for scattering into the backward hemisphere as a function of energy in the energy range shown. The inset to Figure 2 records the variation with energy of the ratio of the backward to integral cross-section, R, as a function of electron kinetic energy. As a useful check on the data at very low energy, the inset shows that R is asymptotically 0.5, within experimental error, representing pure s-wave scattering as $E \to 0$. Note that the ratio passes below 0.5 at ~ 95 meV. The remainder of the article is devoted to the origin of the suppression of backward scattering and a demonstration that it can be explained through p-wave interference.

3. *Ab initio* calculations

We describe first an *ab initio* theory whose results will be used as a guide to identify the partial waves that are dominant at low energy and their relative importance, in particular in relation to the p_z and $p_{x,y}$ contributions. In the following *ab initio* calculations we use a model potential in a local form

$$V_{\rm int}(\vec{r}) = V_{\rm st} + V_{\rm ex} + V_{\rm cp}, \tag{1}$$

where $V_{\rm st}$ is the Coulombic potential characterized by a highly anisotropic short-range part, with a weak long range quadrupole interaction, and $V_{\rm ex}$ representing the exchange interaction. This is estimated using the TFEGE approximation (Telega et al. 2004, Morrison & Collins 1978) in which the target electron cloud is represented by a free electron gas and the incident electron as a plane wave. $V_{\rm cp}$ is the correlation-polarization potential which incorporates dynamical effects which distort the target electron cloud. The electron correlation at long range essentially describes the charge-induced dipole effect, computed here using the local density approximation (Perdew & Zunger 1981). Asymptotically leading terms in $V_{\rm st}$ and $V_{\rm cp}$ may be written as

$$V_{\rm st} + V_{\rm cp} \stackrel{r\to\infty}{\longrightarrow} -\frac{Q}{r^3}{\rm P}_2(\cos\theta) - \frac{\alpha_0}{2r^4} - \frac{\alpha_2}{2r^4}{\rm P}_2(\cos\theta)\,. \tag{2}$$

Experimental values of the polarizabilities are used: $\alpha_0 = 11.8\,$au, $\alpha_2 = 13.08\,$au (Morrison et al. 1997). The quadrupole moment is computed here from the target Hartree-Fock wave function and has the value of $-1.107\,$au; the experimental value is $-1.09 \pm 0.07\,$au (Morrison et al. 1997). In the region close to the molecule, the value of $V_{\rm ex}$ is typically an order of magnitude greater than $V_{\rm cp}$. $V_{\rm ex}$ however falls exponentially outside the charge density of bound electrons.

3.1. Body-frame approach

Scattering calculations are performed in a body-fixed frame of reference exploiting the conservation of the projection of angular momentum Λ of the scattered electron onto the molecular axis. Using the partial waves expansion, the Schrödinger equation for the incident electron can be written (Boardman et al. 1967), (Lane 1980, p. 48) as

$$\sum_{l'}\left[\left(\frac{{\rm d}^2}{{\rm d}r^2} - \frac{l(l+1)}{r^2} + k_{\rm B}^2\right)\delta_{l,l'} - 2V^{\Lambda}_{l,l'}(r)\right]\psi^{\Lambda}_{l',i}(r) = 0, \tag{3}$$

where $k_{\rm B}$ denotes the body-frame momentum of the incident electron, Λ stands for the projection of its orbital angular momentum onto the molecular axis and finally $V^{\Lambda}_{l,l'}(r)$ represents the matrix element of the interaction potential (1) between respective angular basis elements, namely

$$V^{\Lambda}_{l,l'}(r) = \langle l, \Lambda |\, V_{\rm int}(\vec{r}\,)\, | l', \Lambda \rangle\,, \tag{4}$$

while the interaction potential is expanded into Legendre polynomials (Lane 1980)

$$V_{\rm int}(\vec{r}\,) = V_{\rm int}(r,\theta,\phi) = \sum_L V_L(r)\,{\rm P}_L(\cos(\theta))\,. \tag{5}$$

This explicitly underlines the anticipated cylindrical symmetry of the potential. We note that only terms V_L with even L contribute in case of homonuclear molecules. Substituting (5) into (4) yields

$$\begin{aligned} V^{\Lambda}_{l,l'}(r) &= \sum_L V_L(r)\,\langle l,\Lambda|\,\mathrm{P}_L(\cos(\theta))\,|l',\Lambda\rangle = \\ &= (-1)^{\Lambda}\sqrt{2l+1}\sqrt{2l'+1}\sum_L \frac{V_L(r)}{2L+1}\,C\,(l,l',L;\,0,0)\,C\,(l,l',L;\,-\Lambda,\Lambda) \end{aligned} \quad . \tag{6}$$

By imposing the usual asymptotic behaviour on $\psi^{\Lambda}_{l',l}$ according to

$$\psi^{\Lambda}_{l',l}(r) \overset{r\to\infty}{\longrightarrow} \frac{1}{\sqrt{k_{\mathrm{B}}}}\left[\sin\left(k_{\mathrm{B}}r - l'\frac{\pi}{2}\right)\delta_{l',l} + \cos\left(k_{\mathrm{B}}r - l'\frac{\pi}{2}\right)\mathcal{K}^{\Lambda}_{l',l}\right], \tag{7}$$

we can readily obtain the reactance $\mathcal{K}^{\Lambda}-$matrix and consequently also the cornerstone of the scattering theory, the $\mathcal{T}-$matrix (Morrison & Feldt 2007)

$$\mathcal{T}^{\Lambda} = 2\mathcal{K}^{\Lambda}\,\left(i+\mathcal{K}^{\Lambda}\right)^{-1}. \tag{8}$$

Having obtained the body frame $\mathcal{T}-$matrix we evaluate the total body-frame cross-section according to Huo & Gianturco (1995) via

$$\sigma = \sum_{\Lambda=-l_{\max}}^{l_{\max}} \sigma^{\Lambda},\ \text{with}\ \sigma^{\Lambda} = \frac{\pi}{k_{\mathrm{B}}^2}\sum_{l=0}^{l_{\max}}\sum_{l'=0}^{l_{\max}}\left|\mathcal{T}^{\Lambda}_{l,l'}\right|^2. \tag{9}$$

The angular dependence needed for computation of the backward scattering cross-section σ_{B}, is most readily evaluated using the expansion into Legendre polynomials

$$\left.\frac{\mathrm{d}\sigma}{\mathrm{d}\Omega}\right|_{\mathrm{BF}} = \frac{1}{4k_0^2}\sum_L \mathrm{B}^{\mathrm{BF}}_L\,\mathrm{P}_L(\cos\theta)\,, \tag{10}$$

where

$$\mathrm{B}^{\mathrm{BF}}_L = \sum_{\substack{\Lambda_1,\Lambda_2\\ l_1,l_1',l_2,l_2'}} i^{l_1'-l_1-l_2'+l_2}\,d_L\,(l_1,\,l_2,\,l_1',\,l_2')\,\mathcal{T}^{\Lambda_1}_{l_1',l_1}\mathcal{T}^{\Lambda_2^*}_{l_2',l_2}, \tag{11}$$

with coupling terms (Sun et al. 1995, p. 4)

$$\begin{aligned} d_L\,(l_1,\,l_2,\,l_1',\,l_2') \equiv & \frac{1}{2L+1}\left[(2l_1'+1)(2l_1+1)(2l_2'+1)(2l_2+1)\right]^{1/2} C\,(l_1,l_2,L;\,0,0)\cdot \\ & C\,(l_1',l_2',L;\,0,0)\,C\,(l_1,l_2,L;\,-\Lambda_1,\Lambda_2)\,C\,(l_1',l_2',L;\,-\Lambda_1,\Lambda_2)\,. \end{aligned} \tag{12}$$

3.2. Transformation to the laboratory frame

The $\mathcal{T}-$matrix (8) refers to the body-frame and as such contains no information about the rotational dynamics. For its transformation to the laboratory-frame we employ the adiabatic rotational frame transformation (e.g. Fano & Dill 1972) which connects the body-frame quantum numbers (Λ, l) with laboratory-frame quantization expressed by (j, l), with total angular momentum $\mathbf{J} = \mathbf{j} + \mathbf{l}$ conserved.
This procedure (Huo & Gianturco 1995, Lane 1980) is formally achieved by

$${}^{\mathrm{LF}}\mathcal{T}^{J}_{j'l',jl} \overset{\mathrm{def}}{=} \sum_{\Lambda} A^{J\Lambda}_{j'l'}\,\mathcal{T}^{\Lambda}_{l',l}\,A^{J\Lambda}_{jl}, \tag{13}$$

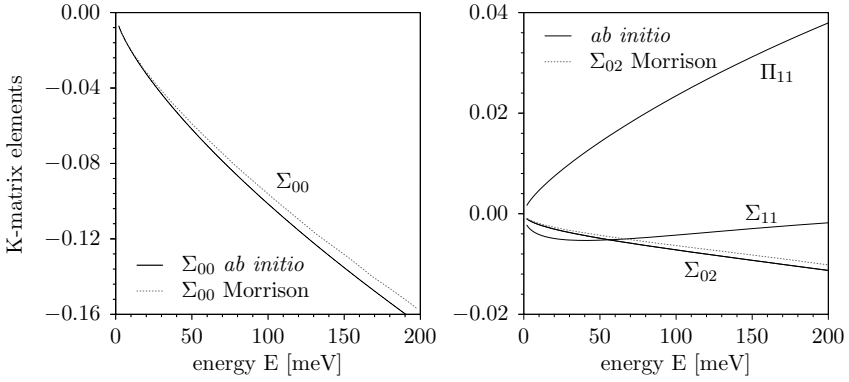

Figure 3. K-matrix elements resulting from the *ab initio* calculations. Dashed lines show the results presented by Morrison et al. (1997).

where the transformation coefficients introduced originally by Fano & Dill (1972) are in simplified form defined as

$$A^{J\Lambda}_{jl} \stackrel{\text{def}}{=} \sqrt{\frac{2j+1}{2J+1}}\,(jl\,J0\,|\Lambda\Lambda\,) = (-1)^{J-\Lambda}\begin{pmatrix} J & l & j \\ -\Lambda & \Lambda & 0 \end{pmatrix}. \tag{14}$$

The individual rotationally elastic and inelastic state-to-state cross-sections are then evaluated as

$$\sigma_{j\to j'} = \frac{\pi}{k_{\mathrm{B}}^2(2j+1)}\sum_{J=0}^{\infty}(2J+1)\sum_{l,l'}\left|{}^{\mathrm{LF}}\mathcal{T}^{J}_{j'l',jl}\right|^2. \tag{15}$$

The formulae for the differential cross-section in the laboratory frame are not needed explicitly in the presented paper and because of their rather lengthy form we refer to Huo & Gianturco (1995).

3.3. Ab initio results

The crux of the numerical procedure consists in the solution of the coupled set of differential equations (3). In our implementation we have used the Volterra integral propagator method (Sams & Kouri 1969, White & Hayes 1972). As mentioned in Huo & Gianturco (1995, p. 154), this technique finds limited use for the wave-function computation, nevertheless it turns out to be a very efficient and fast approach to render the $\mathcal{K}-$matrix.

For practical details concerning the numerical procedure we refer to Huo & Gianturco (1995). In the present calculations we have expanded the continuum wave function $\psi^{\Lambda}_{ll'}(r)$ in Eq. (3) up to $l, l' = 40$. Strictly speaking, these partial waves are then coupled by the radial coefficients $V_L(R)$ in (5) up to $L = 80$. However we found that such a high degree of angular anisotropy is necessary only for the nuclear contribution

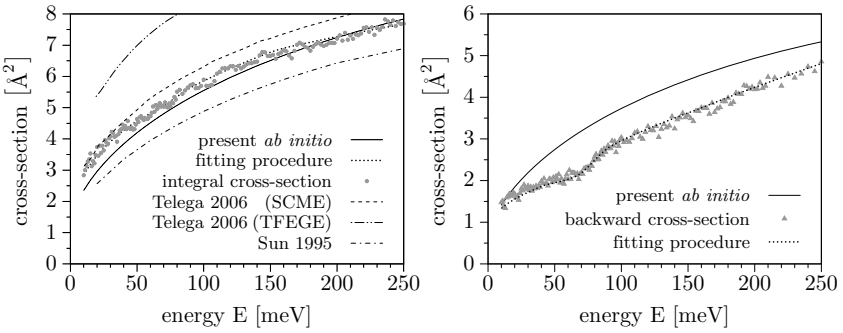

Figure 4. Comparison of theoretical results with the experimental data. Integral and backward cross-sections are displayed in left and right panel, respectively. Present *ab initio* results: solid lines. Telega & Gianturco (2006): dashed; Sun et al. (1995): dash-dot. Fits to experimental data using Σ_g, Σ_u and Π_u phase shifts: dotted.

to V_{st}, while the remaining contributions to V_{int}, namely V_{ex}, V_{cp} and electronic part of V_{st}, are sufficiently accurate with $L \leq 40$.

The numerical integration in the framework of the Volterra method (Rescigno & Orel 1981, Čurík et al. 2000) was done on a discrete radial mesh using composite Simpson's rule with adaptive step size and additional stabilization described for example by Rescigno & Orel (1982) or Morrison et al. (1977). As a practical convergence criterion we have used the eigenphase sums of the various $\mathcal{K}-$matrix Λ-blocks. It has turned out that a radial propagation distance of approx. 400 - 600 a.u. is sufficient to ensure convergence of all the presented quantities below 0.1% for the energy range of 10 - 300 meV. We found this simple approach to the propagation robust and stable and thus we have not incorporated additional tweaks such as Born r- or Λ-completion (Sun et al. 1995).

Figure 3 shows various *ab initio* $\mathcal{K}-$matrix elements compared to the results of other authors (Morrison et al. 1997). Values for the total σ_T and backward σ_B cross-section are depicted in Figure 4. The integral scattering is well reproduced but the method fails to obtain the backward data below 300 meV and gives no hint of the anomalous behaviour below 100 meV. Also shown are results reported by Telega & Gianturco (2006). In passing we note that the present *ab initio* theory reproduces experimental values of rotationally inelastic J=0 to 2 cross-sections with high precision (Morrison et al. 1997, Itikawa & Mason 2005, Telega et al. 2004) as displayed in Figure 5.

4. Connection to the experiment

The goal of this section is to create a simple analytic model for explanation of the anomalous behaviour of the R-ratio visible in the inset of Figure 2. In order to restrict our number of parameters we use our *ab initio* calculations as a guide to tell us what

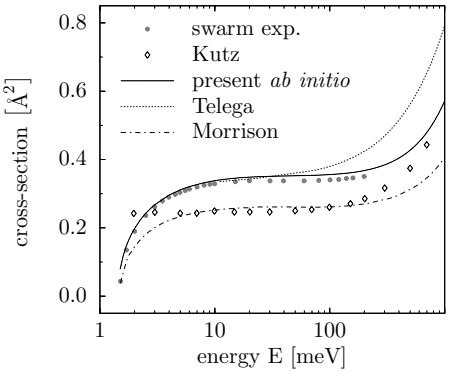

Figure 5. *Ab initio* prediction of $0 \rightarrow 2$ rotational cross-section compared with swarm experiment (Itikawa & Mason 2005) (full circles), Morrison et al.'s (1997) results (dash-dot line), computations by Telega et al. (2004) (dotted line) and Kutz & Meyer (1995) (open diamonds).

are the important partial wave contributions. A significant result stemming from the previous section is that at energies up to 250 meV contributions from waves of $l > 1$ are insignificant. Thus d-waves can be excluded from the analysis with impunity up to ~ 250 meV, greatly reducing the problem of uniqueness in the subsequent fitting procedure involving partial wave phase shifts. We therefore express the integral and backward cross-sections in terms of s- and p- wave phase shifts only. Tangents of phase shifts, which are the elements of the $\mathcal{K}-$matrix, are denoted by Σ_g for the s-wave and Σ_u and Π_u for the p-waves.

It follows that a truncated representation of the K-matrix describing the collisional event takes the form:

$$K = \begin{array}{c} \begin{matrix} \Lambda=0 & \\ \end{matrix} \\ \left(\begin{array}{cc|c} \Sigma_g & 0 & \\ 0 & \Sigma_u & \\ \hline & & \Pi_u \end{array} \right) \\ \begin{matrix} & |\Lambda|=1 \end{matrix} \end{array} \tag{16}$$

Cross-sections and scattering amplitudes are then obtained by an inversion $T = 2K(i+K)^{-1}$, where the T-matrix is essentially the matrix of scattering amplitudes. In our numerical implementation full inversion is used; however the phase shifts here are small and for didactic purposes one may write, to first order in K, that $T = -2iK$. The integral cross-section and the cross-section for scattering into the backward hemisphere, which include rotationally inelastic events through off diagonal terms not shown in the

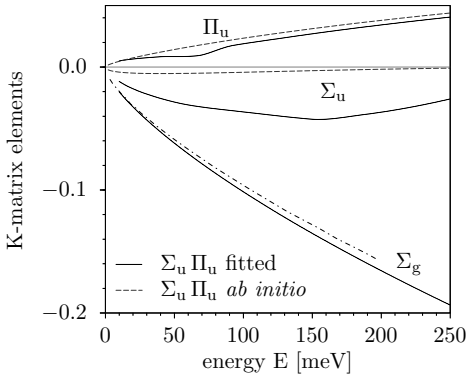

Figure 6. Tangents of the phase shifts (K-matrix elements - see (16)) used to create the fits to integral and backward scattering data (dotted lines in Figure 4). Values of Σ_g were taken from the *ab initio* calculations, Σ_u and Π_u were obtained by fitting to the experiment. Dash-dot line shows the results for Σ_g of Morrison et al. (1997)

truncated matrix in (16), result in the simple formulae:

$$\sigma_{\rm tot} = \frac{4\pi}{k^2}\left(\Sigma_{\rm g}^2 + \Sigma_{\rm u}^2 + 2\Pi_{\rm u}^2\right) \qquad (17a)$$

$$\sigma_{\rm back} = \frac{1}{2}\sigma_{\rm tot} - \frac{2\pi}{k^2}\Sigma_{\rm g}\left(\Sigma_{\rm u} + 2\Pi_{\rm u}\right) \qquad (17b)$$

where k represents the momentum of the incident electron. Note that in the full representation there occur terms in the backward hemisphere scattering cross-section which multiply Σ_u, Π_u and Σ_g phase shifts, illustrating that interference between these waves is somewhat more complex than (17*b*) suggests. Note that terms which generate rotationally inelastic events result in backward-forward symmetric scattering and do not influence our subsequent discussion.

Equation (17*b*) is the crux of the explanation for the anomalous behaviour of the ratio, R, of backward and integral cross-sections shown in Figure 2. The second term in (17*b*) generates a departure from backward-forward equality, that is, $R \neq 0.5$. Our explanation for the variation of R with electron energy is that at energies < 95 meV, the values of Σ_u and Π_u are such as to depress the value of R below 0.5. At 95 meV the terms Σ_u and $2\Pi_u$ become exactly equal and opposite in value, whereby they cancel to zero in (17*b*) giving $R = 0.5$. Thus R starts at 0.5 at zero energy, where $\Sigma_u + 2\Pi_u$ equals zero (see below), and returns to 0.5 once more at 95 meV, reflecting the experimental values of R shown in the inset to Figure 2. The effects of p-wave interference are especially apparent in N_2 since the Σ_g phase shift is small, reflected in the small integral scattering cross-section. The p-waves are therefore able to influence the angular scattering at rather low energy since their values, while considerably less than that of Σ_g, become non-negligible at energies as low as tens of meV.

Our analysis also allows us to determine empirical values of Σ_u and Π_u phase shifts

as follows. A comparison of the spherical component Σ_g calculated using our *ab initio* model with results of Morrison et al. (1997) is shown in Figure 3. Since we see good agreement, we proceed by assuming that the s-wave phase-shift is well described by our *ab initio* model and fix the values of this phase shift to those shown in Figure 3. The phase shifts Σ_u and Π_u then can be determined uniquely by the two sets of experimental data for integral and backward-hemisphere cross sections displayed in Figures 2 and 4. Resulting tangents of phase shifts which create the exact fit to experimental data, shown in Figure 4, are given in Figure 6. It is clear that experimentally determined value of the Π_u phase shift is close to the calculated one. However, the calculated Σ_u phase shift is very small in comparison to the value extracted from the present experiment. This is not surprising, since the experiment requires $\Sigma_u = -2\Pi_u$ at 95 meV. It is necessary to emphasize here that this single discrepancy (shown in Figure 6) between Σ_u determined from experimental data and calculated above is sufficient to explain the difference between calculated and measured backward cross sections displayed in Figure 4. The discrepancy may be attributed to the quality of the local exchange potential V_{ex} used in the computational model (1) since this contribution brings the largest uncertainity to our calculated results.

In the remaining part of this section we first comment on very low-energy (< 20 meV) behaviour of the phase shifts. We include these remarks for the sake of completness as they do not impact our discussion at higher energies. Then we continue with a simplified and pictorial explanation of the p-wave cancelation that occurs at 95 meV.

Returning to the near zero energy regime, the first term in (17*a*), involving Σ_g^2, corresponds to pure s-wave scattering of particles in the zero collision energy limit. In the case of quadrupole interactions, it may be shown analytically that the following limits hold for the Σ_u and Π_u phase shifts:

$$\Sigma_u \xrightarrow{k\to 0} +\frac{Q}{5}k + \mathcal{O}\big(k^2\big) \ , \tag{18a}$$

$$\Pi_u \xrightarrow{k\to 0} -\frac{Q}{10}k + \mathcal{O}\big(k^2\big) \ . \tag{18b}$$

The behaviour in (18*a*) differs from the Wigner threshold law which requires that the phase shift is proportional to k^{2l+1} for short-range interaction. This discrepancy arises from the long-range nature of the quadrupole field, as described in modified effective range theory (Fabrikant 1984, Isaacs & Morrison 1992). However, as $k \to 0$, the Σ_u and Π_u phase shifts both fall to zero and tend to cancel in the second term of (17*b*). Thus p-wave phase shifts are well-behaved at very low energy and tend to the analytical form shown in (18*a*). Note in this connection that (18*a*) contains only first order terms in MERT and therefore is restricted to energies very close to zero.

The physical explanation for interference within the p-manifold is as follows. The distribution of charge around the N_2 molecule is such as to concentrate electrons at each end of the species while between the atoms there is a relative depletion of electron density. This is shown in Figure 7. If we now superpose the Σ_u and Π_u waves on

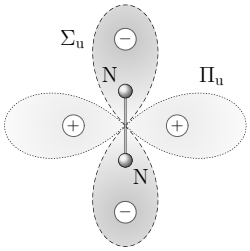

Figure 7. Interaction of the quadrupole field of N_2 with $l = 1$ waves. The quadrupole of the molecule is illustrated by charges displayed in circles. Orientation of the Σ_u and Π_u components show that the waves experience asymptotically different signs for the quadrupole interaction.

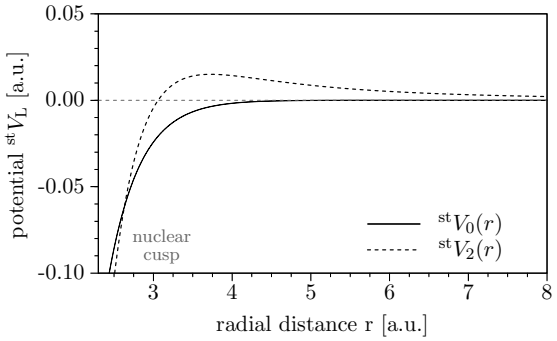

Figure 8. Radial dependence of the $L = 0$ and $L = 2$ components of the static potential V_{st} as defined by the expansion (5). Both Σ_u and Π_u waves are subject to the same centrifugal barrier, nevertheless the sign of the quadrupole interaction differs as explained in the text.

this charge distribution, we see that the Π_u wave interrogates the positive region of the quadrupole and the Σ_u the negative region. Thus in (2), the Σ_u wave sees the quadrupole potential as a repulsion and the Π_u wave sees it as an attraction. For both waves there are equal centrifugal barriers, but for that part of the wave that penetrates into the central region, the Σ_u wave sees the quadrupole as presenting a barrier of maximum height 0.015 au (325 meV) whereas the Π_u wave sees a similar attraction. This behavior can be more formally justified by noting the different sign of the angular prefactor in the potential expansion (6) for Σ_u as compared to Π_u. The barrier quoted is displayed in Figure 8. Its value is derived from our *ab initio* results which show a maximum at ~ 3.7 au, noting that our *ab initio* theory gives a very accurate description of the static potential in (2). On the basis of this description, the Σ_u wave is repelled from the central part of the molecule which by convention gives rise to a negative phase shift,

increasing in absolute magnitude with increasing energy, and the Π_u wave is attracted, which gives rise to a positive phase shift, as shown in Figure 6. The two phases therefore act in opposition and, as our experimental data show, cancel in their effect at 95 meV.

5. Conclusions

We have identified a new form of interference involving interference within the p-manifold of p_z and $p_{x,y}$ waves, which arises from the presence of a quadrupole on the target. This is a general phenomenon but will have readily detectable consequences only if the s-wave interaction is not strongly dominant. Thus it would be difficult to observe in electron scattering in CO_2, with a strong virtual state effect (Field, Jones, Lunt & Ziesel 2001), but could be found for example in H_2 and O_2. The phenomenon could also prove observable in cold ion-molecule scattering with quadrupolar targets.

We have also found that the *ab initio* potential used, sophisticated and adequate as it is in other respects, is unable to describe the necessary Σ_u and Π_u phase shifts. The only means of reproducing this phenomenon is through fitting to the experimental data to obtain the phase shifts. This underlines the general problem in obtaining reliable phase shifts at very low energy, a difficulty well-known in the theoretical determination of scattering lengths.

Acknowledgments

DF would like to acknowledge support by the Danish National Research Foundation through the research centre ACAP (Aarhus Centre for Atomic Physics) and support from the Danish Natural Science Research Council (FNU). NCJ would like to thank the EU EPIC Network for a post-doctoral position during the course of some of this work. We should also like to thank the Directors and Staff at the Institute for Storage Ring Facilities at Aarhus (ISA). MŠ and RČ acknowledge the support of the Czech Ministry of Education (grant OC10046), the Academy of Sciences of the Czech Republic (grant KJB400400803), the Grant Agency of the Czech Republic (grants 202/08/0631, P208/11/0452), the COST Actions CM0601 and CM0805, the Charles University Grant Agency (grant 113210) and the Charles University grant SVV-263301.

References

Boardman A D, Hill A D & Sampanthar S 1967 *Phys. Rev.* **160**(3), 472–475.
Brunger M J & Buckman S J 2002 *Phys. Rep.* **357**(3-5), 215–458.
Fabrikant I I 1984 *J. Phys. B* **17**(20), 4223.
Fano U & Dill D 1972 *Phys. Rev. A* **6**(1), 185–192.
Field D, Jones N C, Lunt S L & Ziesel J P 2001 *Phys. Rev. A* **64**(2), 022708.
Field D, Lunt S L & Ziesel J P 2001 *Acc. Chem. Res.* **34**(4), 291–298.
Field D & Madsen L B 2003 *J. Chem. Phys.* **118**(4), 1679–1683.
Hoffmann S V, Lunt S L, Jones N C, Field D & Ziesel J P 2002 *Rev. Sci. Instr.* **73**(12), 4157–4163.

IOP Publishing Journal of Physics B: Atomic, Molecular and Optical Physics

J. Phys. B: At. Mol. Opt. Phys. **43** (2010) 175205 (8pp) doi:10.1088/0953-4075/43/17/175205

Towards efficient *ab initio* calculations of electron scattering by polyatomic molecules: III. Modelling correlation–polarization interactions

R Čurík and M Šulc

J Heyrovský Institute of Physical Chemistry, Academy of Sciences of the Czech Republic, 18223 Prague 8, Czech Republic

E-mail: roman.curik@jh-inst.cas.cz

Received 11 June 2010, in final form 26 July 2010
Published 23 August 2010
Online at stacks.iop.org/JPhysB/43/175205

Abstract

We explore an implementation of correlation–polarization interactions for electron scattering by polyatomic molecules. The short-range correlation is approximated by local and nonlocal density functional theory (DFT) models commonly used in quantum chemistry and solid-state physics. The long-range polarization is represented by general full tensor components. Furthermore, we propose a robust and stable technique to calculate momentum-space matrix elements of such a composite potential. The quality of several selected DFT potentials is tested by elastic scattering calculations for a class of small hydrocarbon molecules represented by propane and cyclopropane.

1. Introduction

Modification of the static-exchange potential (outlined in the following section) by a local form of interaction accounting for correlation and even polarization of the target's bound orbitals is not a new idea. The first models used the long-range asymptotic form $V_p = -\alpha_0/2r^4$ with a short-range cutoff function in order to remove the singular behaviour at the origin (Morrison and Collins 1978). A single parameter of this model, the cutoff radius, was then determined by adjusting the calculated cross sections to some well-established feature of the results. For modelling the short-range correlation between the scattered electron and the target electron density, use of the density functional theory (DFT) was proposed (O'Connell and Lane 1983, Padial and Norcross 1984). They employed a local spin density (LSD) approximation emerging from the field of solid-state physics (Vosko *et al* 1980, Perdew and Zunger 1981, both later refined by Perdew and Wang (1992)). All these forms of the LSD correlation are based on Green's function Monte Carlo simulation for electrons in a finite volume, subject to periodic boundary conditions. The correlation energy per electron was then extrapolated to infinite volume (Caperley and Alder 1980). The practical accuracy of all these LSD approximations is similar and they are a core component of all modern DFT functionals used in quantum chemistry. They are often referred to as LDA (local density approximation) in the literature of electron–molecule collisions.

A further way to improve LSD approximation came in the form of a generalized gradient approximation (GGA) by Perdew *et al* (1992) (the functional is referred to in the literature as PW91). A different way to incorporate the density gradient corrections was used by Lee *et al* (1988), who turned the correlation-energy formula of Colle and Salvetti (1975) into a DFT functional form by the use of the first and second gradients of electron density (LYP functional).

Development of DFT correlation functionals was accompanied by a simultaneous development of the exchange functionals. Although a Hartree–Fock exchange energy, in principle exact, is computationally cheap, most of the successful exchange-correlation functionals (PBE0, B3LYP, etc) contain a weighted mixture of the Hartree–Fock exchange and gradient-corrected exchange functionals. For example, PBE0 contains 75% of exchange functional constructed by Perdew *et al* (1996). Another highly accurate, gradient-corrected functional is from Becke (1988), which takes 80% of the exchange energy present in the B3LYP exchange-

correlation functional. Both exchange-correlation functionals have been successfully applied to a vast number of molecular systems during the last decade.

We feel that despite the intense development of DFT in solid-state physics and bound-state quantum chemistry, its adaptation for modelling the electron–molecule collisions has been rather slow. One reason may be lack of Hohenberg–Kohn theorem for a continuum $(N+1)$-electron state describing the scattering event. Therefore, many authors employed the DFT correlation potential generated by a closed-shell ground-state density of the target with the density of the continuum orbital excluded. Even with such a minor conceptual discrepancy the addition of a simple LDA correlation potential resulted in calculated cross section being in better agreement with experimental data (among many examples we chose Gianturco and Rodriguez-Ruiz 1993, Čurík and Gianturco 2002a, Telega *et al* 2004, Tonzani and Greene 2005).

Motivated by the success of the LDA exchange and correlation functionals in the electron–molecule computational modelling, here we explore the possibility of their implementation in a framework of discrete momentum representation (DMR) method. Previously Čurík *et al* (2008) employed LDA correlation in the DMR method for calculations of vibrationally inelastic collisions of electrons with methane molecules. The spherically symmetric case is extended in section 3 to a general asymptotic polarization represented by a polarizability tensor. For the short-range parts of the correlation interaction we make use of several DFT functionals commonly used in quantum chemistry. Their quality is assessed in section 4 for propane and cyclopropane molecules.

2. Optical potential

The DMR method belongs to the class of one-electron methods that make use of an optical potential. The method calculates elastic body-frame scattering amplitudes by solving the one-electron Lippmann–Schwinger equation (Polášek *et al* 2000, Čurík and Čársky 2003)

$$\langle \boldsymbol{k}_o|T|\boldsymbol{k}_i\rangle = \langle \boldsymbol{k}_o|V|\boldsymbol{k}_i\rangle + \int \mathrm{d}^3\boldsymbol{k}\frac{\langle \boldsymbol{k}_o|V|\boldsymbol{k}\rangle\langle \boldsymbol{k}|T|\boldsymbol{k}_i\rangle}{k_0^2-k^2+\mathrm{i}\varepsilon}, \quad (1)$$

where $\boldsymbol{k}_i$ and $\boldsymbol{k}_o$ are the momenta of the incoming and outgoing electrons, respectively. Optical potential describing an interaction between the scattered electron and the target molecule is denoted by V. The collision energy E is defined as $E = k_0^2/2$. After some careful treatment of the singular kernel in the above equation one can discretize the integral on the rhs of (1) as shown in greater detail in part I of this series (Čársky 2010a). This technique leads to a set of a linear algebraic equations that can be solved by a matrix inversion (Čurík and Čársky 2003). The optical potential used in the DMR method has been recently extended and now it contains static, exchange and correlation–polarization contributions (Čurík *et al* 2008)

$$V = V_s + V_x + V_{\mathrm{cp}}. \quad (2)$$

The static V_s contribution to the optical potential (2) is obtained from a set of N doubly occupied Hartree–Fock orbitals $\varphi_i(\boldsymbol{r})$ of the closed-shell target as

$$\langle \boldsymbol{r}|V_s|f\rangle = 2\sum_i^N \int \mathrm{d}^3\boldsymbol{r}'\frac{|\varphi_i(\boldsymbol{r}')|^2}{|\boldsymbol{r}-\boldsymbol{r}'|}f(\boldsymbol{r}) - \sum_j \frac{Z_j}{|\boldsymbol{r}-\boldsymbol{R}_j|}f(\boldsymbol{r}). \quad (3)$$

The first term in this equation describes a repulsion with the electronic charge density, while the second term corresponds to an attraction to the molecular nuclei positioned at $\boldsymbol{R}_j$. Similarly, action of the exchange interaction on the continuum function f can be written as

$$\langle \boldsymbol{r}|V_x|f\rangle = -\sum_i^N \int \mathrm{d}^3\boldsymbol{r}'\frac{\varphi_i(\boldsymbol{r}')f(\boldsymbol{r}')}{|\boldsymbol{r}-\boldsymbol{r}'|}\varphi_i(\boldsymbol{r}). \quad (4)$$

The sum $V_s + V_x$ is *an exact static-exchange* approximation in the literature of electron–molecule collisions and it has been employed by many authors to successfully describe the interaction of continuum electron with a target molecular system. For extensive reviews see Huo and Gianturco (1995), p 79, Lane (1980), p 47.

As can be seen from equation (1) the DMR method requires momentum-space representation of the optical potential. The local parts V_s and V_{cp} are then obtained by FT integrals, while the nonlocal exchange contribution is more computationally demanding. Its efficient implementation via interpolation of complex Shavitt functions is described in part II of this series (Čársky 2010b).

3. Correlation and polarization interaction

The short-range correlation potential is obtained by the DFT models mentioned in section 1. We have chosen to examine three correlation functionals that are widely used and known in quantum chemistry calculations. The first is the LDA correlation potential of Perdew and Wang (1992), although the alternative choices due to Vosko *et al* (1980) or Perdew and Zunger (1981) lead to the same results. Gradient corrections to this potential are then applied with the GGA potential of Perdew *et al* (1992) (PW91 potential) and independently we also employ the gradient corrections of Lee *et al* (1988) (LYP functional).

It is appropriate to address the confusing vocabulary used in two different fields of quantum calculations. In the literature of solid-state physics and quantum chemistry the gradient corrected functionals are referred to as nonlocal as they gather information of the electron density surrounding a point of interest. It is achieved via terms with first and second gradients of the electron density that enter the functional. However, from the strict point of view of quantum mechanics, the corresponding potentials are local as they simply multiply the wavefunction in the Schrödinger equation.

All the three correlation potentials that we explore decrease exponentially outside the molecule following the exponential decay of the bound electron density. This defect

in DFT was noted a long time ago (Umrigar and Gonze 1994, Almbladh and von Barth 1985). Such an incorrect long-range behaviour of the DFT potentials causes many problems in the description of induced moments of delocalized charge densities. Accordingly, special treatment has been undertaken in calculations of charge transfers (Dreuw and Head-Gordon 2004) or dispersion forces (Antony and Grimme 2006, Zhao and Truhlar 2007). Rigourously, the long-range correlation potential should be taken as (Almbladh and von Barth 1985, Umrigar and Gonze 1994)

$$V_p(\boldsymbol{r}) = -\frac{1}{2r^6}\sum_{i,j}^{3}\alpha_{ij}x_i x_j, \tag{5}$$

where the symmetric 3×3 matrix α_{ij} is a polarizability tensor and $r^2 = x_1^2 + x_2^2 + x_3^2$. Therefore, guided by the previous works of Padial and Norcross (1984) or Telega *et al* (2004), we connect the correct long-range term V_p of the correlation interaction (5) with the short-range term V_c described by one of the DFT correlation potentials. Since our technique of such a connection differs from the above-mentioned procedures, we describe it in more detail.

A smooth connection of a general and anisotropic asymptotic form (5) to a short-range anisotropic potential is not uniquely defined. Telega *et al* (2004) suggest finding a crossing point r_c of a spherically symmetric component of the long- and short-range parts. Of course r_c is not a proper crossing point of the higher partial-wave components. Overall smoothness is then achieved by adding the higher order-induced multipoles leading to a modification of the asymptotic form (5) where faster decaying terms are added. In our approach we prefer to keep the asymptotic form (5) and perform the smooth connection for each of the partial waves that come into play. As the first step, we expand the general tensor form (5) into partial waves

$$V_p(\boldsymbol{r}) = \sum_{l=0}^{2}\sum_{m=-l}^{l} v_l^m(r)S_l^m(\hat{\boldsymbol{r}}), \tag{6}$$

where $S_l^m(\hat{\boldsymbol{r}})$ are the normalized real spherical harmonics:

$$S_l^m(\vartheta,\varphi) = \left[\frac{2l+1}{2\pi(1+\delta_{0m})}\frac{(l-m)!}{(l+m)!}\right]^{\frac{1}{2}} \times P_l^m(\cos\vartheta)\begin{cases}\cos m\varphi, & m \geqslant 0\\ \sin m\varphi, & m < 0.\end{cases} \tag{7}$$

The radial functions $v_l^m(r)$ of equation (6) can be obtained analytically as

$$v_l^m(r) = -\frac{\alpha_l^m}{2r^4}, \tag{8}$$

where α_l^m are the irreducible components of the Cartesian tensor of rank 2 (Weissbluth 1978, p 174)

$$\begin{aligned}
\alpha_0^0 &= \frac{\sqrt{4\pi}}{3}(\alpha_{xx}+\alpha_{yy}+\alpha_{xx})\\
\alpha_1^0 &= \alpha_1^1 = \alpha_1^{-1} = 0\\
\alpha_2^0 &= \sqrt{\frac{4\pi}{5}}\left(\alpha_{zz} - \frac{\alpha_{xx}+\alpha_{yy}+\alpha_{xx}}{3}\right)\\
\alpha_2^1 &= -2\sqrt{\frac{4\pi}{15}}\,\alpha_{xz}\\
\alpha_2^{-1} &= -2\sqrt{\frac{4\pi}{15}}\,\alpha_{yz}\\
\alpha_2^2 &= 2\sqrt{\frac{4\pi}{15}}\,\frac{\alpha_{xx}-\alpha_{yy}}{2}\\
\alpha_2^{-2} &= 2\sqrt{\frac{4\pi}{15}}\,\alpha_{xy}.
\end{aligned} \tag{9}$$

For the short-range part V_c we separate the interaction into two orthogonal angular subspaces:

$$V_c(\boldsymbol{r}) = \sum_{l=0}^{2}\sum_{m=-l}^{l} w_l^m(r)S_l^m(\hat{\boldsymbol{r}}) + W_0(\boldsymbol{r}). \tag{10}$$

All the terms on the left- and right-hand sides of equation (10) decay exponentially. Because the DFT form of the short-range correlation potential $V_c(\boldsymbol{r})$ is numerical the radial functions $w_l^m(r)$ are obtained by a numerical angular projection. It follows that $W_0(\boldsymbol{r})$ contains only partial components with $l > 2$.

Having both (short- and long-range) interactions split into the partial waves the connection procedure is readily available. We connect each partial wave of $v_l^m(r)$ and $w_l^m(r)$ independently up to $l = 2$ forming six crossing points R_l^m. Three short-range functions $w_l^m(r)$ with $l = 1$ decay exponentially as they do not have the long-range counterparts $v_l^m(r)$ to connect to. It is a consequence of a symmetry of the polarizability tensor. Therefore, we can define the connected radial functions as

$$u_l^m(r) = \begin{cases} w_l^m(r) & \text{for} \quad r < R_l^m\\ v_l^m(r) & \text{for} \quad r \geqslant R_l^m.\end{cases} \tag{11}$$

The total correlation–polarization potential V_{cp} is then evaluated by the following formula:

$$V_{\mathrm{cp}}(\boldsymbol{r}) = \sum_{l=0}^{2}\sum_{m=-l}^{l} u_l^m(r)S_l^m(\hat{\boldsymbol{r}}) + W_0(\boldsymbol{r}). \tag{12}$$

The above procedure exploited the simple fact that the asymptotic polarization potential V_p is fully contained in the angular space defined by $l = 0$ and $l = 2$. Hence, we made sure that the connection between the short- and long-range parts is smooth in every partial component up to $l = 2$. All the higher components of the resulting potential V_{cp} then decay exponentially.

The final step needed to obtain the momentum-space matrix elements entering the Lippmann–Schwinger equation (1) is a Fourier transform (FT) integral

$$\langle \boldsymbol{k}_1|V_{\mathrm{cp}}|\boldsymbol{k}_2\rangle = \frac{1}{(2\pi)^3}\int \mathrm{d}^3\boldsymbol{r}\; V_{\mathrm{cp}}(\boldsymbol{r})\,\mathrm{e}^{\mathrm{i}(\boldsymbol{k}_2-\boldsymbol{k}_1).\boldsymbol{r}}. \tag{13}$$

The integral in the above equation is typically solved by a discrete fast Fourier transform (FFT) method. This is achieved

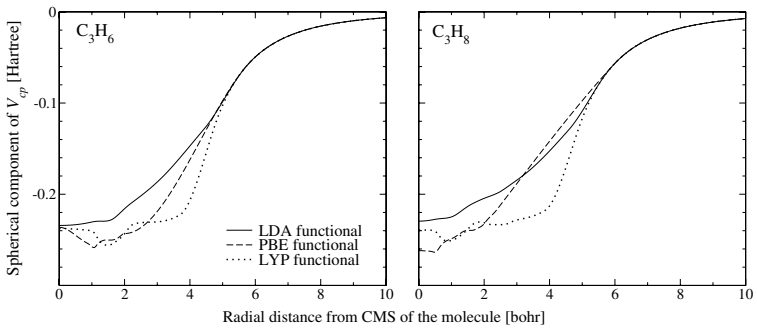

Figure 1. Visual comparison of different correlation functionals used in the present study. For simplicity only the dominant spherical components $u_0^0(r)$ of equations (11) and (12) are displayed. The left panel shows the data for the cyclopropane molecule, and the right panel for the propane molecule.

by bounding the integral in a three-dimensional rectangular volume and by evaluating the argument on a three-dimensional rectangular grid. In our implementation we used a cubic volume. We observed that a cube size of several hundred bohrs is needed in order to achieve a sufficient accuracy of the resulting integrals for the small $\boldsymbol{k}_2 - \boldsymbol{k}_1$ vectors. The cause of the slow size convergence is the long-range nature (5) of the $V_{\rm cp}$ potential. However, with such a large integration volume it becomes difficult to sample the potential with a sufficient density in the area of the molecule, where $V_{\rm cp}$ changes rapidly.

In order to solve this dilemma we subtract and add a well-behaved analytical function that cancels the $V_{\rm cp}$ potential at the long range. We also require this function to have an analytical FT form:

$$V_{\rm cp} = \underbrace{\left[V_{\rm cp} + \frac{1}{2(r^6+a^6)} \sum_{i,j}^{3} \alpha_{ij} x_i x_j \right]}_{\text{numerical FT}\, V_{\rm cp}^n} - \underbrace{\frac{1}{2(r^6+a^6)} \sum_{i,j}^{3} \alpha_{ij} x_i x_j}_{\text{analytical FT}\, V_{\rm cp}^a}. \tag{14}$$

The parameter a is chosen to be sufficiently small in order to achieve the long-range cancellation in the $V_{\rm cp}^n$ term. However, if the cutoff a is chosen too small it may produce a rapidly changing behaviour at the origin. To compromise we have found the procedure very robust and accurate for a being anywhere between 5% and 15% of the FFT cube size. Evaluation of the FT integral for the $V_{\rm cp}^a$ term is described in the appendix. Here we present only the final results:

$$\frac{1}{(2\pi)^3} \sum_{i,j}^{3} \alpha_{ij} \int {\rm d}^3\boldsymbol{r}\ {\rm e}^{{\rm i}\boldsymbol{k}.\boldsymbol{r}}\ \frac{x_i x_j}{2(r^6+a^6)} = \frac{1}{(2\pi)^3} \sum_{ij}^{3} \alpha_{ij}\, G_{ij}(\boldsymbol{k}), \tag{15}$$

with

$$G_{ij}(\boldsymbol{k}) = \frac{F'(k)}{k}\delta_{ij} + \left[\frac{F''(k)}{k^2} - \frac{F'(k)}{k^3} \right] k_i k_j, \tag{16}$$

and

$$F(k) = -\frac{\pi^2}{3a^4 k} {\rm e}^{-ka/2} \left[{\rm e}^{-ka/2} + \sqrt{3} \sin\left(ka\frac{\sqrt{3}}{2} \right) - \cos\left(ka\frac{\sqrt{3}}{2} \right) \right]. \tag{17}$$

For practical implementation one also needs the limit at the origin

$$\lim_{k\to 0} G_{ij}(\boldsymbol{k}) = \frac{2\pi^2}{9a}. \tag{18}$$

4. Application to elastic scattering on small hydrocarbons

In order to test the current implementation of correlation–polarization forces within the DMR method we have selected two similar molecular systems, namely cyclopropane and propane molecules. Both molecules have been intensively studied experimentally (Allan 1994, Allan and Andric 1996, Szmytkowski and Kwitnewski 2002a, 2002b, Makochekanwa *et al* 2006, Boesten *et al* 1994, Tanaka *et al* 1999). While the number of theoretical calculations is thorough for the cyclopropane molecule (Winstead *et al* 1992, Beyer *et al* 1997, Čurík and Gianturco 2002a, 2002b, Makochekanwa *et al* 2006), to our knowledge there is only one SE calculation by Winstead *et al* (1991) for the propane molecule.

A visual comparison of the spherical components $u_0^0(r)$ defined by equation (11) is displayed in figure 1 for both studied polyatomic molecules. The general features of the correlation potentials are as expected. The cyclic C_3H_6 exhibits slightly stronger correlation in the core area of the molecule while the open ring of C_3H_8 allows stronger correlation in the low-density outskirt regions of the molecule resulting in a stronger asymptotic polarizability. As far as the differences among different functionals go, the LYP gradient correction to the LDA potential results in a stronger correlation especially on the peripheral low-density region. This feature is

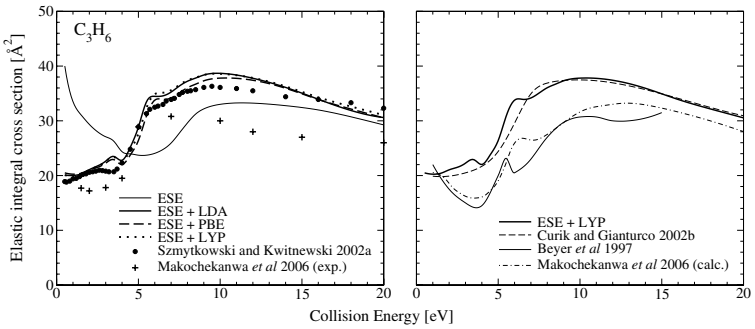

Figure 2. The elastic integral cross sections for electron scattering by cyclopropane molecules. The left panel compares results of various correlation models with available experimental data. The right panel shows the comparison of available calculations.

valid for both presented molecules and it extends even for more unpublished results of polyatomic molecules. On the other hand a behaviour for the PBE potential is not as predictable in the low-density region, as seen for C_3H_6 and C_3H_8 in figure 1. All the calculated correlation potentials smoothly connect to the asymptotic form (5). Polarizability tensor components used in the present calculations were obtained as linear response functions in Kohn–Sham DFT (Rinkevicius *et al* 2003) calculations with B3LYP hybrid functional and Sadlej's polarized VTZ basis sets (Sadlej 1988) as implemented in program Dalton Release 2.0 (2005). The body frame of the reference was chosen by principal axes; thus, the calculated polarizability tensors are diagonal:

$$\alpha(C_3H_6) = \begin{pmatrix} 38.8 & & \\ & 38.8 & \\ & & 33.8 \end{pmatrix},$$

$$\alpha(C_3H_8) = \begin{pmatrix} 38.0 & & \\ & 45.6 & \\ & & 40.2 \end{pmatrix}.$$

Both tensors compare favourably with experimental data for spherical polarizabilities $\alpha_0(C_3H_6) = 38.2$ au (Khristenko *et al* 1998) and $\alpha_0(C_3H_8) = 42.5$ au (Lide 1994).

Parameters for the numerical quadrature of the integral on the rhs of equation (1) are taken, for these two molecules, from table 1 in part I of this series (Čársky 2010a). Calculated fixed-nuclei integral cross sections for all the present correlation–polarization models applied to the cyclopropane molecule are displayed in figure 2. It is clear that the presence of the correlation–polarization interaction leads to some major changes in the magnitude and shape of the cross sections below 10 eV. Moreover, we found the differences among all the three correlation models fairly minor and therefore we chose the LYP model as their representative in the following discussion. The right panel of figure 2 shows a comparison of the available theoretical predictions for the elastic integral cross section. Our calculations are in very good agreement with the calculations of Čurík *et al* (2002a) as a result of very similar interaction models. Čurík and Gianturco (2002a) used a nonlocal separable approximation of the exchange part to be compared to the present exact exchange model. Previous work employed the LDA short-range functional smoothly connected to the spherical polarization potential; however, all the polarization tensor components are used in the present calculations. These small differences between the two models may explain the pronounced structure around 6 eV visible in the present results. The structure was identified by Čurík and Gianturco (2002b) and Allan and Andric (1996) as A_2' shape resonance leading to a selective vibrational excitation of C–C ring stretching mode. Fixed-nuclei calculations of Makochekanwa *et al* (2006) and Beyer *et al* (1997) predict a lower integral cross section than the SEP results discussed above. However, they both predict the presence of the A_2' shape resonance at 6.2 eV and 5.4 eV, respectively.

The elastic DCSs of electrons scattered by cyclopropane are displayed in figure 3. The agreement of the present ESE+LYP model with the experimental angular distributions is again very good at both collision energies: 5 eV (left panel) and 10 eV (right panel). In comparison to the experimental data at 10 eV, present calculations predict a slightly higher cross section at small and large scattering angles. This difference, especially at angles above 140°, may lead to a different experimental extrapolation of the DCS, consequently resulting in a smaller integral cross section visible in figure 2.

In order to make a full use of our tensor description of the asymptotic polarization, we selected a molecular system with a smaller symmetry yet of similar size to our second testing case: the propane molecule. Figure 4 summarizes the available experimental and theoretical data for elastic collisions of electrons with the propane molecules. The left panel compares our correlation models with the measurements of Szmytkowski and Kwitnewski (2002b), Tanaka *et al* (1999) and Boesten *et al* (1994). The experimental cross sections exhibit a strong maximum around 8 eV. Again the presence of the correlation-polarization forces in our model strongly affects the value of our calculated integral cross section below the collision energy of 12 eV. The difference among correlation models is more visible for this system, as seen in figure 1. The strongest correlation provided by the LYP functional shifts the peak in the integral cross section down to 8.5 eV while the PBE

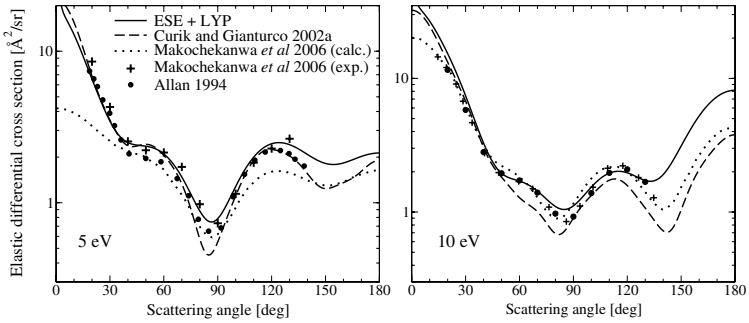

Figure 3. Elastic differential cross sections (DCSs) for electron scattering by cyclopropane molecules. The left panel shows data for the collision energy of 5 eV while the right panel for 10 eV. The data of Čurík and Gianturco (2002a) and Allan (1994) are shown on the left panel for the collision energy 5.5 eV.

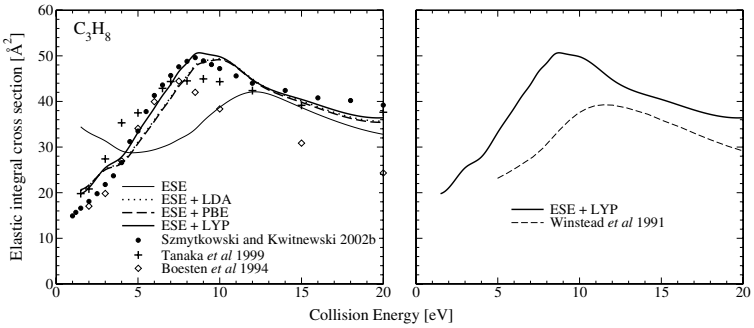

Figure 4. Elastic integral cross sections for electron scattering by propane molecules. The left panel compares results of various correlation models with available experimental data. The right panel shows present results with the LYP functional and the previous SE calculations of Winstead *et al* (1991).

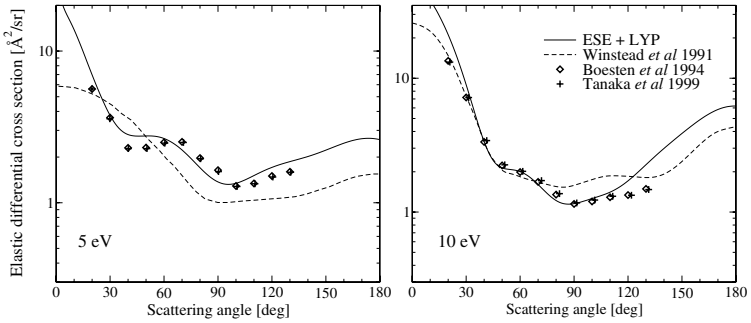

Figure 5. Elastic DCSs for electron scattering by propane molecules. We compare our LYP calculations (full curve) with experimental data of Boesten *et al* (1994) (diamonds) and Tanaka *et al* (1999) (crosses). The broken curve represents the SE calculations of Winstead *et al* (1991).

and LDA functionals point to 9.5 eV. The right panel of figure 4 also shows the SE calculations of Winstead *et al* (1991) that are similar to the present ESE results (the left panel of figure 4).

In order to complete our comparisons we likewise present the angular distributions for the propane molecule in figure 5. The agreement between our calculated results and the experimental data is very good for 5 eV (left panel) while

for 10 eV we observe behaviour similar to the case of the cyclopropane molecule. Our predicted DCSs are slightly higher for the small and large scattering angles resulting in larger integral cross section shown in figure 4.

5. Conclusions

The present study has several goals: first, to extend a previously published spherical polarization model in the DMR method (Čurik *et al* 2008) to a form of the general polarizability tensor; second, to implement and discuss several correlation potentials commonly used in the DFT community and codes (the LDA, PBE and LYP potentials) and third, to test the reliability of the constructed potentials on two simple hydrocarbon molecules, propane and cyclopropane.

Regarding the second and third objectives, the reliability of the potentials is gauged by their agreement with experimental data. In the case of the cyclopropane molecule, all three correlation models led to very similar results. Elastic integral cross sections presented in this paper agree very well with calculations by Čurík and Gianturco (2002b) and total cross-section measurements of Szmytkowski *et al* (2002). Experimental and theoretical integral cross sections of Makochekanwa *et al* (2006) are distinctly lower. However, in terms of angular distributions, the present calculations agree very well with the experimental data suggesting the difference between our integral cross sections and cross-beam integral cross sections might rest in the extrapolation of the cross-beam data to large scattering angles. Similar conclusions can be drawn in the case of the propane molecule with one distinct difference. The stronger LYP correlation model performs considerably better than the LDA and PBE correlation potentials.

In order to draw some general conclusions about the quality of the correlation models in the electron molecule collisions, many more molecular systems should be studied. Computationally, the presented implementation of correlation potentials is very efficient and can be applied to molecules larger than propane and cyclopropane. We hope to provide some data to this open issue in the near future using the methods and model presented in this paper.

Acknowledgments

It is our pleasure to thank Professor Baerends (Free University, Amsterdam) for encouraging discussions and useful suggestions. This work was supported by the Czech Ministry of Education (grants OC10046 and OC09079), the Academy of Sciences of the Czech Republic (grant KJB400400803) and the Grant Agency of the Czech Republic (grant 202/08/0631) and the COST Actions CM0601 (ECCL) and CM0805 (The Chemical Cosmos).

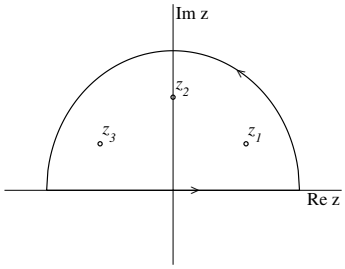

Figure A1. Contour integration path used in equation (A.3) together with the three residual points in the upper plane.

Appendix. Fourier transform of the full tensor asymptotic potential

The aim of the appendix is to evaluate the following FT integrals:

$$G_{ij}(k) = \int \mathrm{d}^3\boldsymbol{r}\, \mathrm{e}^{\mathrm{i}\boldsymbol{k}.\boldsymbol{r}}\, \frac{x_i x_j}{2(r^6 + a^6)}. \tag{A.1}$$

As a first step we define the FT $F(k)$ of the radial component of the potential. The angular part is then integrated out with the only radial integral remaining:

$$F(k) = -\int \mathrm{d}^3\boldsymbol{r}\, \mathrm{e}^{\mathrm{i}\boldsymbol{k}.\boldsymbol{r}}\, \frac{1}{2(r^6 + a^6)} = -\frac{2\pi}{k}\int_0^\infty \mathrm{d}r\, \frac{r \sin kr}{r^6 + a^6}. \tag{A.2}$$

The radial integral can be transformed to a contour integral in the complex plane as follows:

$$\int_0^\infty \mathrm{d}r\, \frac{r \sin kr}{r^6 + a^6} = \frac{1}{2}\int_{-\infty}^\infty \mathrm{d}r\, \frac{r \sin kr}{r^6 + a^6} = \frac{1}{2}\,\mathrm{Im}\int_C \mathrm{d}z\, \frac{z\mathrm{e}^{\mathrm{i}kz}}{z^6 + a^6}, \tag{A.3}$$

with the contour C shown in figure A1. There are three residual points in the upper complex plane that count for the residue theorem:

$$\begin{aligned} z_1 &= a\,\mathrm{e}^{\mathrm{i}\pi/6}, \\ z_2 &= \mathrm{i}a, \\ z_3 &= a\,\mathrm{e}^{\mathrm{i}5\pi/6}. \end{aligned} \tag{A.4}$$

By employing the residue theorem for the last integral in (A.3) we obtain the radial FT $F(k)$ defined in equation (A.2) as follows:

$$F(k) = -\frac{\pi^2}{3a^4 k}\mathrm{e}^{-ka/2}\left[\mathrm{e}^{-ka/2} + \sqrt{3}\sin\left(ka\frac{\sqrt{3}}{2}\right) - \cos\left(ka\frac{\sqrt{3}}{2}\right)\right]. \tag{A.5}$$

By comparing equations (A.1) and (A.2), one can easily see that the general tensor components $G_{ij}(\boldsymbol{k})$ may be obtained by the partial derivatives of the radial function $F(k)$:

$$G_{ij}(\boldsymbol{k}) = \frac{\partial^2}{\partial k_i \partial k_j} F(k). \tag{A.6}$$

The second-order partial derivatives directly lead to equation (16).

References

Allan M and Andric L 1996 *J. Chem. Phys.* **105** 3559
Allan M 1994 *Electron Collisions with Molecules, Clusters and Surfaces* ed H Ehrhardt and L A Morgan (New York: Plenum)
Almbladh C O and von Barth U 1985 *Phys. Rev.* B **31** 3231
Antony J and Grimme S 2006 *Phys. Chem. Chem. Phys.* **8** 5287
Becke A D 1988 *Phys. Rev.* A **38** 3098
Beyer T, Nestmann B M, Sarpal B K and Peyerimhoff S D 1997 *J. Phys. B: At. Mol. Opt. Phys.* **30** 3431
Boesten L, Dillon M A, Tanaka H, Kimura M and Sato H 1994 *J. Phys. B: At. Mol. Opt. Phys.* **27** 1845
Caperley D M and Alder B J 1980 *Phys. Rev. Lett.* **45** 566
Čársky P 2010a *J. Phys. B: At. Mol. Opt. Phys.* Part I **43** 175203
Čársky P 2010b *J. Phys. B: At. Mol. Opt. Phys.* Part II **43** 175204
Colle R and Salvetti D 1975 *Theor. Chim. Acta* **37** 329
Čurík R and Gianturco F A 2002a *J. Phys. B: At. Mol. Opt. Phys.* **35** 717
Čurík R and Gianturco F A 2002b *J. Phys. B: At. Mol. Opt. Phys.* **35** 1235
Čurík R and Čársky P 2003 *J. Phys. B: At. Mol. Opt. Phys.* **36** 2165
Čurík R, Čársky P and Allan M 2008 *J. Phys. B: At. Mol. Opt. Phys.* **41** 115203
Dreuw A and Head-Gordon M 2004 *J. Am. Chem. Soc.* **126** 4007
Gianturco F A and Rodriguez-Ruiz J A 1993 *Phys. Rev.* A **47** 1075
Huo W M and Gianturco F A 1995 *Computational Methods for Electron-Molecule Collisions* (New York: Plenum)
Khristenko S V, Maslov A I and Shevelko V 1998 *Molecules and Their Spectroscopic Properties* (Berlin: Springer)
Lane N F 1980 *Rev. Mod. Phys.* **52** 29
Lee C, Yang W and Parr R 1988 *Phys. Rev.* B **37** 785
Lide D R (ed) 1994 *CRC Handbook of Chemistry and Physics* (Boca Raton, FL: CRC Press)
Makochekanwa C, Kato H, Hoshino M, Tanaka H, Kubo H, Lopes A R, Lima M A P and Ferreira L G 2006 *J. Chem. Phys.* **124** 024323
Morrison M A and Collins L A 1978 *Phys. Rev.* A **17** 918
O'Connel J K and Lane N F 1983 *Phys. Rev.* A **27** 1893
Telega S, Bodo E and Gianturco F A 2004 *Eur. Phys. J.* D **29** 357
Tonzani S and Greene C H 2005 *J. Chem. Phys.* **112** 014111
Padial N T and Norcross D W 1984 *Phys. Rev.* A **29** 1742
Perdew J P, Chevary J A, Vosko S H, Koblar A J, Pederson M R, Singh D J and Fiolhais C 1992 *Phys. Rev.* B **46** 6671
Perdew J P and Wang Y 1992 *Phys. Rev.* B **45** 13244
Perdew J P and Zunger A 1981 *Phys. Rev.* B **23** 5048
Perdew J P, Burke K and Ernzerhof M 1996 *Phys. Rev. Lett.* **77** 3865
Polášek M, Juřek M, Ingr M, Čársky P and Horáček J 2000 *Phys. Rev.* A **61** 032701
Rinkevicius Z, Tunnel I, Salek P, Vahtras O and Hans A 2003 *J. Chem. Phys.* **119** 34
Sadlej J 1988 *Coll. Czech. Chem. Commun.* **53** 1995
Szmytkowski C and Kwitnewski S 2002a *J. Phys. B: At. Mol. Opt. Phys.* **35** 2613
Szmytkowski C and Kwitnewski S 2002b *J. Phys. B: At. Mol. Opt. Phys.* **35** 3781
Tanaka H, Tachibana Y, Kitajima M, Sueoka O, Takaki H, Hamada A and Kimura M 1999 *Phys. Rev.* A **59** 2006
Umrigar C J and Gonze X 1994 *Phys. Rev.* A **50** 3827
Vosko S H, Wilk L and Nusair M 1980 *Can. J. Phys.* **58** 1200
Weissbluth M 1978 *Atoms and Molecules* (New York: Academic)
Winstead C, Hipes P G, Lima M A P and McKoy V 1991 *J. Chem. Phys.* **94** 5455
Winstead C, Sun Q and McKoy V 1992 *J. Chem. Phys.* **96** 4246
Zhao Y and Truhlar D G 2007 *J. Chem. Theory Comput.* **3** 289

LIST OF FIGURES

LIST OF TABLES

BIBLIOGRAPHY

Abramov, D. I. and Komarov, I. V. (1972), 'Weakly bound states of a charged particle in a finite-dipole field', *Theor. Math. Phys.* **13**, 1090–1098.

Abramowitz, M. and Stegun, I. A., eds (1965), *Handbook of Mathematical Functions*, Dover Publications.

Alexander, M. H. and Manolopoulos, D. E. (1987), 'A stable linear reference potential algorithm for solution of the quantum close-coupled equations in molecular scattering theory', *J. Chem. Phys.* **86**(4), 2044–2050.

Alhaidari, A. D. and Bahlouli, H. (2008), 'Electron in the Field of a Molecule with an Electric Dipole Moment', *Phys. Rev. Lett.* **100**(11), 110401.

Allison, A. (1989), 'The numerical solution of the equations of molecular scattering', *Adv. At. Mol. Phys.* **25**, 323–341.

Almbladh, C.-O. and von Barth, U. (1985), 'Exact results for the charge and spin densities, exchange-correlation potentials, and density-functional eigenvalues', *Phys. Rev. B* **31**(6), 3231–3244.

Anastassi, Z. and Simos, T. (2009), 'Numerical multistep methods for the efficient solution of quantum mechanics and related problems', *Phys. Rep.* **482-483**, 1–240.

Arthurs, A. M. and Dalgarno, A. (1960), 'The Theory of Scattering by a Rigid Rotator', *Proc. Roy. Soc. London Sect. A* **256**(1287), 540–551.

Atkinson, D., Johnson, P. W., Mehta, N. and de Roo, M. (1973), 'Crichton's phase-shift ambiguity', *Nucl. Phys. B* **55**(1), 125–131.

Atkinson, D., Kok, L. P. and de Roo, M. (1978), 'Crichton ambiguities with infinitely many partial waves', *Phys. Rev. D* **17**(9), 2492–2502.

Aymar, M., Greene, C. H. and Luc-Koenig, E. (1996), 'Multichannel Rydberg spectroscopy of complex atoms', *Rev. Mod. Phys.* **68**(4), 1015–1123.

Bartlett, M. S. (1951), 'An Inverse Matrix Adjustment Arising in Discriminant Analysis', *Ann. Math. Statist.* **22**(1), 107–111.

Berends, F. A. and Ruijsenaars, S. N. M. (1973), 'Examples of phase-shift ambiguities for spinless elastic scattering', *Nucl. Phys. B* **56**(2), 507–524.

Berends, F. A. and Van Reisen, J. C. J. M. (1976), 'On the existence of phase-shift ambiguities in spinless elastic scattering', *Nucl. Phys. B* **115**(3), 505–508.

Biedenharn, L. C., Blatt, J. M. and Rose, M. E. (1952), 'Some Properties of the Racah and Associated Coefficients', *Rev. Mod. Phys.* **24**(4), 249–257.

Biermann, L. (1943), 'Die Oszillatorenstärken einiger Linien in den Spektren des Na I, K I und Mg II', *Z. Astrophys.* **22**, 157–164.

Blatt, J. M. (1967), 'Practical points concerning the solution of the Schrödinger equation', *J. Comput. Phys.* **1**(3), 382–396.

Blatt, J. M. and Biedenharn, L. C. (1952), 'The Angular Distribution of Scattering and Reaction Cross Sections', *Rev. Mod. Phys.* **24**(4), 258–272.

Bohr, A. and Mottelson, B. R. (1998), *Nuclear structure*, Vol. 1, World Scientific.

Bottcher, C. (1969), 'The formalism of electron-molecule scattering', *Chem. Phys. Lett.* **4**(5), 320–322.

Bottcher, C. (1970), 'The scattering of slow electrons by polar molecules', *Mol. Phys.* **19**, 193–198.

Bouferguene, A., Ema, I. and Weatherford, C. A. (1999), 'Nonadiabatic polarization potentials in electron- and positron-molecule scattering: Application to $e^- + H_2$', *Phys. Rev. A* **59**(4), 2712–2718.

Bouten, M. (1969), 'On the rotation operators in quantum mechanics', *Physica* **42**(4), 572–580.

Breig, E. L. and Lin, C. C. (1965), 'Vibrational Excitation of Diatomic Molecules by Electron Impact', *J. Chem. Phys.* **43**(11), 3839–3845.

Brink, D. and Satchler, G. (1994), *Angular momentum*, 3 edn, Oxford University Press.

Bunker, P. and Jensen, P. (2004), *Fundamentals of Molecular Symmetry*, 1 edn, Taylor & Francis.

Burgess, A., Hummer, D. G. and Tully, J. A. (1970), 'Electron Impact Excitation of Positive Ions', *Phil. Trans. R. Soc. A* **266**(1175), 225–279.

Burke, P. (1979), Theory of Low Energy Electron-Molecule Collisions, Vol. 15 of *Advances in Atomic and Molecular Physics*, Academic Press, pp. 471–506.

Burke, P. G. and Chandra, N. (1972), 'Electron-molecule interactions. III. A pseudopotential method for $e^- - N_2$ scattering', *J. Phys. B* **5**(9), 1696.

Burke, P. G., Hibbert, A. and Robb, W. D. (1971), 'Electron scattering by complex atoms', *J. Phys. B* **4**(2), 153.

Burke, P. G., Mackey, I. and Shimamura, I. (1977), 'R-matrix theory of electron-molecule scattering', *J. Phys. B* **10**(12), 2497.

Burke, P. G. and Tennyson, J. (2005), 'R-matrix theory of electron molecule scattering', *Mol. Phys.* **103**, 2537–2548.

Burke, P. and Robb, W. (1976), The R-Matrix Theory of Atomic Processes, Vol. 11 of *Adv. At. Mol. Phys.*, Academic Press, pp. 143–214.

Buttle, P. J. A. (1967), 'Solution of Coupled Equations by R-Matrix Techniques', *Phys. Rev.* **160**(4), 719–729.

Callaway, J., LaBahn, R. W., Pu, R. T. and Duxler, W. M. (1968), 'Extended Polarization Potential: Applications to Atomic Scattering', *Phys. Rev.* **168**(1), 12–21.

Calogero, F. (1967), *Variable phase approach to potential scattering*, Academic Press, New York.

Carlsten, J. L., Peterson, J. R. and Lineberger, W. C. (1976), 'Binding of an electron by the field of a molecular dipole – $LiCl^{-}$', *Chem. Phys. Lett.* **37**(1), 5–8.

Carr, W. J., Coldwell-Horsfall, R. A. and Fein, A. E. (1961), 'Anharmonic Contribution to the Energy of a Dilute Electron Gas – Interpolation for the Correlation Energy', *Phys. Rev.* **124**(3), 747–752.

Čársky, P. (2010*a*), 'Towards efficient *ab initio* calculations of electron scattering by polyatomic molecules: I. Efficient numerical quadrature of the UGT term', *J. Phys. B* **43**(17), 175203.

Čársky, P. (2010*b*), 'Towards efficient *ab initio* calculations of electron scattering by polyatomic molecules: II. Efficient evaluation of exchange integrals', *J. Phys. B* **43**(17), 175204.

Castillejo, L., Percival, I. C. and Seaton, M. J. (1960), 'On the Theory of Elastic Collisions Between Electrons and Hydrogen Atoms', *Proc. Roy. Soc. London Sect. A* **254**(1277), 259–272.

Ceperley, D. M. and Alder, B. J. (1980), 'Ground State of the Electron Gas by a Stochastic Method', *Phys. Rev. Lett.* **45**(7), 566–569.

CERNLIB (2006).
URL: *http://cernlib.web.cern.ch/cernlib/*

Chan, S.-K., Light, J. C. and Lin, J.-L. (1968), 'Inelastic Molecular Collisions: Exponential Solution of Coupled Equations for Vibration–Translation Energy Transfer', *J. Chem. Phys.* **49**(1), 86–97.

Chandra, N. (1975), 'On the relationship between the adiabatic-nuclei and the frame-transformation theories of e^{-} – molecule scattering', *J. Phys. B* **8**(11), 1953.

Chandra, N. (1977), 'Low-energy electron scattering from CO. II. *Ab initio* study using the frame-transformation theory', *Phys. Rev. A* **16**(1), 80.

Chang, E. S. and Fano, U. (1972), 'Theory of Electron-Molecule Collisions by Frame Transformations', *Phys. Rev. A* **6**(1), 173–185.

Chang, E. S. and Temkin, A. (1969), 'Rotational Excitation of Diatomic Molecules by Electron Impact', *Phys. Rev. Lett.* **23**(8), 399–403.

Chang, E. S. and Temkin, A. (1970), 'Rotational Excitation of Diatomic Molecular Systems. II. H_2^+', *J. Phys. Soc. Jap.* **29**(1), 172–179.

Chase, D. M. (1956), 'Adiabatic Approximation for Scattering Processes', *Phys. Rev.* **104**(3), 838–842.

Child, M. S. (2010), *Molecular Collision Theory*, Dover Publications.

Chin, S. A. (1997), 'Symplectic integrators from composite operator factorizations', *Phys. Lett. A* **226**(6), 344–348.

Clark, C. W. (1977), 'Electron scattering from diatomic polar molecules. I. The limitations of the Born approximation', *Phys. Rev. A* **16**(4), 1419–1422.

Clark, C. W. (1979), 'Electron scattering from diatomic polar molecules. II. Treatment by frame transformations', *Phys. Rev. A* **20**(5), 1875–1889.

Clark, C. W. (1984), 'Eigenphase sum in electron scattering by polar molecules', *Phys. Rev. A* **30**(2), 750–757.

Cohen, J. S. and Pack, R. T. (1974), 'Modified statistical method for intermolecular potentials. Combining rules for higher van der Waals coefficients', *J. Chem. Phys.* **61**(6), 2372–2382.

Colle, R. and Salvetti, O. (1975), 'Approximate calculation of the correlation energy for the closed shells', *Theor. Chem. Acc.* **37**, 329–334.

Collins, L. A. and Norcross, D. W. (1978), 'Electron collisions with highly polar molecules: Comparison of model, static, and static-exchange calculations for alkali-metal halides', *Phys. Rev. A* **18**(2), 467–498.

Collins, L. A., Robb, W. D. and Morrison, M. A. (1980), 'Electron scattering by diatomic molecules: Iterative static-exchange techniques', *Phys. Rev. A* **21**(2), 488–495.

Collins, L. A. and Schneider, B. I. (1981), 'Linear-algebraic approach to electron-molecule collisions: General formulation', *Phys. Rev. A* **24**(5), 2387–2401.

Cornille, H. and Drouffe, J. (1974), 'Phase-shift ambiguities for spinless and $L_{\max} \leq 4$ elastic scatterings', *Nuovo Cimento A* **20**, 401–436.

Crawford, O. (1971), 'Negative ions of polar molecules', *Mol. Phys.* **20**, 585–591.

Crawford, O. and Dalgarno, A. (1967), 'Bound states of an electron in a dipole field', *Chem. Phys. Lett.* **1**(1), 23–23.

Crawford, O. H. (1967), 'Bound states of a charged particle in a dipole field', *Proc. Phys. Soc.* **91**(2), 279.

Crawford, O. H. and Dalgarno, A. (1971), 'The scattering of thermal electrons by carbon monoxide', *J. Phys. B* **4**(4), 494.

Crawford, O. H., Dalgarno, A. and Hays, P. B. (1967), 'Electron collision frequencies in polar gases', *Mol. Phys.* **13**(2), 181–192.

Crawford, O. H. and Garrett, W. R. (1977), 'Electron affinities of polar molecules', *J. Chem. Phys.* **66**(11), 4968–4970.

Crichton, J. (1966), 'Phase-shift ambiguities for spin-independent scattering', *Nuovo Cimento A* **45**, 256–258.

Čurík, R. and Čársky, P. (2003), 'Vibrationally inelastic electron scattering on polyatomic molecules by the discrete momentum representation (DMR) method', *J. Phys. B* **36**(11), 2165.

Čurík, R. and Gianturco, F. A. (2002*a*), 'A computational analysis of low-energy electron scattering from gaseous cyclopropane', *J. Phys. B* **35**(3), 717.

Čurík, R. and Gianturco, F. A. (2002*b*), 'Quantum calculations for resonant vibrational excitations of cyclopropane by electron impact', *J. Phys. B* **35**(5), 1235.

Čurík, R., Gianturco, F. A. and Sanna, N. (2000), 'The separable representation of exchange in electron scattering from polyatomic targets', *J. Phys. B* **33**(14), 2705.

Čurík, R. and Šulc, M. (2010), 'Towards efficient *ab initio* calculations of electron scattering by polyatomic molecules: III. Modelling correlation–polarization interactions', *J. Phys. B* **43**(17), 175205.

Čurík, R., Ziesel, J. P., Jones, N. C., Field, T. A. and Field, D. (2006), 'Rotational Excitation of H_2O by Cold Electrons', *Phys. Rev. Lett.* **97**(12), 123202.

Dalgarno, A. and Lewis, J. T. (1956), 'The Representation of Long Range Forces by Series Expansions I: The Divergence of the Series II: The Complete Perturbation Calculation of Long Range Forces', *Proc. Phys. Soc. A* **69**(1), 57–64.

Davydov, A. S. (1965), *Quantum mechanics*, 1 edn, Pergamon Press.

DeLucia, F. C., Helminger, P. and Kirchhoff, W. H. (1974), 'Microwave Spectra of Molecules of Astrophysical Interest V. Water Vapor', *J. Phys. Chem. Ref. Data* **3**(1), 211–219.

Ding, J. and Zhou, A. (2007), 'Eigenvalues of rank-one updated matrices with some applications', *Appl. Math. Lett.* **20**(12), 1223–1226.

Dixon, D. A., Eades, R. A. and Truhlar, D. G. (1979), '*Ab initio* SCF polarisabilities and electron-molecule adiabatic polarisation potentials. II. Li_2', *J. Phys. B* **12**(16), 2741.

Edmonds, A. R. (1996), *Angular Momentum in Quantum Mechanics*, Princeton University Press.

Elran, Y. and Kay, K. G. (1999), 'Improving the efficiency of the Herman–Kluk propagator by time integration', *J. Chem. Phys.* **110**(8), 3653–3659.

Erdélyi, A. (1954), *Tables of Integral Transforms*, Vol. 2, McGraw-Hill.

Fabrikant, I. I. (1976), 'Scattering of slow electrons by polar molecules', *Zh. Eksp. Teor. Fiz.* **71**, 148–158.

Fabrikant, I. I. (1983*a*), 'Frame transformation effective-range theory: application to interaction of polar molecules with electrons', *J. Phys. B* **16**(7), 1269.

Fabrikant, I. I. (1983*b*), 'Generalised quantum defect theory for electron scattering by polar molecules', *J. Phys. B* **16**(7), 1253.

Fabrikant, I. I. (1984), 'Effective-range analysis of low-energy electron scattering by non-polar molecules', *J. Phys. B* **17**(20), 4223.

Fabrikant, I. I. (1991), 'A model describing inelastic processes in low-energy electron collisions with methyl chloride', *J. Phys. B* **24**(8), 2213.

Faisal, F. H. M. (1970), 'Electron-molecule interactions. I. Single-centre wave functions and potentials', *J. Phys. B* **3**(5), 636.

Fano, U. and Lee, C. M. (1973), 'Variational Calculation of R Matrices. Application to Ar Photoabsorption', *Phys. Rev. Lett.* **31**(27), 1573–1576.

Fano, U. and Racah, G. (1959), *Irreducible tensorial sets*, Academic Press.

Faure, A., Gorfinkiel, J. D. and Tennyson, J. (2004), 'Low-energy electron collisions with water: elastic and rotationally inelastic scattering', *J. Phys. B* **37**(4), 801.

Feldt, A. N. and Morrison, M. A. (2008*a*), 'Analytic Born completion in the calculation of differential cross sections for electron scattering from a linear molecule', *Phys. Rev. A* **77**(1), 012726.

Feldt, A. N. and Morrison, M. A. (2008*b*), 'Analytic Born completion in the calculation of differential cross sections for electron scattering from a linear molecule', *Phys. Rev. A* **77**(1), 012726.

Feng, H., Sun, W. and Morrison, M. A. (2003), 'Parameter-free nonadiabatic correlation-polarization potential for vibrational excitation in electron-molecule scattering: Application to $e^- - N_2$ collisions', *Phys. Rev. A* **68**(6), 062709.

Feng, H., Sun, W., Morrison, M. A. and Feldt, A. N. (2009), 'Exact inclusion of exchange in calculations of cross sections for vibrational excitation of N_2 by low-energy electrons', *J. Phys. B* **42**(17), 175201.

Fermi, E. and Teller, E. (1947), 'The Capture of Negative Mesotrons in Matter', *Phys. Rev.* **72**(5), 399–408.

Fetter, A. L. and Walecka, J. D. (2003), *Quantum Theory of Many-Particle Systems*, Dover Publications.

Field, D. and Jones, N. C. (n.d.), private communication.

Field, D., Lunt, S. L. and Ziesel, J.-P. (2001), 'The Quantum World of Cold Electron Collisions', *Acc. Chem. Res.* **34**(4), 291–298.

Fox, K. (1968), 'Classical motion of an electron in an electric-dipole field II. Point dipole case', *J. Phys. A* **1**(1), 124.

Galassi, M., Davies, J., J.Theiler, Gough, B., Jungman, G., Alken, P., Boot, M. and Rossi, F., eds (2009), *GNU Scientific Library Reference Manual*, 3 edn, Network Theory Ltd.

Garrett, W. (1971*a*), 'Comment on the critical dipole moments for electron binding to a freely rotating electric dipole', *Mol. Phys.* **20**, 751–752.

Garrett, W. R. (1970), 'Critical binding of an electron to a non-stationary electric dipole', *Chem. Phys. Lett.* **5**(7), 393–397.

Garrett, W. R. (1971*b*), 'Critical Binding of an Electron to a Rotationally Excited Dipolar System', *Phys. Rev. A* **3**(3), 961–972.

Garrett, W. R. (1975), 'Molecular scattering: Convergence of close-coupling expansions in the presence of many open channels', *Phys. Rev. A* **11**(4), 1297–1302.

Garrett, W. R. (1980*a*), 'Critical binding of an electron by a nonstationary, point-dipole rotor', *Phys. Rev. A* **22**(4), 1769–1770.

Garrett, W. R. (1980*b*), 'Critical binding of electron–dipole rotor systems; electronically excited states', *J. Chem. Phys.* **73**(11), 5721–5725.

Garrett, W. R., Turner, J. E. and Anderson, V. E. (1969), 'Spherical-Coordinate Analysis of Ground-State Energy Eigenfunctions for an Electron in the Field of a Finite Dipole', *Phys. Rev.* **188**(1), 513–514.

Gáspár, R. (1954), 'Über eine Approximation des Hartree-Fockschen Potentials Durch eine Universelle Potentialfunktion', *Acta physica Academiae Scientiarum Hungaricae* **3**, 263–286.

Gell-Mann, M. and Goldberger, M. L. (1953), 'The Formal Theory of Scattering', *Phys. Rev.* **91**(2), 398–408.

Gerjuoy, E. and Stein, S. (1955), 'Rotational Excitation by Slow Electrons', *Phys. Rev.* **97**(6), 1671–1679.

Gianturco, F. A., Jain, A. and Rodriguez-Ruiz, J. A. (1993), 'Test of local model potentials for positron scattering from rare gases', *Phys. Rev. A* **48**(6), 4321–4332.

Gianturco, F. A. and Rodriguez-Ruiz, J. A. (1992), 'Correlation forces in electron scattering from atoms and molecules: a density functional approach', *J. Mol. Struct. Theochem.* **260**, 99–121.

Gianturco, F. A. and Rodriguez-Ruiz, J. A. (1993), 'Correlation forces in electron-scattering processes via density-functional theory: Electron collisions with closed-shell atoms', *Phys. Rev. A* **47**(2), 1075–1086.

Gibson, T. L. and Morrison, M. A. (1984), '*Ab initio* nonadiabatic polarization potentials for electron-molecule scattering: The $e^- - H_2$ system', *Phys. Rev. A* **29**(5), 2497–2508.

Giri, P. R., Gupta, K. S., Meljanac, S. and Samsarov, A. (2008), 'Electron capture and scaling anomaly in polar molecules', *Phys. Lett. A* **372**(17), 2967–2970.

Goldstein, H., Poole, C. and Safko, J. (2001), *Classical mechanics*, 3 edn, Addison Wesley.

Golub, G. H. and Loan, C. F. V. (1996), *Matrix computations*, 3 edn, The John Hopkins University Press.

Gordon, R. G. (1969), 'New Method for Constructing Wavefunctions for Bound States and Scattering', *J. Chem. Phys.* **51**(1), 14–25.

Gordon, R. G. and Kim, Y. S. (1972), 'Theory for the Forces between Closed-Shell Atoms and Molecules', *J. Chem. Phys.* **56**(6), 3122–3133.

Gradshteyn, I. and Ryzhik, I. (2007), *Table of Integrals, Series, and Products*, 7 edn, Elsevier Academic Press.

Gulley, R. J. and Buckman, S. J. (1994), 'Elastic scattering of low energy electrons from sulphur dioxide', *J. Phys. B* **27**(9), 1833.

Hall, R. T. and Dowling, J. M. (1967), 'Pure Rotational Spectrum of Water Vapor', *J. Chem. Phys.* **47**(7), 2454–2461.

Hara, S. (1967), 'The Scattering of Slow Electrons by Hydrogen Molecules', *J. Phys. Soc. Jap.* **22**(3), 710–718.

Helgaker, T., Jørgensen, P. and Olsen, J. (2000), *Modern Electronic-Structure Theory*, Wiley.

Heller, E. J. (1981), 'Frozen Gaussians: A very simple semiclassical approximation', *J. Chem. Phys.* **75**(6), 2923–2931.

Henry, R. J. W. and Lane, N. F. (1969), 'Polarization and Exchange Effects in Low-Energy Electron-H_2 Scattering', *Phys. Rev.* **183**(1), 221–231.

Herman, M. F. and Kluk, E. (1984), 'A semiclasical justification for the use of non-spreading wavepackets in dynamics calculations', *Chem. Phys.* **91**(1), 27–34.

Herzberg, G. (1956), *Molecular spectra and molecular structure*, Vol. II. Infrared and Raman spectra of polyatomic molecules, van Nostrand.

Herzberg, G. (1991), *Molecular Spectra and Molecular Structure: Infrared and Raman of Polyatomic Molecules*, Krieger Publishing Co.

Hoffmann, S. V., Lunt, S. L., Jones, N. C., Field, D. and Ziesel, J.-P. (2002), 'An undulator-based spherical grating monochromator beamline for low energy electron-molecule scattering experiments', *Rev. Sci. Instr.* **73**(12), 4157–4163.

Hougen, J. T. (1962), 'Classification of Rotational Energy Levels for Symmetric-Top Molecules', *J. Chem. Phys.* **37**(7), 1433–1441.

Hougen, J. T. (1963), 'Classification of Rotational Energy Levels. II', *J. Chem. Phys.* **39**(2), 358–365.

Huo, W. and Gianturco, F. (1995), *Computational methods for Electron–Molecule Collisions*, Plenum Press, New York.

Ingr, M., Polášek, M., Čársky, P. and Horáček, J. (2000), 'Discrete momentum representation method for polar molecules: Calculation of the elastic electron scattering on the H_2O molecule', *Phys. Rev. A* **62**(3), 032703.

Inui, T., Tanabe, Y. and Onodera, Y. (1996), *Group Theory and Its Applications in Physics*, Springer.

Isaacs, W. A. and Morrison, M. A. (1992), 'Modified effective range theory as an alternative to low-energy close-coupling calculations', *J. Phys. B* **25**(3), 703.

Isaacs, W. A. and Morrison, M. A. (1996), 'Analytic Born completion in the calculation of electron-molecule differential cross sections', *Phys. Rev. A* **53**(6), 4215–4221.

Itikawa, Y. (1978), 'Electron scattering by polar molecules', *Phys. Rep.* **46**(4), 117–164.

Itikawa, Y. (2000*a*), 'Electron Scattering from Polar Molecules: Frame Transformation and the Born Closure Approximation', *Physics Essays* **13**(3), 344–349.

Itikawa, Y. (2000*b*), 'The Born closure approximation for the scattering amplitude of an electron-molecule collision', *Theor. Chem. Acc.* **105**, 123–131.

Itikawa, Y. and Mason, N. (2005), 'Rotational excitation of molecules by electron collisions', *Phys. Rep.* **414**(1), 1–41.

Jackson, J. L. (1951), 'A Variational Approach to Nuclear Reactions', *Phys. Rev.* **83**(2), 301–304.

Jain, A. and Norcross, D. W. (1992), 'Slow-electron collisions with CO molecules in an exact-exchange plus parameter-free polarization model', *Phys. Rev. A* **45**(3), 1644–1656.

Johnson, B. R. (1973), 'The multichannel log-derivative method for scattering calculations', *J. Comput. Phys.* **13**(3), 445–449.

Jonker, J. E. and Vries, E. D. (1967), 'A note on orthogonality and completeness of the rotation matrices', *Nucl. Phys. A* **105**(2), 621–626.

Jordan, K. D. and Luken, W. (1976), 'Theoretical study of the binding of an electron to a molecular dipole: $LiCl^-$', *J. Chem. Phys.* **64**(7), 2760–2766.

Kay, K. G. (1994), 'Numerical study of semiclassical initial value methods for dynamics', *J. Chem. Phys.* **100**(6), 4432–4445.

Kay, K. G. (2005), 'Semiclassical Initial Value Treatments of Atoms and Molecules', *Annu. Rev. Phys. Chem.* **56**(1), 255–280.

King, G. W., Hainer, R. M. and Cross, P. C. (1943), 'The Asymmetric Rotor I. Calculation and Symmetry Classification of Energy Levels', *J. Chem. Phys.* **11**(1), 27–42.

Kohn, W. (1948), 'Variational Methods in Nuclear Collision Problems', *Phys. Rev.* **74**(12), 1763–1772.

Kohn, W. and Sham, L. J. (1965), 'Self-Consistent Equations Including Exchange and Correlation Effects', *Phys. Rev.* **140**(4A), A1133–A1138.

Kołos, W. and Wolniewicz, L. (1965), 'Potential-Energy Curves for the $X^1\Sigma_g^+$, $b^3\Sigma_u^+$ and $C^1\Pi_u$ States of the Hydrogen Molecule', *J. Chem. Phys.* **43**(7), 2429–2441.

Kroto, H. W. (1975), *Molecular rotation spectra*, 1 edn, Wiley.

Landau, L. and Lifschitz, E. (1977), *Quantum mechanics*, 3 edn, Pergamon Press Ltd.

Lane, A. M. and Thomas, R. G. (1958), 'R-Matrix Theory of Nuclear Reactions', *Rev. Mod. Phys.* **30**(2), 257–353.

Lane, N. F. (1980), 'The theory of electron-molecule collisions', *Rev. Mod. Phys.* **52**(1), 29.

Lane, N. F. and Henry, R. J. W. (1968), 'Polarization Potential in Low-Energy Electron-H_2 Scattering', *Phys. Rev.* **173**(1), 183–190.

Lebedev, V. I. (1976), 'Quadratures on a sphere', *USSR Comp. Math. Math. Phys.* **16**(2), 10–24.

Lebedev, V. I. (1977), 'Spherical quadrature formulas exact to orders 25–29', *Siberian Mathematical Journal* **18**, 99–107.

Lebedev, V. and Laikov, D. (1999), 'Quadrature formula for the sphere of 131^{th} algebraic order of accuracy', *Dok. Akad. Nauk* **366**(6), 741–745.

Lee, C., Yang, W. and Parr, R. G. (1988), 'Development of the Colle-Salvetti correlation-energy formula into a functional of the electron density', *Phys. Rev. B* **37**(2), 785–789.

Lehman, D. R., Parke, W. C. and Maximon, L. C. (1981), 'Numerical evaluation of integrals containing a spherical Bessel function by product integration', *J. Math. Phys.* **22**(7), 1399–1413.

Lévy-Leblond, J.-M. (1967), 'Electron Capture by Polar Molecules', *Phys. Rev.* **153**(1), 1–4.

Lévy-Leblond, J.-M. and Provost, J. P. (1967), 'Critical scattering of electrons by polar molecules', *Phys. Lett. B* **26**(2), 104–106.

Li, Y., Carter, S., Hirsch, G. and Buenker, R. J. (1993), 'Theoretical calculation of the potential surfaces and vibrational frequencies of the $A\,^2\Sigma^+$ and $X\,^2\Pi$ electronic states of the NCO radical', *Mol. Phys.* **80**(1), 145–152.

Lide, D. R. (2009), *CRC Handbook of Chemistry and Physics*, 90 edn, CRC Press.

Linz, P. (1985), *Analytical and numerical methods for Volterra equations*, Society for Industrial and Applied Mathematics.

Longuet-Higgins, H. C. (1962), 'The symmetry groups of non-rigid molecules', *Mol. Phys.* **6**, 445–460.

Lovas, F. J. (1978), 'Microwave spectral tables II. Triatomic molecules', *J. Phys. Chem. Ref. Data* **7**(4), 1445–1750.

Lucchese, R. R. and McKoy, V. (1979), 'Application of the Schwinger variational principle to electron scattering', *J. Phys. B* **12**(14), L421.

Manolopoulos, D. E., Jamieson, M. J. and Pradhan, A. D. (1993), 'Johnson's Log Derivative Algorithm Rederived', *J. Comput. Phys.* **105**(1), 169–172.

Massey, H. S. W. (1932), 'The collision of electrons with rotating dipoles', *Math. Proc. Camb. Phil. Soc.* **28**, 99–105.

Meyer, H.-D., Horáček, J. and Cederbaum, L. S. (1991), 'Schwinger and anomaly-free Kohn variational principles and a generalized Lanczos algorithm for nonsymmetric operators', *Phys. Rev. A* **43**(7), 3587–3596.

Mil'nikov, G., Nakamura, H. and Horáček, J. (2001), 'Stable and efficient evaluation of Green's function in scattering problem', **135**(3), 278–292.

Morrison, M. A. (1983), 'The physics of low-energy electron-molecule collisions: A guide for the perplexed and the uninitiated', **36**, 239–286.

Morrison, M. A. (1988), Near-Threshold Electron-Molecule Scattering, Vol. 24 of *Advances in Atomic and Molecular Physics*, Academic Press, pp. 51–156.

Morrison, M. A. and Collins, L. A. (1978), 'Exchange in low-energy electron-molecule scattering: Free-electron-gas model exchange potentials and applications to $e^- - H_2$ and $e^- - N_2$ collisions', *Phys. Rev. A* **17**(3), 918–938.

Morrison, M. A. and Feldt, A. N. (2007), 'Through scattering theory with gun and camera: Coping with conventions in collision theory', *Am. J. Phys.* **75**, 67–80.

Morrison, M. A., Feldt, A. N. and Austin, D. (1984), 'Adiabatic approximations for the nuclear excitation of molecules by low-energy electron impact: Rotational excitation of H_2', *Phys. Rev. A* **29**(5), 2518–2540.

Morrison, M. A., Feldt, A. N. and Saha, B. C. (1984), 'Validity of the adiabatic nuclei theory for vibrational excitation of molecules by electron impact: The $e^- - H_2$ system', *Phys. Rev. A* **30**(5), 2811–2813.

Morrison, M. A. and Hay, P. J. (1979), '*Ab initio* adiabatic polarization potentials for low-energy electron-molecule and positronmolecule collisions: The $e^- - N_2$ and $e^- - CO_2$ systems', *Phys. Rev. A* **20**(3), 740–748.

Morrison, M. A., Lane, N. F. and Collins, L. A. (1977), 'Low-energy electron-molecule scattering: Application of coupled-channel theory to $e^- - CO_2$ collisions', *Phys. Rev. A* **15**(6), 2186–2201.

Morrison, M. A. and Parker, G. A. (1987), 'A Guide to Rotations in Quantum Mechanics', *Aust. J. Phys.* **40**(4), 465–497.

Morrison, M. A., Saha, B. C. and Gibson, T. L. (1987), 'Electron-N_2 scattering calculations with a parameter-free model polarization potential', *Phys. Rev. A* **36**(8), 3682–3698.

Morrison, M. A., Sun, W., Isaacs, W. A. and Trail, W. K. (1997), 'Ultrasimple calculation of very-low-energy momentum-transferand rotational-excitation cross sections: e-N_2 scattering', *Phys. Rev. A* **55**(4), 2786–2798.

Motovilov, A. K., Sandhas, W., Sofianos, S. A. and Kolganova, E. A. (2001), 'Binding energies and scattering observables in the $^4He_3$ atomic system', *Eur. Phys. J. D* **13**, 33–41.

Mrugala, F. (1985), 'Log-derivative method for two-potential scattering problems', *J. Comput. Phys.* **58**(1), 113–133.

Mulliken, R. S. (1941), 'Species Classification and Rotational Energy Level Patterns of Non-Linear Triatomic Molecules', *Phys. Rev.* **59**(11), 873–889.

National Institute of Standars and Technology (2008).
URL: *http://physics.nist.gov/cuu/Units/*

Nesbet, R. K. (1979), 'Energy-modified adiabatic approximation for scattering theory', *Phys. Rev. A* **19**(2), 551–556.

Nesbet, R. K. (2004), *Variational Principles and Methods in Theoretical Physics and Chemistry*, Cambridge Univeristy Press.

Norcross, D. W. and Padial, N. T. (1982), 'The multipole-extracted adiabatic-nuclei approximation for electron-molecule collisions', *Phys. Rev. A* **25**(1), 226–238.

Norcross, D. W. and Seaton, M. J. (1973), 'Asymptotic solutions of the coupled equations of electron-atom collision theory for the case of some channels closed', *J. Phys. B* **6**(4), 614.

Oberoi, R. S. and Nesbet, R. K. (1973), 'Variational Formulation of the R Matrix Method for Multichannel Scattering', *Phys. Rev. A* **8**(1), 215–219.

O'Connell, J. K. and Lane, N. F. (1983), 'Nonadjustable exchange-correlation model for electron scattering from closed-shell atoms and molecules', *Phys. Rev. A* **27**(4), 1893–1903.

Onda, K. and Temkin, A. (1983), 'Calculation of the polarization potential for $e^- - N_2$ collisions', *Phys. Rev. A* **28**(2), 621–631.

Padial, N. T. and Norcross, D. W. (1984), 'Parameter-free model of the correlation-polarization potential for electron-molecule collisions', *Phys. Rev. A* **29**(4), 1742–1748.

Padial, N. T., Norcross, D. W. and Collins, L. A. (1981), 'On the use of the unitarised Born approximation in electron collisions with polar molecules', *J. Phys. B* **14**(16), 2901.

Percival, I. and Seaton, M. (1957), 'The partial wave theory of electron-hydrogen atom collisions', *Proc. Cambridge Philos. Soc.* **53**, 654–662.

Perdew, J. P., Chevary, J. A., Vosko, S. H., Jackson, K. A., Pederson, M. R., Singh, D. J. and Fiolhais, C. (1992), 'Atoms, molecules, solids, and surfaces: Applications of the generalized gradient approximation for exchange and correlation', *Phys. Rev. B* **46**(11), 6671–6687.

Perdew, J. P. and Wang, Y. (1992), 'Accurate and simple analytic representation of the electron-gas correlation energy', *Phys. Rev. B* **45**(23), 13244–13249.

Perdew, J. P. and Zunger, A. (1981), 'Self-interaction correction to density-functional approximations for many-electron systems', *Phys. Rev. B* **23**(10), 5048–5079.

Pichl, L. and Horáček, J. (1996), 'Analytical treatment of the Green function singularity in integral equations of scattering theory', *J. Phys. A* **29**(16), L405.

Podolsky, B. (1928), 'Quantum-Mechanically Correct Form of Hamiltonian Function for Conservative Systems', *Phys. Rev.* **32**(5), 812–816.

Polášek, M., Juřek, M., Ingr, M., Čársky, P. and Horáček, J. (2000), 'Discrete momentum representation of the Lippmann-Schwinger equation and its application to electron-molecule scattering', *Phys. Rev. A* **61**(3), 032701.

Press, W. H., Teukolsky, S. A., Vetterling, W. T. and Flannery, B. P. (2007), *Numerical Recipes: The Art of scientific computing*, 3 edn, Cambridge University Press.

Randell, J., Gulley, R. J., Lunt, S. L., Ziesel, J.-P. and Field, D. (1996), 'Very low energy electron scattering in CO', *J. Phys. B* **29**(10), 2049.

Rescigno, T. N. and Orel, A. E. (1981), 'Separable approximation for exchange interactions in electron-molecule scattering', *Phys. Rev. A* **24**(3), 1267–1271.

Rescigno, T. N. and Orel, A. E. (1982), 'Separable approximation for exchange interactions in electron-molecule scattering: Numerical stabilization procedures', *Phys. Rev. A* **25**(4), 2402–2404.

Rescigno, T. N., Orel, A. E. and McCurdy, C. W. (1997), 'Low-energy electron scattering from CH_3Cl', *Phys. Rev. A* **56**(4), 2855–2859.

Riley, M. E. and Truhlar, D. G. (1975), 'Approximations for the exchange potential in electron scattering', *J. Chem. Phys.* **63**(5), 2182–2191.

Robicheaux, F. (1991), 'Driving nuclei with resonant electrons: *Ab initio* study of $(e+H_2)^2\ \Sigma_u^+$', *Phys. Rev. A* **43**(11), 5946–5955.

Rose, M. E. (1995), *Elementary theory of angular momentum*, Dover Publications.

Salvini, S. and Thompson, D. G. (1981), 'Exchange approximations in the scattering of slow electrons by polyatomic molecules', *J. Phys. B* **14**(19), 3797.

Sams, W. N. and Kouri, D. J. (1969*a*), 'Noniterative Solutions of Integral Equations for Scattering. I. Single Channels', *J. Chem. Phys.* **51**(11), 4809–4814.

Sams, W. N. and Kouri, D. J. (1969*b*), 'Noniterative Solutions of Integral Equations for Scattering. II. Coupled Channels', *J. Chem. Phys.* **51**(11), 4815–4819.

Sams, W. N. and Kouri, D. J. (1970*a*), 'Noniterative Solutions of Integral Equations for Scattering. III. Coupled Open and Closed Channels and Eigenvalue Problems', *J. Chem. Phys.* **52**(8), 4144–4150.

Sams, W. N. and Kouri, D. J. (1970*b*), 'Noniterative Solutions of Integral Equations for Scattering. IV. Preliminary Calculations for Coupled Open Channels and Coupled Eigenvalue Problems', *J. Chem. Phys.* **53**(2), 496–501.

Shi, X., Chan, V. K., Gallup, G. A. and Burrow, P. D. (1996), 'Low energy electron scattering from CH_3Cl', *J. Chem. Phys.* **104**(5), 1855–1863.

Shimamura, I. (1977), 'R-matrix theory of atomic continuum processes', *J. Phys. B* **10**(13), 2597.

Shimanouchi, T. (1972), *NIST Chemistry WebBook, NIST Standard Reference Database Number 69*, National Institute of Standards and Technology, chapter Molecular Vibrational Frequencies.

Slater, J. C. (1960), *Quantum Theory of Atomic Structure*, Vol. 2, McGraw-Hill.

Sloan, I. (1968), 'The numerical evaluation of principal-value integrals', *J. Comput. Phys.* **3**(2), 332–333.

Šulc, M. (2007), Numerical solution of scattering integral equations, Master's thesis, Faculty of Mathematics and Physics, Charles University in Prague.

Šulc, M., Čurík, R. and Horáček, J. (2010), 'Efficient solution of scattering equations by combination of R-matrix and Lanczos methods', *Eur. Phys. J. D* **57**, 187–196.

Sullivan, E. C. and Temkin, A. (1982), 'A non-iterative method for solving PDE's arising in electron scattering', *Comp. Phys. Commun.* **25**(1), 97–110.

Sun, W., Morrison, M. A., Isaacs, W. A., Trail, W. K., Alle, D. T., Gulley, R. J., Brennan, M. J. and Buckman, S. J. (1995), 'Detailed theoretical and experimental analysis of low-energy electron-N_2 scattering', *Phys. Rev. A* **52**(2), 1229–1256.

Szabo, A. and Ostlund, N. S. (1996), *Modern Quantum Chemistry: Introduction to Advanced Electronic Structure Theory*, Dover Publications.

Takatsuka, K. and McKoy, V. (1981), 'Extension of the Schwinger variational principle beyond the static-exchange approximation', *Phys. Rev. A* **24**(5), 2473–2480.

Taylor, J. R. (2006), *Scattering theory: The Quantum Theory of Nonrelativistic Collisions*, Dover Publications.

Telega, S., Bodo, E. and Gianturco, F. (2004), 'Rotationally inelastic collisions of electrons with H_2 and N_2 molecules: converged space-frame calculations at low energies', *Eur. Phys. J. D* **29**, 357–365.

Telega, S. and Gianturco, F. A. (2006), 'Modelling electron-N_2 scattering in the resonant region', *Eur. Phys. J. D* **38**, 495–500.

Temkin, A. (1957), 'Polarization and Exchange Effects in the Scattering of Electrons from Atoms with Application to Oxygen', *Phys. Rev.* **107**(4), 1004–1012.

Temkin, A. and Faisal, F. H. M. (1971), 'Adiabatic Theory of Rotational Excitation of Non-Σ States', *Phys. Rev. A* **3**(1), 520–521.

Temkin, A. and Lamkin, J. C. (1961), 'Application of the Method of Polarized Orbitals to the Scattering of Electrons from Hydrogen', *Phys. Rev.* **121**(3), 788–794.

Temkin, A., Vasavada, K. V., Chang, E. S. and Silver, A. (1969), 'Scattering of Electrons from H_2^+. II', *Phys. Rev.* **186**(1), 57–66.

Thompson, D. G. (1966), 'The Elastic Scattering of Slow Electrons by Neon and Argon', *Proc. Roy. Soc. London Sect. A* **294**(1437), 160–174.

Thompson, W. J. (2004), *Angular momentum*, WILEY-VCH Verlag GmbH.

Townes, C. and Schalow, A. (1975), *Microwave spectroscopy*, 2 edn, Dover Publications.

Truhlar, D. G. and Brandt, M. A. (1976), 'Close-coupling calculations of differential cross sections for elastic scattering and rotational excitation of hydrogen molecules by electrons at 10 and 40 eV', *J. Chem. Phys.* **65**(8), 3092–3101.

Truhlar, D. G., Dixon, D. A. and Eades, R. A. (1979), '*Ab initio* SCF probabilities and electron-molecule adiabatic polarisation potentials. I. H_2', *J. Phys. B* **12**(12), 1913.

Truhlar, D. G. and Rice, J. K. (1970), 'Electron Scattering by H_2 with and without Vibrational Excitation. I. Quantum-Mechanical Theory', *J. Chem. Phys.* **52**(9), 4480–4501.

Tully, J. C. and Berry, R. S. (1969), 'Elastic Scattering of Low-Energy Electrons by the Hydrogen Molecule', *J. Chem. Phys.* **51**(5), 2056–2075.

Turner, J. E. (1977), 'Minimum dipole moment required to bind an electron – moleculartheorists rediscover phenomenon mentioned in Fermi-Teller paper twenty years earlier', *Am. J. Phys.* **45**(8), 758–766.

Turner, J. E., Anderson, V. E. and Fox, K. (1968), 'Ground-State Energy Eigenvalues and Eigenfunctions for an Electron in an Electric-Dipole Field', *Phys. Rev.* **174**(1), 81–89.

Turner, J. E. and Fox, K. (1968), 'Classical motion of an electron in an electric-dipole field. I. Finite dipole case', *J. Phys. A* **1**(1), 118.

Turner, J. and Fox, K. (1966), 'Minimum dipole moment required to bind an electron to a finite dipole', *Phys. Lett.* **23**(9), 547–549.

Wallis, R. F., Herman, R. and Milnes, H. W. (1960), 'Energy levels of an electron in the field of a finite dipole', *J. Mol. Spec.* **4**(1-6), 51–74.

Walton, A. R. and Manolopoulos, D. E. (1995), 'Application of the frozen Gaussian approximation to the photodissociation of CO_2', **244**(5-6), 448–455.

Walton, A. R. and Manolopoulos, D. E. (1996), 'A new semiclassical initial value method for Franck-Condon spectra', *Mol. Phys.* **87**(4), 961–978.

Wang, H., Manolopoulos, D. E. and Miller, W. H. (2001), 'Generalized Filinov transformation of the semiclassical initial value representation', *J. Chem. Phys.* **115**(14), 6317–6326.

Watson, G. N. (2008), *A Treatise on the theory of Bessel functions*, Merchant Books.

Watson, J. K. G. (1970), 'The vibration-rotation hamiltonian of linear molecules', *Mol. Phys.* **19**(4), 465–487.

Wehrle, M., Šulc, M. and Vaníček, J. (2011), 'Time-Resolved Electronic Spectra with Efficient Quantum Dynamics Methods', *Chimia* **65**, 334–338.

White, R. A. and Hayes, E. F. (1972), 'Quantum Mechanical Studies of the Vibrational Excitation of H_2 by Li^+', *J. Chem. Phys.* **57**(7), 2985–2993.

Wigner, E. P. and Eisenbud, L. (1947), 'Higher Angular Momenta and Long Range Interaction in Resonance Reactions', *Phys. Rev.* **72**(1), 29–41.

Wilkinson, J. H. (1988), *Algebraic eigenvalue problem*, Oxford University Press.

Wilson, Jr, E. B. (1935), 'The Statistical Weights of the Rotational Levels of Polyatomic Molecules, Including Methane, Ammonia, Benzene, Cyclopropane and Ethylene', *J. Chem. Phys.* **3**(5), 276–285.

Wilson, Jr., E. B., Decius, J. C. and Cross, P. C. (1980), *Molecular Vibrations: The Theory of Infrared and Raman Vibrational Spectra*, Dover Publications.

Winnewisser, G. (1972), 'Millimeter Wave Rotational Spectrum of HSSH and DSSD. II. Anomalous K Doubling Caused by Centrifugal Distortion in DSSD', *J. Chem. Phys.* **56**(6), 2944–2954.

Winstead, C. and McKoy, V. (2007), *Electron Scattering by Small Molecules*, Wiley, pp. 103–190.

Winter, C. V. (1954), 'The asymmetric rotator in quantum mechanics', *Physica* **20**(1-6), 274–292.

Zemach, C. (1964), 'Phase-shift equations for many-channel problems', *Nuovo Cimento* **33**, 939–947.

Zvijac, D. J., Heller, E. J. and Light, J. C. (1975), 'Variational correction to Wigner R-matrix theory of scattering', *J. Phys. B* **8**(7), 1016.